

IL NUOVO CIMENTO

ORGANO DELLA SOCIETÀ ITALIANA DI FISICA
SOTTO GLI AUSPICI DEL CONSIGLIO NAZIONALE DELLE RICERCHE

VOL. XVI, N. 5

Serie decima

1° Giugno 1960

On a Convergent non-local Field Theory. - II.

E. ARNOUS

Centre National de Recherche Scientifique - Paris

W. HEITLER and L. O'RAIFEARTAIGH (*)

Institut für Theoretische Physik, Universität - Zürich

(ricevuto il 20 Gennaio 1960)

Summary. — The general theory of part I is formulated for the case of quantum-electrodynamics. The Lorentz-condition, the gauge transformation, the connexion between potentials and (gauge invariant) field strengths and the (divergence free) current density j_μ all require generalizations which are given. The Schrödinger equation is shown to be gauge invariant and the condition for the gauge invariance of the S -matrix is derived. Throughout the form factor is left open. It is shown that the space integral of j_0 reduces to the ordinary total charge (if the form factor commutes with the field operators). The canonical energy-momentum vector is formally the same as in local theory (the difference lies in the different Hamiltonian). The possibilities for obtaining a gauge invariant energy-momentum vector are discussed.

Introduction.

This paper is a direct continuation of Part I.

We consider here the special case of a non-local electrodynamics with an interaction Hamiltonian

$$H = \int \mathcal{H} d^3x, \quad \mathcal{H} = -ie \int \bar{\psi}(x') \gamma_\mu F(x - x', x - x'', x - x''') \psi(x'') A_\mu(x''') d^4(x' x'' x''').$$

(*) On leave of absence from Dublin Institute for Advanced Studies and National University of Ireland.

The A_μ are the same operators as in local theory and satisfy in interaction representation

$$[A_\mu(x), A_\nu(y)] = iD(x-y)\delta_{\mu\nu}.$$

The case of electrodynamics causes a great deal more complication: the potentials have to satisfy the Lorentz-condition and there is an additional group of transformations, the gauge transformation, against which we would wish the theory to be invariant.

Throughout this paper we imagine the interaction to be switched on adiabatically at $t = -\infty$. This is a simplification which makes it unnecessary to consider wave packets before particles collide or to take into account explicitly the Bloch-Nordsieck transformation from bare to real particles.

It will be seen that all conditions (Lorentz-condition, etc.) and all basic quantities (current, field strengths, etc.) require a generalization and are not identical with those of the local theory, except the total charge which, as already shown in Part I, is the same.

1. - Lorentz-condition.

The Lorentz-condition is, in close analogy to the local theory, formulated as follows: We seek an operator $\chi^+(x', t)$ operating on the state vector $\Psi(t)$ such that

$$(1a) \quad \partial_\mu'^2 \chi^+(x', t) = 0,$$

$$(1b) \quad \chi^+(x', t_0) \Psi(t_0)|_{x'_0=t_0} = 0,$$

$$(1c) \quad \{\partial_4' \chi^+(x', t_0)\}_{x'_0=t_0} \Psi(t_0) = 0.$$

It follows hence that

$$(1d) \quad \chi^+(x', t_0) \Psi(t_0) = 0, \quad \text{for all } x'_0 (\neq t_0).$$

Throughout this paper we denote by d_4 the total derivative

$$d_4 X = \partial_4 X - [X, H], \quad d_i = \partial_i.$$

We demand further

$$(1e) \quad d_4 \chi^+(x', t) = 0.$$

From (1e) it follows then that

$$(1f) \quad \chi^+(x', t) \Psi(t) = 0 \quad \text{for all } t \text{ and } x'.$$

For a free electromagnetic field we must, of course, have

$$\chi^+ = \partial'_\mu A_\mu^+(x')$$

(independent of t).

When the field interacts with electrons we can put quite generally

$$(2) \quad \chi^+(x', t) = S(t) \partial'_\mu A_\mu^+(x') S^\dagger(t),$$

where $S(t)$ is the time dependent S -matrix. We anticipate here the fact that in our non-local theory also an S -matrix exists ⁽¹⁾ which is formally (*i.e.* expressed by H) the same as usual and which fulfils

$$(3) \quad i \frac{\partial S(t)}{\partial t} = H S(t), \quad -i \frac{\partial S^\dagger(t)}{\partial t} = S^\dagger(t) H, \quad S = S(\infty).$$

That (1a) is satisfied is evident. (1e) follows immediately from (3) (note that $\partial'_\mu A_\mu^+(x')$ is independent of t).

So far there is no difference between the local and non-local cases. The difference appears when χ^+ is worked out explicitly. We use the expansion of $S(t)$

$$(4) \quad S(t) = 1 - i \int_0^t H(t_1) dt_1 + (-i)^2 \int_0^t dt_1 \int_0^{t_1} dt_2 H(t_1) H(t_2) + \dots$$

With the help of this expansion $\chi^+(x', t)$ is obtained in form of an infinite series

$$(5) \quad \chi^+(x', t) = \partial'_\mu A_\mu^+(x') + L_1^+(x', t) + L_2^+(x', t) + \dots$$

The calculation is straightforward. We use

$$(6) \quad (\partial'_\nu + \partial''_\nu) \bar{\psi}(y') \gamma_\nu \psi(y'') = 0$$

on account of the Dirac equation (in interaction representation), and

$$[A_\mu^+(x), A_\nu(y)] = [A_\mu^+(x), A_\nu^-(y)] = i D^+(x - y) \delta_{\mu\nu}.$$

For the explicit evaluation we assume F to commute with $\bar{\psi}$, ψ , A_μ .

(1) The S -matrix will be studied in a separate paper by one of us (O'R.).

After some calculation one finds for the first two terms

$$(7_1) \quad L_1^+(x', t) = i^2 e \int_{y_0=t} d^3 y d^4(y' y'' y''') D^+(x' - y''') \bar{\psi}(y') \gamma_4 F(y - y', y - y'', y - y''') \psi(y''),$$

$$(7_2) \quad L_2^+(x', t) = i^4 e^2 \int_{y_{10}=t_1=y_0}^t dt_1 d^3 y_1 d^3 y d^4(y'_1 y''_1 y'''_1) d^4(y' y'' y''') D^+(x' - y''') \cdot \\ \cdot [\bar{\psi}(y_1) \gamma_\nu F(y_1 - y'_1, \dots) \psi(y''_1) A_\nu(y'''_1) \bar{\psi}(y') \gamma_4 F(y - y', \dots) \psi(y'')].$$

The local limit is obtained by putting $F = \delta^4(y - y') \delta^4(y - y'') \delta^4(y - y''')$. We obtain then

$$L_1^+(x', t) = -e \int d^3 y \bar{\psi}(y) \gamma_4 \psi(y) D^+(x' - y),$$

which is the usual expression. The commutator in (7₂) reduces to

$$[\bar{\psi}(y_1) \gamma_\nu \psi(y_1), \bar{\psi}(y) \gamma_4 \psi(y)]_{y_0=y_{10}} = 0$$

because the current densities (of local theory) in 2 different space points but at the same time commute. So L_2^+ vanishes in the local limit, and the same is true for all higher terms. In the above use is made of the assumption that H vanishes at $t = -\infty$.

We establish now some properties of χ . At $t = -\infty$ χ^+ reduces (on account of the assumed switch-on) to

$$(8) \quad \chi^+(x', -\infty) = \partial'_\mu A_\mu^+(x').$$

The commutator of χ^+ and χ^- taken at the same t vanishes:

$$(9a) \quad \left\{ \begin{aligned} [\chi^+(x', t), \chi^-(x'', t)] &= S(t) [\partial'_\mu A_\mu^+(x'), \partial''_\nu A_\nu^-(x'')] S^\dagger(t), \\ &= i S(t) \partial'_\mu \partial''_\mu D^+(x' - x'') S^\dagger(t), \\ &= -i \partial'^2_\mu D^+(x' - x'') = 0. \end{aligned} \right.$$

Evidently, of course

$$(9b) \quad [\chi^+(x', t), \chi^+(x'', t)] = 0$$

(because A^+ commutes with A^+ , always).

If we define

$$(10a) \quad \left\{ \begin{aligned} \chi &= \chi^+ + \chi^-, \\ \bar{\chi} &= \chi^+(x, t=x_0) + \chi^-(x, t=x_0) = S(t) \partial_\mu A_\mu(x) S^\dagger(t)|_{x_0=t} \end{aligned} \right.$$

then it follows that

$$(10b) \quad [\bar{\chi}(x), \bar{\chi}(y)]_{x_0=y_0} = 0.$$

Forming the time derivative of $\bar{\chi}$ and using (3), we get immediately:

$$(11a) \quad d_4 \bar{\chi}(x) = S(t) \partial_4 \partial_\mu A_\mu(x) S(t)^\dagger = \partial_4' \chi(x', t)|_{x'_0=t},$$

$$(11b) \quad d_4^2 \bar{\chi}(x) = \partial_4'^2 \chi(x', t)|_{x'_0=t},$$

whence

$$(11c) \quad d_\mu^2 \bar{\chi}(x) = \partial_\mu'^2 \chi(x', t)|_{x'_0=t} = 0.$$

The following commutators also vanish:

$$(12) \quad [\bar{\chi}(x), d_4 \bar{\chi}(y)]_{x_0=y_0} = [d_4 \bar{\chi}(x), d_4 \bar{\chi}(y)]_{x_0=y_0} = 0.$$

The expansion of $\bar{\chi}(x)$ is immediately obtained from (7) by replacing D^+ by D and putting $t = x_0$.

$$(13) \quad \left\{ \begin{aligned} \bar{\chi}(x) &= \hat{c}_\mu A_\mu + L_1(x) + L_2(x) + \dots, \\ L_1(x) &= i^2 e \int_{y_0=t} d^3 y d^4(y' y'' y''') D(x - y''') \bar{\psi}(y') \gamma_4 F(y - y', \dots) \psi(y''), \\ L_2(x) &= e^2 \int_{y_{10}=t_1=y_0}^{x_0} dt_1 d^3 y_1 d^3 y d^4(y'_1 y''_1 y'''_1) d^4(y' y'' y''') D(x - y''') \cdot \\ &\quad \cdot [\bar{\psi}(y'_1) \gamma_\nu F(y_1 - y'_1, \dots) \psi(y''_1) A_\nu(y'''_1), \bar{\psi}(y') \gamma_4 F(y - y', \dots) \psi(y'')]. \end{aligned} \right.$$

We also give here explicitly the expansion for $d_4 \bar{\chi}$:

$$(13') \quad d_4 \bar{\chi}(x) = \partial_4 \hat{c}_\mu A_\mu - Q_4 + e^2 \int_{y_{10}=y_0=t}^t dt_1 d^3 y_1 d^3 y d^4(y'_1 y''_1 y'''_1) d^4(y' y'' y''') \partial_4 D(x - y''') \cdot \\ \cdot [\bar{\psi}(y'_1) \gamma_\nu F(y_1 - y'_1, \dots) \psi(y''_1) A_\nu(y'''_1), \bar{\psi}(y') \gamma_4 F(y - y', \dots) \psi(y'')],$$

where

$$(14) \quad Q_\mu(x) \equiv [\partial_4 A_\mu(x), H] = e \int_{x_0=y_0} d^3 y d^4(y' y'' y''') \partial_4 D(x - y''') \cdot \\ \cdot \bar{\psi}(y') \gamma_\mu F(y - y', \dots) \psi(y'').$$

The notation Q_μ does not imply that Q_μ is a 4-vector. The same applies to

$F_{\mu\nu}$, j_μ , etc., Sections 3, 4. In general such quantities are exact tensors only in the local limit ⁽²⁾.

In the local limit $\partial_4 D(x-y)|_{x_0=y_0} = i\delta^3(\mathbf{x}-\mathbf{y})$ and Q_μ reduces to the local current density j_μ . The e^2 -term of (13) then vanishes. $\bar{\chi}$ itself reduces simply to $\partial_\mu A_\mu$ because $D(x-y)|_{x_0=y_0} = 0$. Thus in the local limit we have the usual relations

$$(14') \quad \begin{cases} \bar{\chi}(x) = \partial_\mu A_\mu(x), \\ d_4 \bar{\chi}(x) = \partial_4 \partial_\mu A_\mu(x) - j_4. \end{cases}$$

2. - The gauge transformation.

We can follow again, rather closely, the pattern of the local theory ⁽³⁾. The main difference will be that the quantities $\partial_\mu A_\mu$ will be replaced by our more complicated $\bar{\chi}$.

We seek a transformation which changes

$$(15) \quad A_\mu(x) \rightarrow A_\mu(x) + \partial_\mu A(x),$$

where A is a c -number. This, as in the local theory, is effected by a canonical transformation $\exp[iG_1]$,

$$(16) \quad iG_1 = \int d^3x \{ A \partial_4 \partial_\mu A_\mu - (\partial_4 A) \partial_\mu A_\mu \},$$

$$(16') \quad \partial_\mu^2 A = 0.$$

Then indeed

$$(17) \quad \exp[iG_1] A_\mu \exp[-iG_1] = A_\mu + [iG_1, A_\mu] + \dots = A_\mu + \partial_\mu A,$$

G_1 is time independent

$$(16'') \quad \partial_4 G_1 = \int d^3x \{ A \partial_4^2 (\partial_\mu A_\mu) - (\partial_4^2 A) \partial_\mu A_\mu \} = \int d^3x A \partial_4^2 (\partial_\mu A_\mu) = 0,$$

using (16') and partial integration. We can then regard G_1 also as the gauge transformation at $t = -\infty$.

⁽²⁾ In part I conditions for the invariance of the S -matrix are given but we refrain from giving similar conditions for the covariance of j_μ etc.

⁽³⁾ Compare J. M. JAUCH and F. ROHRICH. *Theory of Photons and Electrons* (Cambridge, 1955).

We now transform all operators occurring by $\exp [iG_1]$ such that quite generally ($\psi =$ Dirac field)

$$(17') \quad O' = \exp [iG_1] O \exp [-iG_1], \quad A'_\mu = A_\mu + \partial_\mu A, \quad \psi' = \psi.$$

If the Schrödinger equation is to be invariant, the state vector has to be transformed also. To find the transformation we apply $S(t)$, $S(t)^\dagger$ to G_1 . It was shown in the previous section that

$$S(t) \partial_\mu A_\mu(x) S(t)^\dagger = \chi(x, t)$$

and also

$$S(t) \partial_4 \partial_\mu A_\mu(x) S(t)^\dagger|_{x_0=t} = d_4 \bar{\chi}(x).$$

It follows then that

$$(18) \quad iG = S(t) iG_1 S(t)^\dagger = \int d^3x \{ A d_4 \bar{\chi} - (\partial_4 A) \bar{\chi} \}.$$

Similarly

$$(18') \quad \exp [iG] = S(t) \exp [iG_1] S(t)^\dagger.$$

The *total* time derivative of G vanishes

$$(18'') \quad d_4 G = S(t) \partial_4 G_1 S(t)^\dagger = 0.$$

Since G is independent of \mathbf{x} , we can also state

$$(18''') \quad d_i G = 0 \quad (d_i = \partial_i \text{ for } i = 1, 2, 3).$$

From the commutation relations (12) it follows further that

$$(19) \quad [\bar{\chi}(x), G(t)]_{x_0=t} = [d_4 \bar{\chi}(x), G(t)]_{x_0=t} = 0$$

and from (9) also

$$(19') \quad [\chi^+(x', t), G(t)] = 0.$$

If the interaction is switched off at $t = -\infty$,

$$(20) \quad G(-\infty) = G_1.$$

We next define a second transformation G_2 by

$$(21) \quad \exp [iG_2] = \exp [iG] \exp [-iG_1],$$

G and G_1 do not in general commute. It is now G_2 , by which the state vector

is transformed:

$$(22) \quad \Psi' = \exp[-iG_2]\Psi.$$

We now show that the Schrödinger equation remains invariant, if (i) the operators are transformed according to (17') and (ii) the state vector according to (22). We have

$$\begin{aligned} i\dot{\Psi}' &= i\left(\frac{\partial}{\partial t} \exp[-iG_2]\Psi\right) = i\left(\frac{\partial}{\partial t} \exp[-iG_2]\right)\Psi + \exp[-iG_2](i\dot{\Psi}) = \\ &= i\left(\frac{\partial}{\partial t} \exp[-iG_2]\right) \exp[iG_2]\Psi' + \exp[-iG_2]H \exp[iG_2]\Psi' \equiv H'\Psi', \end{aligned}$$

where H' is so far defined as factor of Ψ' . Since

$$\partial_t G_1 = 0,$$

$$\left(\frac{\partial}{\partial t} \exp[-iG_2]\right) \exp[iG_2] = \exp[iG_1] \left(\frac{\partial}{\partial t} \exp[-iG]\right) \exp[iG] \exp[-iG_1].$$

We thus have

$$\begin{aligned} H' &= \exp[iG_1] \left(\frac{\partial}{\partial t} i \exp[-iG]\right) \exp[iG] \exp[-iG_1] + \exp[-iG_2]H \exp[iG_2] = \\ &= \exp[iG_1] \left\{ \left(\frac{\partial}{\partial t} i \exp[-iG]\right) \exp[iG] + \exp[-iG]H \exp[iG] \right\} \exp[-iG_1]. \end{aligned}$$

Now, by expansion of the exponentials, and combining $\partial G/\partial t$ with the commutator $[G, H]$, (which leads to $d_4 G = 0$) it is easily seen that the {...} reduces to H itself.

Thus

$$H' = \exp[iG_1]H \exp[-iG_1] = H(A_\mu + \partial_\mu A).$$

This is just the transformation of the operators stated above. Thus we have shown that the Schrödinger equation is invariant under the above transformation.

In the local limit $\bar{\chi} = \partial_\mu A_\mu$, and as G differs from G_1 only in that $\partial_4 \bar{\chi}$ is replaced by $d_4 \bar{\chi}$,

$$(23) \quad iG - iG_1 = -\int d^3x A[\bar{\chi}, H] = -\int d^3x A \bar{\psi} \gamma_4 \psi = iG_2.$$

The right hand side commutes with G_1 (because G_1 does not contain ψ). In the non-local case G_1 and G_2 , however, do not commute.

If an operator O commutes with G , its expectation value is gauge invariant.

$$(24) \quad \left\{ \begin{aligned} \langle 0 \rangle' &= \langle \Psi'^* O \Psi' \rangle = \langle \Psi^* \exp [iG_2] \exp [iG_1] O \exp [-iG_1] \exp [-iG_2] \Psi \rangle \\ &= \langle \Psi^* \exp [iG] O \exp [-iG] \Psi \rangle = \langle \Psi^* O \Psi \rangle . \end{aligned} \right.$$

Of course $\langle O \rangle$ may be gauge invariant without O commuting with G . For example if $O = O_1 + O_2$ where $[O_1, G] = 0$ and $\langle O_2 \rangle = 0$ ($[O_2, G] \neq 0$) then $\langle O \rangle$ is also gauge invariant.

The above proof of invariance of the Schrödinger equation is quite independent of the form of H . Any Hamiltonian $H(\psi, \bar{\psi}, A_\mu)$ leads to a gauge invariant Schrödinger equation, in agreement with the general considerations of Part I. This does not mean that quantities like the S -matrix are gauge invariant. For this purpose additional requirements have to be fulfilled.

The Lorentz condition $\chi^+(x', t) \Psi(t) = 0$ is gauge invariant. With

$$\chi^{+'} = \exp [iG_1] \chi^+(x', t) \exp [-iG_1], \quad \Psi'(t) = \exp [-iG_2] \Psi(t)$$

(G_1 is independent of t) we have on account of (19')

$$(25) \quad \chi^{+'} \Psi' = \exp [iG_1] \chi^+(x', t) \exp [-iG] \Psi = \exp [iG_1] \exp [-iG] \chi^+ \Psi = 0 .$$

We consider now the condition under which the S -matrix is invariant. We define, as usual

$$(26) \quad S = S(\infty), \quad \Psi(t) = S(t) \Psi(-\infty) .$$

Let $\psi(-\infty)$ be a definite state (element of \mathcal{H}) Ψ_k , say, before the interaction is switched on, so that $\exp [-iG_2] \Psi(-\infty) = \Psi(-\infty)$ (on account of (20) $G_2(-\infty) = 0$). The transformed equation to (26) reads then

$$(26') \quad \exp [-iG_2(\infty)] \Psi(\infty) = S' \psi(-\infty) = S' \Psi_k ,$$

$\Psi(-\infty)$ is a definite state Ψ_k ($\Psi(t)$ is the solution with the initial condition $\Psi(-\infty) = \Psi_k$). What is required, if we say that S is invariant, is that the elements of S between two definite states should be invariant, i.e.

$$(27) \quad S_{ik} = \langle \Psi_i^* S(\infty) \Psi_k \rangle = S'_{ik} .$$

This means now that

$$(27') \quad \langle \Psi_i^* \exp [-iG_2(\infty)] \Psi(\infty) \rangle = \langle \Psi_i^* \Psi(\infty) \rangle .$$

It follows that

$$(28) \quad G_2(\infty) = 0$$

is a sufficient and probably necessary condition for the invariance of *all* the S -matrix elements. In the local theory, G_2 is given by (23). (28) can be considered as fulfilled if the interaction is switched off at $t = +\infty$, or if the fields are represented by wave packets well separated at $t = +\infty$, so that no interaction takes place. In the non-local theory (28) is not so easily fulfilled, in fact it is definitely not fulfilled for certain choices of the form factor. (28), of course, corresponds to the general condition (13) of Part I.

3. - Field strengths.

The chief property of the field strengths, making them the basic quantities in classical theory is their gauge invariance. In quantum theory, local case, (here $[A_\mu, H] = 0$, therefore $d_\mu A_\nu = \partial_\mu A_\nu$)

$$(29) \quad \overset{(0)}{F}_{\mu\nu} = \partial_\mu A_\nu - \partial_\nu A_\mu$$

commutes with G_1 , so that $\exp[iG_1] \overset{(0)}{F}_{\mu\nu} \exp[-iG_1] = \overset{(0)}{F}_{\mu\nu}$ (∂_ν also commutes with G_1 , see (18'''). $\overset{(0)}{F}_{\mu\nu}$ also commutes with G_2 (which in the local theory is given by (23)) and hence with G so that the expectation value $\langle \overset{(0)}{F}_{\mu\nu} \rangle$ is gauge invariant.

In our non local theory these simple connexions cannot be maintained. It is still true that $\overset{(0)}{F}_{\mu\nu}$ commutes with G_1 because G_1 is the same as in local theory but it is no longer true that $\overset{(0)}{F}_{\mu\nu}$ commutes with G , because $\bar{\chi}$ is a complicated expression (see Section 1), and G_2 no longer commutes with G_1 . Thus $\langle \overset{(0)}{F}_{\mu\nu} \rangle$ is not gauge invariant.

We can, however, obtain gauge invariant quantities which we shall call « field strengths » by generalizing the connexion (29) between potentials and field strengths. We shall need these gauge invariant field strenghts to define the current density later.

It is true that in this way we assign a more prominent rôle to the potentials than that of the mere auxiliary aids to calculation which they are in classical theory. However, this is already the case to some extent in local quantum electrodynamics which can hardly be formulated in a simple manner in terms of the field strengths alone ⁽⁴⁾.

⁽⁴⁾ For example the gauge transformations one considers there only change A_μ within the Lorentz gauge and usually by a c -number. A transformation changing the operators A_μ to the *full* extent to which they could be changed in classical theory, has never — to our knowledge — been formulated.

We put

$$(30) \quad F_{\mu\nu} = \overset{(0)}{F}_{\mu\nu} + \overset{(1)}{F}_{\mu\nu} + \overset{(2)}{F}_{\mu\nu} + \dots,$$

which may be regarded as an expansion in e , similar to the expansions of χ in Section 1. We make the following demands on $F_{\mu\nu}$:

$$(31) \quad F_{\mu\nu} = -F_{\nu\mu},$$

$$(31') \quad d_\mu F_{\nu\lambda} + d_\nu F_{\lambda\mu} + d_\lambda F_{\mu\nu} = 0.$$

Thus we demand the validity of one set of Maxwell's equations as operator equations, (as in local theory). The gauge invariance of $F_{\mu\nu}$ means

$$(31'') \quad \exp[iG]F_{\mu\nu}\exp[-iG] = F_{\mu\nu}.$$

This secures the invariance of $\langle F_{\mu\nu} \rangle$. In the local case we must, of course, obtain $\overset{(0)}{F}_{\mu\nu}$, so that $\overset{(1)}{F}_{\mu\nu}$, etc., vanish in the local limit. There is no need to demand that $F_{\mu\nu}$ should commute with G_1 , all that is wanted is the invariance of $\langle F_{\mu\nu} \rangle$.

From (31') it follows that $F_{\mu\nu}$ can be represented in the form

$$(31''') \quad F_{\mu\nu} = d_\mu \alpha_\nu - d_\nu \alpha_\mu$$

(note that $[d_\mu, d_\nu] = 0$). Thus generalized potentials α_μ exist, of which $F_{\mu\nu}$ are the *usual* derivatives. Our problem reduces to find

$$(32) \quad \alpha_\mu = A_\mu + \overset{(1)}{\alpha}_\mu + \overset{(2)}{\alpha}_\mu + \dots$$

On account of $[d_\nu G] = 0$ (eq. (18''')), (31') is fulfilled if

$$(33) \quad \exp[iG]\alpha_\nu\exp[-iG] = \alpha_\nu + \partial_\nu A$$

or

$$(33') \quad [iG, \alpha_\nu] = \partial_\nu A.$$

Since $\bar{\chi}$ is given by the expansion (13), G is likewise expanded

$$(34) \quad G = \overset{(0)}{G} + \overset{(1)}{G} + \overset{(2)}{G} + \dots,$$

with

$$i\overset{(0)}{G} = \int d^3x \{A \partial_4 (\partial_\mu A_\mu) - \partial_4 A (\partial_\mu A_\mu)\} = iG_1$$

Consequently

$$(34') \quad [i\overset{(0)}{G}, \overset{(0)}{\alpha}_\nu] = [iG_1, A_\nu] = \hat{c}_\nu A.$$

Hence (33) splits up into

$$(35_1) \quad [\overset{(1)}{G}, A_\nu] + [\overset{(0)}{G}, \overset{(1)}{\alpha}_\nu] = 0,$$

$$(35_2) \quad [\overset{(2)}{G}, A_\nu] + [\overset{(1)}{G}, \overset{(1)}{\alpha}_\nu] + [\overset{(0)}{G}, \overset{(2)}{\alpha}_\nu] = 0,$$

.

These are equations from which $\overset{(1)}{\alpha}, \overset{(2)}{\alpha}, \dots$ etc., can be determined successively.

We discuss the existence of solutions of these equations a little further for the case where F commutes with $\bar{\psi}, \psi, A_\mu$. L_1 does not contain A so that the first term of (35₁) vanishes. We can then put $\overset{(1)}{\alpha}_\nu = 0$. This is not really necessary: $\overset{(0)}{G}$ does not contain the electron-field and therefore any function of $\psi, \bar{\psi}$ would solve (35₁) for $\overset{(1)}{\alpha}$. Thus it is clear that the solutions of (35) cannot be unambiguous. However, our purpose is merely to show, that solutions exist. We therefore put $\overset{(1)}{\alpha}_\nu = 0$, and then we have to solve

$$(35') \quad [\overset{(0)}{G}, \overset{(2)}{\alpha}_\nu] = -[\overset{(2)}{G}_2, A_\nu].$$

$\overset{(0)}{G}$ is independent of ψ and linear in A . $\overset{(2)}{G}$ is also linear in A . $[\overset{(2)}{G}, A_\mu]$ depends on $\psi, \bar{\psi}$ only. We can therefore put $\overset{(2)}{\alpha}_\nu$ also linear in A , for example

$$\overset{(2)}{\alpha}_\nu(x) = \int_{y_0=x_0} d^3y X_{\nu 0}(x, y) A_0(y),$$

where X is an operator composed of ψ and $\bar{\psi}$ but independent of A .

We obtain an integral equation for X . A closer analysis of this shows that it always has solutions. For example, a solution for $\overset{(2)}{\alpha}_\nu$ can be given explicitly. We introduce the singular function D_σ defined by

$$D_4 = D, \quad \partial_j D_j = \partial_4 D$$

or

$$D_\sigma(y) = \frac{1}{(2\pi)^3} \int d^4k \exp [iky] (-1)^{\delta_{04}} \frac{k_\sigma}{k_0} \delta(k^2) \varepsilon(k_0).$$

Let us further, for simplicity, assume that

$$F(x-x', \dots) = G(x-x', x-x'') \delta^4(x-x''')$$

and let therefore

$$Q_v(x) = ie \int d^4(x'x'') \bar{\psi}(x') \gamma_v \psi(x'') G(x - x', x - x''),$$

then X is found to be

$$X_{v\sigma}(x, y) = i \int_{y_1=y_2=0}^{x_0} d^4y_1 d^4y_2 D(x - y_1) D_\sigma(y - y_2) [Q_v(y_1), Q_\sigma(y_2)].$$

This is stated without derivation merely to show that solutions for $\alpha_v^{(2)}$ exist. We shall not make explicit use of the solution.

4. - Current density.

A divergence-free and gauge invariant current density can be found with the help of the field strengths and the second set of Maxwell's equations. We first define a « current density » J_v by

$$(36) \quad d_\mu F_{\mu\nu} = -J_\nu.$$

From $F_{\mu\nu} = -F_{\nu\mu}$ and $[d_\mu, d_\nu] = 0$ it follows at once that

$$(36') \quad d_\nu J_\nu = 0.$$

This J_v , however, which also exists in local theory, is not the usual current. In the zero'th approximation ($F = \overset{(0)}{E}$, local theory) it is a quantity depending on A and not on the electron field. We therefore next define

$$(37) \quad j_\nu = J_\nu - d_\nu \bar{\chi}.$$

From $d_\nu^2 \bar{\chi} = 0$ (11c) it follows that also j_ν is divergence free

$$(37') \quad d_\nu j_\nu = 0.$$

Both J_v and j_v commute with G and have therefore gauge invariant expectation values. This follows immediately from $[d_\nu, G] = 0$, $[F_{\mu\nu}, G] = 0$ and $[\bar{\chi}, G] = 0$

$$(37'') \quad [J_\nu, G] = [j_\nu, G] = 0,$$

j_ν is the generalization of the usual Dirac-current, as will be seen presently. We first remark that, on account of the Lorentz condition $\langle \chi \rangle = 0$, the expectation values of J_ν and j_ν are the same and Maxwell's second set of equations are satisfied as relations between expectation values ⁽⁵⁾

$$(38) \quad J_\mu = \langle j_\mu \rangle, \quad \partial_\mu F_{\mu\nu} = -\langle j_\nu \rangle$$

(note that $\langle d_\mu \cdot \rangle = \partial_\mu \langle \cdot \rangle$).

We can expand j_ν in the same manner as $F_{\mu\nu}$ and $\bar{\chi}$. With the expansion (13) for $\bar{\chi}$ and $F_{\mu\nu}$ (30) we obtain

$$(39a) \quad j_i = Q_i - \partial_i P_4 - \partial_\mu (F_{\mu i}^{(1)} + F_{\mu i}^{(2)} + \dots) + \\ + [F_{4i}^{(1)} + F_{4i}^{(2)} + \dots, H] - \partial_i [L^{(1)} + L^{(2)} + \dots],$$

$$(39b) \quad j_4 = Q_4 - \partial_i P_i - \partial_i (F_{i4}^{(1)} + F_{i4}^{(2)} + \dots) + [L^{(2)} + \dots, H] - \partial_4 [L^{(2)} + \dots],$$

where

$$(39') \quad Q_\mu = [\partial_4 A_\mu, H], \quad P_\mu = [A_\mu, H]$$

(we have used, of course, $\partial_\mu^2 A_\nu = 0$).

In the local limit $L^{(1)} = F_{\mu\nu}^{(1)} = \dots = 0$. Furthermore $P_\mu \rightarrow 0$ (as A_μ commutes with H at the same time), and Q_μ reduces to the usual Dirac current

$$(39'') \quad Q_\mu(x) \rightarrow ie \bar{\psi}(x) \gamma_\mu \psi(x).$$

Thus (37) is the generalization of the Dirac current. It follows, of course, from (37') that

$$(40) \quad d_4 \int j_4 d^3x = 0.$$

Thus $\int j_0 d^3x$ is the total charge integral.

For the remainder of this section we assume that F commutes with $\bar{\psi}$, ψ , A_μ . For this case we have already shown in Part I that the total charge of the local theory $e \int \bar{\psi} \gamma_4 \psi d^3x$ is an integral also in the non-local case. We shall now show that without further specification of F

$$(41) \quad Q \equiv \int j_0 d^3x = Q_D \equiv e \int \bar{\psi} \gamma_4 \psi d^3x.$$

⁽⁵⁾ Expectation values need here only be regarded as averaged over longitudinal and scalar photon variables but need not concern other variables.

In fact Q will reduce to the integral of our Q_0 which then reduces to Q_D . If F commutes with A_μ , Q_ν is given explicitly by

$$(42) \quad Q_\nu = e \int_{x_0=y_0} \bar{\psi}(x') \gamma_\nu F(x-x', \dots) \partial_4 D(y-x'') \psi(x'') d^3x d^4(x'x''x''').$$

First it is easy to show that

$$(42') \quad \partial_\nu Q_\nu = 0.$$

For this purpose one shifts the differentiation on x''' , hence on F (note that in the term $\partial_4 Q_4$ also F has to be differentiated with respect to $x_0 = y_0$) and uses $(\partial'_\mu + \partial''_\mu) \bar{\psi}(x') \gamma_\mu \psi(x'') = 0$. Several partial integrations lead to (42'). It follows that

$$(43) \quad \partial_4 \int Q_4 d^3x = 0.$$

We next show that $\hat{Q} - \int Q_0 d^3x$ is identical with Q_D . We know, of course, that as a consequence of the Dirac equations valid in interaction representation $\partial_4 Q_D = 0$. Hence $\hat{Q} - Q_D = \text{constant}$. We then form the time integral $\int dy_4 (\hat{Q} - Q_D) \equiv I$. If I can be shown to vanish, $\hat{Q} - Q_D$ must vanish because the integrand is constant and the time integral can only vanish if this constant is zero. Now

$$\int dy_4 \hat{Q} = e \int_{x_0=y_0} \bar{\psi}(x') \gamma_4 \psi(x'') \partial_4 D(y-x''') F(x-x', \dots) d^3x d^4y d^4(x'x''x''').$$

From the properties of the D -function it follows that

$$(44) \quad \int \partial_4 D(y-x''') d^3y = 1$$

and since $x_0 = y_0$

$$\int dy_4 \hat{Q} = e \int \bar{\psi}(x') \gamma_4 \psi(x'') F(x-x', \dots) d^4x d^4(x'x''x''').$$

We use now the essential normalization property of F discussed in Part I,

$$(45) \quad \int F(x-x', \dots) d^4x d^4x''' = \delta^4(x'-x''),$$

and obtain therefore

$$\int dy_4 \hat{Q} = e \int \bar{\psi}(x) \gamma_4 \psi(x) d^4x = \int dx_4 Q_D.$$

Hence $I = 0$ and

$$(46) \quad \int Q_0 d^3x = e \int \bar{\psi}(x) \gamma_4 \psi(x) d^3x \equiv Q_D.$$

It remains to show that the further terms of (39b) give no contribution to the space integral. The spatial divergences $\partial_i P_i$ and $\partial_i (\overset{(1)}{F}_{i4} + \dots)$, of course, vanish. What we have therefore to show is that

$$\int d_4(L^{(2)} + \dots) d^3x = 0.$$

$d_4 L^{(2)}$ is given by the last term (written explicitly) of (13'). For the space integration we can use (44) again. The second factor in the commutator of (13') is then identical with \hat{Q} :

$$e \int \bar{\psi}(y') \gamma_4 \psi(y'') F(y - y', \dots) d^4(y' y'' y''') d^3y = \hat{Q}.$$

We have, however, proved above that $\hat{Q} = Q_D = e \int \bar{\psi}(y) \gamma_4 \psi(y) d^3y$ which is independent of y_0 . We have also proved in Part I that Q_D commutes with H . Thus the commutator in (13') vanishes. Similar considerations apply to higher orders.

We have thus proved that

$$(47) \quad Q = \int j_0 d^3x = Q_D = e \int \bar{\psi}(x) \gamma_4 \psi(x) d^3x.$$

For this theorem to hold it has only been assumed that F commutes with $\bar{\psi}$, ψ , A_μ and satisfies (44).

With the total charge given simply by the Dirac expression, it follows also that

$$(48) \quad [Q, \psi] = -e\psi, \quad [Q, \bar{\psi}] = e\bar{\psi},$$

the usual commutation relations. Q is, of course, as in the local theory, Lorentz-invariant.

5. - Energy momentum vector.

In the local theory the so-called canonical energy-momentum tensor is given by

$$(49) \quad T_{\mu\nu}^{(0)} = \frac{1}{2} (\bar{\psi} \gamma_\nu \partial_\mu \psi - (\partial_\mu \bar{\psi}) \gamma_\nu \psi) - \frac{1}{2} \delta_{\mu\nu} (\bar{\psi} \gamma_\lambda \partial_\lambda \psi - (\partial_\lambda \bar{\psi}) \gamma_\lambda \psi) - \\ - \delta_{\mu\nu} \bar{\psi} m \psi + \partial_\mu A_\lambda \partial_\nu A_\lambda - \frac{1}{2} \delta_{\mu\nu} \partial_\lambda A_\sigma \partial_\lambda A_\sigma.$$

$T_{\mu\nu}^{(0)}$ is neither symmetrical nor gauge invariant. We use this tensor first to define the zero order of the energy momentum vector

$$(50) \quad i P_\mu^{(0)} = \int d^3x T_{\mu 4}^{(0)}(x).$$

Since

$$(51) \quad \partial_\nu T_{\mu\nu}^{(0)} = 0,$$

on account of the wave equations (this is independent of H , therefore also valid in the non local case) it follows that

$$(52) \quad \partial_4 P_\mu^{(0)} = 0,$$

$P_4^{(0)}$ is in fact nothing but the Hamiltonian of the free fields H_0 .

It also follows that

$$(53) \quad i[A(x) P_\nu^{(0)}] = \partial_\nu A(x),$$

$$(54) \quad i[\psi(x) P_\nu^{(0)}] = \partial_\nu \psi(x).$$

The conservation of P_ν requires of course $d_4 P_\nu = 0$ and not (52). For this purpose we consider the commutator $i[H, P_\nu^{(0)}]$.

Because of the translational invariance of $F(x - x', x - x'', \dots)$ the derivatives of $A_\mu(x'')$, $\bar{\psi}(x')$, $\psi(x'')$ can be shifted under the integral on F as a derivative with respect to the variable x . For the same reason we may well make the assumption that $P_\nu^{(0)}$ commutes with F . Then it follows that (*)

$$(55) \quad i[H P_\nu^{(0)}] = \delta_{\nu 4} \partial_4 H.$$

Hence it follows that our energy-momentum vector is

$$(56) \quad P_\nu = P_\nu^{(0)} + i \delta_{\nu 4} H,$$

(*) In (55) the time factor due to the adiabatic switching on at $t = -\infty$ is not differentiated. (55) is valid only after the interaction is fully switched on.

and satisfies

$$(56') \quad d_4 P_\nu = 0.$$

Thus, there is no difference between the local and non-local cases, except, of course, that H is different. If we could interpret P_ν as energy and momentum we would find the Hamiltonian to be the energy. However, this is not so simple now. P_ν arises from the canonical tensor and is not gauge invariant. In the local theory one can go over to a gauge invariant vector (also to a corresponding energy-momentum tensor) by adding to P_ν another vector θ_ν such that

$$(57) \quad \langle \theta_\nu \rangle = 0$$

and such that $P_\nu^\theta = P_\nu + \theta_\nu$ is gauge invariant and $\partial_4 \langle P_\nu^\theta \rangle = 0$. (The expectation value $\langle \rangle$, of course, only refers to longitudinal and scalar photons.) It follows then that $\langle P_\nu^\theta \rangle = \langle P_\nu \rangle$ is gauge invariant. The existence of such a θ_ν hinges on the fact that the expectation value $\langle P_\nu \rangle$ is gauge invariant although P_ν is not. In the non-local theory this is not so simple. It is not always possible to find a corresponding θ_ν . The gauge invariance of $\langle P_\nu \rangle$ imposes a condition, similar to that for the invariance of S , which we now derive. The question is relevant to P_1 only, because P_i derives directly from the free fields and is gauge invariant.

Consider the expectation value of P_4 , formed with $\Psi(t)$. As we are not interested in the H_0 part of P_4 but only in the radiative corrections we consider the radiative corrections to P_4

$$(58) \quad X = \langle \Psi^*(t) P_4 \Psi(t) \rangle - \langle \Psi^*(-T) H_0 \Psi(-T) \rangle \equiv \langle t | P_4 | t \rangle - \langle -T | H_0 | -T \rangle.$$

We now introduce a change of gauge, and we denote the change of (58) due to it by ΔX . According to Section 2 this is given by (note that at $t = -\infty$, $G \rightarrow G_1$)

$$(58') \quad \Delta X = \langle t | \exp [iG] P_4 \exp [-iG] - P_4 | t \rangle - \\ - \langle -T | \exp [iG_1] H_0 \exp [-iG_1] - H_0 | -T \rangle.$$

Using $|t\rangle = S(t)|-T\rangle$ and (18') we obtain

$$(59) \quad \left\{ \begin{aligned} \Delta X &= \langle -T | \exp [iG_1] S^\dagger(t) P_4 S(t) \exp [-iG_1] - S^\dagger(t) P_4 S(t) | -T \rangle - \\ &\quad - \langle -T | \exp [iG_1] H_0 \exp [-iG_1] - H_0 | -T \rangle = \\ &= \langle -T | \exp [iG_1] \{ S^\dagger(t) P_4 S(t) - H_0 \} \exp [-iG_1] - \\ &\quad - \{ S^\dagger(t) P_4 S(t) - H_0 \} | -T \rangle. \end{aligned} \right.$$

We now make use of the following theorem:

If $|k\rangle$ is any free field state then ⁽⁷⁾

$$(60) \quad \langle k | S^\dagger(t) P_4 S(t) - H_0 | k \rangle = \lim_{T \rightarrow \infty} \frac{i}{2T} \langle k | S(T) - S^\dagger(T) | k \rangle = \\ = \lim_{T \rightarrow \infty} \frac{i}{T} \langle k | S(T) - 1 | k \rangle .$$

At the time t the interaction is fully switched on. The left hand side is, however, independent of t . On the right $S(T) - S^\dagger(T)$ taken between two equal states (and again calculated with a switch-on) is proportional to T for large T which just cancels the $1/T$ written explicitly. (Note that $\langle k | S(T) - 1 | k \rangle$ is pure imaginary). The theorem holds for any interaction H and only presupposes the usual expansion of S in terms of H . It states essentially that the self-energy (left hand side) is given by the diagonal elements of the S -matrix. The states $|-T\rangle$ and $\exp[-iG_1] |-T\rangle$ both qualify as free field states. Thus (59) becomes

$$(61) \quad \Delta X = \frac{i}{T} \langle -T | \exp[iG_1](S-1) \exp[-iG_1] - (S-1) | -T \rangle = \\ = \frac{i}{T} \langle -T | \exp[iG_1] S \exp[-iG_1] - S | -T \rangle .$$

This can still be written in another form. Consider the quantity

$$(62) \quad \begin{cases} Y(t) = \exp[iG_1] S(t) \exp[-iG_1] - \exp[iG_2(t)] S(t) , \\ \quad = \exp[iG_1] (S(t) - \exp[iG(t)] S(t) \exp[iG_1]) \exp[-iG_1] . \end{cases}$$

(G_1 is independent of t). Using $i\dot{S}(t) = H S(t)$ and $d_t \exp[iG] = 0$ it appears that

$$(63) \quad i \frac{\partial Y}{\partial t} = \exp[iG_1] H \exp[-iG_1] Y ,$$

obviously $Y(-\infty) = 0$, because $S(-\infty) = 1$ and $\langle G_2(-\infty) \rangle = 0$. The only solution of (63) with the initial condition $Y(-\infty) = 0$ is $Y(t) = 0$ at all times. Inserting this for $t = +T \rightarrow \infty$ in (61) we find

$$(64) \quad \Delta X = \lim_{T \rightarrow \infty} \frac{1}{T} \langle -T | \exp[iG_2(T)] S - S | -T \rangle .$$

In Section 2 we have seen that a general condition for all S -matrix elements to be gauge invariant is $G_2(+\infty) = 0$. This condition is therefore also sufficient to make $\Delta X = 0$ or to make $\langle P_4 \rangle$ gauge invariant. (64) may, however,

(7) The proof of (60) is straightforward but very lengthy. In energy representation the essentials of it are given in H. UMEZAWA: *Quantum Theory of Fields* (Amsterdam, 1956), pp. 220-222.

be somewhat less restrictive than $G_2(+\infty) = 0$. If $G_2(\infty) = 0$ one can show that we can put

$$(65) \quad i\theta_v = \int d^3x (\alpha_v d_4 \bar{\chi} - (\partial_4 \alpha_v) \bar{\chi} + \frac{1}{2} \delta_{v4} \bar{\chi}^2) .$$

If $\Delta X \neq 0$ then it is impossible that $\langle P_4 \rangle$ is gauge invariant, and no θ_v with $\langle \theta_v \rangle = 0$ exists such that $\langle P_v^\theta \rangle = \langle P_v \rangle$ is gauge invariant. One may perhaps drop the condition $\langle \theta_v \rangle = 0$ and merely demand $\hat{c}_4 \langle \theta_v \rangle = 0$. In this case one can see that *many possibilities* exist, and therefore a variety of P_v^θ exist, all satisfying $\langle d_v P_v^\theta \rangle = 0$, and P_v^θ is gauge invariant. We may interpret P_v^θ as the proper (gauge invariant) energy-momentum, but the Hamiltonian would be a different quantity and $H_0 + H$ (although conserved) would not be identical with the total energy. The possibilities have not been fully investigated yet.

6. - Discussion.

The purpose of this work was to create a frame work for a theory which embodies the possibility of convergence. In a recent note (ref. (3) Part I) a special form factor has been suggested which fulfils at least the requirements of convergence, namely:

$$(66) \quad \begin{cases} F(x - x', x - x'', x - x''') = G(x - x', x - x'') \delta^4(x - x''') , \\ G(x, y) = \int \varrho(p, q) \exp [i(px - qy)] d^4p d^4q , \\ \varrho(p, q) = \varrho[-p^2 q^2 + (pq)^2] . \end{cases}$$

If for ϱ (of the one argument $p^2 q^2 - (pq)^2$) a function is chosen that decreases suitably with the argument, for example $\lambda/(\lambda - p^2 q^2 \pm (pq)^2)$, it can be shown that the theory converges throughout (8). So at least the possibility of convergence exists.

This in itself is an encouraging fact, because so far no convergent field theory exists, which contains as a limiting case the usual local theory in the relativistic region. (65) is C , P , T invariant separately, leads to a hermitian H and is a generalization of the extended source model. For if $p = 0$, the argument of ϱ reduces to $p_0^2 q^2 - m^2 q^2$ thus leading to a 3-dimensional cut-off of q . (65) itself is Lorentz-invariant. Consequently the first order of perturbation theory is still Lorentz-invariant, but the results, of course, show a departure from the predictions of the local theory at high energies. However, this form factor does not fulfil the conditions of (i) Lorentz-invariance of the

(8) Cfr. a separate paper by O'R., to be published.

S -matrix (Part I, eq. (19)) or of (ii) gauge invariance of the S -matrix (eq. (28)). The violation of both, of course, is restricted to the inside of the source (*i.e.* to higher than the first orders and to the radiative corrections). The lack of exact Lorentz-invariance can, at present hardly be said to be in contradiction with the experimental facts (cf. the introduction to Part I), because no sufficiently accurate tests are available. The violation of gauge invariance is more serious, especially when an external field is present⁽⁹⁾. On the other hand, it seems possible to have at least a gauge invariant energy-momentum P_ν^0 (Section 5) which would enable one to treat static problems like self-energies, etc. But a variety of possibilities exist and so far this problem is ambiguous.

The form factor (65) is certainly not the only one that secures convergence. It remains to be seen whether other convergent form factors exist (possibly q -number form factors) which at the same time lead to a more satisfactory aspect of the problem of gauge invariance and possibly also of Lorentz-invariance.

* * *

One of us (L. O'R.) would like to thank the Swiss National Fonds for a research grant, and one of us (E.A.) thanks the same Institution for financial aid while temporarily in Zürich. We wish to thank Professors TOLHOEK and JÁNOSSY for interesting discussions.

⁽⁹⁾ For virtual fields one may even go as far as to visualize the possibility of assigning an absolute rôle to the potentials inside the particles. Even in local quantum electrodynamics the potentials seem far more important — and almost unavoidable — than in classical theory (compare the remarks in Sect. 3).

RIASSUNTO (*)

La teoria generale della I parte viene qui formulata per il caso della elettrodinamica quantistica. La condizione di Lorentz, la trasformazione di gauge, la connessione fra potenziale e intensità di campo (gauge invariante), e la densità di corrente (priva di divergenza) j_μ , richiedono tutte generalizzazioni, che vengono esposte. Si dimostra che l'equazione di Schrödinger è gauge invariante e si deriva la condizione per l'invarianza di gauge della matrice S . Dappertutto il fattore di forma è lasciato indefinito. Si dimostra che l'integrale spaziale di j_0 si riduce alla carica totale ordinaria (se il fattore di forma commuta con gli operatori di campo). Il vettore canonico energia-momento è formalmente lo stesso che nella teoria locale (la differenza sta nel diverso Hamiltoniano). Si discutono le possibilità di ottenere un vettore energia-momento gauge invariante.

(*) Traduzione a cura della Redazione.

The Lagrange Function in a General Problem.

M. BORNEAS

Physical Laboratory of the Polytechnic Institute - Timișoara

(ricevuto il 21 Gennaio 1960)

Summary. — A general formalism, based upon the use of a Lagrange function with n -order derivatives with respect to σ independent variables, is presented.

The development of field theory starting from the variational principle has become very widespread. For this aim one chooses Lagrange functions of appropriate forms, in which various physical magnitudes are considered as generalized co-ordinates, and space-time co-ordinates as independent variables. These functions generally contain first-order derivatives, with few exceptions. For instance BOPP ⁽¹⁾ introduces into the Lagrange function second-order derivatives of the potentials.

In the present paper we shall develop a formalism based on a Lagrange function containing n -order derivatives with respect to σ independent variables. This represents a further generalization of the Lagrange function formerly introduced by us ⁽²⁾, containing time-derivatives of the co-ordinates up to s -th order: thus we have established the fundamental equations of a generalized Lagrangian mechanics. With the help of the function now introduced we shall go beyond the domain of mechanics.

For convenience we shall make first some notations.

The n -th order derivative of q_k with respect to the independent variables

⁽¹⁾ F. BOPP: *Ann. d. Phys.*, **38**, 345 (1940).

⁽²⁾ M. BORNEAS: *Amer. Journ. Phys.*, **27**, 265 (1959).

can be written in the general form as follows

$$\underbrace{\hat{c}^n q_k / \partial x_\lambda \partial x_\mu \dots}_{(n)} = q_{k'\lambda\dots}^{(n)}$$

where λ, μ, \dots take all values from 1 to σ .

We shall denote

$$\underbrace{\int \int \dots \int}_{(\sigma)} = \int_{(\sigma)}; \quad \underbrace{\sum_{\lambda=0}^{\sigma} \sum_{\mu=0}^{\sigma} \dots}_{(n)} = \sum_{(n)};$$

$$\partial L / \partial q_{k'\lambda\dots}^{(n)} = L_{,k(n[\lambda\dots])}; \quad \partial L / \partial x_\pi = L_{,\pi}.$$

We shall write the n -th order derivative of a magnitude M_q with respect to x_λ, x_μ, \dots (also by the intermediation of other variables depending on x_λ, x_μ, \dots , if there are any)

$$D_{\lambda\mu\dots}^n M_q = M_q^{(n;\lambda\dots)}.$$

We shall not indicate the limits of integrals, and we shall not write the sign for summation over k , this being understood when k appears twice.

Consider now the function

$$(1) \quad L = L(x_1, \dots, x_\lambda, \dots, q_{k'\lambda\dots}^{(n)}, \dots) \quad (\lambda = 1, 2, \dots, \sigma; k = 1, 2, \dots, r; n = 0, 1, \dots, s).$$

The variational principle can be written

$$(2) \quad \delta \int_{(\sigma)} L dx_1 \dots dx_\lambda \dots = \int_{(\sigma)} \sum_{n=0}^s \sum_{(n)} \lambda_{,n} L_{,k(n[\lambda\dots])} \delta q_{k'\lambda\dots}^{(n)} dx_1 \dots dx_\lambda \dots = 0.$$

This leads to the Euler-Lagrange equations for our case. We integrate with respect to x_λ the general term

$$\int_{(\sigma)} L_{,k(n[\lambda\dots])} \delta q_{k'\lambda\dots}^{(n)} dx_1 \dots dx_\lambda \dots = \int_{(\sigma)} L_{,k(n[\lambda\dots])} D_\lambda \delta q_{k'\mu\dots}^{(n-1)} dx_1 \dots dx_\lambda \dots,$$

and, knowing that the integrated part becomes zero at limits, we obtain the integral

$$\int_{(\sigma-1)} \left[- \int_{(1;\lambda)} L_{,k(n[\lambda\dots])} \delta q_{k'\mu\dots}^{(n-1)} dx_\lambda \right] dx_1 \dots dx_{\lambda-1} dx_{\lambda+1} \dots$$

This can be also transformed as before. Continuing in the same manner we come at last to the expression

$$(-1)^n \int_{(\sigma)} L_{k(n[\lambda \dots])}^{(n; \lambda \dots)} \delta q_k dx_1 \dots dx_\lambda \dots,$$

which allows to write (2) in this way

$$(2') \quad \int_{(\sigma)} \sum_{n=0}^s \sum_{\lambda \dots}^{(n)} (-1)^n L_{k(n[\lambda \dots])}^{(n; \lambda \dots)} \delta q_k dx_1 \dots dx_\lambda \dots = 0.$$

Thus the Euler-Lagrange equations are

$$(3) \quad \sum_{n=0}^s \sum_{\lambda \dots}^{(n)} (-1)^n L_{k(n[\lambda \dots])}^{(n; \lambda \dots)} = 0.$$

The derivative of L with respect to a certain variable x_π is

$$(4) \quad D_\pi L = L_{,\pi} + \sum_{n=0}^s \sum_{\lambda \dots}^{(n)} L_{k(n[\lambda \dots])} \dot{q}_{k^* \pi \lambda \dots}^{(n+1)}.$$

In order to transform this expression, we write the relation

$$(5) \quad L_{k(n[\lambda \dots])}^{(l; \lambda \dots)} \dot{q}_{k^* \varrho \pi \alpha \beta}^{(n-l+1)} = D_\varrho [L_{k(n[\lambda \dots])}^{(l; \lambda \dots)} \dot{q}_{k^* \pi \alpha \beta \dots}^{(n-l)}] - L_{k(n[\lambda \dots])}^{(l+1; \varrho \lambda \dots)} \dot{q}_{k^* \pi \alpha \beta \dots}^{(n-l)},$$

where $\varrho = \underline{\lambda+l}$, $\alpha = \underline{\lambda+l+1}$, $\beta = \underline{\lambda+l+2}$, etc. (with the convention $\mu = \underline{\lambda+1}$, $v = \underline{\mu+1}$, ...).

With the help of formula (5), making $l=0$, we substitute all terms of the sum $\sum_{n=0}^s$ from (4), except the first, by other two terms, so that the sum is replaced by other two sums $\sum_{n=1}^s$. In the second of these sums we substitute again all terms, except the first, if we make $l=1$ in formula (5). Similarly, making, $l=2, 3, \dots$, etc., in relation (5), we substitute always the terms of the last sum, except the first. So we write eq. (4) into the form

$$(6) \quad D_\pi L = L_{,\pi} + \sum_{l=0}^{s-1} \sum_{n=l+1}^s \sum_{\lambda \dots}^{(n)} (-1)^l D_\varrho [L_{k(n[\lambda \dots])}^{(l; \lambda \dots)} \dot{q}_{k^* \pi \alpha \beta \dots}^{(n-l)}] + \sum_{i=0}^s \sum_{\lambda \dots}^{(i)} (-1)^i L_{k(i[\lambda \dots])}^{(i; \lambda \dots)} \dot{q}_{k^* \pi}^{(1)}.$$

Because of eq. (3) the last group of sums is zero. Therefore we can write the σ relations (6) as follows

$$(6') \quad \sum_{l=0}^{s-1} \sum_{n=l+1}^s \sum_{(\pi)} \lambda \dots (-1)^l D_{\varrho} [L_{k(n[\lambda \dots])}^{(l; \lambda \dots)} q_{k' \pi \alpha \dots}^{(n-l)}] - D_{\pi} L = -L_{\pi}.$$

We observe that for every value of l , $\varrho = \lambda + l$ has once the value j ($j = 1, 2, \dots, \sigma$), no matter which of the indices λ, μ, \dots is represented by it. Namely, ϱ has the value j in that term of the sum $\sum_{\lambda+l=1}^{\sigma}$ for which $\lambda+l = j$. This term is

$$(7) \quad \sum_{l=0}^{s-1} \sum_{n=l+1}^s \sum_{(\pi)} |\lambda+l| (-1)^l D_j [L_{k(n[\dots \lambda+l=j \dots])}^{(l; \dots \lambda+l=j \dots)} q_{k' \pi \alpha \dots}^{(n-l)}],$$

where by the $|\lambda+l|$ we indicate that the sum over the index $|\lambda+l|$ from the group of sums $\sum_{(n-1)}$, disappears.

Consequently eq. (6') can be written

$$(8) \quad \sum_{j=1}^{\sigma} D_j \sum_{l=0}^{s-1} \sum_{n=l+1}^s \sum_{(\pi)} |\lambda+l| (-1)^l L_{k(n[\dots \lambda+l=j \dots])}^{(l; \dots \lambda+l=j \dots)} q_{k' \pi \alpha \dots}^{(n-l)} - \sum_{j=1}^{\sigma} D_j L \delta_{\pi j} = L_{\pi},$$

$\delta_{\pi j}$ being the symbol of Kronecker.

Thus the tensor

$$(9) \quad N_{\pi j} = \sum_{l=0}^{s-1} \sum_{n=l+1}^s \sum_{(\pi)} |\lambda+l| (-1)^l L_{k(n[\dots \lambda+l=j \dots])}^{(l; \dots \lambda+l=j \dots)} q_{k' \pi \alpha \dots}^{(n-l)} - L \delta_{\pi j}$$

satisfies the equation

$$(10) \quad D_j N_{\pi j} = -L_{\pi},$$

$N_{\pi j}$ is a generalization of the energy-momentum density tensor, from the field theories ($T_{\pi j}$).

The equalization with zero of the divergence of $T_{\pi j}$ leads to conservation laws for energy and momentum⁽³⁾. Equation

$$(11) \quad D_j N_{\pi j} = 0$$

⁽³⁾ See, for example, A. SOKOLOV and D. IVANENKO: *Kvantovaya teoriya polia* (Moscow-Leningrad, 1952).

leads also to laws which for $\sigma = 4$ ($x_1 = x$, $x_2 = y$, $x_3 = z$, $x_4 = ict$) reduce to the mentioned conservation laws, but containing derivatives of the field functions up to s -th order.

On the other hand, for $x_1 = t$, $x_2 = x_3 = \dots = 0$, $N_{\pi j}$ reduces to the generalized Hamiltonian function, previously established by us ⁽²⁾.

Eqs. (3) and (10) can constitute starting points for the development of a more comprising field theory.

RIASSUNTO (*)

Si espone un formalismo generale basato sull'uso di una funzione di Lagrange con derivate di n -esimo ordine rispetto a σ variabili indipendenti.

(*) Traduzione a cura della Redazione.

On the Double Compton Process and Some Calculations of Polarization Effects. - II.

M. CARRASSI and G. PASSATORE

Istituto di Fisica dell'Università - Genova

Istituto Nazionale di Fisica Nucleare - Sezione di Genova

(ricevuto il 25 Gennaio 1960)

Summary. — Using a method already developed in another paper, the transition amplitudes among the basic polarization states of all particles involved in the double Compton effect have been deduced and numerically calculated. The cross-section and various polarization effects have also been discussed in several cases. The cross sections as a function of the energy of one of the emitted photons show in general an infra-red divergence at the ends of the spectrum, a forward concentration with the increase of the incident energy, and in the case of symmetric geometry for the two photons, a minimum when the energies of the emitted photons are nearly equal. Some effects of linear and circular polarizations have been considered in detail and a comparison with the single Compton effect has always been made. Linear polarization effects show some qualitative difference from the single Compton scattering.

1. — Introduction.

In a previous paper ⁽¹⁾ we developed a method which enables us to discuss easily any polarization effect for a process involving photons and spin $\frac{1}{2}$ particles. We have used such a method to calculate the differential cross-section for the double Compton effect and to describe certain polarization effects of particular interest in this process.

The double Compton effect was first considered by HEITLER and NORDHEIM ⁽²⁾. Assuming that the two photons share the same energy, HEITLER

⁽¹⁾ M. CARRASSI and G. PASSATORE: *Nuovo Cimento*, **13**, 944 (1959). (In the following we shall refer to this paper as I).

⁽²⁾ W. HEITLER and L. NORDHEIM: *Physica*, **1**, 1059 (1934).

and NORDHEIM showed that the order of magnitude of the double process is smaller, by a factor 137, than the single Compton scattering process. Later ELIEZER ⁽³⁾ obtained the exact expression for the differential cross-section but he only carried out the analysis in the particular case of a very soft photon. In this case he obtained a considerable increase in the cross-section compared with the value of HEITLER and NORDHEIM, corresponding to the «infra-red catastrophe». The ELIEZER result has recently been generalized by MAJUMDAR MATHUR and DHAR ⁽⁴⁾ for Compton scattering of any multiplicity.

The differential cross-section for the double Compton effect has also been calculated by MANDL and SKYRME ⁽⁵⁾ using covariant formalism and under most general conditions. They also examined in detail some particular cases of remarkable interest. A computation of the cross-section, when the two final photons are the same, has been carried out by DE TOLLIS and LIOTTA ⁽⁶⁾.

In all these works one obtains the transition probability by averaging and summing on initial and final states of polarizations. Therefore it is impossible to examine the polarization effects.

In the present work, following the method described in I, without directly calculating the transition probability, we set up the exact expression for the transition amplitudes among the basic states of polarization of all the particles involved in the process. By means of particular combination of these amplitudes (formula (I.7)) we obtain the differential cross-section and the description of polarization effects. In Section 2, we show the explicit dependence of the amplitudes on the dynamical variables of all the particles. The numerical values of these amplitudes have been obtained by the use of a IBM 650 computer.

As far as the cross-sections are concerned they are in full agreement with the special cases considered by MANDL and SKYRME. In Section 3 we discuss some polarization effects. Some of these effects are already well-known in the simple Compton process and they provide the principle on which the polarimeters and analyzers are based.

In these cases we find that the polarization effects are of the same order of magnitude as those of the simple Compton process and, qualitatively, their dependence on the angles of emission and on the energy of the incident photon is of the same kind. Naturally in the double Compton process the polarization effects, and particularly the linear polarization, have a more complex structure because of the introduction of an asymmetric element due to the second photon which does not exist in the single Compton effect. We have also con-

⁽³⁾ C. S. ELIEZER: *Proc. Roy. Soc.*, **187**, 210 (1946).

⁽⁴⁾ R. C. MAJUMDAR, V. S. MATHUR and J. DHAR: *Nuovo Cimento*, **12**, 97 (1959).

⁽⁵⁾ F. MANDL and T. H. R. SKYRME: *Proc. Roy. Soc.*, **215**, 497 (1952).

⁽⁶⁾ B. DE TOLLIS and R. LIOTTA: *Nuovo Cimento*, **5**, 947 (1957).

sidered correlations between states of circular polarization, particularly interesting for the dynamics of the process, apart from their possible use for production or analysis of polarized photons.

All numerical calculations of the present paper refer to the case in which the final photons are emitted in two perpendicular planes. Since the validity of the formulae is quite general we will later give other evaluations relating to other special cases.

2. - Transition amplitudes for the double Compton effect.

For the meaning of the symbols here used we refer to I.

The differential cross-section for the double Compton effect can be written as follows.

$$(1) \quad \frac{d\sigma}{d\Omega_1 d\Omega_2 dk_1} = \frac{1}{e} \sum_{\text{in}}^* \sum_{\text{fin}}^* |A_{\text{fin, in}}|^2,$$

where

$$(2) \quad A_{\text{fin, in}} = M' \langle \mathbf{e}^1, \mathbf{e}^2, u | H | \mathbf{e}^0, u^0 \rangle,$$

with

$$(3) \quad \begin{cases} M' = M \frac{e^3}{4\mu} \left[\frac{(2\pi\hbar^2 c^2)^3}{k_0 k_1 k_2} \right]^{\frac{1}{2}}; \\ M = \left\{ \frac{2\pi}{\hbar} \frac{k_1^2 k_2^2 E}{(2\pi\hbar c)^6 [\mu + k_0(1 - \cos \alpha_2) - k_1(1 - \cos \alpha_{12})]} \right\}^{\frac{1}{2}}. \end{cases}$$

The matrix element for the transition is:

$$(4) \quad \langle \mathbf{e}^1, \mathbf{e}^2, u | H | \mathbf{e}^0, u^0 \rangle = u^* Q u^0,$$

where Q is a 4×4 matrix given by the sum of six terms, the first being:

$$(5) \quad \frac{(\boldsymbol{\alpha} \cdot \mathbf{e}^{2*}) [\mu(1 + \beta) + k_0 - k_1 + \boldsymbol{\alpha} \cdot (\mathbf{k}_0 - \mathbf{k}_1)] (\boldsymbol{\alpha} \cdot \mathbf{e}^{1*}) [\mu(1 - \beta) + k_0 + (\boldsymbol{\alpha} \cdot \mathbf{k}_0)] (\boldsymbol{\alpha} \cdot \mathbf{e}^0)}{k_0 [\mu(k_0 - k_1) + k_0 k_1 - \mathbf{k}_0 \cdot \mathbf{k}_1]}.$$

The second and third term derive from (5) by means of the following exchanges

$$\mathbf{k}_0 \rightleftharpoons \mathbf{k}_1, \quad k_0 \rightleftharpoons k_1, \quad \mathbf{e}^0 \rightleftharpoons \mathbf{e}^1; \quad \mathbf{k}_0 \rightleftharpoons \mathbf{k}_2, \quad k_0 \rightleftharpoons k_2, \quad \mathbf{e}^0 \rightleftharpoons \mathbf{e}^2,$$

respectively; the other three can be obtained from the preceding one by means of interchanging index 1 with index 2.

We have chosen the basic states of polarization and the Stokes parameters as in I. With α_1 and β_1 we indicate the polar angles of the photon of energy k_1 and with α_2 and β_2 those of the photon of energy k_2 .

The transition amplitudes $\langle e_{\alpha_1} e_{\alpha_2} u_{\gamma} | H | e_{\beta}^0 u_{\delta}^0 \rangle = H^{\alpha_1 \alpha_2 \beta \gamma \delta}$ have been calculated directly for general geometry. These amplitudes are 2⁵ and there exist among them, as in the simple Compton effect, the following relations expressing the conservation of parity

$$(6) \quad H^{\alpha_1 \alpha_2 \beta \gamma \delta} = \eta \text{ c.c. } H^{\alpha'_1 \alpha'_2 \beta' \gamma' \delta'} \quad \begin{cases} \eta = +1 & \text{for } \gamma = \delta, \\ \eta = -1 & \text{for } \gamma \neq \delta, \end{cases}$$

with

$$\alpha_1 \neq \alpha'_1, \quad \alpha_2 \neq \alpha'_2, \quad \beta \neq \beta', \quad \gamma \neq \gamma', \quad \delta \neq \delta'.$$

By means of these relations the independent amplitudes are reduced to 16 and furthermore have the following properties: eight amplitudes, corresponding to the same values of the indices α_1 and α_2 , are symmetric functions of the vectors k_1 and k_2 ; the remaining eight, corresponding to different values of the indices α_1 and α_2 and the same value of the indices β, γ, δ , are obtained one from the other by interchanging k_1 with k_2 . These properties are expressed analytically by the following relation

$$(7) \quad \langle e_{\alpha_1} e_{\alpha_2} u_{\gamma} | H | e_{\beta}^0 u_{\delta}^0 \rangle = A^{\alpha_1 \alpha_2 \beta \gamma \delta}(k_1, k_2) + A^{\alpha_2 \alpha_1 \beta \gamma \delta}(k_2 k_1).$$

The explicit expression of the quantities $A^{\alpha_1 \alpha_2 \beta \gamma \delta}$ in terms of the variables $k_0, k_1, k_2, p, \alpha_1, \alpha_2, \beta_1$ and β_2 are:

$$(8) \quad \left\{ \begin{aligned} A^{1111}(k_1, k_2) &= -D_{01} [\bar{B} k_{1+} \hat{T}_{2+}^2 + \bar{B} k_{1+} S_{1+}^2 Z_{2-}^2 + 2\mu p S_{1+}^2 T_{2+}^2] - \\ &\quad - D_{12} \bar{B} (p + p_z) p_+ R_{1+2-}^{22}, \\ A^{1121}(k_1, k_2) &= D_{01} [B k_{1+} \hat{Z}_{2+}^2 - B k_{1+} S_{1+}^2 T_{2-}^2 - 2\mu p S_{1+}^2 Z_{2+}^2] + \\ &\quad + D_{12} B (p_+)^2 R_{1+2-}^{22}, \\ A^{1112}(k_1, k_2) &= D_{01} [(2k_0 B + \bar{C}_-) \hat{T}_{2+}^2 - \bar{B} k_{1+} Z_{2-}^2 + 2\mu p S_{1+}^2 Z_{2-}^2] - \\ &\quad - D_{12} (p + p_z) \bar{Y}_+ R_{1+2-}^{22}, \\ A^{1122}(k_1, k_2) &= -D_{01} [(2k_0 \bar{B} + C_-) \hat{Z}_{2+}^2 + B k_{1+} \hat{T}_{2-}^2 - 2\mu p S_{1+}^2 T_{2-}^2] + \\ &\quad + D_{12} p_+ Y_- R_{1+2+}^{22}, \\ A^{2211}(k_1, k_2) &= -D_{01} [B k_{1+} S_{1+}^2 Z_{2-}^2 + (A - C_+) S_{1+}^2 T_{2+}^2] - \\ &\quad - D_{12} B (p + p_z) p_+ R_{1+2-}^{11}, \end{aligned} \right.$$

$$\begin{aligned}
 A^{22121}(\mathbf{k}_1, \mathbf{k}_2) &= -D_{01}[\bar{B}k_{1+}S_{1+}^1T_{2-}^1 - (\bar{A} - \bar{C}_+)S_{1+}^1Z_{2+}^1] + D_{12}\bar{B}(p_+)^2R_{1+2-}^{11}, \\
 A^{22112}(\mathbf{k}_1, \mathbf{k}_2) &= D_{01}[C_-\hat{T}_{2+}^1 + (C_- + 2\mu p)S_{1+}^1Z_{2-}^1] - D_{12}(p + p_z)Y_-R_{1-2+}^{11}, \\
 A^{22122}(\mathbf{k}_1, \mathbf{k}_2) &= -D_{01}[\bar{C}_-\hat{Z}_{2+}^1 - (\bar{C}_- - 2\mu p)S_{1+}^1T_{2-}^1] + D_{12}p_+\bar{Y}_-R_{1-2+}^{11}, \\
 A^{12111}(\mathbf{k}_1, \mathbf{k}_2) &= -D_{01}[\bar{B}k_{1+}\hat{T}_{2+}^1 + \bar{B}k_{1+}S_{1+}^2Z_{2-}^1 + 2\mu pS_{1+}^2T_{2+}^1] - \\
 &\quad - D_{12}(p + p_z)[\bar{B}p_+R_{1+2-}^{21} - \bar{Y}_+X_{1+2+}^{21}], \\
 A^{12121}(\mathbf{k}_1, \mathbf{k}_2) &= D_{01}[Bk_{1+}\hat{Z}_{2+}^1 - Bk_{1+}S_{1+}^2T_{2-}^1 - 2\mu pS_{1+}^2Z_{2+}^1] + \\
 &\quad + D_{12}p_+[Bp_+R_{1+2-}^{21} - Y_+X_{1+2+}^{21}], \\
 A^{12112}(\mathbf{k}_1, \mathbf{k}_2) &= D_{01}[(2k_0B + \bar{C}_-)\hat{T}_{2+}^1 - \bar{B}k_{1+}\hat{Z}_{2-}^1 - 2\mu pS_{1+}^2Z_{2-}^1] - \\
 &\quad - D_{12}(p + p_z)[\bar{B}p_+X_{1-2-}^{21} + \bar{Y}_+R_{1-2+}^{21}], \\
 A^{12122}(\mathbf{k}_1, \mathbf{k}_2) &= -D_{01}[(2k_0\bar{B} + C_-)\hat{Z}_{2+}^1 + Bk_{1+}\hat{T}_{2-}^1 + 2\mu pS_{1+}^2T_{2-}^1] + \\
 &\quad + D_{12}p_+[Bp_+X_{1-2-}^{21} + Y_+R_{1-2+}^{21}], \\
 A^{21111}(\mathbf{k}_1, \mathbf{k}_2) &= -D_{01}[Bk_{1+}S_{1+}^1Z_{2-}^2 + (A - C_+)S_{1+}^1T_{2+}^2] - \\
 &\quad - D_{12}(p + p_z)[Bp_+R_{1+2-}^{12} - \bar{Y}_-X_{1+2+}^{12}], \\
 A^{21121}(\mathbf{k}_1, \mathbf{k}_2) &= -D_{01}[\bar{B}k_{1+}S_{1+}^1T_{2-}^2 - (\bar{A} - \bar{C}_+)S_{1+}^1Z_{2+}^2] + \\
 &\quad + D_{12}p_+[\bar{B}p_+R_{1+2-}^{12} - \bar{Y}_-X_{1+2+}^{12}], \\
 A^{21112}(\mathbf{k}_1, \mathbf{k}_2) &= D_{01}[C_+\hat{T}_{2+}^2 + (C_- + 2\mu p)S_{1+}^1Z_{2-}^2] - \\
 &\quad - D_{12}(p + p_z)[Bp_+X_{1-2-}^{12} + Y_+R_{1-2+}^{12}], \\
 A^{21122}(\mathbf{k}_1, \mathbf{k}_2) &= -D_{01}[\bar{C}_-\hat{Z}_{2+}^2 - (\bar{C}_- - 2\mu p)S_{1+}^1T_{2-}^2] + \\
 &\quad + D_{12}p_+[\bar{B}p_+X_{1-2-}^{12} + \bar{Y}_-R_{1-2+}^{12}],
 \end{aligned}
 \tag{8}$$

where the meaning of the symbols used is as follows:

$$\begin{aligned}
 A &= 2(k_0B + \mu p); & B &= E + \mu + p; & C_{\pm} &= Bk_1(\cos \alpha_1 \pm 1); \\
 \bar{A} &= 2(k_0\bar{B} - \mu p); & \bar{B} &= E + \mu - p; & \bar{C}_{\pm} &= \bar{B}k_1(\cos \alpha_1 \pm 1); \\
 D_{01} &= (N/\sqrt{2})[\mu(k_0 - k_1) - k_0k_1(1 - \cos \alpha_1)]^{-1}; \\
 D_{12} &= (N/\sqrt{2})[\mu(k_1 + k_2) - k_1k_2(1 - \cos \alpha_{12})]^{-1}; \\
 N &= [4pE(p + p_z)(E + \mu)]^{-\frac{1}{2}}; & \alpha_{12} &= \widehat{\mathbf{k}_1\mathbf{k}_2}; \\
 Y_{\mp}^{\pm} &= B[k_1(\cos \alpha_1 \mp 1) + k_2(\cos \alpha_2 \mp 1)] \pm 2\mu p;
 \end{aligned}$$

$$\begin{aligned}
\bar{Y}_{\pm}^{\pm} &= \bar{B}[k_1(\cos \alpha_1 \pm 1) + k_2(\cos \alpha_2 \pm 1) \pm 2\mu p]; \\
Z_{j\pm}^1 &= (p + p_z) \exp[\pm i\beta_j](\cos \alpha_j \mp 1) + p_{\pm} \sin \alpha_j; \\
Z_{j\pm}^2 &= (p + p_z) \exp[\pm i\beta_j](\cos \alpha_j \pm 1) + p_{\pm} \sin \alpha_j; \\
T_{j\pm}^1 &= (p + p_z) \sin \alpha_j - p_{\mp} \exp[\pm i\beta_j](\cos \alpha_j \mp 1); \\
T_{j\pm}^2 &= (p + p_z) \sin \alpha_j - p_{\mp} \exp[\pm i\beta_j](\cos \alpha_j \pm 1); \\
\hat{Z}_{j\pm}^r &= \sin \alpha_j Z_{j\pm}^r; & \hat{T}_{j\pm}^r &= \sin \alpha_j T_{j\pm}^r; \\
S_{j\pm}^1 &= \exp[\pm i\beta_j](\cos \alpha_j \mp 1); & S_{j\pm}^2 &= \exp[\pm i\beta_j](\cos \alpha_j \pm 1); \\
R_{i\pm j\mp}^{11} &= \sin \alpha_i \sin \alpha_j + S_{i\pm}^1 S_{j\mp}^1; & R_{i\pm j\mp}^{22} &= \sin \alpha_i \sin \alpha_j + S_{i\pm}^2 S_{j\mp}^2; \\
R_{i\pm j\mp}^{12} &= \sin \alpha_i \sin \alpha_j + S_{i\pm}^1 S_{j\mp}^2; & R_{i\pm j\mp}^{21} &= \sin \alpha_i \sin \alpha_j + S_{i\pm}^2 S_{j\mp}^1; \\
X_{i\pm j\pm}^{12} &= -[S_{i\pm}^1 \sin \alpha_j - S_{j\pm}^2 \sin \alpha_i]; & X_{i\pm j\pm}^{21} &= -[S_{i\pm}^2 \sin \alpha_j - S_{j\pm}^1 \sin \alpha_i].
\end{aligned}$$

These amplitudes have been calculated numerically for $k_0 = 0.5, 1, 2, 20$ where the energy values are always expressed in mc^2 unity. We have always considered the case in which the planes $k_0 k_1$ and $k_0 k_2$ are perpendicular among themselves. The values of α_1 and α_2 which have been considered are: $\alpha_1 = \alpha_2 = 90^\circ$; $\alpha_1 = \alpha_2 = 30^\circ$; $\alpha_1 = 10^\circ$, $\alpha_2 = 90^\circ$.

3. - Cross-sections.

Using once more the notations introduced in I, the differential cross-section may be expressed in the following manner:

$$(9) \quad \frac{d\sigma}{d\Omega_1 d\Omega_2 dk_1} = \frac{M'^2}{c} [\Phi_0 + \Phi_1 + \Phi_2 + \Phi_3 + \Phi_4 + \Phi_5],$$

where the Φ in equation (9) are like those introduced in I for the simple Compton effect. The differential cross-section, averaged over the initial states of polarization and summed over the final ones, results as follows:

$$(10) \quad \frac{d\sigma}{d\Omega_1 d\Omega_2 dk_1} = \varepsilon^3 \frac{M'^2}{c} \Phi_0,$$

and Φ_0 is given by

$$(11) \quad \Phi_0 = (1/2^5) H^{\alpha_1 \alpha_2 \beta \gamma \delta} \bar{H}_{\alpha_1 \alpha_2 \beta \gamma \delta},$$

where we use the summation convention.

Let us discuss now some particular cases:

i) *The forward cross-section.* For $\alpha_1 = \alpha_2 = 0$ the cross-section vanishes. This fact, as is well known ⁽⁵⁾, is due to the impossibility of a photon disintegrating into two photons without interaction with something. However the cross-section does not vanish if we take the case in which α_1 and α_2 are so small that all terms of order higher than the second are negligible. In this case only 24 of the 32 amplitudes are different from zero and their expressions are very simple compared with the general expressions (8), so that it is possible to obtain the cross-section explicitly as follows:

$$(12) \quad \frac{d\sigma}{d\Omega_1 d\Omega_2 dk_1} = \frac{1}{(2\pi)^2} \frac{e^2}{\hbar c} r_0^2 \frac{k_1 k_2}{\mu^2 k_0} \cdot E \left(\frac{k_0^2}{k_1^2 k_2^2} - \frac{k_1^2}{k_0^2 k_2^2} - \frac{k_2^2}{k_0^2 k_1^2} \right) [k_0 k_1 (1 - \cos \alpha_1) - k_0 k_2 (1 - \cos \alpha_2) - k_1 k_2 (1 - \cos \alpha_{12})].$$

α_{12} is the angle between \mathbf{k}_1 and \mathbf{k}_2 and $r_0 = e^2/mc^2$. Putting $(k_1/k_0) = \xi_1$, $(k_2/k_0) = \xi_2$ and assuming $\xi_1 + \xi_2 = 1$, as is possible in our approximation, we see easily that (12) is the same result obtained by MANDL and SKYRME.

ii) *Cross-section for other special cases.* We consider here the cases in which the incident photon energy is $k = 0.5, 1, 2, 20$ and the angles are as follows: $\alpha_1 = \alpha_2 = 30^\circ$; $\alpha_1 = \alpha_2 = 90^\circ$; $\alpha_1 = 10^\circ$, $\alpha_2 = 90^\circ$, the final photons being always emitted in two perpendicular planes ($\beta_1 - \beta_2 = 90^\circ$). In Figs. 1, 2, 3

$$I_k = \frac{16\pi^2}{\alpha_0^2} \frac{d\sigma}{d\Omega_1 d\Omega_2 dk_1},$$

is plotted against the energy k_1 of one photon for fixed direction of emission of both photons. A peculiarity present in all cases is the divergence of the cross-section at the ends of the energy range, a divergence corresponding to « infra-red catastrophe ». All these functions have only one minimum. In the cases in which the angles of emission of both photons are the same the curve is nearly symmetric with respect to the middle of the range; the deviation from symmetry is due to the factor $[\mu + k_0(1 - \cos \alpha_2) - k_1(1 - \cos \alpha_{12})]^{-1}$ caused by the density of the final states. Let us now consider several cases separately and closely examine the behaviour, with the incident energy, of the cross-section integrated over k_1 .

a) $\alpha_1 = \alpha_2 = 30^\circ$. With the increase of the incident energy the cross-section, integrated over k_1 , increases (Fig. 1); this rise is particularly large passing from $k_0 = 2$ to $k_0 = 20$. The cross-section increases with the range of k_1 and with the rise of the minimum of the differential cross-section. This

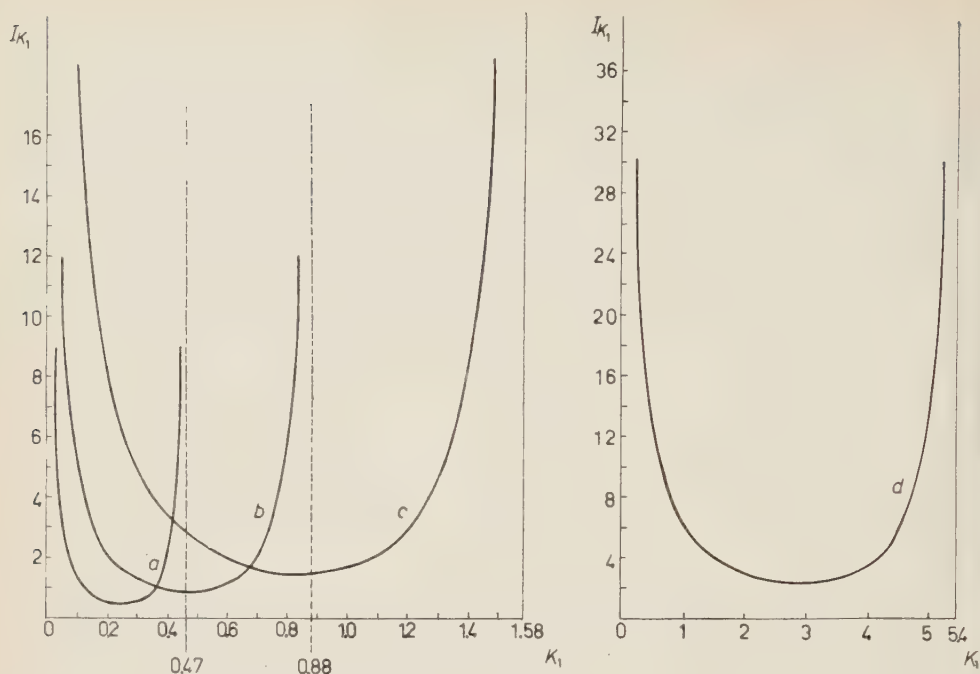


Fig. 1. - Cross-sections for the double Compton effect against the energy of one emitted photon: $\alpha_1 = \alpha_2 = 30^\circ$, $\beta_1 = \beta_2 = 90^\circ$. a) $k_0 = 0.5$, $k_{1\max} = 0.47$; b) $k_0 = 1$, $k_{1\max} = 0.88$; c) $k_0 = 2$, $k_{1\max} = 1.58$; d) $k_0 = 20$, $k_{1\max} = 5.44$.

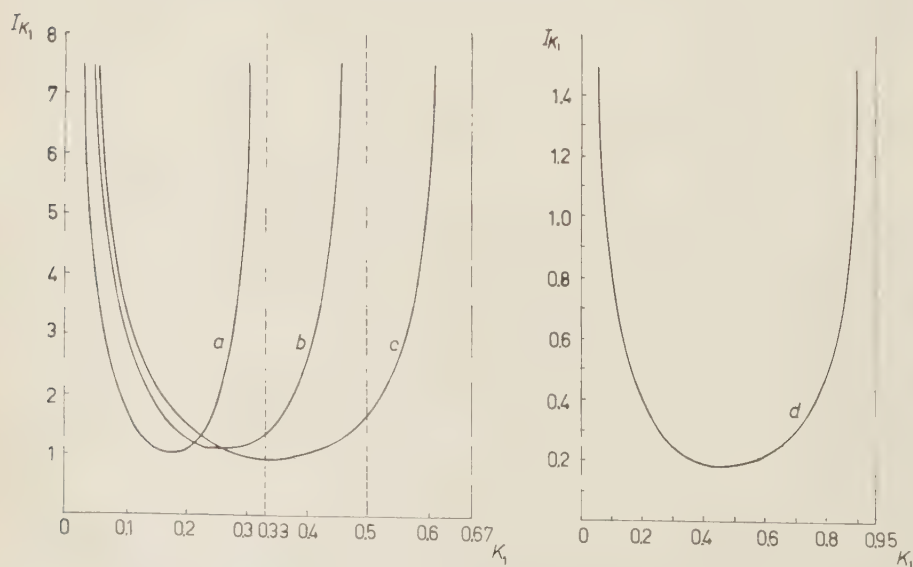


Fig. 2. - Cross-sections for the double Compton effect against the energy of one emitted photon: $\alpha_1 = \alpha_2 = 90^\circ$, $\beta_1 = \beta_2 = 90^\circ$. a) $k_0 = 0.5$, $k_{1\max} = 0.33$; b) $k_0 = 1$, $k_{1\max} = 0.50$; c) $k_0 = 2$, $k_{1\max} = 0.67$; d) $k_0 = 20$, $k_{1\max} = 0.95$.

is physically clear since with the increasing of k_0 , the forward emission is predominant, *i.e.* the emission of the photons tends towards smaller and smaller solid angles with the increasing of k_0 . Consequently, the rise of the cross-section in this case shows that the photons, at least up to $k_0 = 20$, are emitted into a cone larger than 30° .

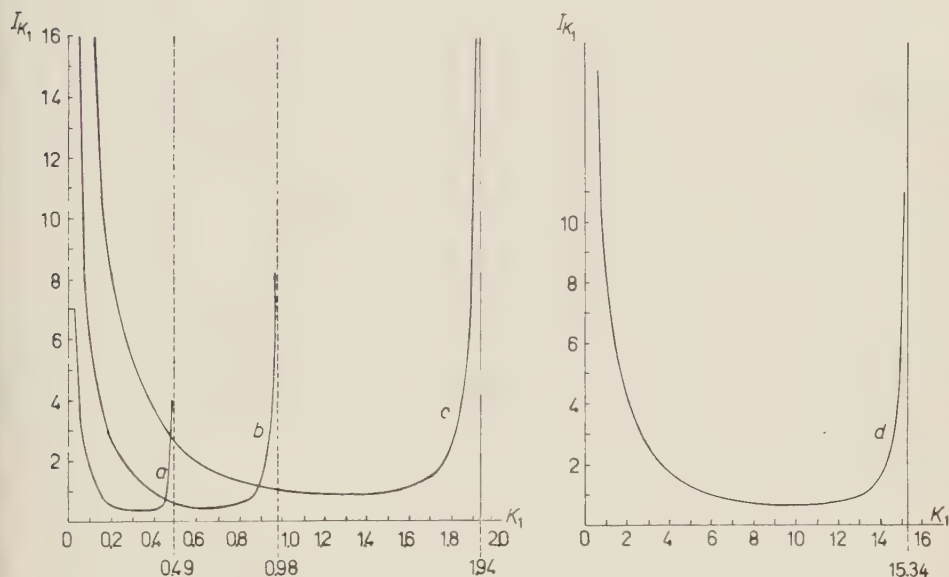


Fig. 3. — Cross-sections for the double Compton effect against the energy of one emitted photon: $\alpha_1 = 16^\circ$, $\alpha_2 = 90^\circ$, $\beta_1 - \beta_2 = 90^\circ$. a) $k_0 = 0.5$, $k_{1\max} = 0.49$; b) $k_0 = 1$, $k_{1\max} = 0.98$; c) $k_0 = 2$, $k_{1\max} = 1.94$; d) $k_0 = 20$, $k_{1\max} = 15.34$.

b) $\alpha_1 = \alpha_2 = 90^\circ$. With the increasing of the incident energy from $k_0 = 2$ to $k_0 = 20$ the cross-section integrated over k_1 decreases considerably owing to the forward concentration of photon emission within a cone less than 90° (Fig. 2). On the contrary the cross-section for k_0 going from 0.5 to 1 increases as in the case a). This evidently means that for such low values of the incident energy the photon emission is not yet sufficiently forward; in other words, the photons are preferably emitted within a cone greater than 90° . However at $k_0 = 2$, the lowering of the minimum of the spectrum already shows that the forward emission is prevalent. By lowering the minimum of the spectrum when increasing the incident energy, at a certain point the cross-section integrated over k_1 will also begin to decrease. We note at last that the results here obtained in the case of $k_0 = 2$ agree with those of MANDL and SKYRME.

c) $\alpha_1 = 10^\circ$, $\alpha_2 = 90^\circ$. The dependence on k_0 of the cross-section integrated over k_1 is, qualitatively, as in the case b) (Fig. 3).

The minimum of I_{k_1} now begins to decrease at a value of the incident energy slightly smaller than $k_0 = 20$.

4. - Polarization effects.

To discuss easily the polarization effects we look at the expression (9) of the cross-section depending on all polarization states and the relations (7) of I which enables us to construct the q 's in terms of the amplitudes $H^{\alpha_1\alpha_2\gamma\delta}$.

Among the possible polarization effects and correlations we have considered those which we believed to be particularly significant. In studying these effects we employed the quantities «asymmetry ratio» and «polarization degree» defined in the usual manner.

4.1. Effects related to the polarization of one particle only.

i) Dependence of the cross-section on the polarization of the incident beam. If the incident beam is polarized, the cross-section is:

$$(13) \quad \frac{d\sigma}{d\Omega_1 d\Omega_2 dk_1} = 2^3 \frac{M'^2}{c} [\Phi_0 + \Phi_1(U^0)],$$

where Φ_0 is given by (11), and

$$(14) \quad \begin{aligned} \Phi_1(U^0) &= (1/2^5) [2 \operatorname{Re} (H^{\alpha_1\alpha_21\gamma\delta} \bar{H}^{\alpha_1\alpha_22\gamma\delta}) U_1^0 + 2 \operatorname{Im} (H^{\alpha_1\alpha_21\gamma\delta} \bar{H}^{\alpha_1\alpha_2\gamma\delta}) U_2^0 + \\ &+ (H^{\alpha_1\alpha_21\gamma\delta} \bar{H}^{\alpha_1\alpha_21\gamma\delta} - H^{\alpha_1\alpha_22\gamma\delta} \bar{H}^{\alpha_1\alpha_22\gamma\delta}) U_3^0] = \\ &= A^{(0)} [U_1^0 \cos 2\beta_1 + U_2^0 \sin 2\beta_1] + B^{(0)} [-U_1^0 \sin 2\beta_1 + U_2^0 \cos 2\beta_1]. \end{aligned}$$

As in the single Compton effect, the cross-section does not depend on U_3^0 , as one can see immediately from the relations (7) among the amplitudes. The $A^{(0)}$ and $B^{(0)}$ quantities depend on the azimuths β_1 and β_2 only through the difference $\beta_1 - \beta_2$ (as is shown in the Appendix) so that, when this difference is kept fixed, the only azimuthal dependence is the one explicitly shown. One sees that the azimuthal dependence is the same as in the single Compton effect when it concerns the $A^{(0)}$ term, but now there also exists the $B^{(0)}$ term. This describes the dependence of the cross-section on the polarization degree (*) at 45°

(*) With «polarization direction» we understand always the direction of the electric vector.

with the scattering plane of the k_1 photon: this dependence does not exist in the single Compton effect by symmetry, while in the double Compton effect the symmetry to right and left of the scattering plane is destroyed by the direction of the k_2 photon.

It is always possible to assume that $U_2^0 = 0$ and so (14) becomes:

$$(15) \quad \Phi_1(U^0) = [A^{(0)} \cos 2\beta_1 - B^{(0)} \sin 2\beta_1] U_1^0,$$

showing in a quite simple way the azimuthal dependence of the cross-section. To discuss this in greater detail it is convenient to introduce the «asymmetry ratio»

$$(16) \quad \delta = \frac{A^{(0)} \cos 2\beta_1 - B^{(0)} \sin 2\beta_1}{\Phi_0},$$

which expresses the ratio between the difference and the sum of the cross-sections for opposite states of polarization of the incident beam. In general this asymmetry ratio depends on β_1 , which relates the polarization direction of the incident beam to the scattering plane of the k_1 photon.

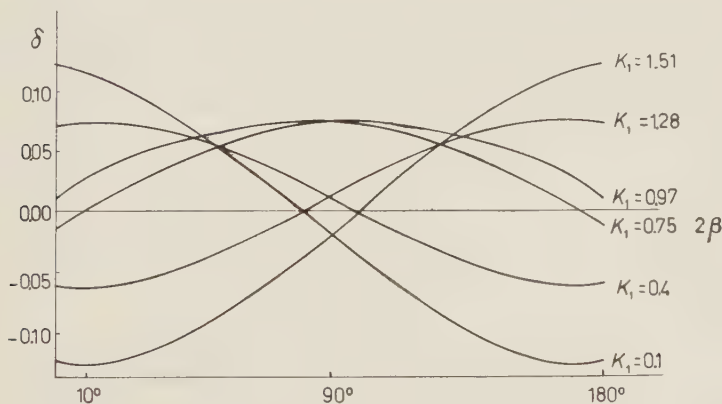
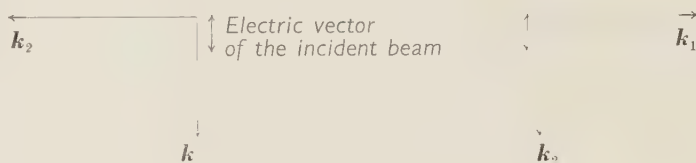


Fig. 4. - Asymmetry ratio against the angle between the plane of polarization of the incident beam and the scattering plane of the k_1 photon - $k_0 = 2$, $\alpha_1 = \alpha_2 = 30^\circ$, $\beta_1 - \beta_2 = 90^\circ$.

In Fig. 4 δ is shown as a function of β_1 for $k_0 = 2$, $\alpha_1 = \alpha_2 = 30$ and for various values of k_1 . It may be interesting to discuss the dependence of these curves on k_1 , and to compare then with the single Compton effect. In the single Compton effect the asymmetry ratio depends only on $\cos 2\beta$ and it is zero for $\beta = \pi/4$ because the cross-section cannot depend on the polarization of the incident beam at 45° with the scattering plane.

In the double Compton effect, where this dependence exists, the asymmetry ratio depends on the azimuth through a linear combination of $\cos 2\beta_1$, and $\sin 2\beta_1$, whose coefficients depend on k_1 . In particular for $k_1 = k_2$, $A^{(0)} = 0$ and δ depends only on $\sin 2\beta_1$. In this case the asymmetry ratio has a maximum, whereas in the single Compton effect it was zero, and vice versa. It is easy to understand that for $k_1 = k_2$ it must be $A^{(0)} = 0$ because for $k_1 = k_2$ the situations showed in the figure below



are related by spatial inversion.

The curves of Fig. 2 that intersect for $2\beta = \pi/2$ correspond to the values of k_1 and k_2 interchanged. One can easily see that this property and also the symmetric behaviour of those curves with respect to $2\beta = \pi/2$, is a consequence of the invariance for spatial inversion.

In the case of a soft photon the asymmetry ratio behaves like the single Compton effect, as the curves of Fig. 2 for $k_1 = 0.1$ and $k_1 = 1.51$ show. As far as the values of the asymmetry ratio are concerned, Fig. 2 shows that in the limiting case of vanishing energy of one photon the single Compton effect values are obtained, while in the other cases the asymmetry ratio is always lower.

ii) Polarization degree of a scattered photon. If one observes the polarization state of the k_1 photon, the cross-section is expressed by

$$(17) \quad \frac{d\sigma}{d\Omega_1 d\Omega_2 dk_1} = 2^2 (M^2/c) [\Phi_0 + \Phi_1(U^1)],$$

where $\Phi_1(U^1)$ is given by:

$$(18) \quad \begin{aligned} \Phi_1(U^1) = (1/2^5) [2 \operatorname{Re} (H^{2\alpha_2 \beta \gamma \delta} \bar{H}^{1\alpha_1 \beta \gamma \delta}) U_1^1 + 2 \operatorname{Im} (H^{2\alpha_2 \beta \gamma \delta} \bar{H}^{1\alpha_2 \beta \gamma \delta}) U_2^1 + \\ + (H^{1\alpha_2 \beta \gamma \delta} \bar{H}^{1\alpha_2 \beta \gamma \delta} - H^{2\alpha_2 \beta \gamma \delta} \bar{H}^{2\alpha_2 \beta \gamma \delta}) U_3^1]. \end{aligned}$$

By means of relations (7) one sees immediately that the coefficient of U_3^1 (that is the circular polarization degree of the scattered beam) is zero. Therefore (18) becomes:

$$(19) \quad \Phi_1(U^1) = A^{(1)} U_1^1 + B^{(1)} U_2^1,$$

and $A^{(1)}/\Phi_0$, $B^{(1)}/\Phi_0$ are respectively the polarization degree of the k_1 photon in the scattering plane and in the plane at 45° degrees anticlockwise. While $A^{(1)}/\Phi_0$ corresponds to the polarizing effect in the single Compton scattering, $B^{(1)}/\Phi_0$ has no analogy in the single Compton scattering, because there, for symmetry reasons, the scattered beam is unpolarized at 45° degrees with the scattering plane. This is not the case for the double Compton scattering, due to the direction of emission of the second photon. Therefore in the double Compton effect the k_1 photon in general will not be polarized normally to the scattering plane.

The degree of linear polarization is given by $[(A^{(1)}/\Phi_0)^2 + (B^{(1)}/\Phi_0)^2]^{1/2}$ and the polarization direction is represented in the Poincaré sphere by polar angles $\theta = \pi/2$, $\psi = \arctg(B^{(1)}/A^{(1)})$.

Fig. 5 shows, in the case $k_0 = 2$, $\alpha_1 = \alpha_2 = 90^\circ$, the polarization direction of

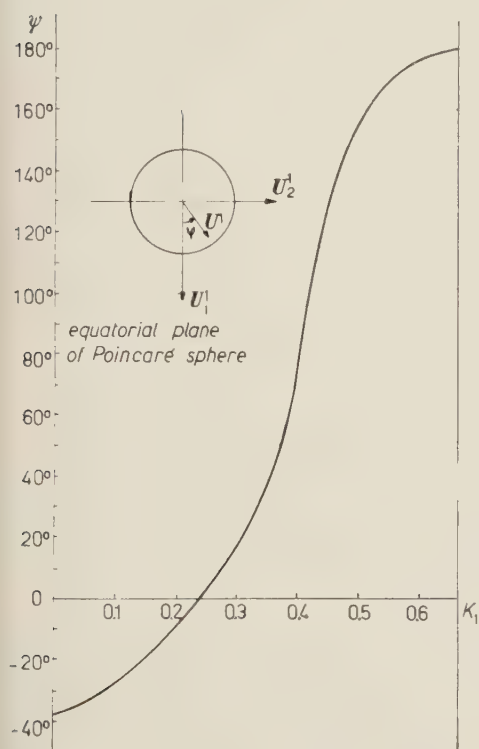


Fig. 5. — Polarization direction of the k_1 photon against its energy - $k_0 = 2$, $\alpha_1 = \alpha_2 = 90^\circ$, $\beta_1 = \beta_2 = 90^\circ$.

the k_1 photon against its energy, and Fig. 6 the polarization degree against the polarization direction. The polarization direction is specified by the angle ψ defined above: $\psi = 0$ means polarization in the scattering plane ($U_1^1 > 0$, $U_2^1 = 0$), $\psi = \pi/2$ polarization perpendicular to the scattering plane, $\psi = \pi/2$ and $\psi = 3\pi/2$ polarization in the planes at 45° with the scattering plane.

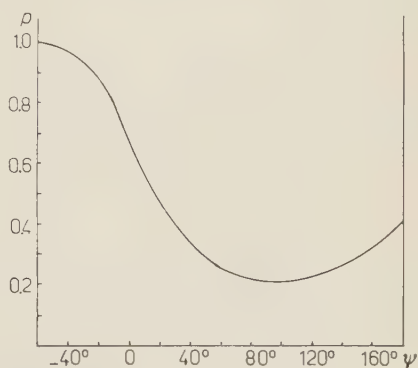


Fig. 6. — Polarization degree of the k_1 photon against the polarization direction - $k_0 = 2$, $\alpha_1 = \alpha_2 = 90^\circ$, $\beta_1 = \beta_2 = 90^\circ$.

At the end of spectrum for $k_1 \rightarrow k_{1,\text{max}}$ ($k_2 \rightarrow 0$) the polarization direction becomes that of the single Compton effect (perpendicular to the scattering

plane) and also the polarization degree ($\sim 42\%$) while at the other end of the spectrum ($k_1 \rightarrow 0$) the polarization degree tends to unity, and has a minimum for the polarization direction at 45° with the scattering plane.

In the case of $k=2$, $\alpha_1=\alpha_2=30^\circ$ for $k_1 \rightarrow k_{\text{max}}$ the direction and the degree of polarization tend to the single Compton values, and for $k_1 \rightarrow 0$ the polarization degree tends to unity.

iii) Independence of the cross-section on the polarization degree of the initial and final electrons. It follows immediately from the relation (7) among the matrix elements that $\Phi_1(V^0)=0$, $\Phi_1(V^1)=0$, as in the single Compton effect.

4.2. Correlation between the polarization states of two particles.

i) Dependence of the cross-section on the circular polarization degree of the incident photons for polarized target electrons. In this case the differential cross-section is as follows:

$$(20) \quad \frac{d\sigma}{d\Omega_1 d\Omega_2 dk_1} = 2^3 \frac{M'^2}{c} [\Phi_0 + \Phi_2(U_3^0, V^0)].$$

We will consider the case of electron polarization along the direction of incident photons. Relation (20) becomes:

$$(21) \quad \frac{d\sigma}{d\Omega_1 d\Omega_2 dk_1} = 2^3 \frac{M'^2}{c} [\Phi_0 + \Phi_2(U_3^0 V_3^0)],$$

where

$$(22) \quad \Phi_2(U_3^0 V_3^0) = (1/2^4) [H^{\alpha_1 \alpha_2 1 \gamma 1} \bar{H}^{\alpha_1 \alpha_2 1 \gamma 1} - H^{\alpha_1 \alpha_2 1 \gamma 2} \bar{H}^{\alpha_1 \alpha_2 1 \gamma 2}].$$

The ratio

$$\varepsilon = \frac{1}{U_3^0 V_3^0} \frac{\Phi_2(U_3^0 V_3^0)}{\Phi_0},$$

between the part of the cross-section sensitive to spin and circular polarization and the part independent from polarizations has been numerically calculated for $k_0=2$, $k_0=20$, $\alpha_1=\alpha_2=30^\circ$, $\alpha_1=\alpha_2=90^\circ$ and for several values of k_1 .

Figs. 7 a) b) c) d), show ε against k_1 in these cases. At both ends of the spectrum (where the energy of one of the emitted photons tends to zero) ε has the same value as in the single Compton effect (^{1,7,8}). In the case $\alpha_1=\alpha_2=90^\circ$

(⁷) F. W. LIPPS and H. A. THOLHOEK: *Physica*, **20**, 395 (1954).

(⁸) H. A. THOLHOEK: *Rev. Mod. Phys.*, **28**, 217 (1956).

while in the single Compton effect ε is zero, in the double effect it reaches a maximum of 30% for $k_0=2$ and of 45% for $k_0=20$ when the emitted photons are of same energy.

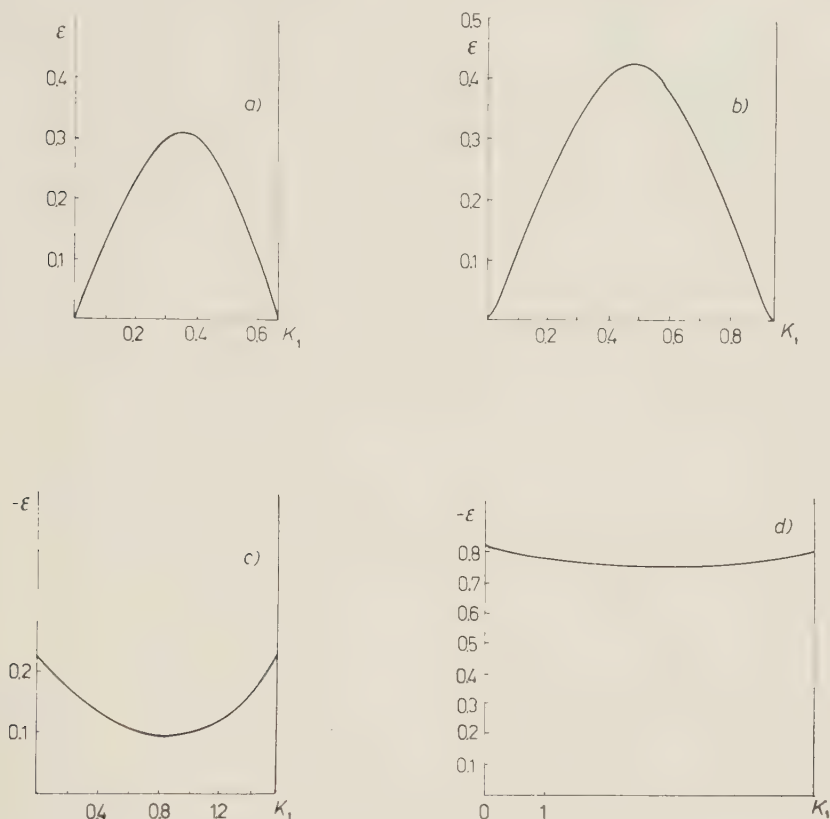


Fig. 7. — Ratio between the part of the cross-section sensitive to spin and circular polarization, and the part independent from them - a) $\alpha_1=\alpha_2=90^\circ$, $k_0=2$; b) $\alpha_1=\alpha_2=90^\circ$, $k_0=20$; c) $\alpha_1=\alpha_2=30^\circ$, $k_0=2$; d) $\alpha_1=\alpha_2=30^\circ$ $k_0=20$.

ii) Correlations between states of circular polarization of two of the three photons. We examined the correlation between the circular polarization of the incident and of a scattered photon, and between the circular polarizations of the two scattered photons. These correlations are interesting more to gain knowledge of the process than from the experimental point of view, since more efficient methods for producing and analysing polarized beams are now available ⁽⁸⁾.

a) Correlation between the circular polarization of the incident and of a scattered photon. If the incident beam is cir-

cularly polarized and one observes the circular polarization of the k_1 photons, the cross-section is expressed by:

$$(23) \quad \frac{d\sigma}{d\Omega_1 d\Omega_2 dk_1} = 2^2 \frac{M'^2}{c} [\Phi_0 + \Phi_2(U_3^0 U_3^1)],$$

where

$$(24) \quad \Phi_2(U_3^0 U_3^1) = (1/2^4) [H^{1\alpha_2 1\gamma\delta} \bar{H}^{1\alpha_2 1\gamma\delta} - H^{1\alpha_2 2\gamma\delta} \bar{H}^{1\alpha_2 2\gamma\delta}] U_3^0 U_3^1.$$

The quantity $\eta_1 = (1/U_3^0 U_3^1) (\Phi_2(U_3^0 U_3^1)/\Phi_0)$ is the degree of circular polarization of the scattered beam with momentum k_1 , if the incident beam is circularly polarized. This polarization degree has been evaluated, for several k_1 values, in the cases of $\alpha_1 = \alpha_2 = 30^\circ$, $\alpha_1 = \alpha_2 = 90^\circ$; $k_0 = 2$, $k_0 = 20$, Fig. 8 a) b), shows η_1 and $\eta_2 = (1/U_3^0 U_3^1) (\Phi_2(U_3^0 U_3^1)/\Phi_0)$ against k_1 for $k_0 = 2$, $k_0 = 20$, $\alpha_1 = \alpha_2 = 30^\circ$. At the end of the spectrum η_1 and η_2 tend to the very large values that they have in the single Compton effect. On the other hand, the polarization degree is only a few percent.

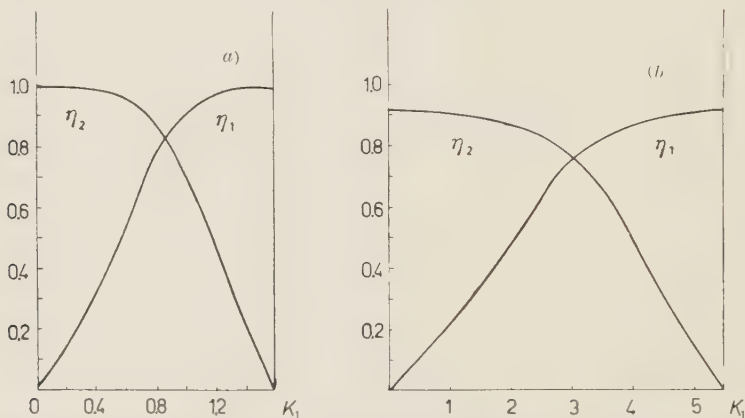


Fig. 8. - Circular polarization degrees of scattered photons for incident beam circularly polarized. - a) $\alpha_1 = \alpha_2 = 30^\circ$, $k_0 = 2$ b) $\alpha_1 = \alpha_2 = 30^\circ$, $k_0 = 20$.

We note at last that there is no correlation between the linear and circular polarization states of the two photons, as in the single Compton effect.

b) Correlation between circular polarizations of the two scattered photons. If one observes the circular polarization of the two scattered photons, the cross-section has the expression:

$$(25) \quad \frac{d\sigma}{d\Omega_1 d\Omega_2 dk_1} = 2 \frac{M'^2}{c} [\Phi_0 + \Phi_2(U_3^1 U_3^2)],$$

where

$$(26) \quad \Phi_2(U_3^1 U_3^2) = (1/2^4) [H^{11\beta\gamma\delta} \bar{H}^{11\beta\gamma\delta} - H^{21\beta\gamma\delta} \bar{H}^{21\beta\gamma\delta}].$$

The quantity $\lambda = (1/U_3^1 U_3^2)(\Phi_2(U_3^1 U_3^2)/\Phi_0)$ is the circular polarization degree of the photons of momentum k_1 counted in coincidence with the circularly polarized photons of momentum k_2 . This polarization degree has been evaluated for several k_1 values in the cases $\alpha_1 = \alpha_2 = 30^\circ$, $\alpha_1 = \alpha_2 = 90^\circ$, $k_0 = 2$, $k_0 = 20$. One observes that in general the beam of k_1 photons in coincidence with the totally circularly polarized k_2 photons is only partially polarized. The polarization degree tends to zero at both ends of the spectrum; it reaches a maximum for $k_1 = k_2$, Fig. 9 a) b) c) d) shows $\lambda(k_1)$ for $k_0 = 2$; $k_0 = 20$, $\alpha_1 = \alpha_2 = 30^\circ$ $\alpha_1 = \alpha_2 = 90^\circ$.

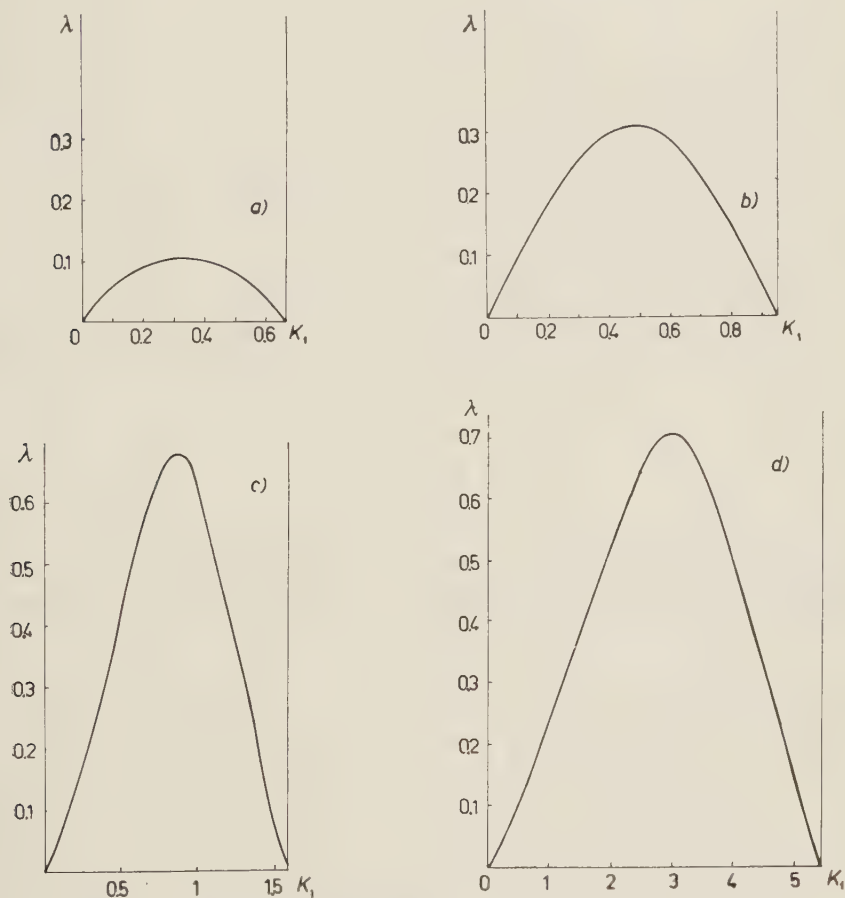


Fig. 9. - Circular polarization degree of k_1 photons counted in coincidence with k_2 photons circularly polarized. - a) $\alpha_1 = \alpha_2 = 90^\circ$, $k_0 = 2$; b) $\alpha_1 = \alpha_2 = 90^\circ$, $k_0 = 20$
c) $\alpha_1 = \alpha_2 = 30^\circ$, $k_0 = 2$; d) $\alpha_1 = \alpha_2 = 30^\circ$, $k_0 = 20$.

We also note that in this case there is no correlation between linear and circular polarization states of the two scattered photons.

* * *

The authors wish to warmly thank Prof. A. BORSELLINO for his constant encouragement during the course of this work, Dr. L. REBOLIA for his vital contribution to the programming and elaboration of the numerical computations, and Dr. C. GULMINELLI for the facilities kindly accorded and for the the useful advice in using the IBM 650 computer besides his great personal interest.

APPENDIX

The azimuthal dependence of the quantities $H^{\alpha_1\alpha_2[\gamma\delta]}$ is of a very simple type. We put:

$$(A.1) \quad H^{\alpha_1\alpha_2[\gamma\delta]} = \exp[\pm i\varphi/2] \exp[in\beta_1] V^{\alpha_1\alpha_2[\gamma\delta]}$$

and the others sixteen amplitudes $H^{\alpha_1\alpha_2 2\gamma\delta}$ are related to these through the relation (7).

The quantities $V^{\alpha_1\alpha_2[\gamma\delta]}$ are independent of the azimuth φ of the electron momentum, while they depend on β_1 and β_2 only through the difference $\beta_1 - \beta_2$ and their integral multiples.

In the relation (A.1) sign \pm holds according to $\gamma = 1$ or 2, and besides

$$(A.2) \quad n = \begin{cases} 0 & \text{for } \gamma = 1, \delta = 2, \\ 1 & \text{for } \gamma = \delta, \\ 2 & \text{for } \gamma = 2, \delta = 1. \end{cases}$$

The relation (A.1) enables us to write explicitly, using only the amplitudes combination rule, the azimuthal dependence of all polarization effects. For example it is easy to obtain the relation (14) and (19) of Section 4.

RIASSUNTO

Le ampiezze di transizione tra tutti gli stati base di polarizzazione di ogni particella che interviene nel doppio effetto Compton sono state dedotte e calcolate numericamente usando un metodo già sviluppato in un altro lavoro. La sezione d'urto e alcuni effetti di polarizzazione sono stati anche discussi in vari casi. La sezione d'urto, come funzione dell'energia di uno dei fotoni emessi, mostra in ogni caso la caratteristica divergenza infrarossa agli estremi dello spettro, una concentrazione dei fotoni in avanti con il crescere dell'energia, e nel caso di uguali condizioni geometriche per i due fotoni diffusi, mostra un minimo quando le energie dei fotoni emessi sono circa uguali. Sono stati inoltre considerati in dettaglio alcuni effetti di polarizzazione lineare e circolare ed i risultati sono stati, per quanto è possibile, confrontati con i corrispondenti dell'effetto Compton semplice. Gli effetti di polarizzazione lineare mostrano alcune differenze qualitative rispetto allo scattering Compton singolo.

On the Gamma Rays Emitted in the Decay of $^{141}_{51}\text{Pr}$.

S. JHA, R. K. GUPTA and H. G. DEVARE

Tata Institute of Fundamental Research - Bombay

(ricevuto il 4 Febbraio 1960)

Summary. — The γ -rays from ^{140}Nd - ^{140}Pr mixture have been studied in a scintillation spectrometer. The new γ -rays of energies (900 ± 20) , (1600 ± 30) and (2500 ± 50) keV have been detected and their intensities in comparison to the 511 keV annihilation radiation are $(0.15 \pm 0.05)\%$, $(0.50 \pm 0.10)\%$ and $(0.02 \pm 0.01)\%$ respectively. The branching ratio from the decay of ^{140}Pr to the ground state, 1600 keV state and 2500 keV state of ^{140}Ce have been estimated, from the photon intensities, to be 99%, $\sim 1\%$ and $\sim 0.2\%$ respectively giving the value of $\log ft \sim 5$ for all these branches. An assignment of 1^+ for ^{140}Pr is suggested.

1. — Introduction.

The isotope ^{140}Pr is known ⁽¹⁾ to decay, with a half-life of 3.5 minutes, by the emission of positons of maximum energy of 2.23 MeV to the ground state of $^{140}_{58}\text{Ce}$. BROWNE *et al.* ⁽²⁾ saw a meagre indication of radiation of energy 1.0 to 1.2 MeV in the decay of the series $^{141}_{60}\text{Nd} \rightarrow ^{140}_{59}\text{Pr} \rightarrow ^{140}_{58}\text{Ce}$. Since the decay energy of ^{140}Nd has been estimated to be (105 ± 40) keV ⁽²⁾, γ -rays, even if emitted in the decay of ^{140}Nd itself, will have energies less than 100 keV. Any high energy γ -rays seen in this decay series, therefore, must originate in the decay of ^{140}Pr .

From the knowledge of the excited states of ^{140}Ce , one can make a fair guess as to the energies of the γ -rays, which are likely to be emitted in the decay of ^{140}Pr . The excited states of ^{140}Ce , fed from the β^- -decay of ^{140}La ,

⁽¹⁾ D. STROMINGER, J. M. HOLLANDER and G. T. SEABORG: *Rev. Mod. Phys.*, **30**, 585 (1959).

⁽²⁾ C. T. BROWNE, J. O. RASMUSSEN, J. P. SURLS and D. F. MARTIN: *Phys. Rev.*, **85**, 146 (1952).

are rather well-known, through the careful work of DZELEPOW *et al.* ^(3,4) and CORK *et al.* ⁽⁵⁾. The excited states of ^{140}Ce have been found at 1596 keV (2^+) 1902 keV (0^+), 2083 keV (4^+), 2343 keV (3^\pm or 4^+), 2515 keV (2^+ or 3^+) and 2890 keV ^(6,9). The shell model prediction and the observed predominant positron decay of ^{140}Pr to the ground state (0^+) of ^{140}Ce indicate that the spin of ^{140}Pr presumably is 0^+ or 1^+ . Since there is about 1600 keV energy available for the positron and the electron capture transition to lead to the first excited (2^+) state of ^{140}Ce , it seemed worth-while looking for the existence of a 1600 keV γ -ray in the decay series $^{140}\text{Nd} \rightarrow ^{140}\text{Pr} \rightarrow ^{140}\text{Ce}$ as the existence or otherwise of this γ -ray would give an important clue as to the spin of the ground state of ^{140}Pr .

2. - Details of the present studies.

About 100 mg of spectroscopically pure Pr_2O_3 were irradiated by the proton beam of the Harwell cyclotron for about 20 minutes, the energy of the proton beam being about 30 MeV. After irradiation, the target was flown to Bombay. After a lapse of about 48 hours from the termination of the bombardment, the studies of the γ -rays emitted by the sample were started. No chemical separation of ^{140}Nd from the praseodymium target was thought necessary.

The γ -rays were studied with a scintillation spectrometer, using a NaI crystal $1\frac{3}{4}$ in. in diameter and 2 in. high coupled to a Dumont 6292 photomultiplier. Spectra were recorded with a single channel analyser. For the study of the low energy γ -ray spectrum (in the region of 50 keV to 600 keV) a weak source was placed at a distance of about 5 cm. In order to look for low intensity, high energy γ -rays, a lead piece about 4 mm thick was inserted between a strong source and the scintillation crystal. In each case, the source was sandwiched between two aluminium discs to ensure the complete annihilation of the positron at the source position. The contribution of the annihilation in flight was subtracted from the γ -ray spectrum. This contri-

(3) B. S. DZELEPOW, YU. V. Kholnov and V. P. PRIKHODTSEVA: *Nucl. Phys.*, **9**, 665 (1958-59).

(4) B. S. DZELEPOW, YU. V. Kholnov and V. P. PRIKHODTSEVA: *Izv. Akad. Nauk SSSR Ser. fiz.*, **22**, 179 (1958).

(5) J. M. CORK, J. LE BLANK, A. STODDARD, D. MARTIN, C. BRANYAN and W. CHILDS: *Phys. Rev.*, **83**, 856 (1951).

(6) H. H. BOLOTIN, C. H. PRUETT, P. L. ROGGENKAMP and R. G. WILKINSON: *Phys. Rev.*, **99**, 62 (1955).

(7) G. R. BISHOP and J. P. PEREZ Y. JORBA: *Phys. Rev.*, **98**, 89 (1955).

(8) W. H. KELLY and M. L. WIEDENBECK: *Phys. Rev.*, **102**, 1130 (1956).

(9) D. F. COLEMAN: *Nucl. Phys.*, **7**, 488 (1958).

From the observation of the decay in time of the intensities of these γ -rays, it was concluded that all of them originated in ^{140}Nd decay. In order to establish the coincidence relationship between the γ -rays, the γ -ray spectrum was taken inside the well of a NaI crystal, 4 in. in diameter and 4 in. high, and compared with the γ -ray spectrum taken with the source outside the crystal. There appears to be a low intensity sum-peak at 2100 keV. The intensity of the peak at 2500 keV did not increase appreciably when the spectrum was taken with the source inside the crystal compared to its intensity when the source was outside the crystal.

3. - Discussion.

From the observation of 1600 keV, 900 keV and 2500 keV γ -rays emitted in the decay series $^{140}\text{Nd} \rightarrow ^{140}\text{Pr} \rightarrow ^{140}\text{Ce}$, and from the knowledge of the levels

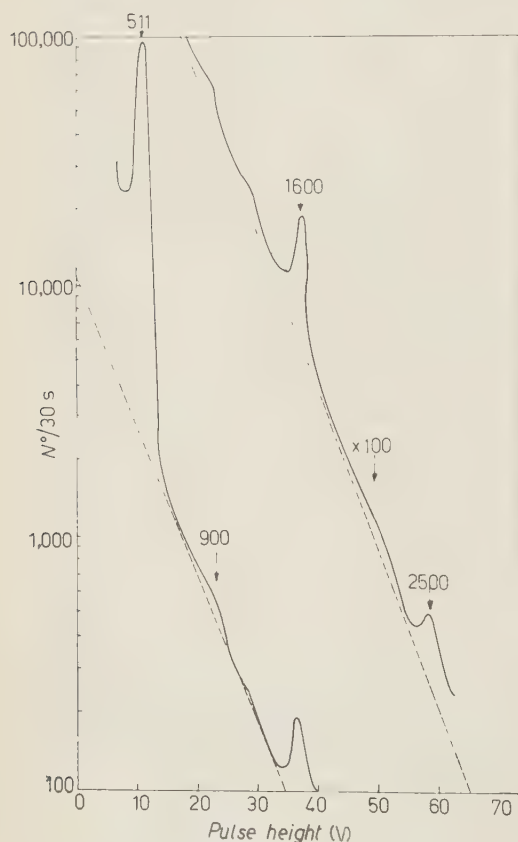


Fig. 2. - Decay scheme of $^{140}\text{Nd} \rightarrow ^{140}\text{Pr} \rightarrow ^{140}\text{Ce}$ and ^{140}La .

in ^{140}Ce from the decay of ^{140}La (Fig. 2), it seems fair to conclude that the decay of ^{140}Pr feeds the ground state, the 1596 keV first excited state, and the 2515 keV state of ^{140}Ce . The predominant transition to the ground state takes place by positron emission. The observation of a small sum-peak at 2100 keV (1600 keV + 510 keV) points to the conclusion that there is a small positron branching to the 1600 keV also. Although no significant increase in the peak area of the 2500 keV γ -rays was observed when the source was placed inside the crystal, it is difficult to interpret the emission of the 900 keV γ -ray in any way other than that it arises from the transition from the 2500 keV state to the 1596 keV state. If one takes into account the relative intensities of the 900 keV γ -ray and the 2500 keV γ -ray and their photoefficiencies in a 4 in. \times 4 in. NaI(Tl) crystal, one can see that

the expected increase in the peak area at 2500 keV would not be appreciable. It may be pointed out here that the ratio of the intensities of the stop-over transition (900 keV γ -ray) and the cross-over transition (2500 keV γ -ray) is 7 ± 4 as compared to 3 ± 2 found by COLEMAN (8). In the light of this discussion and from the relative intensities given in Table I, the branching ratios to the ground state, 1596 keV state and the 2500 keV state have been estimated to be 99%, 1% and 0.2% respectively. The $\log ft$ values for all these decay branches are about 5.

From the fact that the 1596 keV state and the 2500 keV state have been assigned (5-8) spin and parity 2^- , and that the decay of ^{140}Pr leads to the ground state and to both these excited states with the allowed $\log ft$ value of about 5, one could safely conclude that the spin and the parity of the ground state of ^{140}Pr is 1^+ .

In this connection, it may be pointed out that a level in ^{140}Ce has been detected at 1902 keV (3, 4) which is assigned the spin and parity 0^+ . One would think that some electron-capture decay of ^{140}Pr should lead to this state also. This state would decay to the ground state by electron emission only, and therefore would not show up in the scintillation γ -ray spectrometer. The low energy portion of the spectrum of the γ -ray was carefully analysed to see if one could find any evidence of the presence of a γ -ray of energy about 300 keV due to the transition from the 1902 keV state to the 1596 keV state. Beyond placing an upper limit of about 1% as to the intensity of this possible γ -ray in comparison to the annihilation γ -ray intensity, no definite statement can be made about the level at 1902 keV being fed in the decay of ^{140}Pr .

B. S. DZHELEPOV, I. F. UCHEVATKIN and S. A. SHESTOPALOVA (*Žurn. Éxp. Teor. Fiz.*, **37**(10) 611 (1960)) have recently observed the conversion electron of the transition from 1902 keV state to the ground state of $^{140}\text{Ce}(\nu^+ \rightarrow 0^+)$ in the decay of ^{140}Pr .

RIASSUNTO (*)

I raggi γ provenienti da una miscela di ^{140}Nd - ^{140}Pr sono stati studiati in uno spettrometro a scintillazione. Sono stati individuati nuovi raggi γ di energia (900 ± 20) , (1600 ± 30) e (2500 ± 50) keV e le loro intensità confrontate alla radiazione di annichilazione di 511 keV sono $(0.15 \pm 0.05)\%$, $(0.50 \pm 0.10)\%$ e $(0.02 \pm 7.01)\%$ rispettivamente. Dalle intensità dei fotoni si è valutato che il rapporto di branching per il decadimento del ^{140}Pr allo stato base, allo stato a 1600 keV ed allo stato a 2500 keV del ^{140}Ce , è 99%, $\sim 1\%$ e $\sim 0.2\%$ rispettivamente, che danno il valore di $\log ft \sim 5$ per tutte queste ramificazioni. Si suggerisce di assegnare 1^+ al ^{140}Pr .

(*) Traduzione a cura della Redazione.

Reduction of Spurious Scattering in Ilford G-5 and K-5 Emulsions.

B. JUDEK

Division of Pure Physics, National Research Council - Ottawa

(ricevuto l'8 Febbraio 1960)

Summary. — In an attempt to reduce the amount of spurious scattering in the emulsions, two batches of Ilford G-5 and two batches of Ilford K-5 stripped emulsions, 600 μm thick, have been exposed to the 6.2 GeV internal proton beam from the Berkeley Bevatron, and developed in several different ways. The methods of development used included isothermal development at 5 °C, 10 °C and 15 °C, and temperature cycle development with the warm stages at 10 °C, 15 °C and 20 °C with the plates immersed in a boric acid-potassium bromide solution. For comparison some emulsions were also developed with the « dry », warm development at 25 °C which was usually employed in previous work. As a further precaution against distortions in the emulsions potassium alum hardener has been added to the fixing bath, and the emulsions were dried slowly at a temperature below 10 °C. Scattering measurements performed on the 6.2 GeV proton tracks in the emulsions have shown that the spurious scattering has been reduced to about half of the value which has usually been obtained previously and by other workers. This applies to all the plates, except for a G-5 emulsion from one batch and developed at 25 °C. It has been observed that the amount of spurious scattering depends on the development temperature: (i) It does not change between temperatures of 5 °C and 10 °C. (ii) Above 10 °C there is a gradual increase with temperature. (iii) In some batches of emulsions a marked increase of spurious scattering occurs at a temperature of about 25 °C. Some variation in the amount of spurious scattering present in the different batches of emulsions used has been observed, but there appears to be no difference in that respect between the G-5 and the K-5 emulsions. Good grain densities on minimum tracks and improved uniformity of development with depth in both the G-5 and the K-5 emulsions have been obtained using the temperature cycle methods of development with warm stages at 10 °C, 15 °C and 20 °C.

1. - Introduction.

The effect of the spurious scattering distortion of tracks, caused by small local dislocations occurring in the emulsions, has first been observed and studied by BISWAS, PETERS and RAMA ⁽¹⁾, and then by several other investigators ⁽²⁻⁶⁾ in stacks of Ilford G-5 emulsions exposed to cosmic rays and also to mono-energetic high energy particles from the Berkeley Bevatron. The presence of this type of distortion was found to impair greatly the reliability of measurements of multiple coulomb scattering of fast charged particles in the emulsions. In fact, the various investigations mentioned above show that above energies varying between five and one GeV per unit charge, according to the amount of spurious scattering present in a particular plate, energy determinations from direct scattering measurements are not possible.

The presence of the spurious scattering distortion is usually attributed partly to the imperfections of the emulsion itself and partly to the methods of processing. Until now very similar procedures based on the temperature cycle method of Dilworth *et al.* ⁽⁷⁾ with the warm development stage at temperatures varying from 24 °C to 30 °C were used by most workers. It has been observed recently by the author ⁽⁸⁾ that in a cosmic ray stack of G-5 stripped emulsions, for which the warm development temperature has been reduced to 10 °C, the amount of spurious scattering present was about half of the value usually obtained. This result is in agreement with the generally recognized fact that swelling and softening of wet gelatine, especially at higher temperatures close to its melting point, is one of the factors causing distortions in the emulsions.

In the present work an attempt has been made to reduce the amount of spurious scattering by modifying the methods of processing of the emulsions. Special emphasis has been laid on the lowering of the development temperature and on the elimination of the « dry » stage, the latter having proved rather cumbersome in handling large stacks of emulsions. Several new developing procedures have been tried including temperature cycle development with

(1) S. BISWAS, B. PETERS and H. RAMA: *Proc. Ind. Acad. Sci.*, A **41**, 154 (1955).

(2) H. FAY: *Zeits. f. Naturfor.*, **10a**, 572 (1955).

(3) E. LOHRMANN and M. TEUCHER: *Nuovo Cimento*, **3**, 59 (1956).

(4) F. A. BRISBOUT, C. DAHANAYAKE, A. ENGLER, P. H. FOWLER and P. B. JONES: *Nuovo Cimento*, **3**, 1400 (1956).

(5) A. J. APOSTOLAKIS, J. O. CLARKE and J. V. MAJOR: *Nuovo Cimento*, **5**, 377 (1957).

(6) F. W. FISHER and J. J. LORD: *Nuovo Cimento*, **11**, 44 (1959).

(7) C. C. DILWORTH, G. OCCHIALINI and L. VERMAESEN: *Bull. Centre Phys. Nucléaire Univ. Libre Bruxelles*, Note 13a (1950).

(8) B. JUDEK: *Can. Journ. Phys.*, **37**, 102 (1959).

warm stages at 10 °C, 15 °C and 20 °C, as well as isothermal development at 5 °C, 10 °C and 15 °C. In order to reduce the amount of swelling of the emulsions (especially during their final washing) potassium alum hardener was added to the fixing bath. As a further precaution against distortion the plates were dried slowly in a refrigerator at a temperature below 10 °C.

Two batches of Ilford G-5 and two batches of Ilford K-5 stripped emulsions, 600 μm thick, exposed to the 6.2 GeV internal proton beam from the Berkeley Bevatron were used in these experiments.

2. - Experimental details.

One stack consisting of Ilford G-5 stripped emulsions, 600 μm thick batch Z1401, and Ilford K-5 emulsions, batch Z1398 and one stack of G-5 emulsions, batch Z1284, and K-5 emulsions, batch Z1285, have been exposed to the 6.2 GeV internal proton beam from the Berkeley Bevatron. The direction of the beam was almost parallel to the plane of the emulsions and the average track length in a single sheet of emulsion was greater than 5 cm in the first stack and about 3 cm in the second stack. At the time of the exposure the emulsions in the first stack were six weeks old, and in the second stack three months old. Prior to the exposure they were stored at 0 °C. After the exposure they were also stored and transported under refrigeration. The first stack was processed five days, and the second three weeks, after the exposure.

2.1. Processing.

(i) Mounting: The emulsions were mounted on glass one day before the processing using the mounting procedure described previously ⁽⁸⁾. In order to improve the adherence to the glass a more concentrated gelatine solution (2%) was used for treatment of both the glass and the emulsion. The plates were dried in an inverted position after mounting over trays containing calcium chloride as drying agent and were stored overnight in a refrigerator at about 5 °C.

(ii) Development: The plates were developed in several different ways. Two methods of isothermal development at 5 °C, 10 °C and 15 °C were tried as well as temperature cycle development with warm stages at 10 °C, 15 °C and 20 °C. The «dry» development stage has been replaced by soaking of the emulsions in a boric acid solution to which potassium bromide restrainer has been added. Amidol developers of different concentrations and pH were used. In order to obtain uniform grain densities throughout the whole depth of the emulsion two methods of compensating for the quicker penetration of the developer to its top layers were used. In the first, the bottom of the emul-

sion was maintained at a higher pH than the top during actual development by presoaking the plates in a borax-boric acid buffer solution of pH higher than that of the developer (amidol with boric acid) ⁽⁹⁾. In the second method, by replacing the «dry» development stage by immersion of the emulsions in the boric acid-potassium bromide solution after they have been soaked in the developer, a gradual dilution of the developer with the simultaneous lowering of its pH, starting at the top of the emulsions, has been obtained. For comparison, some plates were developed by the temperature cycle method which had been employed previously and used with a dry warm stage at 25 °C.

TABLE I. — *Isothermal development procedures.*

Temperature	Presoaking		Soaking in developer		Dilution of developer		Stop bath (1% acetic acid at 5 °C)
	Solution	Time	Developer	Time	Solution	Time	
5 °C (a)	Borax pH 9.3	2.5 h	Acid amidol	5.5 h	Boric acid potassium bromide (a)	3 h	30 min
5 °C (b)	Distilled water	2.5 h	Normal amidol ($\frac{2}{3}$ strength)	5.5 h	Boric acid potassium bromide (a)	3 h	30 min
10 °C (a)	Borax pH 9.3	2 h	Acid amidol	3.5 h	Boric acid potassium bromide (a)	2 h	30 min
10 °C (b)	Distilled water	2 h	Normal amidol ($\frac{2}{3}$ strength)	3.5 h	Boric acid potassium bromide (a)	2 h	30 min
15 °C (a)	Borax- boric acid pH 8.5	1.5 h	Acid amidol	2 h	Boric acid potassium bromide (b)	1.5 h	30 min
15 °C (b)	Distilled water	1.5 h	Normal amidol ($\frac{1}{2}$ strength)	2 h	Boric acid potassium bromide (a)	1.5 h	30 min

The details of the various developing procedures are given in Tables I and II. The chemical compositions of the solutions used are given in the Appendix.

⁽⁹⁾ H. G. DE CARVALHO: private communication, 2^e Colloque International de Photographie Corpusculaire (Montreal, 1958).

TABLE II. - *Temperature cycle development procedures.*

Temperature of the warm stage	Presoaking in distilled water at 5 °C	Soaking in developer at 5 °C		Dilution of developer at warm stage temperature		Stop bath (1% acetic acid at 5 °C)
		Developer	Time	Solution	Time	
10 °C	2.5 h	Normal amidol	4 h	Boric acid-potassium bromide (a)	2 h	30 min
15 °C	2.5 h	Normal amidol	4 h	Boric acid-potassium bromide (a)	1.5 h	30 min
20 °C	2.5 h	Normal amidol	4 h	Boric acid-potassium bromide (b)	1 h	30 min
25 °C	2.5 h	Acid amidol	2.5 h	« Dry » development	50 min	2.5 h

(iii) Fixation, Washing and Drying: An acid fixing bath of chemical composition recommended by THURO and PAIC⁽¹⁰⁾, to which potassium alum hardener has been added, was used. As some preliminary tests have shown, the presence of hardener in the fixer completely checks the additional swelling of the emulsions such as usually occurs during their final washing. It was also found to have the effect of reducing the number and size of « bubbles » formed due to the imperfections of mounting. It has been observed, however, that emulsions fixed in a bath containing a hardening agent have a greater tendency for stripping from the glass, at low humidities. Soaking the emulsions in a glycerine solution of higher concentration than it was customary before drying, or protecting them from loss of moisture by covering their surface with transparent varnish, may prevent this. As a protection against corrosion of the developed grains some silver bromide has been dissolved in the fixer⁽¹¹⁾, prior to its use. The chemical composition of the fixing bath is given in the Appendix.

The emulsions were fixed at 6 °C for about 4 days, and then after gradual dilution of the fixer, they were washed at the same temperature for two days. After washing they were soaked for 6 hours at 6 °C in a 30% alcohol and 3% glycerine solution, and dried slowly in an inverted position over trays containing calcium chloride in a refrigerator at a temperature of about (5 ÷ 10) °C,

⁽¹⁰⁾ G. THURO and M. PAIC: *Nuovo Cimento*, **4**, 887 (1956).

⁽¹¹⁾ H. BRAUN, G. CORNIL and G. MEULEMANS: *Proc. Bagnères Conf.* (1953), p. 61.

2'2. *Measurements of spurious scattering.* — Multiple scattering measurements were made in the usual way ⁽¹²⁾ using a Koristka MS-2 microscope. In the case of the first stack of G-5 and K-5 emulsions measurements were made on plates developed by all the different methods described above. In the case of the second stack, measurements were made only in emulsions for which the four temperature cycle procedures and one isothermal method at 5° were used. The tracks were selected at random throughout the whole depth of the emulsions. Basic cell lengths of 500 μm and 1000 μm were used. The measurements with 500, 1000, 2000, and 4000 μm cell lengths include respectively about 300, 250, 120, and 50 independent cells in each plate. The standard 4X cut-off procedure without replacement has been applied to the observations. The values of the mean sagitta of spurious scattering (D_{ss}) were calculated from the measurements of the observed scattering (D_o) by the usual relation:

$$D_{ss}^2 = D_o^2 - D_r^2 - \epsilon_{RG}^2.$$

The theoretical values of the sagitta of the multiple coulomb scattering (D_r) for the 6.2 GeV protons ($p\beta = 7.0 \text{ GeV}/c$) were calculated using Molière's scattering constants ⁽¹³⁾. The grain and reading noise (ϵ_{RG}) was determined for the G-5 and the K-5 emulsions separately by the method of Peters ⁽¹⁾, taking scattering measurements with cell lengths of 50 μm . At this cell length both real and spurious scattering can be assumed as negligible in comparison with the reading and grain noise. The noise level of the Koristka microscope was assumed to be negligible.

2'3. *Measurements of grain densities.* — For comparison of the degree and uniformity of development with depth obtained using the various methods of processing of the emulsions, 2500 \div 3000 blobs were counted in each plate, on the 6.2 GeV proton tracks at the depth of (50 \div 70) μm of emulsion thickness before processing below the surface, and at (50 \div 70) μm above the glass. These measurements were carried out in the G-5 and the K-5 emulsions from the first stack only.

3. — Results and discussion.

3'1. *Spurious scattering.* — The results of the scattering measurements performed in the emulsions are shown in the tables below. Table III gives the

⁽¹²⁾ P. H. FOWLER: *Phil. Mag.*, **41**, 169 (1950).

⁽¹³⁾ K. GOTTSTEIN, M. G. K. MENON, J. H. MULVEY, C. O'CEALLAIGH and O. ROCHAT: *Phil. Mag.*, **42**, 708 (1951).

theoretical values of the mean sagittae of multiple coulomb scattering for the 6.2 GeV protons. The actual observations made in the different plates

TABLE III. - *Theoretical values of sagittae of multiple scattering of 6.2 GeV protons (D_T).*

Cell length D_T	500 μm .070 μm	1 000 μm .207 μm	2 000 μm .605 μm	4 000 μm 1.76 μm
----------------------	---	---	---	---

in the four batches of emulsions used are given in Tables IV, *a*, *b*, *c*, and *d*. The reading and grain noise was found to be $(.087 \pm .002) \mu\text{m}$ in the G-5, and $(.068 \pm .002) \mu\text{m}$ in the K-5 emulsions. The calculated mean values of the sagittae of spurious scattering at different development temperatures in the four batches of emulsions are given in Tables V, *a*, *b*, *c*, and *d*.

The values of D_{ss} at 1000 μm cell length are probably most suitable as a basis of comparison between the plates. Their magnitude is comparable with that of the real scattering of the 6.2 GeV protons, and twice as high as the reading and grain noise. With higher cell lengths the measurements are probably affected by long range distortions in the emulsions due to the fact that the pellicles are not always perfectly flat and therefore become distorted on mounting them on glass. Moreover, the values of the theoretical scattering constant used in the calculation of spurious scattering have not yet been verified with sufficient accuracy for longer cell lengths and high energies.

The results can be summarized as follows:

- 1) In all the plates for which the measurements have been carried out, except for the G-5 Z1401 emulsion developed at 25 °C (Tables V, *a-d*), a much lower amount of spurious scattering has been obtained in this experiment than in most of the previous investigations. Its magnitude at 1000 μm cell length varies between .13 and .24 μm with an average of .17 μm . This is about half of the value of .34 μm which has been observed in glass backed emulsion by FISHER and LORD (*) who have also made the measurements on tracks of the 6.2 GeV protons. This general reduction of the spurious scattering may be due to an improvement, in this respect, of the quality of the particular batches of emulsions used. On the other hand, improvements in the processing techniques may have been made. Comparison with other published work is made difficult by the fact that exact details of processing are not given in most of the reports. It is possible that even the 25 °C development temperature (which seems to be on the borderline for the increase in the amount of spurious scattering) is lower than temperatures employed by the other workers in their investigations. The introduction of the hardener into the fixing bath, and the low temperature drying, may have also contributed to the general reduction of the amount of spurious scattering present in the plates.

TABLE IV. - *Observed values of mean sagittae of scattering of 6.2 GeV protons in the emulsions (D_0 in μm).*

Method of development	Cell length			
	500 μm	1 000 μm	2 000 μm	4 000 μm
(a) G-5 Z1401 emulsions				
5 °C isothermal (a)	.134 \pm .006	.338 \pm .015	.83 \pm .06	2.78 \pm 0.25
5 °C isothermal (b)	.131	.261	.69	1.83
Mean	.132 \pm .004	.235 \pm .01	.76 \pm .04	2.30 \pm 0.2
10 °C isothermal (a)	.154 \pm .006	.278 \pm .015	.73 \pm .06	1.92 \pm 0.25
10 °C isothermal (b)	.126	.266	.68	2.21
10 °C temperature cycle	.146	.315	.79	2.28
Mean	.142 \pm .004	.286 \pm .01	.73 \pm .04	2.13 \pm 0.2
15 °C isothermal (a)	.130 \pm .006	.270 \pm .015	.74 \pm .06	1.85 \pm 0.25
15 °C isothermal (b)	.144	.309	.90	2.72
15 °C temperature cycle	.154	.295	.84	1.97
Mean	.143 \pm .004	.291 \pm .01	.83 \pm .04	2.18 \pm 0.2
20 °C temperature cycle	.154 \pm .006	.299 \pm .015	.75 \pm .06	2.15 \pm 0.3
25 °C temperature cycle	.200 \pm .007	.425 \pm .02	1.04 \pm .08	2.37 \pm 0.3
(b) G-5 Z1284 emulsions				
5 °C isothermal	.137 \pm .006	.278 \pm .015	.81 \pm .06	1.95 \pm 0.25
10 °C temperature cycle	.115	.262	.62	1.62
15 °C temperature cycle	.128	.276	.76	2.22
20 °C temperature cycle	.156	.332	.79	2.08
25 °C temperature cycle	.145	.294	.72	1.83
(c) K-5 Z1398 emulsions				
5 °C isothermal (a)	.131 \pm .006	.241 \pm .015	.64 \pm .06	1.75 \pm 0.25
5 °C isothermal (b)	.149	.288	.80	2.15
Mean	.140 \pm .004	.265 \pm .01	.72 \pm .04	1.95 \pm 0.2
10 °C isothermal (a)	.142 \pm .006	.289 \pm .015	.71 \pm .06	1.61 \pm 0.25
10 °C isothermal (b)	.139	.306	.74	1.98
10 °C temperature cycle	.128	.251	.64	1.95
Mean	.136 \pm .004	.282 \pm .01	.70 \pm .04	1.85 \pm 0.2
15 °C isothermal (a)	.141 \pm .006	.307 \pm .015	.72 \pm .06	1.86 \pm 0.25
15 °C isothermal (b)	.128	.288	.86	2.60
15 °C temperature cycle	.141	.269	.71	2.16
Mean	.137 \pm .004	.288 \pm .010	.76 \pm .04	2.21 \pm 0.2
20 °C temperature cycle	.156 \pm .006	.307 \pm .015	.76 \pm .06	2.38 \pm 0.25
25 °C temperature cycle	.154 \pm .006	.283 \pm .015	.75 \pm .06	2.20 \pm 0.25
(d) K-5 Z1285 emulsions				
5 °C isothermal	.120 \pm .006	.253 \pm .015	.60 \pm .06	1.76 \pm 0.25
10 °C temperature cycle	.115	.257	.81	2.32
15 °C temperature cycle	.131	.265	.80	2.34
20 °C temperature cycle	.134	.264	.71	2.19
25 °C temperature cycle	.146	.290	.77	2.49

2) Some variation of the amount of the spurious scattering in the different batches of emulsions can be observed (Tables V, *a-d*), the G-5 and K-5 emulsions from the first stack having higher spurious scattering than the G-5 and K-5 emulsions from the second stack. On the other hand, there appears to be no difference, in this respect, between G-5 and K-5 emulsions.

TABLE V. - *Values of mean sagittae of spurious scattering in the emulsions (D_{83} in μm).*

Development temperature	Cell length			
	500 μm	1 000 μm	2 000 μm	4 000 μm
(a) G-5 Z1401 emulsions				
5 °C	.070 \pm .006	.175 \pm .02	.45 \pm .1	1.48 \pm 0.3
10 °C	.088	.177	.40	1.20
15 °C	.089	.185	.56	1.28
20 °C	.092	.197	.44	1.23
25 °C	.166	.360	.84	1.59
(b) G-5 Z1284 emulsions				
5 °C	.079 \pm .006	.165 \pm .02	.54 \pm .1	0.84 \pm 0.3
10 °C	.027	.135	.13	0.0
15 °C	.062	.160	.45	1.35
20 °C	.109	.244	.52	1.10
25 °C	.092	.190	.39	0.50
(c) K-5 Z1398 emulsions				
5 °C	.100 \pm .006	.151 \pm .02	.38 \pm .1	.84 \pm 0.3
10 °C	.095	.179	.34	.57
15 °C	.096	.188	.45	1.33
20 °C	.122	.216	.45	1.60
25 °C	.119	.183	.44	1.32
(d) K-5 Z1285 emulsions				
5 °C	.070 \pm .006	.129 \pm .02	.00 \pm .1	0.0 \pm 0.3
10 °C	.061	.136	.53	1.51
15 °C	.088	.151	.52	1.54
20 °C	.092	.149	.36	1.30
25 °C	.108	.191	.47	1.76
(e) Average values				
5 °C	.080 \pm .003	.155 \pm .01	.342 \pm .05	.79 \pm .15
10 °C	.068	.157	.350	.82
15 °C	.084	.171	.495	1.37
20 °C	.104	.201	.442	1.41
25 °C	.121	.231	.535	1.25

3) The results of measurements on individual plates (Tables IV, *a-d*) show that for a given development temperature the amount of spurious scattering present in the emulsion does not appear to depend on the particular method of development chosen (involving use of solutions of various pH values, sudden changes of temperature, etc.). The random variations from plate to plate, however, seem to be greater than expected from statistical considerations.

4) An effect of an increase of the amount of spurious scattering with development temperature has been observed. This can be most clearly seen

TABLE VI. — *Blob densities in Ilford G-5 and K-5 emulsions.*

Method of development	Type of emulsion	Blobs per 100 μm			Depth (*) variation %
		near surface	near glass	average	
5 °C isothermal (<i>a</i>)	G-5	14.2 ± 0.5	13.8 ± 0.4	14.0 ± 0.3	3 ± 4
	K-5	12.7 ± 0.4	12.2 ± 0.4	12.5 ± 0.3	4 ± 4
5 °C isothermal (<i>b</i>)	G-5	15.6 ± 0.4	14.4 ± 0.4	15.0 ± 0.3	8 ± 4
	K-5	14.8 ± 0.4	12.9 ± 0.4	13.9 ± 0.3	13 ± 4
10 °C isothermal (<i>a</i>)	G-5	16.1 ± 0.4	15.4 ± 0.4	15.8 ± 0.3	4.5 ± 4
	K-5	14.2 ± 0.4	12.7 ± 0.4	13.5 ± 0.3	11 ± 4
10 °C isothermal (<i>b</i>)	G-5	16.3 ± 0.4	14.9 ± 0.4	15.6 ± 0.3	9 ± 4
	K-5	14.9 ± 0.4	13.5 ± 0.4	14.2 ± 0.3	11 ± 4
15 °C isothermal (<i>a</i>)	G-5	17.7 ± 0.4	14.0 ± 0.4	15.9 ± 0.3	23 ± 4
	K-5	15.4 ± 0.4	11.4 ± 0.3	13.4 ± 0.3	30 ± 4
15 °C isothermal (<i>b</i>)	G-5	17.1 ± 0.4	13.6 ± 0.4	15.4 ± 0.3	23 ± 4
	K-5	14.7 ± 0.4	11.9 ± 0.3	13.3 ± 0.3	21 ± 4
10 °C temperature cycle	G-5	17.4 ± 0.4	16.3 ± 0.3	16.9 ± 0.3	6.5 ± 3
	K-5	15.4 ± 0.4	15.0 ± 0.4	15.2 ± 0.3	2.6 ± 4
15 °C temperature cycle	G-5	18.2 ± 0.4	17.8 ± 0.4	18.0 ± 0.3	2.2 ± 4
	K-5	15.2 ± 0.4	15.8 ± 0.4	15.5 ± 0.3	— 4 ± 4
20 °C temperature cycle	G-5	19.3 ± 0.4	20.0 ± 0.4	19.7 ± 0.3	— 3.5 ± 3
	K-5	17.3 ± 0.4	16.8 ± 0.4	17.1 ± 0.3	3 ± 3
25 °C temperature cycle	G-5	19.1 ± 0.4	17.4 ± 0.4	18.3 ± 0.3	9.5 ± 3
	K-5	18.9 ± 0.4	15.2 ± 0.4	17.1 ± 0.3	22 ± 3

(*) Depth variation = $\frac{(\text{blob density near surface}) - (\text{blob density near glass})}{\text{average blob density}}$

from Table V(e) in which the values obtained for all the four batches of emulsions have been averaged; i) there is no change in the amount of spurious scattering between temperatures of 5 °C and 10 °C; ii) above 10 °C a gradual increase with temperature can be observed; iii) in some batches of emulsions a more marked increase of spurious scattering occurs at a temperature of 25 °C or even 20 °C. This, for example can be observed at 25 °C in G₅ Z 1401 and K₅ Z 1285 emulsions, and possibly at 20 °C in G₅ Z 1284 emulsions.

3'2. *Comparison of the different methods of development.* – The results of the blob density measurements on the 6.2 GeV proton tracks in the G-5 and the K-5 emulsions developed by the different methods are given in Table VI. It can be seen that the best results have been obtained using the temperature cycle development with warm stages at all three temperatures of 20 °C, 15 °C and 10 °C with the plates immersed in the boric acid-potassium bromide solution. The grain densities on the minimum tracks are comparable with those obtained using the « standard » development with the dry warm stage at 25 °C while the uniformity of development with depth in the emulsion is much better. This is what should be expected since in this method the temperature change, gradual dilution of the developer, and lowering of its pH at the top of the emulsion, are all combined to compensate for the quicker penetration of the developer to the top layers of the emulsion. The isothermal development at 5 °C and 10 °C also gives a good uniformity of development with depth, although the grain densities on the minimum tracks are rather low.

It can be observed that in the present results the grain densities in the K-5 emulsions are always lower than in the corresponding G-5 emulsions. However, in some preliminary development tests for which different emulsion batches were used, the same or even higher grain densities in the K-5 than in the G-5 emulsions have been obtained with the same development.

4. – Conclusions.

In the present investigation a considerable reduction of the spurious scattering distortion in the emulsions has been obtained. Several new developing procedures have been tried and the results show that lowering of the development temperature has the effect of decreasing the amount of spurious scattering present in the emulsions, while at the same time good grain densities on minimum tracks and uniformity of development with depth, can be obtained. With the level of spurious scattering obtained in the present experiments it may be possible to extend the measurements of multiple scattering in the emulsions to particles of energies up to about 10 GeV per unit charge.

* * *

I wish to thank Dr. E. J. LOFGREN and the Staff of the Berkeley Bevatron, and also Dr. I. J. VAN HEERDEN for exposing the emulsion stacks to the 6.2 GeV proton beam.

APPENDIX

Chemical formulas of solutions used for processing of the emulsions.

Borax, pH 9.3

Borax	19.1	g
Distilled water	1000	cm ³

Borax boric acid, pH 8.5

Borax	19.1	g
Boric acid (crystals)	12.4	g
Distilled water	2000	cm ³

Normal amidol developer

Sodium sulphite (anhydrous)	18	g
Amidol	4.5	g
Potassium bromide (10% solution)	8	cm ³
Distilled water	1000	cm ³

Normal amidol developer ($\frac{2}{3}$ strength)

Sodium sulphite (anhydrous)	12	g
Amidol	3	g
Potassium bromide (10% solution)	8	cm ³
Distilled water	1000	cm ³

Normal amidol developer ($\frac{1}{2}$ strength)

Sodium sulphite (anhydrous)	9	g
Amidol	2.25	g
Potassium bromide (10% solution)	8	cm ³
Distilled water	1000	cm ³

Acid amidol developer

Sodium sulphite (anhydrous)	18	g
Boric acid (crystals)	35	g
Amidol	4.5	g
Potassium bromide (10% solution)	8	cm ³
Distilled water	1000	cm ³

Boric acid-potassium bromide solution (a)

Boric acid (crystals)	12.4	g
Potassium bromide (10% solution)	8	cm ³
Distilled water	1000	cm ³

Boric acid-potassium bromide solution (b)

Boric acid (crystals)	35	g
Potassium bromide (10% solution)	8	cm ³
Distilled water	1000	cm ³

Stop bath

Acetic acid - 1% solution

Fixer

Sodium thiosulphate	300	g
Sodium sulphite (anhydrous).	5	g
Acetic acid.	4	cm ³
Potassium alum	10	g
Distilled water to.	1000	cm ³

Concentration of Ag⁺ ions in the fixer (2 ÷ 4) g per 1000 c.c.

RIASSUNTO (*)

Nel tentativo di ridurre l'ammontare di scattering spurio nelle emulsioni, due pacchi di pellicole staccate Ilford G-5 e due di Ilford K-5, dello spessore di 600 μm sono stati esposti al fascio interno di protoni da 6.2 GeV del Bevatrone di Berkeley, e sono stati sviluppati con diversi procedimenti. I metodi seguiti comprendevano lo sviluppo isoteramico a 5 °C, 10 °C e 15 °C e lo sviluppo a ciclo di temperatura con gli stadi caldi a 10 °C, 15 °C e 20 °C mentre le lastre erano immerse in una soluzione di acido borico e bromuro di potassio. Per confronto alcune pellicole vennero anche sviluppate col metodo di sviluppo caldo « a secco » a 25 °C che è stato di solito usato nei lavori precedenti. Come ulteriore precauzione contro le deformazioni delle pellicole al bagno di fissaggio fu aggiunto allume potassico come indurente, e le pellicole furono fatte asciugare.

(*) Traduzione a cura della Redazione.

gare lentamente a temperatura inferiore a 10°C . Le misure di scattering eseguite sulle tracce dei protoni di 6.2 GeV nelle emulsioni hanno dimostrato che lo scattering spurio è stato ridotto a metà del valore precedentemente ottenuto da noi e da altri autori. Questo vale per tutte le lastre, tranne per una pellicola G-5 di un pacco sviluppata a 25°C . Si è osservato che l'ammontare di scattering spurio dipende dalla temperatura di sviluppo come segue: *a*) non varia tra le temperature di 5°C e 10°C ; *b*) al disopra dei 10°C si ha un graduale incremento con la temperatura; *c*) in qualche pacco di emulsioni si osserva un marcato aumento dello scattering spurio a temperature di circa 25°C . Al di sotto della temperatura critica si è riscontrato un piccolo aumento dello scattering spurio con la temperatura. Si sono osservate alcune variazioni nell'ammontare dello scattering spurio presente nei differenti pacchi di pellicole, ma non sembra ci sia alcuna differenza a questo riguardo fra le emulsioni G-5 e K-5. Buone densità di grana su tracce minime e migliore uniformità di sviluppo nello spessore nelle emulsioni G-5 e K-5 sono state ottenute usando i metodi di sviluppo a ciclo di temperatura con lo stadio caldo a 10°C , 15°C e 20°C .

Die elastische und inelastische Streuung von negativen K-Mesonen an freien Protonen bei Energien bis 90 MeV.

H. GÖING

Max-Planck-Institut für Physik und Astrophysik - München

(ricevuto il 12 Febbraio 1960)

Summary. — In the present work the total and differential cross-sections for elastic and inelastic scattering of negative K-mesons from free protons for energies up to 90 MeV in nuclear emulsions have been determined. The track length followed is 671.78 m. The differential cross-sections show that *S*-scattering suffices for the description of these processes and Coulomb-scattering can be neglected for the angles here considered ($> 20^\circ$). A simple theory has been employed for the description of these interactions and a phase-shift-analysis carried out for both possible isotopic spin states $T=0$ and $T=1$. It turns out that absorption and shadow-scattering in the state $T=0$ is greater than in the state $T=1$. The scattering length calculated here has been used to calculate the cross-sections at high energies. They agree very well with the experimental values.

Einleitung.

Wechselwirkungen zwischen negativen K-Mesonen und Wasserstoffkernen, d.h. freien Protonen wurden in einem Block aus 105 600 μm dicken Ilford G-5 Emulsionen mit den Gesamtabmessungen $(13.5 \times 8.5 \times 6.3)$ cm untersucht, der am 300 MeV/c K^- -Strahl des Bevatrons in Berkeley (Cal.) exponiert worden war. Etwa 20 000 K^- -Mesonen wurden in Zusammenarbeit mit den Instituten in Paris (10%), Bologna (31%) und Parma (14%) nahe beim Eintritt in den Block gefunden und bis zum Ende verfolgt. Die Verteilung der Spurlängen in den einzelnen Energieintervallen zeigt Fig. 1.

Die auftretenden Reaktionen mit Wasserstoffkernen lassen sich in zwei Gruppen einteilen:

1.) elastische Streuung $K^- + p \rightarrow K^- + p$

2.) inelastische Streuung $K^- + p \rightarrow \begin{cases} \bar{K}^0 + n \text{ Ladungsaustausch} \\ Y + \pi \text{ Erzeugung von Hyperonen} \end{cases}$

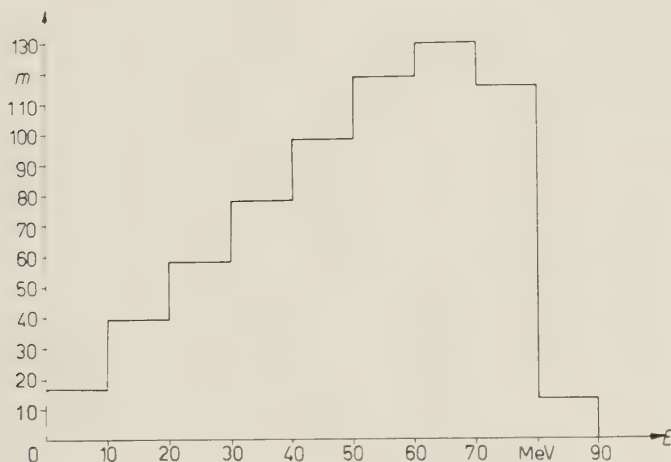


Fig. 1. - Verteilung der Spurlängen in den einzelnen Energie-Intervallen.

1. - Ergebnisse zur elastischen Streuung.

Die Analyse geschah mit Hilfe der Kinematik. Zur Vermeidung von Verwechslungen mit Streuungen an komplexen Kernen wurden solche Ereignisse fortgelassen, bei denen die Reichweite des Protons $\leq 5 \mu\text{m}$ war. Solche Ereignisse treten nur bei sehr kleinen Streuwinkeln ϑ (Schwerpunktsystem) auf. Unter Voraussetzung von Isotropie im Schwerpunktsystem kann man auf $\vartheta = 0$ extrapolieren. Um Fehler durch Verzerrungen zu vermeiden, wurden nur solche Ereignisse analysiert, die mehr als $5 \mu\text{m}$ von der Ober- bzw. Unterseite der geschrumpften Emulsion entfernt lagen. Dies wurde durch einen Korrekturfaktor berücksichtigt. Fig. 2 zeigt die Mikrophotographie einer elastischen Streuung.

Der totale Wirkungsquerschnitt ergibt sich zu

$$\sigma(E) = \frac{1}{\varrho \cdot L(E)}.$$

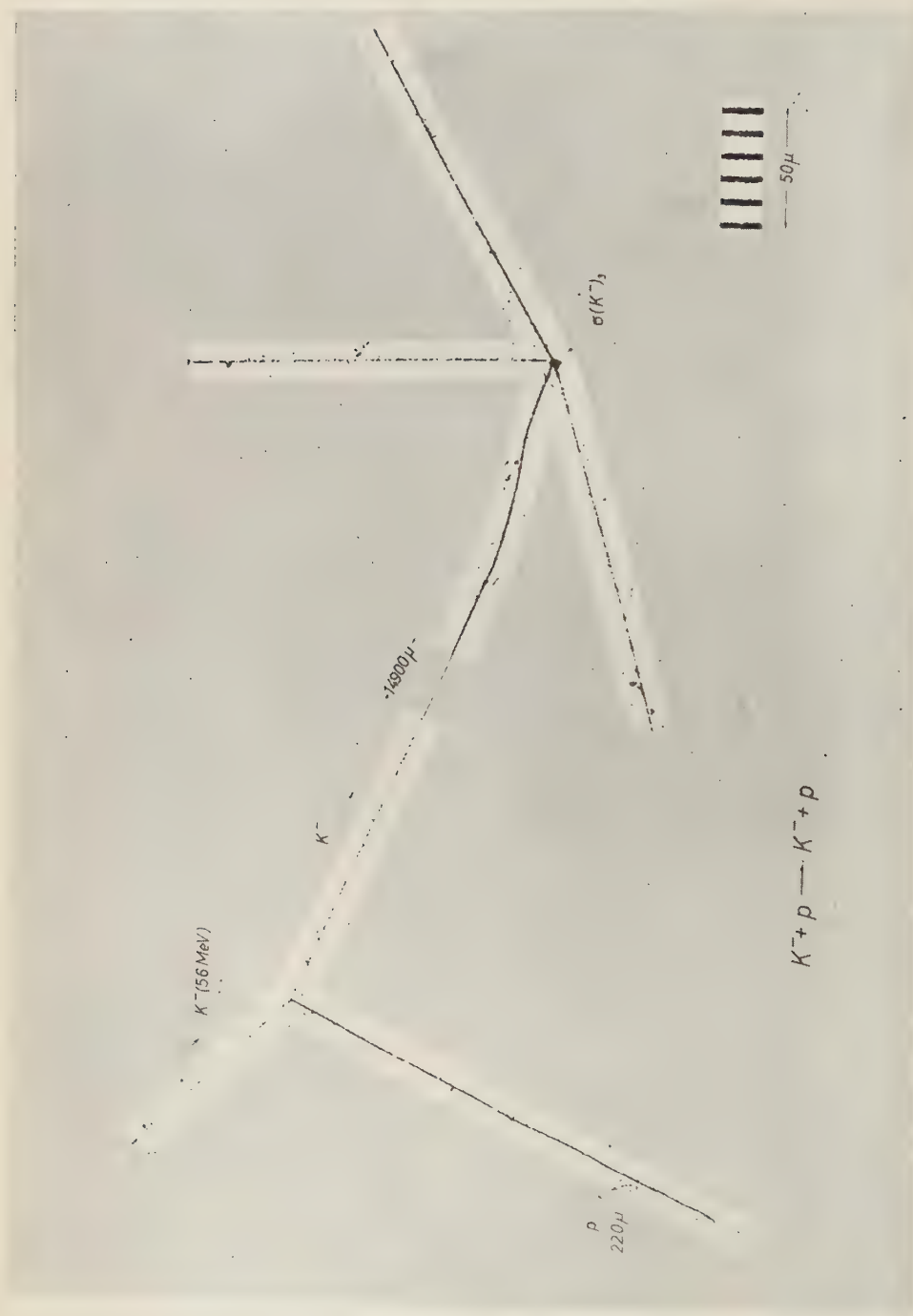


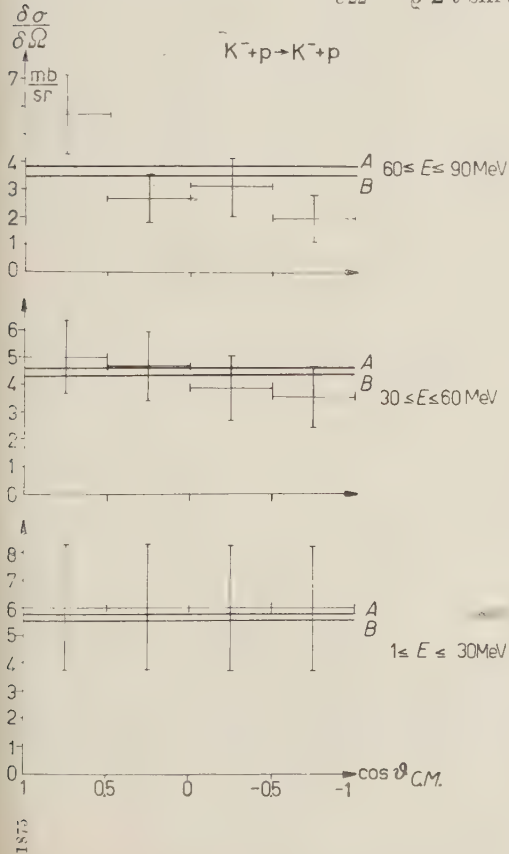
Fig. 2. - Mikrophotographie einer elastischen Streuung.

Hier ist ϱ die Anzahl der H-Atome/cm³ in der Kernemulsion und $l(E)$ die mittlere freie Weglänge für eine elastische Streuung eines K-Mesons bei der Energie E . Fig. 3 zeigt die Abhängigkeit des totalen Wirkungsquerschnitts von der Energie. Die durchgezogenen Kurven sind die mit Hilfe einer Phasenanalyse theoretisch berechneten Wirkungsquerschnitte.

Darauf kommen wir weiter unten zu sprechen.

Der differentielle Wirkungsquerschnitt berechnet sich ganz entsprechend zu

$$\frac{\partial \sigma}{\partial \Omega} = \frac{1}{\varrho} \frac{1}{2\pi \sin \vartheta} \frac{\partial^2 N}{\partial \vartheta \partial S(E)}$$



Hier ist $d\Omega = 2\pi \sin \vartheta d\vartheta$ das Raumwinklelement, in das die Streuung erfolgt. $\partial^2 N = dn(E, \vartheta) \cdot dE \cdot d\vartheta$ ist die Anzahl der Ereignisse im Energieintervall $(E, \Delta E)$ und im Winkelintervall $(\vartheta, \Delta \vartheta)$. Fig. 4 zeigt die Ergebnisse. Die Verteilungen sind bis 60 MeV innerhalb der Fehlergrenzen isotrop. Ein Überwiegen der Vorwärtsstreuung macht sich erst im Intervall $(60 \div 90)$ MeV bemerkbar. Dies kann jedoch nicht von der Coulomb-Streuung herrühren, da ihr Anteil bei höherer Energie

Fig. 4. – Differentieller Wirkungsquerschnitt für elastische Streuung.

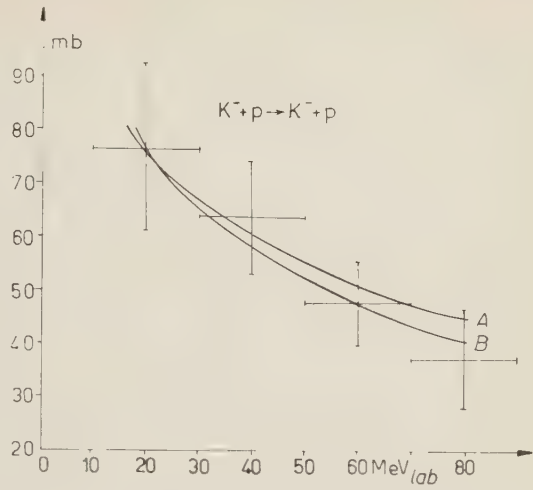


Fig. 3. – Abhängigkeit des totalen Wirkungsquerschnitts für elastische Streuung von der Energie.

kleiner wird. Die durchgezogenen Kurven geben wieder die später zu besprechenden theoretischen Ergebnisse.

2. – Ergebnisse zur inelastischen Streuung.

a) *Ladungsaustausch.* Wegen der fehlenden Ladung der Sekundärprodukte können solche Ereignisse nicht direkt in Emulsionen beobachtet werden. Eine rohe Abschätzung kann etwa folgendermaßen vor sich gehen: Man bestimme im Intervall 10 bis 30 MeV, die Anzahl derjenigen K^- -Wechselwirkungen, bei denen ein geladenes Σ -Hyperon und ein geladenes π -Meson ohne zusätzliche Spur erzeugt werden (N_1). Dann besteht eine große Wahrscheinlichkeit dafür, daß die Sekundärprodukte keine weiteren Wechselwirkungen im komplexen Kern eingegangen sind, d.h. es liegen nahezu ausschließlich primäre Wechselwirkungen mit Protonen vor. Sodann bestimme man in diesem Intervall die Anzahl der Spurenden ohne Sekundärspur. Sie muß näherungsweise gleich der Gesamtzahl N_2 der an gebundenen und freien Protonen erzeugten Σ^0 und Λ^0 und der Ladungsaustausch-Reaktionen sein. Unter der Voraussetzung, daß die von ALVAREZ *et al.* an freien Protonen gefundenen Erzeugungsraten von Hyperonen ($\Sigma^-:\Sigma^+:\Sigma^0:\Lambda = 4:2:2:0.5$) auch für gebundene Protonen gelten, läßt sich aus N_1 die Summe $N(\Sigma^0) + N(\Lambda^0)$ bestimmen (N_3). Dann ist $N_2 - N_3$ die Anzahl der Ladungsaustausch-Ereignisse. Unter der weiteren Voraussetzung, daß das Verhältnis der Zahl der Ladungsaustausch-Ereignisse zur Zahl der erzeugten geladenen Hyperonen an gebundenen Protonen dasselbe ist wie an freien Protonen, läßt sich daraus die Anzahl der Ladungsaustausch-Ereignisse an freien Protonen in diesem Energieintervall berechnen. Es ergibt sich:

$$\sigma_{ex} = (15 \pm 7) \text{ mb} \quad \text{bei} \quad E_{K^-} = 20 \text{ MeV}.$$

b) *Absorption.* Es sind folgende Reaktionen möglich:

$$K^- + p = \begin{cases} \Sigma^+ + \pi^- + 103.1 \text{ MeV} \\ \Sigma^- + \pi^+ + 96.3 \text{ MeV} \\ \Sigma^0 + \pi^0 + 105.3 \text{ MeV} \\ \Lambda^0 + \pi^0 + 181.8 \text{ MeV} \end{cases}$$

Zur Analyse wurden die Streuwinkel und die Reichweite des Hyperons ausgemessen. Da die Primärenergie besonders bei großen Pion-Winkeln sehr empfindlich von diesen Größen abhängt, wurde die wegen möglicher Verzerrungen nicht ausgemessene Zone auf je 50 μm bei der ungeschrumpften Emulsion er-

weitert. Fig. 5 zeigt die Ergebnisse. Auch hier ist ein starker Abfall des totalen Wirkungsquerschnittes zu beobachten. Fig. 6 zeigt den differentiellen Wirkungsquerschnitt für die Erzeugung von geladenen Hyperonen. Auch hier ist die Winkelverteilung praktisch isotrop. Fig. 7 zeigt die Mikrophotographie einer Absorption.

In Fig. 8 ist der Schwerpunkts-Streuwinkel über der Laborenergie des K^- aufgetragen. In der Vergleichskurve wurde für den differentiellen Wirkungsquerschnitt für Coulomb-Streuung der Wert 1 mb/sr eingesetzt. Man sieht, daß außer 2 inelastischen und 3 elastischen Ereignissen alle Streuungen jenseits dieser Kurve liegen, d.h. außerhalb des Bereiches, in dem die Coulomb-Streuung einen nennenswerten Beitrag liefert. Zum andern wurde die Kurve

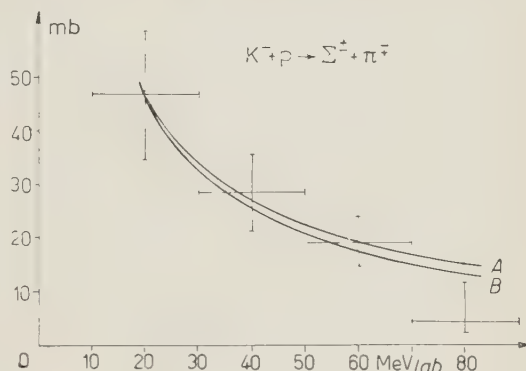


Fig. 5. – Abhängigkeit des totalen Wirkungsquerschnittes für Erzeugung von geladenen Hyperonen von der Energie.

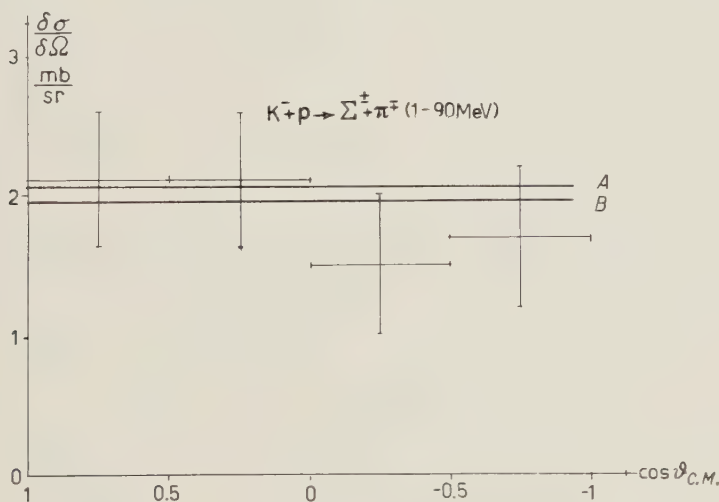


Fig. 6. – Differentieller Wirkungsquerschnitt für die Erzeugung von geladenen Hyperonen.

ingezeichnet, die sich ergibt, wenn das Proton bei der elastischen Streuung die Grenz-Reichweite von $5 \mu\text{m}$ besitzt.



Fig. 7. - Mikrophotographie einer Absorption.

Zusammenfassend ist also zu sagen, daß die Coulomb-Streuung vernachlässigt werden kann und die S -Streuung zur Beschreibung ausreicht.

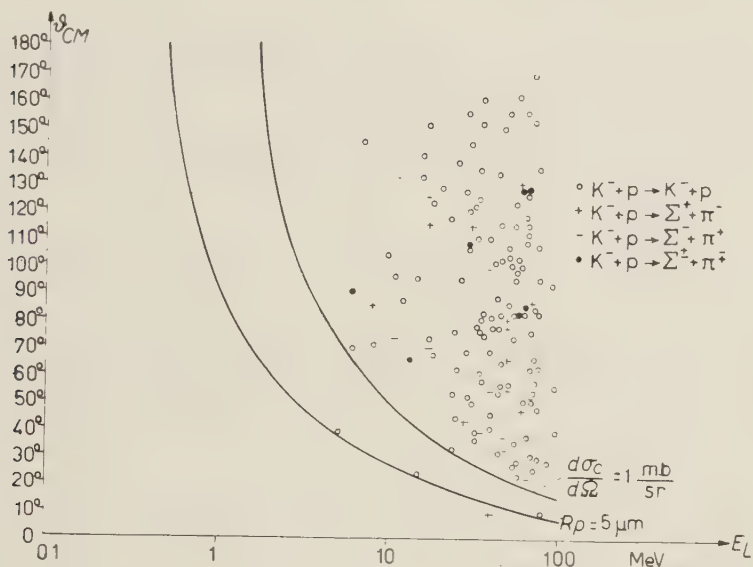


Fig. 8. — Abhängigkeit des Schwerpunkt-Streuwinkels von der Laborenergie der K^- -Mesonen. Einmal wurde als Parameter der differentielle Wirkungsquerschnitt für Coulomb-Streuung von 1 mb benutzt. Zum andern die $5\ \mu\text{m}$ -Grenze der Proton-Reichweite.

3. — Phasenanalyse und Bestimmung der Streulängen.

Beschränken wir uns nur auf S -Wellen, so werden die Wirkungsquerschnitte eine Funktion der Amplitude $n_{0,1} = \exp[2i\delta^{0,1}]$ der auslaufenden S -Wellen sein, wobei $\delta^{0,1}$ die zu den beiden möglichen Isospin-Zuständen $T=0$ und $T=1$ gehörigen Phasenverschiebungen der ankommenden gegen die gesamte Welle außerhalb der Reichweite der Wechselwirkung ist. Hierbei ist $\delta^{0,1}$ komplex anzusetzen, um die Absorption zu beschreiben. Um die 4 Unbekannten zu bestimmen, haben wir einmal 3 Gleichungen für die Wirkungsquerschnitte: Elastische Streuung:

$$(1) \quad \sigma_{\text{tot}} = \frac{\pi}{4k^2} |(\exp[2i\delta^1] - 1) + (\exp[2i\delta^0] - 1)|^2.$$

Ladungsaustausch:

$$(2) \quad \sigma_{\text{tot}} = \frac{\pi}{4k^2} |(\exp[2i\delta^1] - 1) - (\exp[2i\delta^0] - 1)|^2.$$

Absorption:

$$(3) \quad \sigma_{\text{tot}} = \frac{\pi}{2k^2} (1 - |\exp [2i\delta^0]|^2 + 1 - |\exp [2i\delta^1]|^2) .$$

Beobachten kann man nur die geladenen Hyperonen. Nun wird Σ^0 nur im Zustand $T=0$ und zwar zu $\frac{1}{3}$ der gesamten Produktion erzeugt, während Λ^0 natürlich nur im Zustand $T=1$ erzeugt werden kann ⁽¹⁾. Damit ergibt sich für den totalen Wirkungsquerschnitt für Erzeugung von geladenen Hyperonen:

$$(4) \quad \sigma_{\Sigma^\pm} = \frac{\pi}{2k^2} \left[\frac{2}{3} (1 - |\exp [2i\delta^1]|^2) + (1 - f_\Lambda) (1 - |\exp [2i\delta^1]|^2) \right] .$$

f_Λ ist der Teil der $T=1$ Absorption, der zu Λ^0 -Produktion führt. Um diesen Faktor bei kleinen Energien zu berechnen, benutzen wir wieder das Verhältnis der Erzeugungsraten von ALVAREZ *et al.* und erhalten:

$$(5) \quad \frac{\sigma_{\Sigma^\pm}}{\sigma_{\Sigma^\pm\Lambda}} = \frac{12}{13} \wedge \sigma_{\Sigma^\pm} = \frac{12}{13} \sigma_{\Sigma^\pm\Lambda} .$$

Mit (4) und (5) ergibt sich:

$$\begin{aligned} \frac{12}{13} \frac{\pi}{2k^2} \left[\frac{2}{3} (1 - |\exp [2i\delta^0]|^2) + (1 - |\exp [2i\delta^1]|^2) \right] = \\ = \frac{\pi}{2k^2} \left[\frac{2}{3} (1 - |\exp [2i\delta^0]|^2) + (1 - f_\Lambda) (1 - |\exp [2i\delta^1]|^2) \right] . \end{aligned}$$

Hieraus folgt für f_Λ :

$$(6) \quad f_\Lambda = \frac{1}{13} \left[\frac{2}{3} \frac{1 - |\exp [2i\delta^0]|^2}{1 - |\exp [2i\delta^1]|^2} + 1 \right] .$$

Für das Verhältnis $\sigma_{\text{ab}}(T=1)/\sigma_{\text{ab}}(T=0)$ ergibt sich nach den Überlegungen von DALITZ ⁽²⁾

$$(7) \quad \frac{1 - |\exp [2i\delta^1]|^2}{1 - |\exp [2i\delta^0]|^2} = 0.42 \pm 0.13 ,$$

(7) ist nun die gesuchte 4. Gleichung neben (1), (2) und (4) zur Berechnung der Phasen.

⁽¹⁾ M. KOSHIBA: *Nuovo Cimento*, **4**, 357 (1956).

⁽²⁾ R. H. DALITZ: *Annual Intern. Conf. on High Energy Physics at CERN* (1958), S. 187 ff.

Für f_{Λ} folgt:

$$f_{\Lambda} = 0.2 \pm 0.07.$$

Gleichsetzen der beobachteten Wirkungsquerschnitte bei 20 MeV mit den Formeln liefert Bestimmungsgleichungen für die Phasen.

TABELLE I. - Phasen bei $E_{K^-} = 20$ MeV.

Lösung	Realteil (Grade)		Imaginärteil (Grade)	
	A	B	A	B
Isospin 0	$+ 8.75^{+9}_{-10}$	$+ 37.3^{+17}_{-13}$	$+ 14.8 \pm 4.5$	$+ 14.8 \pm 4.5$
Isospin 1	$+ 33 \quad ^{+9}_{-10}$	$+ 13 \quad ^{+17}_{-13}$	$+ 4.5 \pm 2.5$	$+ 4.5 \pm 2.5$

Für die Realteile ergeben sich zwei Lösungen mit unbestimmten Vorzeichen. Aus der Mathematik folgt nur, daß, wenn $\text{Re } \delta_{A,B}^1$ ein bestimmtes Vorzeichen hat, $\text{Re } \delta_{A,B}^0$ dasselbe Vorzeichen haben muß. Nun gehört bekanntlich eine positive Phase zu einem anziehenden Potential, und zwar ist sie um so größer, je größer das Potential ist. Man weiss nun ziemlich sicher, daß das Potential zwischen einem negativen K-Meson und einem komplexen Kern anziehend ist ⁽³⁾. Nimmt man das auch für die K⁻-Proton-Wechselwirkung an, so ergibt sich für die größere der beiden Phasen ein positives Vorzeichen. Das bedeutet bei uns ein positives Vorzeichen für alle Phasen ^(*).

TABELLE II. - Streulängen.

Lösung	Realteil (10^{-13} cm)		Imaginärteil b (10^{-13} cm)	
	A	B	A	B
Isospin 0	$- 0.31 \pm 0.35$	$- 1.48 \pm 0.4$	$- 0.55 \pm 0.2$	$- 0.83 \pm 0.3$
Isospin 1	$- 1.39 \pm 0.4$	$- 0.49 \pm 0.5$	$- 0.236 \pm 0.12$	$- 0.176 \pm 0.09$

⁽³⁾ E. FERREIRA: *Nuovo Cimento*, **11**, 880 (1959); J. D. JACKSON: *The Physics of Elementary Particles* (Princeton, 1958), S. 67.

^(*) In Tabelle I sind daher nur die positiven Werte mit den sich aus den Experimenten ergebenden Fehlern eingetragen.

Nach der « effective-range-theory » ist der Zusammenhang zwischen den Phasen und den Streulängen bei nicht zu hoher Energie gegeben durch

$$(8) \quad k \operatorname{ctg} \delta = -\frac{1}{a + i \cdot b}.$$

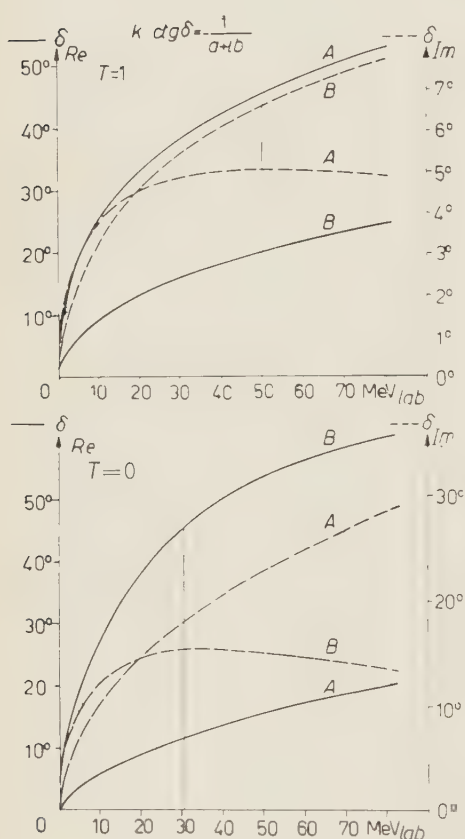


Fig. 9. – Abhängigkeit der Phasen von der Energie bei $T=0$ und $T=1$.

Wenn die obigen Überlegungen zutreffen, erhalten wir also negative Streulängen. Das bedeutet bekanntlich, daß die Streuung von einem ungebundenen Zustand aus erfolgt. Auch erkennt man, daß die Absorption und die Schattenstreuung im Zustand $T=0$ größer ist als im Zustand $T=1$.

In Übereinstimmung mit DALITZ⁽²⁾ nehmen wir an, daß diese Streulängen in guter Näherung energieunabhängig sind. Mit (8) läßt sich daher die Energieabhängigkeit der Phasen darstellen (Fig. 9). Die durchgezogenen Kurven stellen die Realteile, die gestrichelten die Imaginärteile der Phasen dar. Die letzteren besitzen dort ein Maximum, wo die zugehörigen Realteile 45° erreichen. Jenseits dieser Grenze wird der Wirkungsquerschnitt für die Absorption und die Schattenstreuung also wieder kleiner.

Setzen wir die Streulängen in die Formeln für die Wirkungsquerschnitte ein, so erhalten wir:

Elastische Streuung:

$$(9) \quad \sigma_{\text{tot}} = \pi \left| \frac{a_1 + ib_1}{1 + ika_1 - kb_1} + \frac{a_0 + ib_0}{1 + ika_0 - kb_0} \right|^2.$$

Ladungsaustausch:

$$(10) \quad \sigma_{\text{tot}} = \pi \left| \frac{a_1 + ib_1}{1 + ika_1 - kb_1} - \frac{a_0 + ib_0}{1 + ika_0 - kb_0} \right|^2.$$

Absorption:

$$(11) \quad \sigma_{\Sigma^{\pm}} = \frac{\pi}{2k^2} \left[\frac{2}{3} \left(1 - \left| \frac{1 + kb_0 - ka_0 i}{1 - kb_0 + ka_0 i} \right|^2 \right) + 0.8 \left(1 - \left| \frac{1 + kb_1 - ka_1 i}{1 - kb_1 + ka_1 i} \right|^2 \right) \right].$$

In Fig. 3 und Fig. 5 sind diese Abhängigkeiten eingezeichnet. Sie stimmen bei höheren Energien mit den experimentellen Werten recht gut überein. In Fig. 10 ist der totale Wirkungsquerschnitt für Ladungsaustausch dargestellt. Fig. 11 zeigt die Abhängigkeit des totalen Wirkungsquerschnittes für die Erzeugung von geladenen und ungeladenen Hyperonen in Abhängigkeit von der Energie. (Formel (11) ohne die Faktoren $\frac{2}{3}$ und 0.8).

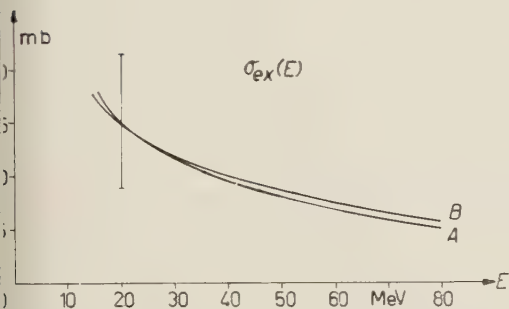


Fig. 10. – Totaler Wirkungsquerschnitt für Ladungsaustausch in Abhängigkeit von der Energie, berechnet über die Streulängen.

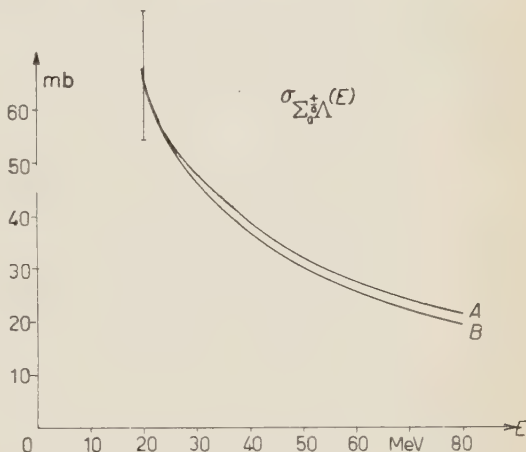


Fig. 11. – Abhängigkeit des totalen Wirkungsquerschnittes für die Erzeugung von geladenen und ungeladenen Hyperonen von der Energie, berechnet über die Streulängen.

Da S -Streuung vorliegt, ergeben sich die differentiellen Wirkungsquerschnitte einfach zu

$$\frac{\partial \sigma}{\partial \Omega} = \frac{1}{4\pi} \sigma_{\text{tot}}.$$

Diese über die Energieintervalle gemittelten Kurven sind in Fig. 4 und Fig. 6 eingetragen. Auch sie geben die experimentellen Werte recht gut wieder. Nur im Energieintervall (60 ÷ 90) MeV bei der elastischen Streuung macht sich die P -Welle bemerkbar.

4. – Diskussion.

R. H. DALITZ ⁽²⁾ hat auf der « 1958 Intern. Conf. on High Energy Physics at CERN » in ähnlicher Weise berechnete Streulängen angegeben. Seine Lösungen stimmen mit unseren Lösungen überein. Leider liegen die Lösungen A, B

so dicht beieinander, daß es nicht möglich ist, eine Lösung auszuschließen. Die gute Übereinstimmung der über die Streulängen berechneten Wirkungsquerschnitte mit den experimentellen Werten zeigt, daß die geforderte Energieunabhängigkeit der Streulängen bei den vorliegenden Energien noch gut erfüllt ist.

* * *

Ich danke Herrn Dr. GOTTSTEIN für die Anregung zu dieser Arbeit. Herrn Dr. MITTELSTAEDT und Herrn Dr. ZORN bin ich für viele klärende Aussprachen zu Dank verpflichtet.

Dem Max-Planck-Institut für Physik und Astrophysik München möchte ich für ein Stipendium danken.

RIASSUNTO (*)

In questo lavoro sono state determinate in emulsioni nucleari le sezioni trasversali totali e differenziali per lo scattering elastico ed anelastico di mesoni K negativi su protoni liberi per energie sino a 90 MeV. La lunghezza di traccia osservata è di 617.78 m. La sezione trasversale differenziale mostra che lo scattering S è sufficiente per la descrizione di questi processi e che lo scattering di Coulomb può essere trascurato per gli angoli qui considerati ($> 20^\circ$). Si è usata una teoria semplice per la descrizione di queste interazioni e si è eseguita un'analisi degli spostamenti di fase per i due possibili stati di spin isotopico $T=0$ e $T=1$. Ne risulta che l'assorbimento e lo shadow-scattering qui determinati sono stati usati per calcolare le sezioni trasversali alle alte energie. Esse si accordano abbastanza bene con i valori sperimentali.

(*) Traduzione a cura della Redazione.

On the Electronic Spectrum of Formyl Fluoride (*).

A. FOFFANI, I. ZANON, G. GIACOMETTI, U. MAZZUCATO,
G. FAVARO and G. SEMERANO

Istituto di Chimica Fisica dell'Università - Padova

(ricevuto il 25 Febbraio 1960)

Summary. — The vapour spectrum of formyl fluoride in the range $(2200 \div 2700) \text{ \AA}$ shows about 60 non-diffuse bands. The comparison with the solution spectrum and the temperature effect allow to isolate two main progressions of the excited state, with a pass of about 1100 and 640 cm^{-1} , assigned respectively to the carbonyl stretching and to the FCO deformation modes. The transition is probably of the singlet-singlet $n\text{-}\pi$ type, with the origin at 37500 cm^{-1} .

Introduction.

Recently the analysis of the electronic spectrum of formaldehyde has been completed ⁽¹⁾, and has given sufficiently detailed information on the structure of the first excited state of this molecule. This makes interesting the study of electronic spectra of like molecules. We have undertaken the examination of the absorption spectrum of the HFCO molecule, whose ground state geometry is sufficiently well known from the results of recent measurements of electron diffraction ⁽²⁾, microwave ⁽³⁾ and infrared spectroscopy ⁽⁴⁾.

(*) The research reported here has been sponsored in part by the Office, Chief of Research and Development, U.S. Dept. of Army, through its European Office, under contract no. DA-91-508-EUC-275.

(1) J. C. D. BRAND: *Journ. Chem. Soc.*, 858 (1956); G. W. ROBINSON: *Can. Journ. Phys.*, **34**, 699 (1956); P. J. DYNE: *Journ. Chem. Phys.*, **20**, 811 (1952).

(2) M. E. JONES, H. HEDBERG and V. SHOMAKER: *Journ. Am. Chem. Soc.*, **77**, 5278 (1955).

(3) P. FAVERO, A. M. MIRRI and J. G. BACKER: *Journ. Chem. Phys.*, **31**, 566 (1959); E. FERRONATO, L. GRIFONE, A. GUARNIERI and G. ZULIANI: *Proc. Int. Meet. Mol. Spect.* (Bologna, 7-12 Sept. 1959).

(4) H. W. MORGAN, P. A. STAATS and J. H. GOLDSTEIN: *Journ. Chem. Phys.*, **25**, 337 (1956).

We report here on experiments in the near ultraviolet performed under medium resolution both in the liquid and vapour phase, and on a first attempt of vibrational analysis of the observed transition.

1. - Experimental.

For vapour spectra a Large Littrow quartz Bausch and Lomb spectrograph has been used (plate factor: 2 \AA/mm at 2000 \AA , 10 \AA/mm at 4000 \AA); the light source was a high-pressure xenon quartz bulb (Osram XBO 162 W); photographic plates were Ferrania «*foto-meccaniche orto*». We used linear cells up to 70 cm length, with pressures ranging from 20 to 760 mm Hg and temperature from -20 to -40°C . Exposure times: up to 10 min ; absence of appreciable photodecomposition for such intervals was checked.

Solution spectra (in *n*-hexane and cyclohexane) were obtained with an Optica grating spectrophotometer (plate factor 6.5 \AA/mm); the concentration ranged from $2 \cdot 10^{-2}$ to $5 \cdot 10^{-3}$ moles liter, in which interval Beer's law was obeyed. The stability of these solutions was satisfactory and in any case sufficient for our measurements.

Formyl fluoride was prepared by addition of benzoyl chloride to a mixture of KF and anhydrous HCOOH ⁽³⁾, and purified by repeated low temperature distillations until a constant vapour pressure was obtained (20 mm Hg at -80°C). A check of the purity of the product was made by infrared spectroscopy ⁽⁴⁾.

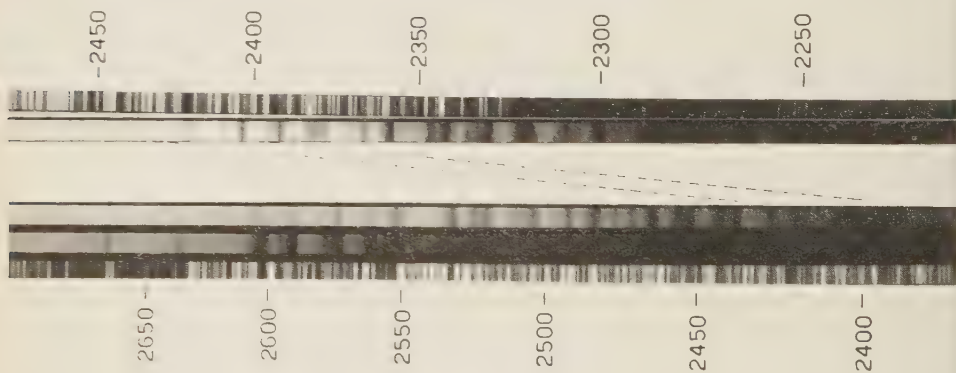


Fig. 1.

Fig. 1. shows some vapour phase spectrograms under different conditions and Fig. 2 a solution spectrum in cyclohexane.

³ A. N. NESMEYANOV and E. J. KAHN: *Ber. deut. chem. Ges.*, B **67**, 370 (1954).

The observed vapour phase spectrum consists of about 60 non-diffuse bands, well developed in their fine structure, in the range $(2\,200 \div 2\,700)$ Å. Temperature lowering does not affect appreciably the relative intensity of the bands. The solution spectrum consists of a single electronic band of medium intensity (molar extinction coefficient at the maximum is about 50) in the same spectral region. Vibrational structure is evident, corresponding to a pass of the order of 1100 cm^{-1} .

2. - Discussion.

It is very likely that the observed transition is a singlet-singlet $n\text{-}\pi$ transition, as the analogous one for formaldehyde⁽¹⁾. This is consistent with the low value of the intensity and in agreement with comparative semi-empirical calculations for the two molecules⁽⁶⁾. On this basis the vibrational separation observed in solution is of a reasonable order of magnitude for a stretching $\text{C}=\text{O}$ mode in the excited state (see below). It was appealing to attempt a vibrational analysis of the vapour phase spectrum on supposing that only progressions deriving from the multiple excitation of this vibrational quantum were active; but this was soon proved to be impossible. It would not be surprising indeed that the $n\text{-}\pi$ transition in formyl fluoride causes the excitation of some other vibration involving the fluorine atom, partially conjugated with the carbonyl double bond.

We actually succeeded in carrying out a first attempt of assignment covering the large majority of the observed bands on the basis of two main progressions of vibrations of the excited state ($\nu_2 = 1100\text{ cm}^{-1}$ and $\nu_5 = 460\text{ cm}^{-1}$) and their combinations. The value 460 cm^{-1} is a reasonable one for the FCO deformation of the excited state, considering the value of 650 cm^{-1} for the same mode in the ground state of the molecule⁽⁴⁾. A few more bands are also assigned to the excitation of a single quantum of two other vibrations of the

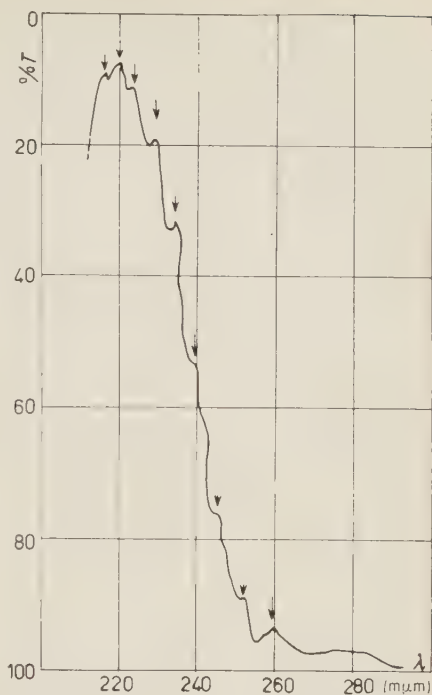


Fig. 2.

⁽⁶⁾ G. GIACOMETTI, G. RIGATTI and G. SEMERANO: *Nuovo Cimento*, **16**, 939 (1960) and references therein contained.

excited state ($\nu_3 = 1260 \text{ cm}^{-1}$ and $\nu_1 = 3000 \text{ cm}^{-1}$ corresponding to the in plane and out of plane C—H vibrations of the ground state), alone or in combination with quanta of the principal progressions. The absence of any selective effect of the temperature indicates a vibrationless ground state. The situation is illustrated in Table I, where all observed bands are reported, and in Fig. 3 where a sketch is given of the assignments, with an approximate evaluation of the relative intensities. Frequency intervals of occurrence of the solution maxima are also reported: intervals and not average values are given because, owing to the very steep form of the electronic band envelope, the positions of the maxima are affected differently by the experimental conditions and have

TABLE I. — *Frequencies (in cm^{-1}) and vibrational assignment of vapour and solution spectra.*

Vapour	Assign.	Solution	Vapour	Assign.	Solution
37.492		37.350 (?)	41.675	$3\nu_2 + 2\nu_5$	
37.615			41.823		
37.951	$1\nu_5$		41.893	$4\nu_2$	41.700 ÷ 42.150
38.052			42.031	$3\nu_2 + 1\nu_3$	
38.292			42.114	$3\nu_2 + 3\nu_5$	
38.410	$2\nu_5$	38.250 ÷ 38.500	42.230		
38.557			42.319	$4\nu_2 + 1\nu_5$	
38.617	$1\nu_2$		42.444	$3\nu_2 + 1\nu_3 + 1\nu_5$	
38.699			42.553	$3\nu_2 + 4\nu_5$	
38.782	$1\nu_3$ (?)		42.644	$2\nu_2 + 1\nu_1$	
38.868	$3\nu_5$		42.725	$4\nu_2 + 2\nu_5$	
39.055	$1\nu_2 + 1\nu_5$		42.882		42.750 ÷ 42.900
39.210	$1\nu_3 + 1\nu_5$		42.955	$5\nu_2$	
39.316	$4\nu_5$		43.122	$4\nu_2 + 3\nu_5$	
39.521	$1\nu_2 + 2\nu_5$	39.400 ÷ 39.600	43.290		
39.645			43.384	$5\nu_2 + 1\nu_5$	
39.714	$2\nu_2$		43.478	$4\nu_2 + 1\nu_3 + 1\nu_5$	
39.885	$1\nu_2 + 1\nu_3$		43.554	$4\nu_2 + 4\nu_5$	
39.968	$1\nu_2 + 3\nu_5$		43.620		
40.161	$2\nu_2 + 1\nu_5$		43.687	$3\nu_2 + 1\nu_1$	43.550 ÷ 43.900
40.306	$1\nu_2 + 1\nu_3 + 1\nu_5$		43.762	$5\nu_2 + 2\nu_5$	
40.404	$1\nu_2 + 4\nu_5$		43.898		
40.494	$1\nu_1$ (?)		44.033	$6\nu_2$	
40.609	$2\nu_2 + 2\nu_5$		44.189		
40.745			44.326		
40.806	$3\nu_2$	40.750 ÷ 41.000	44.464		
40.933	$2\nu_2 + 1\nu_3$		44.603		
41.059	$2\nu_2 + 3\nu_5$		44.803		44.700 ÷ 44.900
41.237	$3\nu_2 + 1\nu_5$				45.500 ÷ 45.700
41.382	$2\nu_2 + 1\nu_3 + 1\nu_5$				46.200 ÷ 46.550
41.494	$2\nu_2 + 3\nu_5$				
41.589	$1\nu_2 + 1\nu_1$				

to be considered only a rough indication of the true positions. Bearing this in mind, the solution maxima correspond reasonably well with the main carbonyl progression bands in the vapour.

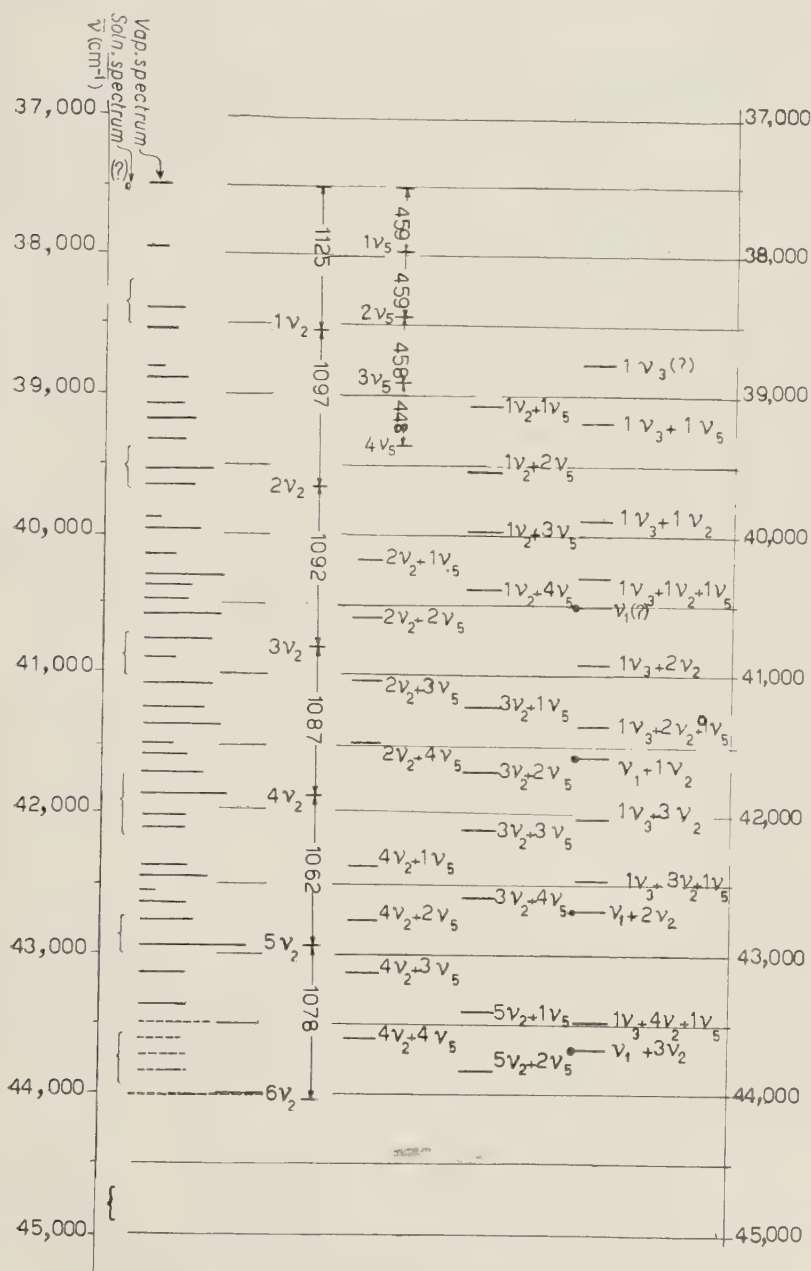


Fig. 3.

The carbonyl stretching progression ν_2 shows a regular anharmonicity effect and its mean value is 1100 cm^{-1} . This value is only a little smaller than the one for the analogous vibration on the 1A_2 state of Formaldehyde, while in the ground state the two values are 1750 cm^{-1} for the latter and 1850 cm^{-1} for Formyl Fluoride ⁽¹⁾, the increase being attributed to the effect of the electronegativity of Fluorine.

The proposed assignment would locate the origin of the transition (0-0 band) at 37500 cm^{-1} . It is however to be noted that the two running quanta are almost exactly in the frequency ratio of 5:2 and one cannot exclude as yet an origin located $2\nu_2\text{ cm}^{-1}$ further to the red. A check of this possibility must wait for the examination of the spectral region with multiple path cells. A further check on the origin will also come indirectly from the examination of the deuterated species of the molecule to confirm the assignment of the progressions containing the C-H vibrations ν_3 and ν_1 .

A detailed examination of the vibro-rotational structure requires obviously a greater resolution but some main features of the bands are already apparent. All the bands show an evident *K*-type sub-band structure degraded toward the red. A great number of them contain two apparent heads, the one at lower wave length being always weaker. Generally speaking the appearance of the bands is much more complicated than in the Formaldehyde case and this is probably due to the fact that, owing to the lower symmetry, we are here confronted with hybrid bands beside the perpendiculare ones.

RIASSUNTO

Lo spettro in vapore del fluoruro di formile nell'intervallo $(2200\div 2700)\text{ \AA}$ consiste di circa 60 bande non diffuse. Il confronto con lo spettro in soluzione e l'effetto della temperatura consentono di isolare due progressioni principali dello stato eccitato, con passo di circa 1100 e 460 cm^{-1} , assegnate rispettivamente al modo d'allungamento carbonilico ed a quello di deformazione FCO. La transizione è probabilmente del tipo singoletto-singoletto $n-\pi$, con origine a 37500 cm^{-1} .

Remarks on the Appearance of Ghost States in Relativistic Field Theories (*).

E. FERRARI

Istituto di Fisica dell'Università - Roma
Istituto Nazionale di Fisica Nucleare - Sezione di Roma

G. JONA-LASINIO (**)

The Enrico Fermi Institute for Nuclear Studies
The University of Chicago - Chicago, Ill.

(ricevuto il 3 Marzo 1960)

Summary. — A subtraction procedure to eliminate ghosts from propagators recently proposed by Redmond is examined from the standpoint of axiomatic field theory. This procedure is found to be equivalent to the introduction of a special vertex function which in principle can be chosen among functions having the analyticity properties prescribed by the axioms. This situation is shown to exist both in the case of boson and fermion fields. In the above discussion Lehmann integral representation of propagators is taken as an axiom by itself. The modifications brought into the discussion of ghost problems by a subtracted Lehmann dispersion formula are then examined. Of some interest are the consequences on the high frequency behaviour of form factors.

1. — Introduction.

1.1. — Recently new interest has been raised on perturbation calculations in field theory by a paper by REDMOND ⁽¹⁾. He shows that combining a well-known expression of the causal propagator of the boson field, derived in per-

(*) Work supported in part by the U.S. Atomic Energy Commission, Contract no. AT(11-1)-264.

(**) Fulbright Fellow. On leave of absence from Istituto di Fisica dell'Università, Roma and Istituto Nazionale di Fisica Nucleare, Sezione di Roma.

(1) P. J. REDMOND: *Phys. Rev.*, **112**, 1404 (1958).

turbation theory, with Lehmann's integral representation and some additional assumptions, an approximate method of calculation can be developed which gives finite results without unphysical features. In particular he finds a finite value for the boson wave function renormalization constant Z_3^{-1} . The clue of Redmond's procedure is to subtract from the conventionally calculated propagator the ghost pole with the correct residue, and then show that the expression obtained satisfies Lehmann's representation. Explicit calculations have been carried out by REDMOND for the meson propagator at the second order of perturbation theory.

In this note the above procedure is examined from the standpoint of axiomatic field theory.

It is well known that the appearance of ghosts in propagators can be connected with the high frequency behaviour of higher order vacuum functions⁽²⁾. In particular when the contribution of the intermediate state with a nucleon-antinucleon pair to the meson propagator is considered, the appearance of unphysical features is determined by the high energy behaviour of the vertex function. So it is not surprising that a ghost appears when this contribution is calculated at the lowest order of perturbation theory, when the vertex function is reduced to the coupling constant g . As the result of a very simple discussion it will be shown in this paper that the subtraction used to eliminate the ghost is equivalent, at the second order of perturbation theory, to the introduction of a special vertex (form factor) (always of the order g but no longer a constant) in the place of the perturbative point vertex.

Only the absolute value on the positive real axis of this special vertex is determined by the propagator and in principle functions with the correct analyticity properties and the prescribed absolute value can be constructed. The introduction of the new vertex implies a modification of the original Hamiltonian of the theory^(3,4).

1'2. — We give now a brief outline of our discussion. It is first recognized that the «perturbative» standard expression of the propagator used by REDMOND (see eq. (1) below) is equivalent to an exact and already known expres-

⁽²⁾ H. LEHMANN, K. SYMANZIK and W. ZIMMERMANN: *Nuovo Cimento*, **2**, 425 (1955).

⁽³⁾ Any attempt to eliminate ghosts probably introduces non-local conditions in the theory. This point has been discussed in detail by BOGOLIUBOV, MEDVEDEV and POLIVANOV. After this paper was sent to the publisher a work by B. V. MEDVEDEV and M. V. POLIVANOV discussing similar problems in the case of the Lee model appeared in *Sov. Phys. Dokl.*, **4**, 829 (1960) (English translation).

⁽⁴⁾ The fact that the results of usual perturbation theory are found by expanding the modified propagator in powers of g agrees with the general statement by FORE (see ref. ⁽⁸⁾) that in the weak coupling limit the ghost would disappear faster than any power of g .

sion of the same propagator derived under very general assumptions. This exact expression is obtained as a solution of an integral equation derived from Lehmann's representation and reduction formula. The above identification will allow us to compare the contribution of the intermediate state with a nucleon-antinucleon pair, calculated in perturbation theory, with the corresponding « exact » quantity. The equivalence of the subtraction procedure to the introduction of a special vertex I' in the place of the point vertex g then follows.

At this order it is found that on the cut corresponding to the two-particle intermediate state the equality holds $|I'| = |\Delta'_F/\Delta_F^*|$, where Δ'_F is the conventional propagator with the ghost and Δ_F^* the propagator modified according to Redmond's prescription. The problem of determining a function I' satisfying the axioms and the above condition on the absolute value is then examined in some detail.

It is finally shown that a completely analogous situation occurs also for the fermion propagator S'_F . In this case the conventional perturbative expression must be compared with exact expressions derived by the authors in a previous paper (5). Some further properties of S'_F which were not given in our previous work will be made explicit here and a close correspondence between the properties of the functions Δ'_F and S'_F will be established, provided the suitable integral representation is chosen in each case.

1'3. — We wish to remark that when we speak of axiomatic field theory Lehmann's unsubtracted representation must be considered as an axiom by itself which in some way specifies a particular theory (6). In fact nothing is known about the number of subtractions to be made in the general case. In any case, it may be of some interest to know the modifications brought into the discussion of the ghost problem by assuming a subtracted dispersion relation for the propagator. The modified formulae are considered in the last section of this paper. The most remarkable points are the different conditions following on the asymptotic behaviour of the vertex: it is found that the usual statement that form factors must vanish for high frequencies does not hold in the general case. It will be easily recognized that all previous arguments as to the consistency of eliminating ghosts by subtractions still apply with only minor modifications.

(5) E. FERRARI and G. JONA-LASINIO: *Nuovo Cimento*, **10**, 310 (1958), hereafter referred to as I.

(6) N. N. BOGOLIUBOV and D. V. SHIRKOV: *Introduction to the Quantized Field Theory* (New York). We are indebted to Dr. ОЕНМЕ for having called our attention to this point.

2. - Discussion on the boson propagator.

2'1. - The topological and analytical properties of diagrams lead in perturbation theory to the well known expression for the complete propagator Δ'_F ⁽⁷⁾ of a boson field (mass μ)

$$(1) \quad \Delta'_F(-k^2) = - \frac{1}{(k^2 + \mu^2) \left[1 - (k^2 + \mu^2) \int_{(2\mu)^2}^{\infty} \frac{f(\kappa^2)}{k^2 + \kappa^2 - i\varepsilon} d\kappa^2 \right]},$$

which can be also written

$$(1') \quad \Delta'_F(\omega) = \frac{1}{\omega \left[1 + \omega \int_{8\mu^2}^{\infty} \frac{F(\omega') d\omega'}{\omega'^2(\omega' - \omega - i\varepsilon)} \right]},$$

with the positions

$$f(\kappa^2) = \frac{F(\omega')}{\omega'^2}, \quad \begin{aligned} -k^2 - \mu^2 &= \omega, \\ \kappa^2 - \mu^2 &= \omega'. \end{aligned}$$

Eq. (1') is a particular solution of the integral equation

$$(2) \quad \Delta'_F(\omega) = \frac{1}{\omega} - \int_{8\mu^2}^{\infty} \frac{F(\omega') |\Delta'_F(\omega')|^2}{\omega' - \omega - i\varepsilon} d\omega',$$

provided the function $F(\omega')$ satisfies the limitation

$$(3) \quad I = \int_{8\mu^2}^{\infty} \frac{F(\omega')}{\omega'^2} d\omega' \leq 1,$$

as it has been shown first by FORD ⁽⁸⁾. The point of interest is that eq. (2) is a direct consequence of the axioms of field theory so that without further reference to perturbation theory we may look at eq. (3) as the condition for

⁽⁷⁾ A factor i is often included in the definition of $\Delta'_F(-k^2)$; cfr. ⁽²⁾. This has been omitted here to simplify the notation. The boson field is assumed to be pseudoscalar.

⁽⁸⁾ K. W. FORD: *Phys. Rev.*, **105**, 320 (1957). See this paper for a detailed discussion of the above equations.

any physically reasonable theory to have a solution in a strict mathematical sense. The structure of the function F can also be deduced from the axioms and it turns out to be a sum of positive contributions from all the intermediate physical states with different number of particles, each contribution satisfying

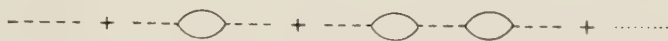
$$(4) \quad I^{(2)} = \int_{\mu^2}^{\infty} \frac{F^{(n)}(\omega')}{\omega'^2} d\omega' < 1.$$

The first term contributing to the meson propagator is $F^{(2)}$ ($^{(2)}$ stands here for a nucleon-antinucleon pair) which can be written ($^{(2)}$).

$$(5) \quad F^{(2)}(\omega') = \frac{1}{4\pi^2} \theta(\omega' + \mu^2 - 4M^2) (\omega' + \mu^2)^{\frac{1}{2}} (\omega' + \mu^2 - 4M^2)^{\frac{1}{2}} |f(\omega')|^2,$$

M = nucleon mass, $\theta(a) = 0$ for $a < 0$, $= 1$ for $a > 0$.

The function $f(\omega')$ is the vertex as defined in (2) and, because of (4), $\lim_{\omega \rightarrow \infty} f = 0$, otherwise the ghost appears. Putting $f = g$ in (1') the result of the lowest perturbation theory is found, which corresponds to the sum of all the diagrams



In this case condition (4) and then eq. (2) are no longer satisfied: $I^{(2)}$ is logarithmically divergent and the ghost appears.

Different points of view have been expressed on the possible ways in which the extra unphysical pole would arise in eq. (1') (9).

We would like to adopt the view that the inclusion of the lowest order self-energy corrections without the corresponding corrections to the vertex is not a consistent procedure: the constant vertex makes the theory equivalent in respect to the Lee model and the richer possibilities of relativistic fields are not used in this approximation. If the corrections to the vertex are included there is the possibility for the whole function I to exhibit the correct asymptotic behaviour in which case no ghost would appear in the propagator. In this case we would be left with the possibility of a ghost in the vertex itself which in turn would depend on the approximation of the four point function.

2'2. - Let us now turn our attention to the subtraction procedure for the elimination of the unphysical poles. We shall consider in general the problem

(9) N. N. BOGOLIUBOV, A. A. LOGUNOV and D. V. SHIRKOV: *Dispersion relations and perturbation theory*, preprint.

of this pole appearing in eq. (1') without particular reference, in this section, to second order perturbation theory and we generalize this way of handling the equations, applying it not only to approximate evaluations of the propagator (which probably induce ghosts due to the approximation), but also to the possible case of a theory not satisfying condition (3) also when the «complete» function F is taken into account. Such a theory would have no solution in a strict mathematical sense, and the unphysical features would be something «inherent» in it; let us try if a prescription can be given, through which the theory can be made mathematically consistent and quantities which have a physical meaning can be defined.

If $I > 1$, expression (1'), does no longer satisfy eq. (2), but an equation obtained from it simply by the addition of the contribution of the ghost pole, at $\omega = -\lambda$ ($\lambda > 0$) with the correct residue, which will be now called K ($K < 0$),

$$(6) \quad \Delta'_F(\omega) = \frac{1}{\omega} - \int_{s\mu^2}^{\infty} \frac{F(\omega') |\Delta'_F(\omega')|^2}{\omega' - \omega - i\varepsilon} d\omega' + \frac{K}{\omega + \lambda}.$$

Of course the function $\Delta'_F(\omega)$ will no longer satisfy even the usual spectral representation⁽⁸⁾, but the contribution of the ghost will be considered explicitly,

$$(7) \quad \Delta'_F(\omega) = \frac{1}{\omega} - \int_{s\mu^2}^{\infty} \frac{\sigma(\omega')}{\omega' - \omega - i\varepsilon} d\omega' + \frac{K}{\omega + \lambda}.$$

$\sigma(\omega') = F(\omega') |\Delta'_F|^2$ is a non negative function: the renormalization constant Z_3^{-1} is defined in terms of it by

$$(8) \quad Z_3^{-1} = 1 + \int_{s\mu^2}^{\infty} \sigma(\omega') d\omega'.$$

It is always $0 \leq Z_3 \leq 1$.

If we consider eq. (6), we note that Redmond's procedure can be applied also to this case: namely one simply brings the term $K/(\omega + \lambda)$ on the left hand side of eq. (6) and redefines the «modified propagator» $\Delta_F^*(\omega)$

$$(9) \quad \Delta_F^*(\omega) = \Delta'_F(\omega) - \frac{K}{\omega + \lambda},$$

which does no longer contain the ghost. From (7) and (8) it is easily seen that Δ_F^* satisfies Lehmann's integral representation

$$(10) \quad \Delta_F^*(\omega) = \frac{1}{\omega} - \int_{s\mu^2}^{\infty} \frac{\sigma(\omega')}{\omega' - \omega - i\varepsilon} d\omega',$$

and it is found that

$$\lim_{\omega \rightarrow -\infty} \omega \Delta_F^*(\omega) = Z_3^{-1}.$$

The residue K of the ghost pole is connected to Z_3^{-1} . Multiplying eq. (9) by ω and taking the limit $\omega \rightarrow -\infty$ we get

$$(11) \quad Z_3^{-1} = -K + \lim_{\omega \rightarrow -\infty} \omega \Delta'_F(\omega).$$

By virtue of eq. (1'), which is still valid, we get

$$(12) \quad Z_3^{-1} = -K + \frac{1}{1-I},$$

and then we see that the residue K equals $-Z_3^{-1}$ only in the case and at the orders in which I is divergent, in particular in the Redmond's case. In the following we shall be mainly interested in the case I divergent. The case $1 < I < \infty$ can be handled in the way indicated by SYMANZIK⁽¹⁰⁾ by suitably modifying the high momentum behaviour of the propagator which in turn is connected with the number of its zeros.

In order to see whether with these redefined quantities the theory is made consistent, we will try to bring the modified equations to a form similar to the one which holds in the case of no ghost poles. We can introduce a « modified spectral function » F^* , by putting

$$(13) \quad F^* = F \left| \frac{\Delta'_F}{\Delta_F^*} \right|^2.$$

This function is still positive, definite and real. It is defined only in terms of F , because the values of Δ'_F , Δ_F^* to be inserted here are given by (1') and (9) respectively: K and λ can be determined uniquely once F is known. Substituting (9) in (6) and introducing the function F^* we get

$$(14) \quad \Delta_F^*(\omega) = \frac{1}{\omega} - \int_{s\mu^2}^{\infty} \frac{|\Delta_F^*(\omega')|^2 F^*(\omega')}{\omega' - \omega - i\varepsilon} d\omega'.$$

This equation admits a solution of the Ford's type only if

$$(15) \quad I^* = \int_{s\mu^2}^{\infty} \frac{F^*(\omega')}{\omega'^2} d\omega' \leq 1.$$

⁽¹⁰⁾ K. SYMANZIK: preprint. This paper was brought to our knowledge when the present work was already completed.

If it could be proved that eq. (15) holds for all cases, then the procedure of redefinition could bring the theory from a mathematically inconsistent scheme to a consistent one. A general proof however is not possible: one can always think that (15) may be verified or not. In the first case, as pointed out, the theory can be made consistent, and the redefined quantities can be thought as having a physical meaning.

In particular, it can be shown that in this case the magnitude of the re-normalization constant is always finite. This can be seen from (12) and from the fact that K is never infinite. A vanishing Z_3 can therefore arise only if $I = 1$, and is irrespective to the value of I^* . We will then assume to be in the case of $I^* < 1$, and try to derive some consequences which could be also interpreted from a physical point of view.

Eqs. (13) and (14) will hold, of course, at any order of approximation of the functions involved ⁽¹¹⁾. In the following the case of the two intermediate nucleons approximation will be again considered.

2.3. — We will work here in the approximation mentioned in the preceding sections: we will consider only the contributions to F , Δ'_F , Δ_F^* of the intermediate state of two nucleons (mass M) with a point vertex ($f(\omega) = g$). We shall omit in this section the label ⁽²⁾, but it will be intended that all functions are calculated in this approximation.

We recall eq. (13)

$$(16) \quad F^* = F \frac{|\Delta'_F|^2}{|\Delta_F^*|^2} = F |I|^2.$$

We see that the «physical» contribution of the nucleon antinucleon pair (namely, the contribution after the ghost has been eliminated) is obtained simply by the substitution of the point vertex g with the function gI . This function I then plays the role of a form factor, which makes the physical vertex not to be point-like even in the lowest perturbative approximation. In other words: the elimination of the ghost is equivalent, in this approximation, to the introduction of a form factor in the elementary interaction. Notice that if the function $|I|$ is expanded in powers of g we find $|I| = 1$ at any order of approximation.

However this form factor, in order to be consistent with the axioms, must

⁽¹¹⁾ The approximations are made initially on the function F , by limiting the number of intermediate states. The corresponding approximations *e.g.* for Δ'_F are obtained by eq. (1') by inserting the corresponding approximate expressions for F in it.

satisfy some analyticity conditions ⁽¹²⁾. These conditions may be summarized in the fact that the form factor is an analytical function in the complex ω plane with a cut on the positive real axis starting from the mass of the lowest intermediate state. From examples in perturbation theory it may be inferred that a dispersion formula in some cases might not be sufficient to represent the vertex and additional poles or cuts can appear being connected with possible bound states. However these additional singularities are always confined to the positive real axis.

We cannot then simply identify $\Gamma = \Delta'_F / \Delta_F^* = \Gamma_0$ since in this case the ghost would be automatically reintroduced in the vertex violating again the axioms. The problem is to determine a function Γ analytic in the cut plane which satisfies the condition on the absolute value $|\Gamma| = |\Gamma_0|$ for $\omega = 4M^2 - \mu^2$ ⁽¹³⁾. It may not be useless to remark at this point that there is not a unique way to satisfy the axioms of field theory and that we have no definite criterion of choice among different possibilities. For this reason we shall confine the following discussion to the problem of finding an analytic function with the prescribed absolute value which avoids the ghost contained in Γ_0 : It is clear that for $\omega \geq 4M^2 - \mu^2$ it must be possible to write

$$\Gamma(\omega+) = \Gamma_0(\omega+) \exp[i\delta(\omega+)],$$

where $\delta(\omega)$ is a real phase factor to be chosen properly. Γ_0 contains a term of the form $\gamma_0/(\omega+\lambda)$ corresponding to the ghost which gives rise to a contribution $\{\gamma_0/(\omega+\lambda)\} \exp[i\delta(\omega)]$. Consider now the function

$$f(\omega) = \frac{\sqrt{\lambda} - \sqrt{-\omega}}{\sqrt{\lambda} + \sqrt{-\omega}},$$

with the following prescriptions on the real axis

$$(17) \quad \begin{cases} \omega > 0 & \begin{aligned} f(\omega+) &= \frac{\sqrt{\lambda} + i\sqrt{\omega}}{\sqrt{\lambda} - i\sqrt{\omega}}, \\ f(\omega-) &= f^*(\omega+), \end{aligned} \\ \omega < 0 & f(\omega) = \frac{\sqrt{\lambda} - \sqrt{|\omega|}}{\sqrt{\lambda} + \sqrt{|\omega|}}, \end{cases}$$

(this correspond to the choice of the Riemann sheet of the square root defined by $-\pi < \arg \omega < \pi$). Then define $\exp[i\delta(\omega+)] = f(\omega+)$. With this choice of

⁽¹²⁾ R. OEHME: *Nuovo Cimento*, **13**, 778 (1959) and UCRL-8838 (1959) to be published in *Phys. Rev.*

⁽¹³⁾ We are indebted to Dr. SYMANZIK who pointed out to us a wrong conclusion contained in the manuscript. The discussion of the example quoted below ((Eq. 17)) was proposed by Dr. OEHME.

the phase factor the vertex function Γ is analytic in the cut plane and we have no trouble with ghosts or other possible poles ($f(\omega)$ has no pole in the sheet we have chosen). The cut starts in this case at $\omega = 0$. A generalization of the procedure used can make the cut of the square root start at any $\omega > 0$.

3. - The fermion propagator.

3.1. - The above conclusions can be obtained also in the case of a fermion fields (mass M) as it has been pointed out in I Section 2. We will simply start the proof without carrying out the calculations extensively, since the procedure is quite similar to the one previously explained. It is necessary, however to give some supplementary properties of the exact fermion propagator S'_F first: these properties will complete the description treated in I, and will make possible a parallel development of both the boson and fermion cases (^{13 bis}). We will first rearrange the expressions (10) of I (hereafter indicated as (10_I)), determining the two constants C and A . We will require the expressions (for the notation see I)

$$\lambda_1(\omega) = -i\chi S'_1(\chi), \quad \lambda_2(\omega) = -i\chi S'_2(\chi),$$

to have a pole at $\omega = (-1)^{1/2}\omega_0$ with residue equal to 1 (as it is apparent from system (9_I)). We find

$$(18) \quad A = 1 - I_1 - I_2 - \sum_n \frac{R_n}{(\omega_n - \omega_0)^2},$$

with

$$(19) \quad I_1 = \frac{1}{\pi} \int_{\Omega}^{\infty} \frac{G_1(\omega')}{(\omega' + \omega_0)^2} d\omega', \quad I_2 = \frac{1}{\pi} \int_{\Omega}^{\infty} \frac{G_2(\omega')}{(\omega' - \omega_0)^2} d\omega',$$

and

$$(20) \quad \frac{1}{C} = \omega_0 \left[1 + \frac{\omega_0}{\pi} \int_{\Omega}^{\infty} \left[\frac{G_1(\omega')}{\omega'(\omega' + \omega_0)^2} - \frac{G_2(\omega')}{\omega'(\omega' - \omega_0)^2} \right] d\omega' - \omega_0 \sum_n \frac{R_n}{\omega_n(\omega_n - \omega_0)^2} \right].$$

(^{13bis}) In this Section the lower limit of all the integrals involving spectral functions will be more generally denoted by $\Omega = M + \mu$ (i.e. the sum of the masses of the fermion and the boson).

Substituting (18), (19) and (20) in the solutions (10_I) $\lambda_1(\omega)$ and $\lambda_2(\omega)$ are given by

$$(21) \quad \left\{ \begin{aligned} \frac{1}{\lambda_1(\omega)} &= (\omega + \omega_0) \left\{ 1 + \frac{\omega + \omega_0}{\pi} \int_{\Omega}^{\infty} \left[\frac{G_1(\omega')}{(\omega' + \omega_0)^2 (\omega' - \omega - i\varepsilon)} - \right. \right. \\ &\quad \left. \left. - \frac{G_2(\omega')}{(\omega' - \omega_0)^2 (\omega' + \omega + i\varepsilon)} \right] d\omega' - (\omega + \omega_0) \sum_n \frac{R_n}{(\omega_n - \omega_0)^2 (\omega_n - \omega)} \right\}, \\ \frac{1}{\lambda_2(\omega)} &= (\omega - \omega_0) \left\{ 1 + \frac{\omega - \omega_0}{\pi} \int_{\Omega}^{\infty} \left[\frac{G_2(\omega')}{(\omega' - \omega_0)^2 (\omega' - \omega - i\varepsilon)} - \right. \right. \\ &\quad \left. \left. - \frac{G_1(\omega')}{(\omega' + \omega_0)^2 (\omega' + \omega + i\varepsilon)} \right] d\omega' + (\omega - \omega_0) \sum_n \frac{R_n}{(\omega_n - \omega_0)^2 (\omega_n - \omega)} \right\}. \end{aligned} \right.$$

By requiring that the functions λ_1 and λ_2 have no other poles in the complex ω -plane than $\pm \omega_0$ it is easy to conclude that:

1) If the constant A is ≥ 0 , additional poles do not exist, the propagator has no ghosts and the theory admits solutions in the strict mathematical sense. From (18) (since all R_n are > 0) we get the important restrictions on G_1 and G_2

$$(22) \quad I_1 + I_2 \leq 1 \quad \text{which implies} \quad I_1 \leq 1, \quad I_2 \leq 1.$$

These limitations look very similar to (3).

2) If (22) is not fulfilled (*i.e.* if $A < 0$), the propagator has poles in the complex plane⁽¹⁴⁾. From the symmetry of the solution (13_I), if λ_1 has a pole at $\omega = \omega_1$, it has also a pole at $\omega = \omega_1^*$, and λ_2 has poles at $-\omega_1$ and $-\omega_1^*$. The residue at complex conjugate points are complex conjugate too. These poles can be in any point of the complex plane off the real axis⁽¹⁵⁾, according to the structure of the functions G_1 and G_2 : The number and the location of such poles cannot be established without further information on these functions.

⁽¹⁴⁾ If $A < 0$ the function (13_I) are no longer generalized R -functions and the result is inconsistent with the method used to find the solution. This situation occurs also in the boson case (see ⁽⁸⁾ for a detailed discussion).

⁽¹⁵⁾ A couple of (equal and opposite) additional poles can arise on the real axis, between $-\Omega$ and $+\Omega$, only in very special cases, namely if one of the two function G_1 and G_2 is particularly «enhanced» with respect to the other (in particular if one of them is zero). In eq. (23) below we will not consider this possibility.

3) It can be shown that $A = Z_2$, where Z_2 is the renormalization constant of the fermion field. If the theory is mathematically consistent Z_2 lies always in the interval $(0, 1)$ (since A can never be > 1). If we have ghosts, we get, on the contrary, a negative renormalization constant.

4) In the case of the appearance of the ghosts, the functions λ_1 and λ_2 do no longer satisfy Syst. (9₁) but a system in which the ghost poles are introduced explicitly, with their correct residues: *e.g.* in the case of only one value for ω_1 , we would get

$$(23) \quad \left\{ \begin{aligned} \lambda_1(\omega) &= \frac{1}{\omega + \omega_0} - \frac{1}{\pi} \int_{\Omega}^{\infty} \frac{G_1(\omega') |\lambda_1(\omega')|^2}{\omega' - \omega - i\varepsilon} d\omega' + \frac{1}{\pi} \int_{\Omega}^{\infty} \frac{G_2(\omega') |\lambda_2(\omega')|^2}{\omega' + \omega + i\varepsilon} d\omega' + \\ &\quad + \frac{K}{\omega - \omega_1} + \frac{K^*}{\omega - \omega_1^*}, \\ \lambda_2(\omega) &= \frac{1}{\omega - \omega_0} - \frac{1}{\pi} \int_{\Omega}^{\infty} \frac{G_2(\omega') |\lambda_2(\omega')|^2}{\omega' - \omega - i\varepsilon} d\omega' + \frac{1}{\pi} \int_{\Omega}^{\infty} \frac{G_1(\omega') |\lambda_1(\omega')|^2}{\omega' + \omega + i\varepsilon} d\omega' + \\ &\quad + \frac{K^*}{\omega + \omega_1} + \frac{K}{\omega + \omega_1^*} \end{aligned} \right.$$

3'2. — Once these properties of S'_F have been established, a line of calculation analogous to the one developed in Section 2 can be started, as it will be shown in the following. The closest correspondence with the boson case is obtained by using throughout the invariant decomposition of the fermion propagator introduced in I by means of the projection operators

$$(24) \quad \begin{cases} A = i\mathbf{k} + \sqrt{-k^2}, \\ B = i\mathbf{k} - \sqrt{-k^2}, \end{cases} \quad \mathbf{k} = \sum_{\mu} \gamma^{\mu} k_{\mu},$$

satisfying

$$(24') \quad A^2 = 2\sqrt{-k^2}A, \quad B^2 = -2\sqrt{-k^2}B, \quad AB = BA = 0.$$

This decomposition leads (as in I) to a spectral representation and analytical properties with respect to the variable $\sqrt{-k^2}$ which is much more convenient than the representation with respect to the variable $-k^2$. It is however easy to find the properties of the propagator as a function of $-k^2$, since, due to the symmetry properties of the solutions λ_1 and λ_2 , the « components » $S'_1 + S'_2$ and $\sqrt{-k^2}(S'_1 - S'_2)$ turn out to be functions of $-k^2$ only.

One can then always work out the calculations in the $\sqrt{-k^2}$ -plane, remembering that two points symmetrical with respect to the origin in this plane are equivalent to one point in the $-k^2$ -plane.

The following decompositions are introduced quite naturally:

$$(25) \quad \begin{cases} S'_F = \frac{1}{2}(AS'_1 + BS'_2), & S_F = \frac{1}{2}(AS_1 + BS_2), \\ \Sigma^* = A\Sigma_1^* + B\Sigma_2^*, \end{cases}$$

where Σ^* is the sum over all the proper graphs occurring in the well known equation derived from topological and analytical properties of diagrams in perturbation theory:

$$(26) \quad S'_F = S_F + S_F \Sigma^* S'_F.$$

By inserting (25) and separating the factors of the operators A and B we get two independent equations for S'_1 and S'_2 , and can then write an expression for both these functions analogous to form. (1) ⁽¹⁶⁾ (α and β are spectral functions)

$$\begin{cases} \sqrt{-k^2} S'_1 = \frac{1}{(\sqrt{-k^2} + M) \left\{ 1 + (\sqrt{-k^2} + M) \left[-\int_{M+\mu}^{\infty} \frac{\alpha(\kappa) d\kappa}{(\kappa + \sqrt{-k^2} + i\varepsilon)} + \int_{M+\mu}^{\infty} \frac{\beta(\kappa) d\kappa}{(\kappa - \sqrt{-k^2} - i\varepsilon)} \right] \right\}}, \\ \sqrt{-k^2} S'_2 = \frac{1}{(\sqrt{-k^2} - M) \left\{ 1 + (\sqrt{-k^2} - M) \left[-\int_{M+\mu}^{\infty} \frac{\beta(\kappa) d\kappa}{(\kappa + \sqrt{-k^2} + i\varepsilon)} + \int_{M+\mu}^{\infty} \frac{\alpha(\kappa) d\kappa}{(\kappa - \sqrt{-k^2} - i\varepsilon)} \right] \right\}}. \end{cases}$$

These equations can be discussed in the same way as eq. (1) has been discussed in (1). We should point out that also in this case, with the positions

$$(28) \quad \begin{cases} \sqrt{-k^2} = \omega, & \kappa = \omega', & M = \omega_0, & \sqrt{-k^2} S_i(k) = \lambda_i(\omega), \\ \beta(\kappa) = \frac{G_1(\omega')}{(\omega' + \omega_0)^2}, & \alpha(\kappa) = \frac{G_2(\omega')}{(\omega' - \omega_0)^2}, \end{cases}$$

they can be brought exactly to the form (21) (with all the constants R_n equal to zero; see below) and then considered as exact solitons of Syst. (9)

⁽¹⁶⁾ Also here a factor $(-i)$ has been suppressed in the definition of S'_1 and S'_2 .

if conditions (22) are satisfied. If (22) are not satisfied, the ghosts appear, and the procedure indicated in Section 2'2 and 2'3 can be applied to this case too.

The constants R_n might be connected with the existence of bound states, and cannot be obtained in a perturbative treatment. Also in the boson case, as pointed by FORD (5), the general expression for Δ'_F contains a set of such constants, which have been considered equal to zero in all the remaining work on the subject. We have included these constants in formulae from (18) to (21) only for the sake of completeness.

4. - Subtractions in propagators and high frequency behaviour of the vertex.

We shall assume in this section that propagators satisfy a subtracted dispersion formula. We shall limit our remarks to the boson case, the extension to the fermion case being straightforward. Let us suppose the Δ'_F function to be bounded by a polynomial of order n when $|\omega| \rightarrow \infty$. Then we can write the following dispersion relation

$$(29) \quad \Delta'_F(\omega) = \frac{1}{\omega} - (-\omega)^{n+1} \int_{s_0^2}^{\infty} \frac{F(\omega') |\Delta'_F(\omega')|^2}{\omega'^{n+1} (\omega' - \omega - i\varepsilon)} d\omega' + \sum_0^n a_k (-\omega)^k,$$

with $a_0 = 0$ and a_k real. By defining $\delta(\omega) = \Delta'_F(\omega)/(-\omega)^{n+1}$ eq. (29) becomes

$$(30) \quad \delta(\omega) = \frac{(-1)^{n+1}}{\omega^{n+2}} - \int_{s_0^2}^{\infty} \frac{F(\omega') \omega'^{n+1} |\delta(\omega')|^2}{\omega' - \omega - i\varepsilon} d\omega' + \sum_0^n a_k (-\omega)^{k-n-1} = \\ = G(\omega) - \int_{s_0^2}^{\infty} \frac{D(\omega') |\delta(\omega')|^2}{\omega' - \omega - i\varepsilon} d\omega',$$

where

$$G(\omega) = \frac{(-1)^{n+1}}{\omega^{n+2}} + \sum_0^n a_k (-\omega)^{k-n-1},$$

$$D(\omega') = F(\omega') \omega'^{n+1}.$$

It is now very easy to verify by a contour integration in the cut ω -plane that eq. (30) has the solution

$$(31) \quad \delta(\omega) = G(\omega) \frac{1}{1 - \omega \int_{s_0^2}^{\infty} \frac{G(\omega') D(\omega')}{\omega' (\omega' - \omega - i\varepsilon)} d\omega'}.$$

provided

$$(32) \quad I(\omega) = -\omega \int_{8\mu^2}^{\infty} \frac{G(\omega') D(\omega')}{\omega'(\omega' - \omega)} d\omega' \leq 1,$$

for all $\omega < 8\mu^2$ ⁽¹⁷⁾. We remark that in this case $I(\omega)$ is by no means a positive definite quantity so that eq. (32) does not imply also $|I(\omega)| \leq 1$. We are then left with two possibilities as to the asymptotic value of $I(\omega)$,

$$(33) \quad \lim_{\omega \rightarrow -\infty} I(\omega) = \text{finite} \leq 1,$$

$$(34) \quad \lim_{\omega \rightarrow \infty} I(\omega) = -\infty.$$

If eq. (33) holds then

$$\int_{8\mu^2}^{\infty} F(\omega') \omega'^{n-1} d\omega' < \infty,$$

which implies in turn $|I|^2 \xrightarrow{\omega \rightarrow \infty} 0$ stronger than $\omega^{-(n+1)}$. If eq. (34) is the correct one then

$$\int_{8\mu^2}^{\infty} F(\omega') \omega'^{n-1} d\omega' = \infty,$$

but

$$\int_{8\mu^2}^{\infty} F(\omega') \omega'^{n-2} d\omega' < \infty,$$

and we find $|I|^2 \xrightarrow{\omega \rightarrow \infty} 0$ stronger than ω^{-n} . From the above conditions prescriptions on the asymptotic behaviour of form factors can now be obtained. A form factor is usually defined as a matrix element of the type $\langle p' | J(0) | p \rangle$ (where $J(x)$ is some boson current) and by use of reduction formula can be written in the form

$$\langle p' | J(0) | p \rangle \propto V(\omega) = \omega \Delta'_p(\omega) I(\omega) \quad \omega = -(p' - p)^2 - \mu^2.$$

⁽¹⁷⁾ Expression (31) does not represent the more general solution of eq. (30) but is sufficient for the following discussion. Conditions similar to (33) and (34) have also been obtained by SYMANZIK (loc. cit.) with a different method and by S. WEINBERG (private communication).

A very simple discussion shows that $V(\omega)$ is bounded at infinity by $\omega^{(n+1)/2}$ or by $\omega^{-1/2}$ in correspondence with the two possibilities mentioned above. In general therefore we cannot conclude that the $V(\omega)$ vertex must vanish asymptotically as a consequence of the axioms. Only in the very special case in which the absorptive part ρ of Δ'_F converges stronger than ω^{-1} (independently from the behaviour assumed for the whole Δ'_F function) $V(\omega) \rightarrow 0$ when $\omega \rightarrow \infty$. This case corresponds to a finite renormalization constant Z_3^{-1} . In other words we arrive at the general statement that a finite renormalization constant is a sufficient condition to make the vertex $V(\omega)$ converge for high frequencies. Viceversa if $V(\omega)$ diverges for high frequencies then Z_3^{-1} is certainly infinite. This simple discussion shows clearly that a sufficiently detailed experimental knowledge of form factors would allow us, at least in principle, to draw some conclusion on the finiteness or infiniteness of renormalization constants independently from the number of subtractions needed to represent propagators.

Finally we remark that if condition (32) is not satisfied a ghost may appear and all conclusions of the preceding sections as to the possibility of its elimination by subtractions obviously apply also to this more general case. In the following Appendix we will discuss a mathematical feature of the procedure used. In this work as well as in all the reference quoted, all the results stated rest on the applicability of the theorem which will be presented, *i.e.* on the assumption that all the unknown functions which occur as spectral functions in the integral representations satisfy the regularity conditions required for the theorem to be valid. These conditions are not at all stringent, and the most part of «reasonable» functions which can be thought fulfil them. In any case we think it useful to point out the existence of these sufficient conditions and to remark that the application of a mathematical relation used so far is equivalent to postulating that the unknown functions brought in by the theory have, in a certain sense, a «not too strange» behaviour.

* * *

We wish to thank Dr. R. OEHME for his interest in this work and for many stimulating discussions and suggestions. We express our gratitude also to Professor M. CINI, Professor Y. NAMBU and Dr. K. SYMANZIK for useful discussion and criticism.

For the results quoted in the Appendix we are greatly indebted to Professor W. GROSS of the Istituto Nazionale per le Applicazioni del Calcolo who worked out the rigorous proof of the theorem. We thank also Professor C. PUCCI.

APPENDIX

The mathematical procedure we want to discuss in this appendix deals with the evaluation of a limit of the following type:

$$(A.1) \quad \lim_{\omega \rightarrow \infty} \omega P \int_a^{\infty} \frac{\varphi(\omega')}{\omega - \omega'} d\omega',$$

where $\varphi(\omega)$ is a function defined in the interval (a, ∞) , and such as to let integral (A.1) converge.

Such expressions occur very often in connection with the high-energy behaviour of the propagators: so far in practice, the following rather immediate evaluation of (A.1) has been made:

$$(A.2) \quad \lim_{\omega \rightarrow \infty} \omega P \int_a^{\infty} \frac{\varphi(\omega') d\omega'}{\omega - \omega'} = \int_a^{\infty} \varphi(\omega') d\omega',$$

either for integrable or for not integrable $\varphi(\omega')$ (in the latter case it is intended that in the limit expression (A.1) diverges) ⁽¹⁸⁾.

We now will look for the conditions to be satisfied by $\varphi(\omega')$ for formula (A.2) to be valid: we shall find only a set of sufficient conditions, which are however fulfilled by a very wide class of functions $\varphi(\omega')$. To assume that formula (A.2) holds is equivalent to assuming that the spectral functions brought in by the theory are sufficiently «well behaved» as to be enclosed in this class.

In the proof of the theorem we restricted ourselves only to non negative functions defined in the interval (a, ∞) with $a \geq 0$, since this is the case which occurs in practice.

Let us state the theorem, and consider the cases of integrable and non-integrable functions separately.

Let $f(x)$ be a real, non negative, derivable function in the interval (a, ∞) ($a \geq 0$).

1) If $f(x)$ is integrable in this interval we have (z real $> a$)

$$(A.3) \quad \lim_{z \rightarrow \infty} z P \int_a^{\infty} \frac{f(x)}{z - x} dx = \int_a^{\infty} f(x) dx,$$

⁽¹⁸⁾ In the boson case the results of interest are generally obtained by taking the limit $\omega \rightarrow -\infty$ in expressions like (A.1); in this case the principal value plays no role and one can think that the condition (A.4) on the derivative can be dropped. However the validity of our theorem is still important, since it ensures that one obtains the same results by taking either the limit $\omega \rightarrow -\infty$ or the limit $\omega \rightarrow +\infty$. Failure of this circumstance would be rather unpleasant.

under the following conditions for $f(x)$ and its derivative:

$$(A.4) \quad \lim_{x \rightarrow \infty} x \log x f(x) = 0 \quad \lim_{x \rightarrow \infty} \frac{f'(x)}{x^N} = 0,$$

for every integer N larger of a certain value N_0 .

2) If $f(x)$ is not integrable in (a, ∞) the limit of

$$zP \int_a^{\infty} \frac{f(x)}{z-x} dx,$$

generally is infinite ⁽¹⁹⁾, but does not diverge more rapidly than

$$\int_a^z f(x) dx.$$

Then we have

$$(A.5) \quad \lim_{z \rightarrow \infty} \frac{zP \int_a^{\infty} \frac{f(x)}{z-x} dx}{\int_a^z f(x) dx} = \text{finite}.$$

This can be proved if the function $f(x)$ can be written as the sum of an integrable function and of a linear combination of a finite number of functions of the type

$$(A.6) \quad f_{\gamma}(x) = x^{-\gamma}, \quad (0 < \gamma \leq 1),$$

and

$$(A.7) \quad g_{\gamma n}(x) = x^{-\gamma} (\log x)^n. \quad (n \text{ integer} > 0, 0 < \gamma \leq 1):$$

We add some remarks to the above statements.

In the case 1) form. (A.3) can be proved to be valid, also, if conditions (A.4) are replaced with different sets of conditions, less and less stringent for the function and correspondingly more stringent for its derivative. However it can be seen that functions satisfying these new conditions and *not* satisfying (A.4) can be constructed only in a very «artificial» way, and from the practical point of view (A.4) represents the more general condition.

⁽¹⁹⁾ A relevant exception occurs when the divergent part of $f(x)$ behaves at infinity like $x^{-\frac{1}{2}}$ (cfr. form. (A.8) below).

In the case 2) the class of functions considered is somewhat restricted, but still includes a wide variety of functions; namely all functions for which the divergent part is due to one or more dominant terms of the type (A.6) or (A.7). Investigation of the case of a term of the type (A.6) has been already made by OMNÈS⁽²⁰⁾: we will complete his argument and give the value of the limit (A.5) in the case of $f(x) \equiv f_\gamma(x)$. We have

$$(A.8) \quad \lim_{z \rightarrow \infty} \frac{zP \int_a^\infty \frac{x^{-\gamma} dx}{z-x}}{\int_a^\infty x^{-\gamma} dx} = -\pi(1-\gamma) \cotg \pi\gamma.$$

For $\gamma = 1$ the right hand side of (A.8) has to be taken as a limit; the result is 1.

⁽²⁰⁾ R. OMNÈS: *Nuovo Cimento*, **8**, 316 (1958).

RIASSUNTO

Un procedimento di sottrazione proposto recentemente da Redmond per eliminare i « ghosts » dai propagatori viene esaminato dal punto di vista della teoria assiomatica dei campi. Si trova che questo procedimento è equivalente all'introduzione di una speciale funzione vertice che in linea di principio può essere scelta tra le funzioni che hanno le proprietà di analiticità prescritte dagli assiomi. Si mostra che tale situazione esiste sia nel caso di un campo bosonico che nel caso di un campo fermionico. Nella discussione precedente la rappresentazione integrale di Lehmann per i propagatori è assunta essa stessa come un assioma. Sono poi esaminate le modificazioni introdotte nella discussione del problema dei « ghosts » da una formula dispersiva alla Lehmann sottratta. Sono di un certo interesse le conseguenze sul comportamento dei fattori di forma per alte frequenze.

β - γ Angular Correlation in ^{59}Fe and Parity Conservation in Strong Interactions.

E. FUSCHINI, G. GIACOMELLI, C. MARONI and P. VERONESI

Istituto di Fisica dell'Università - Bologna

Istituto Nazionale di Fisica Nucleare - Sezione di Bologna

(ricevuto il 4 Marzo 1960)

Summary. — Nuclear β -decay leaves the residual nucleus partially polarized in the direction of emission of the β -particle. If parity conservation in nuclear states is violated, an asymmetry about 90° of a β - γ directional correlation can be present (existence of a $\bar{\sigma}_{\text{nucleus}} \cdot \bar{p}_\gamma \propto \cos \theta$ term). The asymmetry has been looked for in a β - γ cascade of ^{59}Fe and was found to be zero within one standard deviation of 0.3%. The bearing of this result on an upper limit for F is discussed (F is the relative amplitude of the irregular wave function with respect to the regular one). As a by-product we obtained (63.1 ± 0.8) days for the life-time of ^{59}Fe .

1. — Introduction.

Since the discovery of parity non-conservation in weak interactions, a number of experiments have been performed to test how well parity is conserved in nuclear interactions ^(1,2). As WILKINSON ⁽²⁾ notices, «the absence of an effect due to parity non-conservation may be due to chance cancellations or other unfavourable and unpredictable situations. Thus, we cannot rely on an isolated observation, but try to build up a number of examples of comparable sensitivity, preferably drawn from all possible types of experimentation». The justification of this experiment lies in these words.

Following the standard procedure we write the nuclear wave functions in the form

$$\psi = \psi_{\text{regular}} + F\psi_{\text{irregular}},$$

⁽¹⁾ N. TANNER: *Phys. Rev.*, **107**, 1203 (1957).

⁽²⁾ D. H. WILKINSON: *Phys. Rev.*, **109**, 1603, 1610, 1614 (1958).

where F is the relative strength of the parity non-conserving coupling. Our task is the determination of F or of an upper limit for F by an experiment on β - γ angular correlations.

In Section 2 we describe the method followed in the present experiment. In the following sections the experiment is discussed and results given.

In most of these experiments a difficulty arises in calculating the sensitivity to F because of an unknown factor R . R is a ratio of matrix elements for γ -ray transitions which measures the intrinsic transition amplitude from, or to the irregular components relative to that from, or to the regular ones. Since very few experimental data are available, R has to be calculated. In light nuclei it may be estimated by using the single particle picture which is expected to be somewhat reliable. In heavier nuclei, other models have to be used, but none is expected to give reliable results.

2. - The method.

In a β - γ directional correlation one looks for the presence or the absence of an odd power of $\cos \theta$, where θ is the angle, the direction of emission of the γ -ray makes with the direction of emission of the β -ray. In order to understand how the term arises, one has to remember that the β -decay of a nucleus X produces a nucleus Y^* polarized in the direction of emission of the β particle. Now one has a polarized nucleus which γ -decays. Odd powers of $\cos \theta$ may arise from the interference of the transitions from the regular and irregular components of the wave functions which carry *orbital* angular momenta differing by one unit ⁽³⁾. In other words, one may construct a pseudoscalar term $\sigma \cdot p_\gamma$ out of the spin of the nucleus Y^* (individuated by the direction of emission of the electron) and of the direction of the emission of the γ -ray. The interference effect is proportional to RF .

Experimentally a γ counter is first placed at an angle θ (let us call it « right ») with respect to the axis defined by the radioactive source and the β counter; coincidence β - γ are registered. Subsequently the γ counter is placed at $\pi - \theta$ (« left ») and the asymmetry

$$A = 2 \frac{\text{right} - \text{left}}{\text{right} + \text{left}},$$

is thus obtained. From what has been said, this asymmetry is of the order

$$A \simeq PRF \sim F_w RF \sim RF,$$

⁽³⁾ C. N. YANG: *Phys. Rev.*, **74**, 771 (1948).

where P is the degree of polarization of the nucleus Y^* and may be calculated by using the $V-A$ theory of weak interactions. P depends on Ve/c where Ve is the velocity of the β -ray and c is the velocity of light; thus P increases, increasing the electron energy. The formula we have given for the order of magnitude of the asymmetry is certainly a very crude approximation, though it may be considered to be all right to establish upper limits. But, in particular, it does not take into account at all the possible θ dependence of the asymmetry. Very recently KRÜGER⁽⁴⁾ has calculated the asymmetry and we refer to this paper for correct values.

It is clear that to have high sensitivity, one should choose decays with large values of R , *i.e.* decays where the irregular component is intrinsically more probable than the regular one. This is so when the regular transition is magnetic in character and thus the irregular one is electric. Even larger values of R may be found when the regular transition is partially forbidden by some selection rule like the isotopic spin selection rule. In this case, the lifetime of the level may be rather long ($> 10^{-10}$ s) and in order to apply the theory of angular correlations, this level cannot be the intermediate one.

This experiment measures F and is thus rather sensitive.

The presence of the term $\vec{\sigma} \cdot \vec{p}_\gamma$ would prove that parity is violated in nuclear interactions, while its absence would not necessarily prove that parity is conserved, though it may strongly suggest it. The experiment is also sensitive to parity admixtures in electro-magnetic interactions, but we assume here that they conserve parity.

3. - β - γ correlation in ^{59}Fe .

Beside what has been already said, some practical considerations should be kept in mind in choosing a source.

A first consideration is that it is by far easier to see a small $\cos \theta$ term on a flat distribution than on a distribution containing higher even powers of $\cos \theta$. In this case the angles can be very poorly defined, while great precision is required when higher even powers of $\cos \theta$ are present.

This consideration limits essentially the choice of the β transitions to allowed ones (but also transitions where the intermediate nucleus has spin $\frac{1}{2}$ give isotropy).

A second consideration is that the life-time of the source should be reasonably long in order to be able to perform coincidence measurements, since we cannot make our source in loco. Moreover, the decay scheme should not be too messy and the various possible channels should be easily separated.

(4) L. KRÜGER: *Zeits. f. Phys.*, **157**, 369 (1955).

The ^{59}Fe source has most of the requirements we look for. Fig. 1 shows the accepted decay scheme as given by references (^{5 6}). We use the 54% channel which leads, via a pure GT transition, to the $5/2^-$ level. The 1.10 MeV γ -ray to the ground state is an $M1$ transition. The other channels either give lower energy β -rays and are thus easily discriminated by a proper bias of the electron counter, or do not give γ -rays at all. Moreover, the 1.10 and 1.29 MeV γ -rays, when detected by means of a NaI(Tl) crystal, give two nice peaks easily resolved.

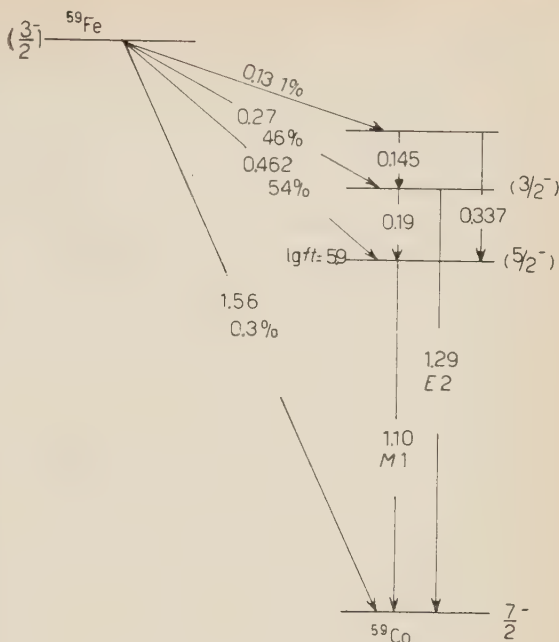


Fig.- 1. ^{59}Fe decay scheme.

4. - Experimental apparatus.

A 50 μC ^{59}Fe source was prepared at Hamersham (United Kingdom) by deposition of mg 0.13 of FeCl_3 in a circle 0.3 cm in diameter on a 2 mg/cm^2 terylene backing. A thin Aluminium strip (0.06 mm) insures the electrical contact and a 1 mg/cm^2 terylene film seals the source.

The β counter is a plastic scintillator 0.9 cm in diameter and 2 mm thickness; it was placed about 3.5 cm from the ^{59}Fe source. A long lucite light pipe connects the scintillator to the photomultiplier.

The γ counter is a cylindrical NaI(Tl) crystal 1 $\frac{3}{4}$ in. in diameter and 2 in. long. Its front face was placed either at 8 cm or at 12 cm from the source.

The counters may slide both radially and azimuthally on precision guides. The photo-tubes are protected by a single mu-metal shield.

The electronics is essentially made of two single channel analysers based on two EFP60 trigger generators differently biased, followed by a diode coincidence circuit and preceded by simple window amplifiers. Single channel output pulses are standard negative pulse about 50 ns long. The resolving time

(⁵) N. B. S. *Nuclear Data Sheets* (1959).

(⁶) D. STROMINGER, J. M. HOLLANDER and G. T. SEABORG: *Rev. Mod. Phys.*, **30**, 585 (1958).

of the diode coincidence circuit is limited by these times. The intrinsic possibilities of the EFP60 tube itself, which may produce sometime uncertainty in the output pulses, does not allow much shorter pulses to be used with safety. With this arrangement we achieve delay curves with about 110 ns full length at half height and a nice plateau 75 ns long.

In practice we have 3 γ -ray counters and the necessary circuitry so that we can count at three angles at the same time. Runs of an hour duration are automatically taken: each hour the coincidence numerators, the β and γ mechanical registers are first photographed and then reset.

5. - Experimental procedure.

The experimental β -ray spectrum shows almost an exponential shape. It may be explained with the relative high probability of electron scattering and degradation in the source itself, in the source backing, in the plastic scintillator and in the surrounding materials. The relatively poor energy resolution of the counter itself (about 30% for the ^{137}Cs line) is another reason. This is not much of a problem for us, since we are interested only in the higher portion of the spectrum. The lower bias of the β channel was set by using the

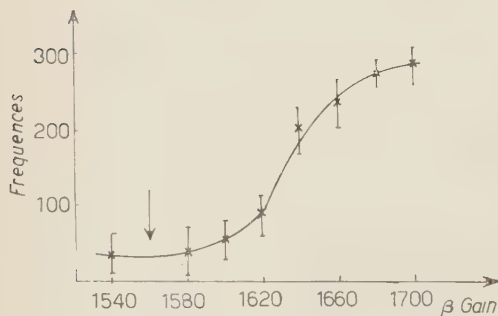


Fig. 2. - Coincidences β - γ 1.29 MeV as function of counter high voltage.

following procedure: the upper bias was removed and coincidences of β -rays with the 1.29 MeV line were taken as function of β gain. Real coincidences should be zero up to the point where β -rays of less than 0.27 MeV come through (see decay scheme). Fig. 2 shows the results with the random counts subtracted. The lower bias was set at the arrow point. Then the upper bias was placed in such a position so as to include all the β -rays up to 0.46 MeV, thus excluding few energy counts from cosmic rays, converted 1.10 and 1.29 MeV γ -rays, etc.

The biases of the γ -ray channels were placed so as to count slightly more than half of the counts in the proper photoelectric peak.

From 20 to 23 one-hour runs per day were taken both with appropriate delay and with delay increased or decreased by 150 ns to measure randoms. The rest of the time was spent on checking the experimental situation.

The signal to noise ratio defined as the number of counts with correct delay minus randoms divided by the number of randoms changed from about 9

to 50, improving slowly with time (as it should, since $((S/N)t - 0)/((S/N)t - t) = \exp[-t/\tau]$). The time spent on randoms was slowly decreased so as to get maximum advantage of statistics.

The data were normalized to the product of the rates of singles and taking into account the lifetime of the source.

The asymmetry about 90° was measured by leaving the counters at a position θ for a few days and then changing them to a position $\pi - \theta$. Thus the results obtained by the same counters were compared. The use of several counters at the same time allows other comparisons to be made, which are very useful for checking the internal consistency of the apparatus.

Since we are looking for a very small asymmetry, a number of precautions and corrections have to be considered.

The first correction comes in because of the resolving time of the registers. SODECO Mechanical Registers were used directly at the output of the coincidence circuits since the coincidence rate was sufficiently slow and scaling was not necessary. The registers have a measured resolving time of $(2.2 \pm 0.2) \cdot 10^{-2}$ s. Thus we have a small counting loss when we are measuring coincidences with correct delay while there is essentially none when we measure randoms. The correction was at most 0.4% and was taken into account.

A serious error may arise because of fluctuations of the electronics. In order to understand it, let us divide the single γ -ray rate in two parts: one coming from the 1.1 MeV γ -rays and the other coming from spurious counts, mainly from Compton degraded 1.29 MeV γ -rays. The before mentioned normalization factors for real counts should be based on true 1.1 MeV singles. Very probably both good counts and spurious counts diminish equally in time and thus, if the electronics biases would remain constant, then normalization factors would be unaffected. The same conclusion holds if the ratio between the two rates remains constant under bias changes.

It may be worthwhile to emphasize that this correction does not arise for random rates, since they are determined only by the number of singles rates in the counters, independently of where they come from.

The knowledge of the structure of the spurious counts is needed to evaluate the importance of the effect. If one makes the reasonable assumption that spurious counts come mainly from the 1.29 MeV line, one may take a radioactive source emitting only 1.29 MeV γ -rays and may look at the Compton region of interest with the same apparatus used for the ^{59}Fe source. By proper normalizations, the structure of the spurious counts is thus found.

^{22}Na is a suitable source and was thus used. We found that 19% of the counts in the 1.1 MeV region are due to Compton degraded 1.29 MeV γ -rays. By changing the channel bias by ± 0.5 V, the ratio changed by $\pm 1.0\%$. Thus for small fluctuations of the electronics the ratio of spurious counts to total counts is not constant, but the change is approximately linear. If the fluctua-

tions are random fluctuations, there is an averaging out of the effect. A change of ± 0.5 V in the channel bias means a reduction of about 1% in the singles γ rates. We thus constructed logarithmic graphs of the rates of singles and only those runs were considered which had a single hourly counting rate within a 1% band determined by the calibration data and the general behaviour. We feel confident that the errors in the normalization average out to a much smaller value (probably to a tenth of the maximum error, which is about $\pm 1.2\%$), provided a sufficient number of runs are used.

A similar situation may arise in the β counter, but here we are looking practically at the top of the spectrum and so fewer spurious counts should be present. A 10% band was thus considered satisfactory.

From $\frac{1}{2}$ to $\frac{2}{3}$ of the data were thrown away, because they did not satisfy these requirements.

Geometrical corrections should be rather small: an error in the angle θ does not make much difference, since the main feature of our β - γ correlation is isotropy. An error in the γ counter to source distance is automatically corrected by our normalization procedure. Other small corrections, like the different γ -ray absorption at different angles, are taken care of by the normalization. The finite solid angle effect does not introduce any error, again because of isotropy. Source uniformity cannot be checked too well, but the smallness of the source and the use of different counters at different positions should minimize the effect.

The decaying nucleus Y^* recoils in the laboratory system with a «mean» velocity of about 4 km/s ($\beta \simeq 1.3 \cdot 10^{-5}$). This produces two effects: *a*) the Doppler effect which changes the energy of the γ -ray and thus the efficiency of the γ -counter, this effect is taken care of by the normalization procedure; and *b*) the aberration effect which changes an isotropic distribution in the c.m. system to a distribution $1 + 2\beta \cos \theta$ in the laboratory. Owing to the smallness of β , it produces an asymmetry of less than 10^{-4} , which is negligible.

6. - Results.

Table I shows the results: θ is the angle the γ -ray makes with the β particle. A is the asymmetry

$$A = 2 \frac{R - L}{R + L},$$

where R (right) is the number of coincidence counts for θ in the region $0 < \theta < \pi/2$ and L (left) for $\pi/2 < \theta < \pi$; both the asymmetries and the errors are in %. Quoted errors represent standard deviations and include sta-

tistical errors only. The values fluctuate somewhat around zero, with which they are certainly consistent, though a best fit line would be somewhat inclined with respect to the θ axis. Assuming the results to be consistent with zero, one may add them up and get the total asymmetry quoted in the last line of Table I.

TABLE I. — *Measured asymmetries as function of the angle. Quoted errors are standard deviations.*

θ	A (%)
30°	+ 1.3 ± 0.7
40°	— 0.7 ± 0.7
50°	+ 0.2 ± 0.5
60°	— 1.0 ± 1.9
70°	— 2.2 ± 1.4
total	+ 0.1 ± 0.3

By using the correct formulae of reference (1), we may write in our case,

$$A \simeq 1.60 RF \cos \theta .$$

By averaging on the cosinus in our case, one obtains for the total value

$$A \simeq RF .$$

The single particle estimate gives (2)

$$R \simeq \frac{m_p cr}{3\hbar} \simeq 7.4 ,$$

where m_p is the mass of the proton, c is the velocity of light in vacuum, r is the nuclear radius, and \hbar Plank's constant divided by 2π .

Classical theory in the dipole approximation yields (7)

$$R \simeq \frac{2m_p cr}{\hbar} \simeq 45 .$$

Thus the single particle estimate gives

$$F < 4 \cdot 10^{-4}$$

(7) See for example, A. E. S. GREEN: *Nuclear Physics* (New York, 1959).

while the classical estimate yields

$$F < 7 \cdot 10^{-5}.$$

Our result has about the same precision and is in agreement with the results of other authors (^{1, 2, 8, 9}).

We feel that the experimental precision reached in this experiment could be somewhat improved with the use of a stronger ⁵⁹Fe source and faster electronics extremely well stabilized.

From the graphs, we obtain as a by-product the life-time of the ⁵⁹Fe source:

$$\tau = (63.1 \pm 0.8) \text{ days}.$$

The error is the standard deviation of the average and it is much larger than the purely statistical error, since it includes the effect of random electronic and other uncertainties.

* * *

It is a pleasure to thank Professor G. PUPPI and Dr. TOMASINI for valuable discussions.

We should also express our thanks to Dr. ZUFFI for the analysis of the data, to Mr. G. BUSACCHI and O. CINELLI for the setting up of the experiment and Mr. J. C. MAYNARD of U.K.A.E.A., for the preparation of the source.

(⁸) F. BOEHM and U. HAUSER: *Bull. Am. Phys. Soc.*, **4**, 460A, P5 (1959).

(⁹) R. HAAS *et al.*: *Phys. Rev.* (to be published).

RIASSUNTO

Il decadimento β polarizza parzialmente il nucleo nella direzione di emissione dell'elettrone. Se si ha violazione della conservazione di parità negli stati nucleari, nella correlazione angolare β - γ può essere presente una asimmetria intorno a 90° (può esistere cioè un termine $\vec{\sigma}_{\text{nucleo}} \cdot \vec{p}_\gamma$ proporzionale a $\cos \theta$). È stato eseguito un esperimento con lo scopo di cercare una tale asimmetria nel decadimento β - γ del ⁵⁹Fe. I risultati hanno mostrato, entro un errore standard del 0.3% che l'asimmetria è zero. Sulla base di tali risultati è stato possibile discutere un limite superiore per F e fissarne il valore (F è l'ampiezza relativa della funzione d'onda irregolare rispetto a quella regolare). L'esperienza ha anche consentito di ricavare la vita media del ⁵⁹Fe ($\tau = (63.1 \pm 0.8)$ giorni).

New Semiphenomenological Proton-Proton Potential (*).

R. A. BRYAN

University of Rochester - Rochester, N. Y.

(ricevuto il 9 Marzo 1960)

Summary. — A static plus spin-orbit proton-proton potential model has been derived semiphenomenologically. The potential resolves asymptotically to the one-pion-exchange potential and has been fixed in the region within $r=1.5\hbar/\mu c$ by matching the 310 MeV MacGregor-Moravcsik-Stapp phase shift solution no. I. The resulting potential gives an improved fit to the p-p scattering data over the 40 to 310 MeV energy range.

1. — Introduction.

The considerably improved fit to the high-energy proton-proton scattering data achieved by the SIGNELL-MARSHAK (SM) ⁽¹⁾ and GAMMEL-THALER (GT) ⁽²⁾ static plus spin-orbit potential models has prompted the development of a new model in which some features of both these approaches have been incorporated to advantage.

The GT model gives fairly good overall agreement with experiment up to the order of 300 MeV through potentials which have been derived essentially by matching the 310 MeV Stapp-Ypsilantis-Metropolis (SYM) phase shift so-

(*) This work supported in part by the IBM Corporation and the U.S. Atomic Energy Commission.

⁽¹⁾ P. S. SIGNELL and R. E. MARSHAK: *Phys. Rev.*, **106**, 832 (1957); **109**, 1229 (1958); P. S. SIGNELL, R. ZINN and R. E. MARSHAK: *Phys. Rev. Lett.*, **1**, 416 (1958). The last is referred to as the SM1 potential.

⁽²⁾ J. L. GAMMEL and R. M. THALER: *Phys. Rev.*, **107**, 291 (1957).

lution No. 1 ⁽³⁾ and the singlet scattering length and effective range. The model lacks a sound basis in meson theory, however, for the potentials have been derived purely phenomenologically. The SM model, on the other hand, has a basis in meson theory, since it employs the Gartenhaus potential, but it gives reasonable overall agreement with experiment only up to 150 MeV.

A direct way to guarantee that a new model will reproduce the data in the 300 MeV region is to fix the potentials by matching a phase shift solution at this energy in the manner of Gammel and Thaler, and judging from their results, this will also tend to produce a reasonable fit down to much lower energies. However, such an approach will not yield potentials with the correct asymptotic dependence. To insure the latter, one of the meson-theoretic calculations of the static potentials can be taken over, leaving just the spin-orbit potential to be derived phenomenologically, as in the SM approach, but now the model will probably be too inflexible to yield a precise fit to the phase shift solution.

To allow flexibility, we took over the one-pion exchange potential (OPEP) and fixed the static potentials phenomenologically in the region where departures from the OPEP become significant. However, various meson-theoretic calculations ⁽⁴⁻⁶⁾ were kept in mind for insight as to more probable forms in this region. It appeared reasonable to represent the static potentials by:

$$(1) \quad V = \sum_{n=2}^5 A_n x^{-n} \exp[-2x] + V_2 \text{ (OPEP)}$$

together with infinite repulsive cores for the central potentials. The pion-nucleon coupling constant $g^2/4\pi$ is taken to be 0.08. Since meson theory provides little insight as to the shape of the spin-orbit potential, except that it is asymptotically weakly attractive and of range $\hbar/2\mu c$ ^(7,8), this component was fixed purely phenomenologically, using the functional form:

$$(2) \quad V = V_0 x^{-n} \exp[-2x]$$

and a straight cut-off at some distance x_c .

⁽³⁾ H. P. STAPP, T. J. YPSILANTIS and N. METROPOLIS: *Phys. Rev.*, **105**, 302 (1957).

⁽⁴⁾ S. GARTENHAUS: *Phys. Rev.*, **100**, 900 (1955).

⁽⁵⁾ M. KONUMA, H. MIYAZAWA and S. OTSUKI: *Progr. Theor. Phys. (Kyoto)*, **19**, 17 (1958).

⁽⁶⁾ M. TAKETANI, S. MACHIDA and S. OHNUMA: *Progr. Theor. Phys. (Kyoto)*, **6**, 638 (1951); **7**, 45 (1952).

⁽⁷⁾ S. OKUBO and S. SATO: *Progr. Theor. Phys. (Kyoto)*, **21**, 383 (1959).

⁽⁸⁾ M. SUGAWARA and S. OKUBO: *Phys. Rev.* (to be published).

2. - Derivation of the potential.

In determining the potentials we relied primarily on the 310 MeV MacGregor-Moravesik-Stapp phase shift solution No. 1 ⁽⁹⁾ (MMS No. 1) (Table I) which supersedes the SYM solutions Nos. 1 and 3. MMS No. 2 was excluded

TABLE I. - Predicted nuclear Blatt and Biedenharn phase shifts ^(*) (in degrees) from 40 to 310 MeV. At 310 MeV, the MacGregor-Moravesik-Stapp phase shift solution no. 1 (MMS no. 1) is also listed.

		1S_0	1D_2	1G_4	3P_0	3P_1	3P_2	ε_2	3F_2
	40 MeV	43.7	0.8	0.0	9.4	- 6.6	3.6	- 16.4	- 0.2
	150 MeV	18.7	5.1	0.5	4.7	- 16.8	13.6	- 13.5	0.2
	210 MeV	9.3	7.8	0.8	- 1.1	- 21.1	16.0	- 11.6	0.6
	310 MeV	- 3.3	12.4	1.2	- 11.0	- 27.4	16.6	- 9.5	0.9
MMS no. 1	310 MeV	- 8.9	11.9	0.8	- 11.3	- 27.5	16.8	- 5.8	1.1
		3F_3	3F_4	ε_4	3H_4	3H_5	3H_6	ε_6	3L_9
	40 MeV	- 0.1	0.0	- 23.2	- 0.0	—	—	—	—
	150 MeV	- 2.0	1.2	- 34.4	- 0.4	- 0.2	0.1	- 34.9	- 0.0
	210 MeV	- 2.7	2.1	- 31.9	- 0.5	- 0.6	0.3	- 38.7	- 0.1
	310 MeV	- 3.6	4.1	- 22.2	- 0.1	- 1.1	0.7	- 39.5	- 0.4
MMS no. 1	310 MeV	- 3.5	4.1	- 21.3	- 0.1	- 1.1	0.2	—	—

(*) These phase shifts have been calculated from the nuclear potential alone.

as being incompatible with a local representation ⁽¹⁰⁾. In utilizing the MMS No. 1 solution, we found the following rule to be quite useful: for a given energy, a phase shift of order L is primarily determined by a corresponding finite region of the potential. (First suggested by calculations in Born approximation, this rule proved to be valid for our purposes except in the case of potentials extremely attractive near the core region.) Since there was little

⁽⁹⁾ M. H. MACGREGOR, M. J. MORAVESIK and H. P. STAPP: *Phys. Rev.*, **116**, 1248 (1959).

⁽¹⁰⁾ It appears improbable that the 310 MeV MMS no. 2 1S_0 and 1D_2 phase shifts could be fit by a static local potential which simultaneously matched the low energy parameters. In addition, the MMS no. 2 F phase shifts seem inconsistent with meson-theoretic tensor potentials.

overlap between regions for a given even or odd potential (Table II), we were able to fix the potentials region by region, by matching the corresponding phase shifts to the MMS solution. The resulting potentials were then checked against experiment at lower energies and adjustment made for a better overall fit over the 40 to 310 MeV range.

TABLE II. - *Approximate regions where potentials are predominantly weighted in the Born approximation solution for a phase shift of angular momentum L at 310 MeV.*

L	S	P	D	F	G	H
x	$0 \div 0.7$	$0.3 \div 1.0$	$0.6 \div 1.3$	$1.0 \div 1.7$	$1.3 \div 2.0$	$1.7 \div 2.4$

The MMS singlet phase shifts suggested a ${}^1V_c^-$ consisting of a repulsive core followed by a monotonic attractive potential, similar to the Gartenhaus potential. The final potential turned out to be more attractive in the « D » region and slightly less so in the « G » region. The analytic form is:

$$(3) \quad {}^1V_c^+(x) = \begin{cases} \infty, & 0 \leq x \leq 0.28 \\ [103.4 - 305.8x + 89.4x^2]x^{-5} \exp[-2x] + {}^1V_{2c}^+(x), & 0.28 < x, \end{cases}$$

in MeV, with x in units of $\hbar/\mu c$.

Simultaneous determination of the three triplet potentials, though more difficult, could be effected since there were now three phase shifts corresponding to each region. The phase shifts were solved for in Born approximation and the resulting 3×3 matrix inverted to give an approximate idea of the contribution of each potential in each region. Examination of these trial potentials showed the central and tensor potentials to be similar to the Gartenhaus potentials, and the spin-orbit to be quite attractive and very short-ranged. Iteration on the IBM 650 ultimately produced the following forms:

$$(4) \quad \begin{cases} {}^3V_c^-(x) = \begin{cases} \infty, & 0 \leq x \leq 0.38 \\ [-55.84 + 132.85x - 96.00x^2]x^{-5} \exp[-2x] + {}^3V_{2c}^-(x), & 0.38 < x \end{cases} \\ {}^3V_T^-(x) = [27.45 - 172.50x + 242.75x^2 - 116.82x^3] \cdot x^{-5} \exp[-2x] + {}^3V_{2T}^-(x) \\ {}^3V_{LS}^-(x) = \begin{cases} -550, & 0 \leq x \leq 0.54 \\ -12.0 x^{-8} \exp[-2x], & 0.54 < x. \end{cases} \end{cases}$$

3. - Discussion.

The ${}^3V_c^-$ potential is similar to the Gartenhaus, and represents the chief difference between our model and the GT model, which employs just a repulsive core in this instance. The strong attractive nature of our ${}^3V_c^-$ near the core region arises primarily as a result of matching the 3P_2 and 3F_4 phase shifts to the MMS values of 17° and 4° . Both phase shifts are quite sensitive to an attractive potential in this region (Born approximation breaks down in this instance) and since the spin-orbit matrix elements is $+3$ in the 3F_4 state, it proves necessary to enhance the central potential at the expense of the spin-orbit to give a 310 MeV 3P_2 value of 17° and yet maintain the 3F_4 at 4° . The ${}^3V_{\sigma^-}$ is chosen to be somewhat weaker than the Gartenhaus, both to avoid excess tensor splitting of the 3P_0 and 3P_1 phases and to reduce the magnitude of the F phases. In contrast, the purely attractive spin-orbit potential is stronger and more short-ranged than either the SM1 or the GT po-

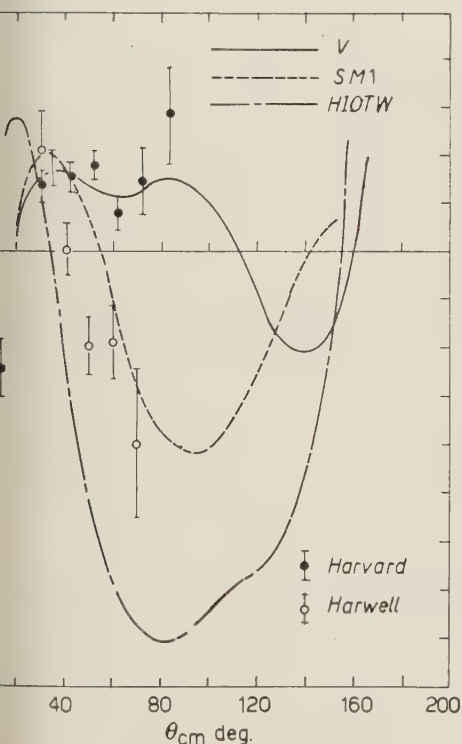


Fig. 1. - Comparison of 150 MeV proton-proton $D(\theta)$ predictions with experiment.

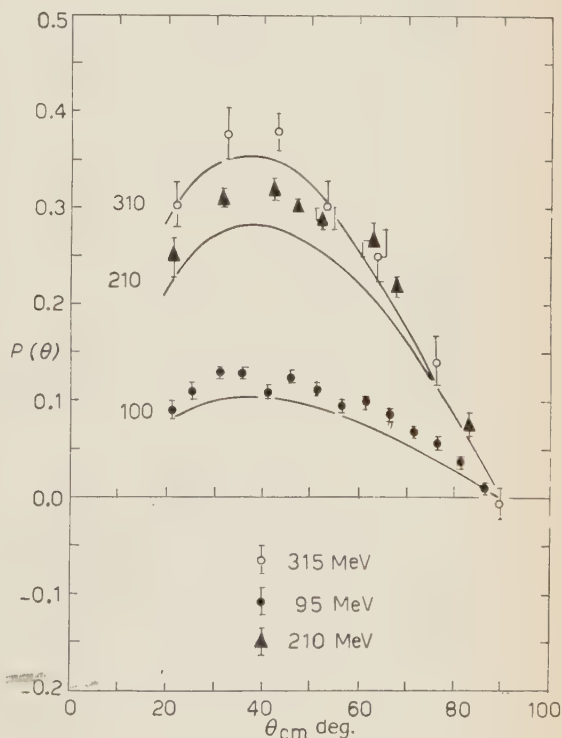


Fig. 2. - Comparison of 100, 210 and 310 MeV proton-proton polarization predictions with experiment.

tentials. This results from the MMS solution requirement for a strong spin-orbit contribution in the « P » region (for adequate depression of the 3P_0 and 3P_1 phases) and yet a very weak contribution in the « F » and « H » regions. A weak spin-orbit potential tail appears to be really needed; if the strength

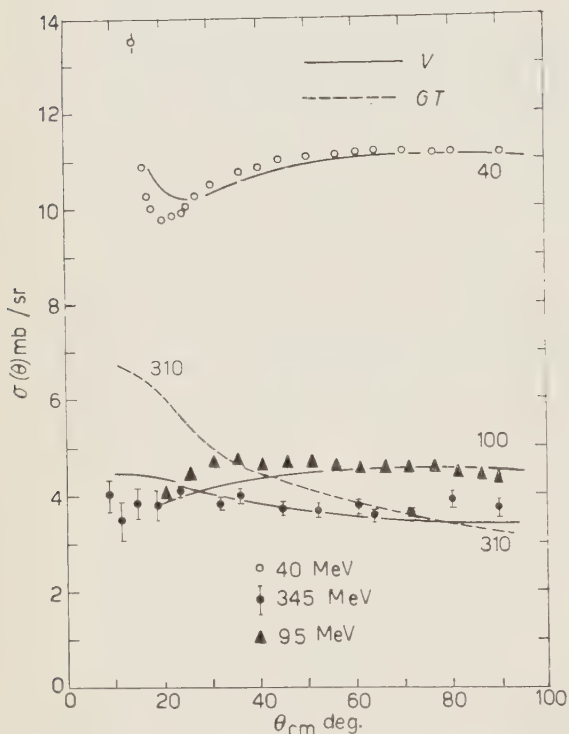


Fig. 3. - Comparison of 40, 100 and 310 MeV proton-proton differential cross-section predictions with experiment. V refers to predictions of the present model.

of the spin-orbit potential were increased to that of the SM1 or GT potentials in the region beyond $x=1$, the one to two degree increase in the 3F_4 phase shift would be sufficient to introduce considerable anisotropy in the predicted differential cross-section at 310 MeV.

HAMADA *et al.* (HIOTW) ⁽¹¹⁾ have questioned the need of introducing a spin-orbit potential at all in fitting the scattering data up to 150 MeV. Although we agree that the spin-orbit potential should be very weak asymptotically, we feel that it should be quite strongly attractive within $x=1$, thereby having a noticeable effect on the 150 MeV P waves. In particular, the spin-orbit potential depresses the 3P_0 phase shift, and, as NIGAM ⁽¹²⁾ has shown, this causes the $D(\theta)$ curve to rise. This effect is illustrated in Fig. 1 where the predicted $D(\theta)$ curves are seen to rise up to the 142 MeV Harvard data as the strength of the spin-orbit potential increases from zero (HIOTW) through that of the SM1 potential to that of the present model. In view of the Harvard data (which is probably to be preferred over the Harwell data) we feel that the spin-orbit interaction is important at 150 MeV.

⁽¹¹⁾ T. HAMADA, J. IWADARE, S. OTSUKI, R. TAMAGAKI and W. WATARI: *Progr. Theor. Phys.*, **22**, 566 (1959).

⁽¹²⁾ B. P. NIGAM: *Progr. Theor. Phys. (Kyoto)*, **23**, 61 (1960).

Our potential model achieves a fairly good fit to the data ⁽¹³⁾ over the 40 to 310 MeV range, although the predicted polarization falls somewhat below experiment (Fig. 2), and some anisotropy appears in the cross-section prediction at 310 MeV (Fig. 3). This latter can be attributed to the deviation of our predicted 310 MeV 1S_0 phase shift of -3° from the MMS value of -9° . To reduce our 1S_0 phase shift to the MMS value at 310 MeV and yet maintain the 40 MeV values of 44° (as required in combination with our other phase shifts) would require too deep a well in the singlet potential to be compatible with the 310 MeV MMS 1D_2 phase shift of 12° .

It is interesting to examine $R(\theta)$ in this connection. NIGAM ⁽¹²⁾ has shown that a decrease in the 1S_0 phase shift causes a noticeable increase in the R parameter in the region of 90° . Our model predicts a 1S_0 phase shift about 5° greater than that of the GT model over the entire 40 to 310 MeV range, and this difference at 150 MeV is reflected in the respective predictions for $R(\theta)$ (Fig. 4).

Another measurement of interest is that of the correlation coefficient C_{nn} for 90° at 320 MeV. The GT model predicts a 310 MeV value of 0.28 while our model predicts 0.56, as compared with the experimental value of 0.77 ± 0.11 .

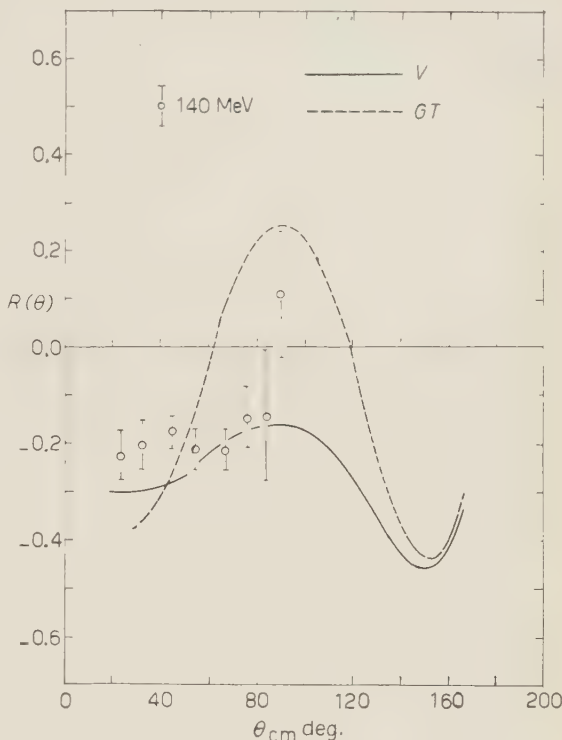


Fig. 4. — Comparison of 150 MeV proton-proton $R(\theta)$ predictions with experiment.

⁽¹³⁾ PP $\sigma(\theta)$ 39.4 MeV: L. H. JOHNSTON and D. A. SWENSON: *Phys. Rev.*, **111**, 212 (1958); $\sigma(\theta)$ and $P(\theta)$ 95 MeV: J. N. PALMIERI, A. M. CORMACK, N. F. RAMSEY and R. WILSON: *Ann. Phys.*, **5**, 299 (1958); $D(\theta)$ 142 MeV (Harvard): C. F. HOANG *et al.*: *Phys. Rev.* (to be published); $R(\theta)$ 140 MeV and $D(\theta)$ 150 MeV (Harwell): A. E. TAYLOR (private communication); $P(\theta)$ 210 MeV: E. BASKIR, E. M. MARSHAK, A. ROBERTS and J. H. TINLOT: *Phys. Rev.*, **106**, 564 (1957); $P(\theta)$ 315 MeV: O. CHAMBERLAIN, E. SEGRÈ, R. D. TRIPP, C. WIEGAND and T. YPSILANTIS: *Phys. Rev.*, **105**, 288 (1957); $\sigma(\theta)$ 345 MeV: O. CHAMBERLAIN, E. SEGRÈ and C. WIEGAND: *Phys. Rev.*, **83**, 923 (1951). Data as reduced by H. P. STAPP, T. J. YPSILANTIS and N. METROPOLIS (ref. ⁽³⁾); C_{nn} 320 MeV: A. ASHMORE (private communication).

* * *

The author would like to express his appreciation to Professor R. E. MARSHAK for the suggestion of this topic and his continuing guidance during the course of the work.

RIASSUNTO (*)

Si è derivato in modo semifenomenologico un modello del potenziale statico positivo spin-orbita nell'interazione protone-protone. Il potenziale si avvicina asintoticamente al potenziale di scambio di un pione ed è stato fissato nella regione entro $r=1.5\hbar/\mu c$ verificando la soluzione no. 1 di MacGregor-Moravcsik-Stapp per lo spostamento di fase a 310 MeV. Il potenziale risultante dà una migliore approssimazione ai dati di scattering nella regione di energia da 40 a 310 MeV.

(*) Traduzione a cura della Redazione.

Surface Effects in (γ, n) and (γ, p) Reactions.

V. DE SABBATA

Istituto di Fisica dell'Università - Ferrara
Istituto Nazionale di Fisica Nucleare - Sezione di Bologna

A. TOMASINI

Istituto di Fisica dell'Università - Bologna
Istituto Nazionale di Fisica Nucleare - Sezione di Bologna

(ricevuto il 14 Marzo 1960)

Summary. — We have studied, in the independent particles model, the contribution to the photonuclear reactions by the surface of the nuclei; we have, in particular, analyzed the angular distributions. The dipole approximation in the case of photoneutrons is good, so the angular distribution is symmetrical around $\pi/2$; the presence of an interference term between the transitions $l \rightarrow l+1$, $l \rightarrow l-1$ results in a possible minimum at $\pi/2$ instead of the usual maximum. In the case of photoprotons, as this approximation no longer holds, we have considered the closed expression without any expansion in multipoles; so the angular distribution results strongly asymmetrical. Numerical calculations have been carried out at various energies for $A=16$, $A=40$ and $r_0=1.2$, $r_0=1.4$. The cross-section results of the order of 10^{-26} cm² and the ratio $\sigma(\gamma, p)/\sigma(\gamma, n)$ of the order of unity.

1. — Introduction.

In a previous paper ⁽¹⁾ we gave some preliminary results on surface effects in photonuclear reactions in which the incident ray interacts merely with the nucleons near the surface of the nucleus. The model is very similar to the AUSTERN, BUTLER, McMANUS ⁽²⁾ one; we assume that the interaction of the γ -ray with

⁽¹⁾ V. DE SABBATA and A. TOMASINI: *Nuovo Cimento*, **13**, 1268 (1959).

⁽²⁾ N. AUSTERN, S. T. BUTLER and M. McMANUS: *Phys. Rev.*, **92**, 350 (1953)

the nucleons inside the nucleus, gives rise essentially to reactions going via compound nucleus, while the interaction with the surface nucleons gives rise to direct reactions.

The initial state of the nucleus has been represented by eigenfunctions of independent particles model in a square well.

«Surface reactions» here means that the integrations in the transition matrix elements have been carried out from the radius $R = r_0 A^{\frac{1}{3}}$ of the nucleus up to the infinity, taking into account only the external tail of the initial wave functions; since the nucleons are «outside» of the nucleus also in the initial state the distortion of their final wave function (due to interaction with other nucleons of the nucleus) should be small; therefore we have assumed a plane wave for the final wave function. This assumption allows to calculate the transition matrix elements in a straightforward way without expanding in multipoles.

LANE⁽³⁾ recently has shown that the external transitions play an important role in photonuclear reactions; in fact we find total cross sections which are of the order of 10^{-26} cm². Perhaps this value is too large, owing probably to the crudeness of the model; anyhow we think that the model, while too crude in order to give correct absolute values, can show some features of the interaction, such as the sensitivity of the differential cross-section to small variations of the nuclear radius and of the γ -ray energy.

In the present paper we have taken into account both (γ, n) and (γ, p) processes; we have chosen two different values for r_0 , namely $r_0 = 1.2$ and $r_0 = 1.4$. The effect of the Coulomb barrier is small, because most of the emitted protons are very energetic; so we have evaluated this effect in an approximated way. Since the protons are near the nuclear surface, we have taken, as internal radius of the barrier, a radius averaged with the external part of the initial wave function. Each cross section is multiplied by a penetration factor evaluated using this average internal radius.

We have neglected the spin of the nucleons, taking into account only electric transitions. In the case of neutrons the dipole approximation is a good one, for γ -ray energies less than 30 MeV and nuclei which are not too light: hence the angular distribution is of the type $a + b \sin^2 \vartheta$, where b can be negative because of the interference between the transitions $l \rightarrow l+1$ and $l \rightarrow l-1$.

In the case of protons one must take into account higher multipoles, or use the complete expression without expanding in multipoles: so the angular distribution is strongly asymmetrical around $\pi/2$.

⁽³⁾ A. M. LANE: *Nucl. Phys.*, **11**, 625 (1959); A. M. LANE and I. E. LYNN: *Nucl. Phys.*, **11**, 646 (1959).

2. - Cross sections.

The cross-section for the process is given by the usual form:

$$(1) \quad \sigma = \frac{8\pi^3\nu}{c} |H|^2 \varrho,$$

where

$$(2) \quad H = \mathbf{e} \cdot \int \psi_f^* \sum_K e_K \mathbf{r}_K \exp[i\mathbf{K} \cdot \mathbf{r}_K] \psi_i d\tau,$$

is the matrix element of the electric moment component of the system in the direction of polarization \mathbf{e} ; ν the frequency of the incident γ -ray; ϱ the density of final states per unity energy interval

$$(3) \quad \varrho = \frac{|\alpha_{nl}| m_2}{\pi^2 \hbar^2},$$

with m_2 the mass of the nucleon, α_{nl} the propagation vector of the emitted nucleon (in (3) the two spin states are taken into account); ψ_i and ψ_f the initial and final wave functions respectively; \mathbf{K} the propagation vector of the incident γ -ray; \mathbf{r}_K the position of the e_K charge.

We treat the nucleon and the residual nucleus as a two body system; if

$$\mathbf{r} = \mathbf{r}_2 - \mathbf{r}_1, \quad \mathbf{r}_0 = \frac{m_1 \mathbf{r}_1 + m_2 \mathbf{r}_2}{m_1 + m_2},$$

are the relative and the baricentric co-ordinates respectively, where index 1 refer to the residual nucleus and 2 to the nucleon, (2) becomes:

$$(4) \quad H = \mathbf{e} \cdot \int \psi_f^* \sum_K e_K \mathbf{r}_K \exp[i\mathbf{K} \cdot \mathbf{r}_K] \psi_i d^3r_0 d^3r, \quad K=1, 2,$$

where

$$\begin{aligned} \psi_f &= \exp\left[\frac{i}{\hbar} \mathbf{p}_f \cdot \mathbf{r}_0\right] u_f(\mathbf{r}), \\ \psi_i &= \exp\left[\frac{i}{\hbar} \mathbf{p}_i \cdot \mathbf{r}_0\right] u_i(\mathbf{r}), \end{aligned} \quad \mathbf{p}_i + \hbar \mathbf{K} = \mathbf{p}_f,$$

With the approximation outlined above the radial part of $u_i(\mathbf{r})$ is represented by a Hankel function $h_i(i\beta r)$ and $u_f(\mathbf{r})$ by a plane wave.

3. - Angular distribution of the photoneutrons.

In the case of neutrons $e_1 = Ze$ and $e_2 = 0$; then (4) becomes:

$$(5) \quad H = -\frac{m_2}{m_1 + m_2} Ze e \cdot \int \exp \left[-i \left[\alpha + \frac{m_2}{m_1 + m_2} \mathbf{K} \right] \mathbf{r} \right] \mathbf{r} u_i(\mathbf{r}) d^3r,$$

where

$$|\alpha| = |\alpha_{nl}| = \left[\frac{2m_2}{\hbar^2} (\hbar\nu - \varepsilon_{nl}) \right]^{\frac{1}{2}},$$

is the level of the square well of finite depth as given by FEENBERG⁽⁴⁾.

Since in our case $|\alpha|$ is always much greater than $[m_2/(m_1 + m_2)]|k|$, for nuclei which are not too light we can put:

$$\alpha + \frac{m_2}{m_1 + m_2} \mathbf{K} \sim \alpha,$$

this means that the dipole approximation is a good one. Assuming the photon circularly polarized, (5) becomes for a given initial level l, m :

$$(6) \quad H \propto \sum_{l'm'} \left[\int_R^\infty j_{l'}(\alpha r) h_l(i\beta r) r^3 dr \cdot \right. \\ \left. \cdot \int Y_{l'}^{m'*}(\vartheta', \varphi') Y_1^1(\vartheta', \varphi') Y_l^m(\vartheta', \varphi') \cdot \sin \vartheta' d\vartheta' d\varphi' \right] Y_{l'}^{m'}(\vartheta, \varphi) = \\ = D_{l'}(\alpha, \beta, R) f_{l'}(\vartheta, \varphi),$$

where

$$\beta = \left[\frac{2m_2 \varepsilon_{nl}}{\hbar^2} \right]^{\frac{1}{2}}.$$

The integrals $D_{l'}(\alpha, \beta, R)$ have been calculated numerically.

For the integrals $f_{l'}(\vartheta, \varphi)$ we have only two possibilities namely

$$l' = l + 1 \quad \text{and} \quad l' = l - 1.$$

We obtain in the two cases for $f_{l'}(\vartheta, \varphi)$:

$$(7) \quad \sum_{m'=-l-1}^{l+1} |Y_{l+1}^{m'}(\vartheta, \varphi)|^2 (l+1 \ 1 \ 0 \ 0 | l \ 0)^2 (l+1 \ 1 \ -m' \ 1 | l - m)^2 \frac{3}{4\pi} \frac{2l-1}{2l+1},$$

$$(8) \quad \sum_{m'=-l+1}^{l-1} |Y_{l-1}^{m'}(\vartheta, \varphi)|^2 (l-1 \ 1 \ 0 \ 0 | l \ 0)^2 (l-1 \ 1 \ -m' \ 1 | l - m)^2 \frac{3}{4\pi} \frac{2l-1}{2l+1},$$

with $m' = m + 1$,

where $(abcd|ef)$ are the usual C.G. coefficients.

(4) E. FEENBERG: *Shell Theory of the Nucleus* (Princeton, 1955), p. 19.

There is also an interference term between the two transitions $l \rightarrow l+1$ and $l \rightarrow l-1$ because the final state is in the continuum.

The sum over m' in the expressions (7) and (8) gives respectively (see Appendix I):

$$(9) \quad \frac{3}{8\pi} \frac{1}{4\pi} \frac{1}{2l+1} \left[l(l+1) + \frac{1}{2} (l+1)(l+2) \sin^2 \vartheta \right],$$

$$(10) \quad \frac{3}{8\pi} \frac{1}{4\pi} \frac{1}{2l+1} \left[l(l+1) + \frac{1}{2} l(l-1) \sin^2 \vartheta \right];$$

the interference term gives (see Appendix I):

$$(11) \quad \frac{3}{8\pi} \frac{1}{4\pi} \frac{1}{2l+1} l(l+1) [2 - 3 \sin^2 \vartheta].$$

Obviously this term disappears when integration over ϑ is carried out in order to evaluate the total cross-section.

The presence of this interference term in the differential cross-section can give in some cases a negative value of the ratio b/a in the $a + b \sin^2 \vartheta$ formula. The angular distribution of the photoneutrons, apart from some constant factors is:

$$(12) \quad \sum_i N_i^2 \frac{|\alpha_{ni}|}{2l+1} \left[l(l+1)(D_{l+1} + D_{l-1})^2 + \left\{ \frac{1}{2} (l+1)(l+2) D_{l+1}^2 + \right. \right. \\ \left. \left. + \frac{1}{2} l(l-1) D_{l-1}^2 - 3l(l+1) D_{l+1} D_{l-1} \right\} \sin^2 \vartheta \right],$$

where D_{l+1} and D_{l-1} are the dipole integrals:

$$(13) \quad D_{l+1} = \int_R^\infty j_{l+1}(\alpha_n r) h_l(i\beta_n r) r^3 dr,$$

$$(14) \quad D_{l-1} = \int_R^\infty j_{l-1}(\alpha_n r) h_l(i\beta_n r) r^3 dr,$$

N_i^2 is the normalization constant. The sum has been made over the levels of the initial nucleus.

4. - Angular distribution of the photoprotons.

For the photoprotons the dipole approximation is not valid. In fact being now $e_1 = (Z-1)e$ and $e_2 = e$, (4) gives

$$(15) \quad H = -\frac{m_2}{m_1 + m_2} (Z-1) e \int u_i^*(\mathbf{r}) \exp \left[-\frac{im_2}{m_1 + m_2} \mathbf{K} \cdot \mathbf{r} \right] \mathbf{e} \cdot \mathbf{r} u_i(\mathbf{r}) d^3r + \\ + \frac{m_1}{m_1 + m_2} e \int u_i^*(\mathbf{r}) \exp \left[i \frac{m_1}{m_1 + m_2} \mathbf{K} \cdot \mathbf{r} \right] \mathbf{e} \cdot \mathbf{r} u_i(\mathbf{r}) d^3r.$$

In the case of circularly polarized photons and plane waves, for the final wave functions (15) becomes:

$$(16) \quad H = -\frac{Z-1}{A} e \int \exp [-i \mathbf{K}_1 \cdot \mathbf{r}] (x + iy) u_i(\mathbf{r}) d^3r + \\ + \frac{A-1}{A} e \int \exp [-i \mathbf{K}_2 \cdot \mathbf{r}] (x + iy) u_i(\mathbf{r}) d^3r,$$

and one can see that while for the first integral the dipole approximation is still valid because $\mathbf{K}_1 = \boldsymbol{\alpha}_{nl} + (1/A) \mathbf{K} \sim \boldsymbol{\alpha}_{nl}$, for the second integral this is not the case being $\mathbf{K}_2 = \boldsymbol{\alpha}_{nl} - ((A-1)/A) \mathbf{K} \sim \boldsymbol{\alpha}_{nl} - \mathbf{K}$. The second integral has itself the form of a dipole integral, but one must pay attention to the fact that the angle between \mathbf{K}_2 and \mathbf{K} is not the observation angle ϑ , rather an angle Θ related to ϑ by:

$$(17) \quad \cos \vartheta = \frac{|\mathbf{K}| + |\mathbf{K}_2| \cos \Theta}{|\boldsymbol{\alpha}_{nl}|},$$

with this in mind one can calculate the second integral in the same way as the first.

The angular distribution will be $((Z-1)/A) \sim \frac{1}{2}$ and $((A-1)/A) \sim 1$;

$$(18) \quad \sum_m \left\{ -\frac{1}{2} \left[\frac{(l+m)(l+m+1)}{(2l+1)(2l+3)} \right]^{\frac{1}{2}} Y_{l+1}^m(\vartheta, \varphi) D_{l+1} - \right. \\ \left. - \frac{1}{2} \left[\frac{(l-m)(l-m+1)}{(2l+1)(2l-1)} \right]^{\frac{1}{2}} Y_{l-1}^m(\vartheta, \varphi) D_{l-1} + \left[\frac{(l+m)(l+m+1)}{(2l+1)(2l+3)} \right]^{\frac{1}{2}} \cdot \right. \\ \left. \cdot Y_{l+1}^m(\Theta\varphi) D_{l+1}' + \left[\frac{(l-m)(l-m+1)}{(2l+1)(2l-1)} \right]^{\frac{1}{2}} Y_{l-1}^m(\Theta\varphi) D_{l-1}' \right\}^2,$$

where D_{l+1} and D_{l-1} are given by (13) and (14) while:

$$(19) \quad D'_{l+1} = \int_R^\infty j_{l+1}(K_2 r) h_l(i\beta_n r) r^3 dr,$$

$$(20) \quad D'_{l-1} = \int_R^\infty j_{l-1}(K_2 r) h_l(i\beta_n r) r^3 dr.$$

The sum over m gives (see Appendix II)

$$(21) \quad \frac{1}{2l+1} \left\{ \frac{1}{4} \text{dipole } \vartheta + \text{dipole } \Theta \right\} - \\ - \frac{1}{2} \frac{1}{2l+1} \left\{ \frac{l(l+1)}{(2l-3)^{\frac{1}{2}}} (4\pi)^{\frac{1}{2}} Y_{l+1}^0(\alpha) + \sin \vartheta \sin \Theta \left[\frac{\partial}{\partial x} P_{l-1}(x) \right]_X \right\} D_{l+1} D'_{l+1} - \\ - \frac{1}{2} \frac{1}{2l+1} \left\{ \frac{l(l+1)}{(2l-1)^{\frac{1}{2}}} (4\pi)^{\frac{1}{2}} Y_{l-1}^0(\alpha) + \sin \vartheta \sin \Theta \left[\frac{\partial}{\partial x} P_{l-1}(x) \right]_X \right\} D_{l-1} D'_{l-1} - \\ - \frac{1}{2} \frac{1}{2l+1} \left\{ (2l+1)^{\frac{3}{2}} (4\pi)^{\frac{1}{2}} \cos \vartheta \cos \Theta Y_l^0(\alpha) - \frac{l^2}{(2l-1)^{\frac{1}{2}}} (4\pi)^{\frac{1}{2}} Y_{l-1}^0(\alpha) - \right. \\ \left. - \frac{(l+1)^2}{(2l+3)^{\frac{1}{2}}} (4\pi)^{\frac{1}{2}} Y_{l+1}^0(\alpha) + \sin \vartheta \sin \Theta \left[\frac{\partial}{\partial x} (P_{l-1}(x) + P_{l+1}(x)) \right]_X \right\} \cdot \\ \cdot \frac{D_{l+1} D'_{l-1} + D_{l-1} D'_{l+1}}{2},$$

where $X = \cos \alpha = \cos \vartheta \cos \Theta + \sin \vartheta \sin \Theta$ and the approximation (33) (see Appendix II) has been used.

Obviously the angular distribution of the photoprotons from a given nucleus is the sum, over the energetic levels of the initial nucleus, of expressions like (21) after multiplication by the appropriate $N_i^2 \alpha_{n i}$.

In (21), dipole ϑ and dipole Θ mean:

$$(22) \quad \text{dipole } \vartheta = l(l+1) [D_{l+1} + D_{l-1}]^2 + \\ + \left\{ \frac{1}{2} l(l+1)(l+2) D_{l+1}^2 + \frac{1}{2} l(l-1) D_{l-1}^2 - 3 D_{l+1} D_{l-1} l(l+1) \right\} \sin^2 \vartheta,$$

$$(23) \quad \text{dipole } \Theta = l(l+1) [D'_{l+1} + D'_{l-1}]^2 + \\ + \left\{ \frac{1}{2} l(l+1)(l+2) D_{l+1}'^2 + \frac{1}{2} l(l-1) D_{l-1}'^2 - 3 D_{l+1}' D_{l-1}' l(l+1) \right\} \sin^2 \Theta.$$

The effect of the coulomb interaction has been evaluated in an approximate way because it is small; so in (21) the radial integrals are multiplied by a

transparence factor to take account of the coulomb barrier. Since the protons are near the nuclear surface, we have taken as internal radius of the barrier a radius averaged with the asymptotical external part of the initial wave function, *i.e.*:

$$\langle r \rangle = \frac{\int_R^\infty (\exp[-\beta r]/\beta r)^2 r^3 dr}{\int_R^\infty (\exp[-\beta r]/\beta r)^2 r^2 dr} = R + \frac{1}{2\beta}.$$

Then we have used the expression

$$\exp \left[-\sqrt{\frac{8m_e Ze^2 b}{\hbar^2}} \left\{ \cos^{-1} \sqrt{\frac{\langle r \rangle}{b}} - \sqrt{\frac{\langle r \rangle}{b} - \frac{\langle r \rangle^2}{b^2}} \right\} \right],$$

for the penetration factor, where b is the external radius of the barrier.

5. - Numerical results and conclusions.

We have evaluated the angular distribution of surface photoneutrons and photoprotons emitted from nuclei with $A = 16$ and $A = 40$ ($Z = N$), for γ -ray energies equal to 17.6 (lithium γ -ray) 20, 22, 24, 26 MeV. We have considered two cases, corresponding to two different values of the nuclear radius ($r_0 = 1.2$ and $r_0 = 1.4$). The angular distribution depends strongly on the choice of r_0 : corresponding to the smaller value of r_0 the potential well is deeper, so that the most internal levels are effective only at greater energy.

An interesting point to be emphasized is that the ratio b/a that appears in $a + b \sin^2 \theta$ formula can be negative because of the presence of the interference terms between the transitions $l \rightarrow l+1$ and $l \rightarrow l-1$ (see Table 1).

TABLE I. - Ratio b/a in the angular distribution of photoneutron ($a + b \sin^2 \theta$) for different values of the parameters.

E_γ	$A = 16$		$A = 40$	
	$r_0 = 1.2$	$r_0 = 1.4$	$r_0 = 1.2$	$r_0 = 1.4$
17.6	1.8	> 200	-0.39	-0.082
20	7.9	> 200	-0.41	1.28
22	35	73	-0.17	4.0
24	> 200	52	-0.21	14
26	—	37	+0.37	44

In the previous paper the results of the angular distribution of photoneutrons (the formula (4) of (1) must be read as (12) of the present paper) has been obtained with preliminary calculations; in the present work new calculations have been performed with a greater precision.

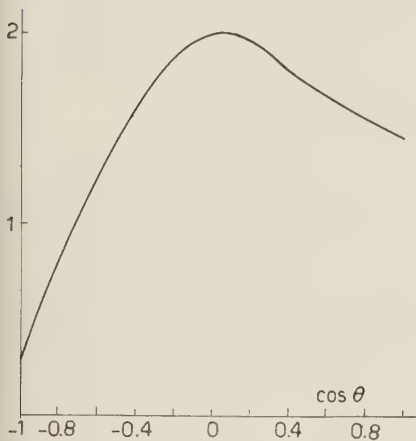


Fig. 1. - $A=16$, $r_0=1.2$, $E=17.6$.

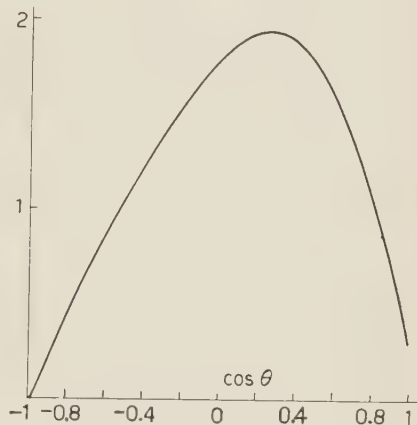


Fig. 2. - $A=16$, $r_0=1.2$, $E=22$.

The angular distribution of the photoprotons is generally very complicated; this is due to the presence in (16) of the second integral. If we put $\mathbf{K}_2 \equiv \alpha_{nl} - ((A-1)/A)\mathbf{K} \sim \alpha_{nl}$ this second integral becomes identical to the first one and we obtain the dipole approximation, as it must be; actually $\mathbf{K}((A-1)/A)$ is not negligible in comparison with α_{nl} , and the dipole approximation is not a good one.

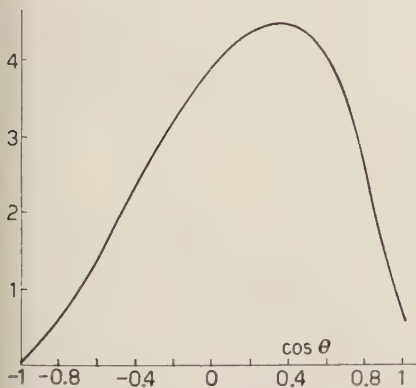


Fig. 3. - $A=16$, $r_0=1.4$, $E=17.6$.

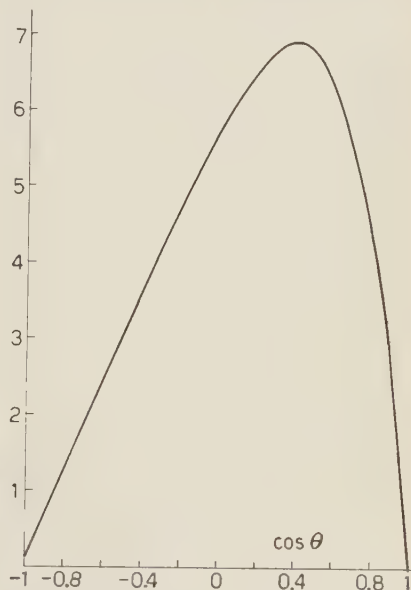
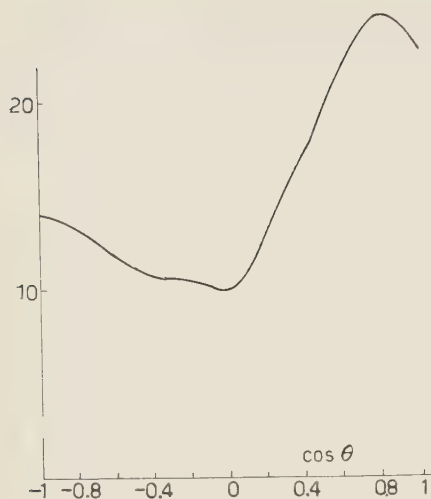
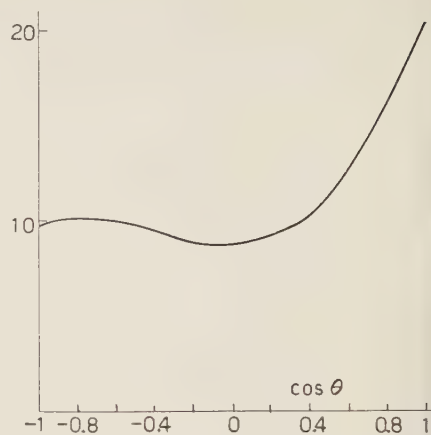


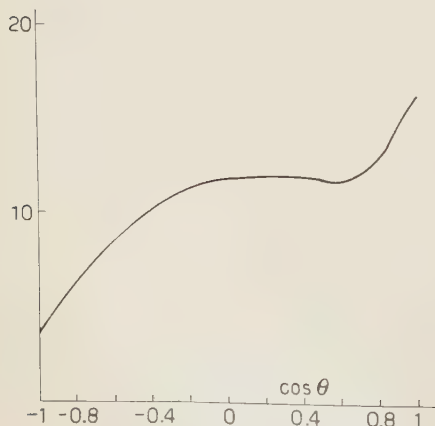
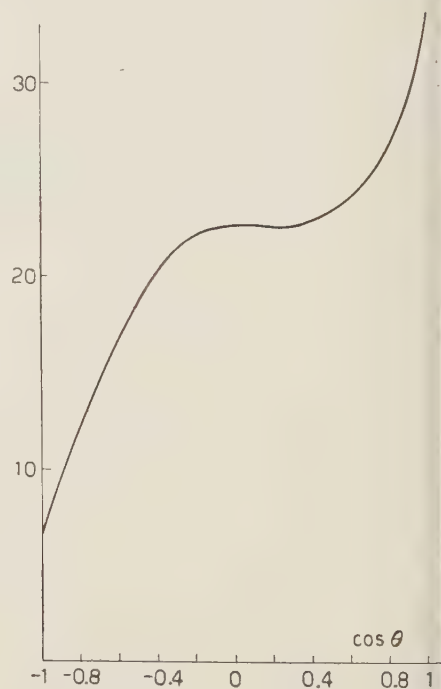
Fig. 4. - $A=16$, $r_0=1.4$, $E=22$.

Fig. 5. - $A=40$, $r_0=1.2$, $E=17.6$.Fig. 6. - $A=40$, $r_0=1.2$, $E=20$.

We can note the following points:

a) If one had not taken into account the dependence on ϑ of the radial part of the second integral, one should obtain an angular distribution asymmetrical around $\pi/2$ with forward maximum.

b) In general, this approximation is not valid and the angular distribution is very complicated (Fig. 1 to 10; in the figures are shown the angular distribution of photo-protons

Fig. 7. - $A=40$, $r_0=1.2$, $E=26$.Fig. 8. - $A=40$, $r_0=1.4$, $E=17.6$.

for different values of the parameters); anyhow in the cases we have examined it is always forward.

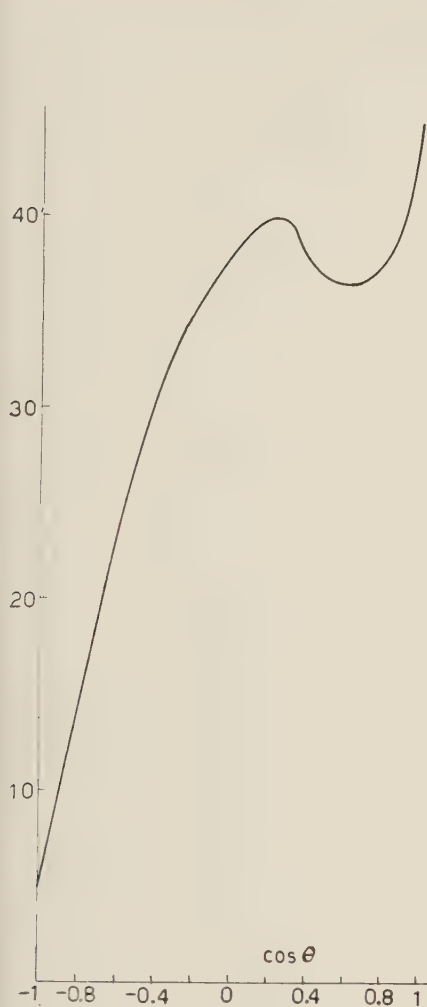


Fig. 9. - $A=40$, $r_0=1.4$, $E=20$.

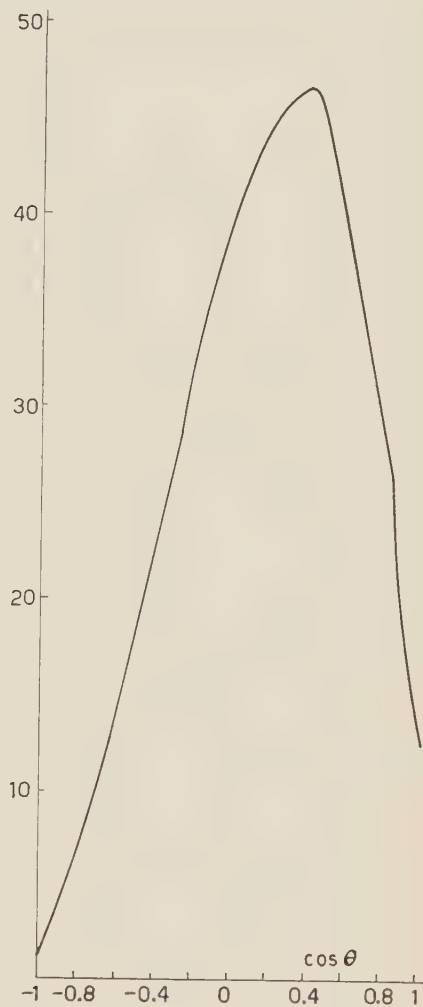


Fig. 10. - $A=40$, $r_0=1.4$, $E=26$.

c) The effect of the Coulomb barrier is small; this is due to the assumption of taking into account only surface protons; this means that the average radius $\langle r \rangle$ in the initial state is fairly equal to the external radius b , and in many cases $\langle r \rangle > b$, i.e. the protons in the initial state have a great probability to be outside the barrier. The Coulomb barrier becomes higher for smaller r_0 , so that its effect is slightly enhanced.

d) The $\sigma(\gamma, p)$ is about 2 or 3 times the $\sigma(\gamma, n)$ at the various energies considered (see Table II).

e) The cross-section is of the order of 10^{-26} cm^2 .

TABLE II. — Ratio of the integrated cross sections $\sigma(\gamma, p)/\sigma(\gamma, n)$ for different values of the parameters.

E_γ	$A=16$		$A=40$	
	$r_0=1.2$	$r_0=1.4$	$r_0=1.2$	$r_0=1.4$
17.6	3.0	2.9	2.7	3.0
20	3.1	1.8	3.1	3.1
22	3.1	2.8	2.1	3.1
24	3.0	3.1	2.4	3.0
26	2.5	3.2	2.7	2.5

APPENDIX I

By writing down explicitly C.G. coefficients and replacing m' with m , (7) and (8) become:

$$\begin{aligned}
 (24) \quad (7) &= \sum_m \frac{3}{8\pi} |Y_{l+1}^m(\vartheta, \varphi)|^2 \frac{l+1}{(2l+3)(2l+1)} \frac{2l+3}{l+1} (l+m+1)(l+m) = \\
 &= \sum_m \frac{3}{8\pi} |Y_{l+1}^m(\vartheta, \varphi)|^2 \frac{(l+m+1)(l+m)}{(2l+3)(2l+1)},
 \end{aligned}$$

and

$$(25) \quad (8) = \sum_m \frac{3}{8\pi} |Y_{l-1}^m(\vartheta, \varphi)|^2 \frac{(l-m)(l-m+1)}{(2l+1)(2l-1)};$$

with the use of:

$$(26) \quad \left\{ \begin{aligned} \sum_m |Y_l^m(\vartheta, \varphi)|^2 &= \frac{2l+1}{4\pi}, \\ \sum_m m^2 |Y_l^m(\vartheta, \varphi)|^2 &= \frac{1}{8\pi} l(l+1)(2l+1) \sin^2 \vartheta, \end{aligned} \right.$$

(24) and (25) respectively become:

$$(27) \quad (24) = \frac{1}{2l+1} \frac{3}{8\pi} \frac{1}{4\pi} \left[l(l+1) + \frac{1}{2} (l+1)(l+2) \sin^2 \vartheta \right],$$

$$(28) \quad (25) = \frac{1}{2l+1} \frac{3}{8\pi} \frac{1}{4\pi} \left[l(l+1) + \frac{1}{2} l(l-1) \sin^2 \vartheta \right].$$

For the interference term one has:

$$(29) \quad \frac{1}{[(2l+3)(2l-1)]^{\frac{1}{2}}} \frac{1}{2l+1} \frac{3}{4\pi} \cdot \sum_m [(l^2 - m^2)\{(l+1)^2 - m^2\}]^{\frac{1}{2}} Y_{l+1}^{m*}(\vartheta, \varphi) Y_{l-1}^m(\vartheta, \varphi),$$

where the sum over m is performed with the aid of

$$\begin{aligned} \cos^2 \vartheta |P_l^m|^2 &= \frac{(l+m)^2}{(2l+1)^2} |P_{l-1}|^2 + \\ &+ \frac{(l-m+1)^2}{(2l+1)^2} |P_{l+1}|^2 + \frac{2(l+m)(l-m+1)}{(2l+1)^2} P_{l-1} P_{l+1}, \end{aligned}$$

with

$$Y_l^m(\vartheta, \varphi) = \left[\frac{2l+1}{4\pi} \frac{(l-m)!}{(l+m)!} \right]^{\frac{1}{2}} P_l^m(\cos \vartheta) \exp [im\varphi].$$

One finds

$$\begin{aligned} \sum_m \{ (l^2 - m^2)[(l+1)^2 - m^2] \}^{\frac{1}{2}} Y_{l+1}^{m*} Y_{l-1}^m &= \\ &= \frac{\{(2l+3)(2l-1)\}^{\frac{1}{2}}}{2} \sum_m \left\{ (2l+1) \cos^2 \vartheta |Y_l^m|^2 - \frac{l^2 - m^2}{2l-1} |Y_{l-1}^m|^2 - \right. \\ &\quad \left. - \frac{[(l+1)^2 - m^2]}{2l+3} |Y_{l+1}^m|^2 \right\} = \frac{[(2l+3)(2l-1)]^{\frac{1}{2}}}{8\pi} l(l+1) \{2 - 3 \sin^2 \vartheta\}. \end{aligned}$$

Then the interference term (29) has the form:

$$(30) \quad \frac{1}{2l+1} \frac{3}{8\pi} \frac{1}{4\pi} l(l+1) \{2 - 3 \sin^2 \vartheta\}.$$

APPENDIX II

In order to carry out the sum over m in (20) one must calculate terms of the type:

$$(31) \quad \sum_m [(l^2 - m^2)\{(l+1)^2 - m^2\}]^{\frac{1}{2}} (Y_{l+1}^{m*}(\vartheta) Y_{l-1}^m(\Theta) D_{l+1} D'_{l-1} + \\ + Y_{l-1}^{m*}(\vartheta) Y_{l+1}^m(\Theta) D_{l-1} D'_{l+1}).$$

We can write:

$$(32) \quad Y_{l+1}^{m*}(\vartheta) Y_{l-1}^m(\Theta) D_{l+1} D'_{l-1} + Y_{l-1}^{m*}(\vartheta) Y_{l+1}^m(\Theta) D_{l-1} D'_{l+1} = \\ = \frac{1}{2} \{ (Y_{l+1}^{m*}(\vartheta) Y_{l-1}^m(\Theta) + Y_{l-1}^{m*}(\vartheta) Y_{l+1}^m(\Theta)) (D_{l+1} D'_{l-1} + D_{l-1} D'_{l+1}) + \\ + (Y_{l+1}^{m*}(\vartheta) Y_{l-1}^m(\Theta) - Y_{l-1}^{m*}(\vartheta) Y_{l+1}^m(\Theta)) (D_{l+1} D'_{l-1} - D_{l-1} D'_{l+1}) \}.$$

In our case the second term is completely negligible; then we have to calculate:

$$(33) \quad \sum_m [(l^2 - m^2)\{(l+1)^2 - m^2\}]^{\frac{1}{2}} \cdot (Y_{l+1}^{m*}(\vartheta) Y_{l-1}^m(\Theta) + Y_{l-1}^{m*}(\vartheta) Y_{l+1}^m(\Theta)) \frac{D_{l+1} D'_{l-1} + D_{l-1} D'_{l+1}}{2}.$$

making use of the

$$z P_l^m(z) = \frac{l+m}{2l+1} P_{l-1}^m(z) + \frac{l-m+1}{2l+1} P_{l+1}^m(z), \quad (z = \cos \vartheta),$$

and the same relation for $z' = \cos \Theta$, we have

$$(34) \quad z z' P_l^m(z) P_l^m(z') = \frac{(l+m)^2}{(2l+1)^2} P_{l-1}^m(z) P_{l-1}^m(z') + \frac{(l-m+1)^2}{(2l+1)^2} P_{l+1}^m(z) P_{l+1}^m(z') + \\ + \frac{(l+m)(l-m+1)}{(2l+1)^2} \{ P_{l-1}^m(z) P_{l+1}^m(z') + P_{l+1}^m(z) P_{l-1}^m(z') \}.$$

Then (33) with the use of (34) becomes

$$(35) \quad \{(2l+3)(2l-1)\}^{\frac{1}{2}} \sum_m \left\{ (2l+1) z z' Y_l^m(z) Y_l^m(z') - \frac{l^2 - m^2}{2l-1} Y_{l-1}^m(z) Y_{l-1}^m(z') - \right. \\ \left. - \frac{[(l+1)^2 - m^2]}{2l+3} Y_{l+1}^m(z) Y_{l+1}^m(z') \right\},$$

and taking into account

$$\sum_m m^2 Y_l^m(\vartheta) Y_l^m(\Theta) = \frac{2l+1}{4\pi} \sin \vartheta \sin \Theta \left[\frac{\partial}{\partial x} P_l(x) \right]_{x = \cos \vartheta \cos \Theta + \sin \vartheta \sin \Theta},$$

one finally obtains

$$\begin{aligned} [(2l+3)(2l-1)]^{\frac{1}{2}} & \left\{ (2l+1) \cos \vartheta \cos \Theta Y_l^0(0) Y_l^0(x) - \frac{l^2}{2l-1} Y_{l-1}^0(0) Y_{l-1}^0(x) - \right. \\ & \left. - \frac{(l+1)^2}{2l+3} Y_{l+1}^0(0) Y_{l+1}^0(x) + \frac{1}{4\pi} \sin \vartheta \sin \Theta \left[\frac{\partial}{\partial x} (P_{l-1}(x) + P_{l+1}(x)) \right]_x \right\}, \end{aligned}$$

with

$$\cos \alpha = X = \cos \vartheta \cos \Theta + \sin \vartheta \sin \Theta.$$

RIASSUNTO

Si è studiato il contributo della superficie del nucleo alle reazioni fotonucleari con un modello a particelle indipendenti; in particolare è stata analizzata la distribuzione angolare. Nel caso dei fotoneutroni l'approssimazione di dipolo è buona e si ha così una distribuzione simmetrica rispetto a 90° ; la presenza di un termine di interferenza tra le transizioni $l \rightarrow l+1$ e $l \rightarrow l-1$ fa sì che tale distribuzione possa presentare anche un minimo a 90° in luogo dell'usuale massimo. Nel caso dei fotoprotoni non essendo più sufficiente l'approssimazione di dipolo, si è tenuto conto dell'espressione completa senza fare lo sviluppo in multipoli e si è così trovata una distribuzione angolare fortemente asimmetrica. I calcoli numerici sono stati eseguiti su due nuclei ($A=16$ e $A=40$) per due diversi valori di r_0 ($r_0=1.2$ e $r_0=1.4$) a varie energie. La sezione d'urto risulta dell'ordine di 10^{-26} cm²; il rapporto $\sigma(\gamma, p)/\sigma(\gamma, n)$ è dell'ordine dell'unità.

Effect of a Pion-Pion Scattering Resonance on Low Energy Pion-Nucleon Scattering.

J. BOWCOCK, W. N. COTTINGHAM and D. LURIE

CERN - Geneva

(ricevuto il 15 Marzo 1960)

Summary. — From the analytic properties of the pion-nucleon scattering amplitude postulated by Mandelstam, we derive a fixed momentum transfer dispersion relation in the energy variable which should be valid at low energies. This formulation allows us to evaluate the effect of a two-pion scattering resonance on pion-nucleon scattering. By a suitable choice of the pion-pion resonance parameters we are able to fit both the experimental pion-nucleon phase shifts and the nucleon electromagnetic form factors.

1. — Introduction.

Experimental evidence has recently appeared which would seem to point to the existence of a strong pion-pion interaction. Evidence for such an interaction has been found, for example, in the analysis of single pion production data in π -p collisions by BONSIGNORI and SELLERI⁽¹⁾ and by DERADO⁽²⁾. In addition, FRAZER and FULCO's work on the electromagnetic structure of the nucleon^(3,4) has shown that the experimental data on the isotopic vector parts of the nucleon form factors may be satisfactorily fitted if one assumes a π - π scattering resonance in the $J=1$, $T=1$ state.

In this paper, we shall investigate, by means of the Cini-Fubini approximate version of the Mandelstam representation⁽⁵⁾, the effect of such a re-

(1) F. BONSIGNORI and F. SELLERI: *Nuovo Cimento*, **15**, 465 (1960).

(2) I. DERADO: *Nuovo Cimento*, **15**, 853 (1960).

(3) W. R. FRAZER and J. R. FULCO: *Phys. Rev. Lett.*, **2**, 365 (1959).

(4) W. R. FRAZER and J. R. FULCO: University of California Radiation Laboratory, Berkeley, UCRL 8880, to be published in *Phys. Rev.*

(5) M. CINI and S. FUBINI: to be published in *Ann. Phys.*

sonance on low-energy pion-nucleon scattering. The use of this representation has the effect of adding to the CHEW, GOLDBERGER, LOW and NAMBU fixed momentum-transfer dispersion relations ⁽⁶⁾ an extra term involving an integral over the absorptive parts of the $\pi + \pi \rightarrow N + \bar{N}$ amplitudes. The addition of this term allows in a natural way for the introduction of a π - π resonance whose width and position may be estimated from available experimental data on the nucleon form factors and the s -wave π - N scattering phase shifts. Although, only the effect of a resonance in the $J=1$, $T=1$ state is considered, the formalism would allow other states as well to be taken into account.

Section 2 is devoted to the kinematics and symmetry properties of the amplitudes under consideration. In Section 3, the Mandelstam representation which the scattering amplitude is assumed to satisfy is written down. From there we pass directly to the Cini-Fubini one dimensional form from which the integral equations for the $\pi + N \rightarrow \pi + N$ and $\pi + \pi \rightarrow N + \bar{N}$ amplitudes may be derived. The latter is identical with that derived recently by FRAZER and FULCO. The expressions derived for the $J=1$, $T=1$, $\pi + \pi \rightarrow N + \bar{N}$ amplitudes involve divergent integrals however, which arise from the incorrect treatment of the high momentum transfer behaviour inherent in the effective range approach of the theory. Our procedure at this point is to express these amplitudes in terms of four arbitrary parameters, three of which may be estimated from the experimental data on the nucleon electromagnetic form factors. This will be done in Section 4 and the expressions for the $\pi + \pi \rightarrow N + \bar{N}$ amplitudes which now involve only one arbitrary parameter will be inserted into the equations for the S , P and D partial waves π - N amplitudes to be derived in Section 5.

A rough determination of the final additional parameter, namely the width of the π - π resonance is given in Section 6, by fitting the experimental s -wave phase shifts. A more thorough comparison of the theory with experimental angular distribution data is at present under way.

2. - Kinematics and symmetry properties.

2.1. Kinematics. - We define first the kinematical variables for the scattering process $\pi + N \rightarrow \pi + N$ (channel I) denoting the four momenta of the pions by q_1 and q_2 and the four-momenta of the nucleons by p_1 and p_2 (Fig. 1).

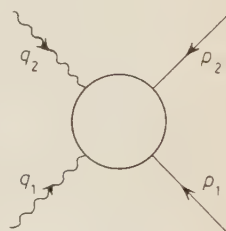


Fig. 1.

⁽⁶⁾ G. F. CHEW, M. L. GOLDBERGER, F. E. LOW and Y. NAMBU: *Phys. Rev.*, **106**, 1337 (1957).

In the centre-of-momentum system take (*)

$$(2.1) \quad \begin{cases} s = -(q_1 + p_1)^2 = (E_p + \omega_q)^2, \\ t = -(q_1 + q_2)^2 = -2q^2(1 - \cos \theta), \\ \bar{s} = -(q_1 + p_2)^2 = (E_p - \omega_q)^2 - 2q^2(1 + \cos \theta), \end{cases}$$

where E_p is the nucleon energy,

ω_q is the meson energy,

q^2 is the square of the magnitude of the meson momentum,

θ is the scattering angle between pion and nucleon where the initial momenta are q_1 and p_1 .

The use of our dispersion relations forces us also to consider the reaction $\pi + \pi \rightarrow \mathcal{N} + \bar{\mathcal{N}}$ (channel II). For this channel denote the angle between incoming pion and final nucleon by φ .

Then

$$(2.2) \quad \begin{cases} s = -p^2 - q^2 + 2pq \cos \varphi, \\ t = 4(q^2 + \mu^2) = 4(p^2 + M^2), \\ \bar{s} = -p^2 - q^2 - 2pq \cos \varphi, \end{cases}$$

where p^2 is the square of the nucleon three-momentum.

In (2.1), (2.2) there are of course only two independent variables since we have the usual relation

$$(2.3) \quad s + \bar{s} + t = 2(M^2 + \mu^2).$$

2.2. Symmetry properties of the T matrix.

i) If the T matrix is defined by

$$S_{fi} = 1 - (2\pi)^4 \delta^4(p_1 + q_1 + p_2 + q_2) \frac{M}{\sqrt{4E_1 E_2 \omega_1 \omega_2}} T_{fi},$$

then it has been shown (*) that if T is to be invariant under Lorentz transformations it must be of the form

$$(2.4) \quad T = -A + \frac{i\gamma \cdot (q_1 - q_2)}{2} B,$$

A and B being scalar functions of q and $\cos \theta$.

(*) We use the metric such that $a \cdot b = a \cdot b - a_0 b_0$.

ii) By also requiring that the meson-nucleon interaction should be charge independent we have that

$$(2.5) \quad \begin{cases} A_{\beta\alpha} = \delta_{\beta\alpha} A^{(+)} + \frac{1}{2} [\tau_{\beta}, \tau_{\alpha}] A^{(-)}, \\ B_{\beta\alpha} = \delta_{\beta\alpha} B^{(+)} + \frac{1}{2} [\tau_{\beta}, \tau_{\alpha}] B^{(-)}, \end{cases}$$

where α, β are the isotopic spin indices of the mesons 1 and 2.

Then for channel I we find

$$(2.6) \quad \begin{cases} A^{(+)} = \frac{1}{3} [A^{(\frac{1}{2})} + 2A^{(\frac{3}{2})}], \\ A^{(-)} = \frac{1}{3} [A^{(\frac{1}{2})} - A^{(\frac{3}{2})}], \end{cases}$$

the indices $(\frac{1}{2})$, $(\frac{3}{2})$ referring to states of total isotopic spin $\frac{1}{2}$, $\frac{3}{2}$.

In channel II, however, the two allowed isotopic spins are 0, 1 and we have

$$(2.7) \quad \begin{cases} A^{(+)} = \frac{1}{\sqrt{6}} A^{(0)}, \\ A^{(-)} = \frac{1}{2} A^{(1)}. \end{cases}$$

iii) The third property of T that we use is that it should satisfy crossing symmetry, *i.e.*

$$(2.8) \quad \begin{cases} A^{(\pm)}(s, \bar{s}, t) = \pm A^{(\pm)}(\bar{s}, s, t), \\ B^{(\pm)}(s, \bar{s}, t) = \mp B^{(\pm)}(\bar{s}, s, t). \end{cases}$$

2.3. *Partial-wave decompositions.* — We give here the way in which the amplitudes in channel I and channel II are decomposed into partial waves.

For channel I we follow the procedure of Ref. (6) and define

$$(2.9) \quad \begin{cases} f_1^{(\pm)} = \frac{E + M}{2W} \left\{ \frac{A^{(\pm)} + (W - M) B^{(\pm)}}{4\pi} \right\}, \\ f_2^{(\pm)} = \frac{E - M}{2W} \left\{ \frac{-A^{(\pm)} + (W + M) B^{(\pm)}}{4\pi} \right\}, \end{cases}$$

W being the total energy for channel I.

Then

$$(2.10) \quad \frac{d\sigma}{d\Omega} = \sum |\langle f | f_1 - \frac{\boldsymbol{\sigma} \cdot \mathbf{q}_2 \boldsymbol{\sigma} \cdot \mathbf{q}_1}{q_1 q_2} f_2 | i \rangle|^2.$$

The decomposition of $f_1^{(\pm)}$ and $f_2^{(\pm)}$ into states of definite angular momentum is given by

$$(2.11) \quad \begin{cases} f_1^{(\pm)} = \sum_{l=0}^{\infty} f_{l+}^{(\pm)} P'_{l+1}(\cos \theta) - \sum_{l=2}^{\infty} f_{l-}^{(\pm)} P'_{l-1}(\cos \theta), \\ f_2^{(\pm)} = \sum_{l=1}^{\infty} (f_{l-}^{(\pm)} - f_{l+}^{(\pm)}) P'_l(\cos \theta), \end{cases}$$

where $f_{l\pm}$ is the scattering amplitude in a state of parity $-(-1)^l$ and total angular momentum $j = 1 \pm \frac{1}{2}$. Thus

$$(2.12) \quad f_{l\pm} = \frac{\exp[i\delta_{l\pm}] \sin \delta_{l\pm}}{q}.$$

It is useful to have a closed expression for l_{\pm} in terms of f_1 and f_2 . This is given by

$$(2.13) \quad f_{l\pm} = \frac{1}{2} \int_{-1}^1 (f_1 P_l(\cos \theta) + f_2 P_{l\pm 1}(\cos \theta)) d \cos \theta.$$

For channel II or the other hand it is convenient to decompose $A^{(\pm)}$ and $B^{(\pm)}$ into states of definite angular momentum and definite helicity as done by FRAZER and FULCO (7). Recalling from (2.2) that in this channel t is the total energy and φ the scattering angle we write

$$(2.14) \quad \begin{cases} A^{(\pm)}(t, \cos \varphi) = \frac{8\pi}{p^2} \sum_J (J + \frac{1}{2})(pq)^J \left\{ M f_{\pm}^{(\pm)J}(t) \frac{1}{\sqrt{J(J+1)}} \cos \varphi P'_J(\cos \varphi) - \right. \\ \left. - f_{\pm}^{(\pm)J}(t) P_J(\cos \varphi) \right\}, \\ B^{(\pm)}(t, \cos \varphi) = 8\pi \sum_J \frac{(J + \frac{1}{2})}{\sqrt{J(J+1)}} (pq)^{J-1} f_{\pm}^{(\pm)J}(t) P'_J(\cos \varphi). \end{cases}$$

For the amplitudes $f_{\pm}^{(\pm)J}(t)$, J refers to the total angular momentum of the state and the subscripts refer to definite helicities of the nucleon anti-nucleon pair; $+$ meaning both particles have the same helicities, $-$ meaning they have opposite helicities.

(7) W. R. FRAZER and J. R. FULCO: UCRL 8806, to be published in *Phys. Rev.*

The inverse of eq. (2.14) is given by

$$(2.15) \quad \begin{cases} f_{+}^{(\pm)J}(t) = \frac{1}{8\pi} \left[-\frac{p^2}{(pq)^J} A_J^{(\pm)} + \frac{M}{(2J+1)(pq)^{J-1}} \{ (J+1)B_{J+1}^{(\pm)} + JB_{J-1}^{(\pm)} \} \right], \\ f_{-}^{(\pm)J}(t) = \frac{1}{8\pi} \frac{\sqrt{J(J+1)}}{2J+1} \frac{1}{(pq)^{J-1}} \{ B_{J-1}^{(\pm)} - B_{J+1}^{(\pm)} \}, \end{cases}$$

where

$$(2.16) \quad [A_J^{(\pm)}(t); B_J^{(\pm)}(t)] = \int_{-1}^1 dx P_J(x) [A^{(\pm)}; B^{(\pm)}].$$

3. - Mandelstam representation and basic assumptions.

We shall make here an approximation to the Mandelstam representation which we hope will give the essential structure of the invariant amplitudes $A^{(\pm)}$ and $B^{(\pm)}$ in the region of low energy and low momentum transfer.

The approximation technique was introduced by CHN and FUBINI⁽⁵⁾ and is based on an analysis of the perturbation graphs for the amplitudes. Consider the analytic properties of the invariant amplitudes as given by the Mandelstam representation⁽⁸⁾ and let us consider explicitly $A^{(+)}$. Then

$$(3.1) \quad A^{(+)}(s, t) = \frac{1}{\pi} \int_{(m+\mu)^2}^{\infty} ds' \alpha^{(+)}(s', t) \left\{ \frac{1}{s' - s} + \frac{1}{s' - \bar{s}} \right\}.$$

This representation automatically satisfies crossing symmetry. For s and t in the physical region of channel I, $\alpha^{(+)}(st) = \text{Im } A^{+}(st)$ and from unitarity this can be expressed as the sum of a contribution from intermediate states involving pion-nucleon scattering and an inelastic contribution where additional mesons are produced in the intermediate state. We therefore write

$$\alpha^{(+)}(s', t) = \alpha_{\text{el}}^{(+)}(s', t) + \alpha_{\text{inel}}^{(+)}(s', t),$$

where

$$\alpha_{\text{inel}}^{(+)}(s', t) = 0 \quad \text{for} \quad s' < (M + 2\mu)^2.$$

The Mandelstam conjecture also states that $\alpha^{(+)}(s', t)$ is of the following

⁽⁸⁾ S. MANDELSTAM: *Phys. Rev.*, **112**, 1344 (1958).

form

$$\alpha^{(+)}(s', t) = \frac{1}{\pi} \int_{L(s')}^{\infty} \frac{u^{(+)}(s', t')}{t' - t} dt' + \frac{1}{\pi} \int_{-\infty}^{M(s')} \frac{v^{(+)}(s', t')}{t' - t} dt'.$$

Fourth order perturbation theory ⁽⁹⁾ indicates that both α_{el}^{+} and α_{inel}^{+} satisfy this representation with

$$M(s') < -4M\mu,$$

$$L(s') \geq 4\mu^2 \quad \text{for} \quad \alpha_{inel}^{(+)},$$

$$L(s') \geq 16\mu^2 \quad \text{for} \quad \alpha_{el}^{(+)}. \quad .$$

We will take this to be so.

Let us write eq. (3.1) as

$$(3.2) \quad \mathcal{A}^{(+)}(s, t) = \frac{1}{\pi} \int_{(m+\mu)^2}^{\infty} ds' \alpha_{el}^{(+)}(s', t) \left\{ \frac{1}{s' - s} + \frac{1}{s' - \bar{s}} \right\} + \frac{1}{\pi} \int_{(m+2\mu)^2}^{\infty} ds' \alpha_{inel}^{(+)} \left\{ \frac{1}{s' - s} + \frac{1}{s' - \bar{s}} \right\}.$$

In the first integral of (3.2) the nearest cut in the t variable begins at $t - 16\mu^2$. For this reason we shall assume the validity of keeping for the integral only the first few terms of a power series expansion in t . For the second integral in (3.2), however, the nearest cut in t begins at $4\mu^2$ whereas the cuts in s and \bar{s} now begin at the inelastic threshold $(m+2\mu)^2$. Accordingly, we shall expand this integral in power series in s and \bar{s} (preserving crossing symmetry), keeping again only the first few terms. Thus the second integral of (3.2) is of the form

$$(3.3) \quad \frac{1}{\pi} \int_{4\mu^2}^{\infty} dt' \frac{a^{(+)}(t', s, \bar{s})}{t' - t} + \frac{1}{\pi} \int_{(m+2\mu)^2}^{\infty} ds' \int_{-\infty}^{M(s')} dt' \frac{v_{inel}(s', t')}{(t' - t)} \left\{ \frac{1}{s' - s} + \frac{1}{s' - \bar{s}} \right\},$$

where

$$(3.4) \quad a^{(+)}(t', s, \bar{s}) = \frac{1}{\pi} \int_{(m+2\mu)^2}^{\infty} ds' u_{inel}^{(+)}(s', t') \left\{ \frac{1}{s' - s} + \frac{1}{s' - \bar{s}} \right\}.$$

The second term in (3.3) should have only a weak dependence on all three variables since the cuts are all distant. We shall replace terms of this form by real constants.

⁽⁹⁾ S. MANDELSTAM: *Phys. Rev.*, **115**, 1752 (1959).

In this manner we obtain a representation of $A^{(+)}$:

$$(3.5a) \quad A^{(+)}(s, t) = \frac{1}{\pi} \int_{(m+\mu)^2}^{\infty} \alpha_{\text{el}}^{(+)}(s', t) \left\{ \frac{1}{s' - s} + \frac{1}{s' - \bar{s}} \right\} dt' + \frac{1}{\pi} \int_{4\mu^2}^{\infty} \frac{a^{(+)}(t', s, \bar{s})}{t' - t} dt' + C_A^{(+)},$$

where $\alpha^{(+)}(s', t)$ is a real polynomial of low degree in t and $a^{(+)}(t', s, \bar{s})$ is a sum of a real polynomial of low degree in s and an identical polynomial in \bar{s} .

$A^{(-)}$ has a similar representation except that from crossing symmetry it must be odd under interchange of s and \bar{s} , so that the arbitrary constant must be zero in this case. Thus

$$(3.5b) \quad A^{(-)}(s, t) = \frac{1}{\pi} \int_{(m+\mu)^2}^{\infty} ds' \alpha_{\text{el}}^{(-)}(s', t) \left\{ \frac{1}{s' - s} - \frac{1}{s' - \bar{s}} \right\} + \frac{1}{\pi} \int_{4\mu^2}^{\infty} \frac{a^{(-)}(t', s, \bar{s})}{t' - t} dt'.$$

Representations of identical form (satisfying the symmetry properties of eq. (2.8)) hold for $B^{(+)}$ and $B^{(-)}$ except that to these must be added the single nucleon pole term, *i.e.*

$$B^{(\pm)} = g_r^2 \left(\frac{1}{M^2 - s} \mp \frac{1}{M^2 - \bar{s}} \right) + \text{terms similar to (3.5)}.$$

Since the weight functions $a^{(+)}$, etc., are real we can make the association

$$(3.6) \quad \text{Im } A^{(+)}(s, t) = \alpha_{\text{el}}^{(+)}(s, t)$$

at least for s and t in the physical region of channel I.

From (2.9) and (2.11) $\text{Im } A^{(+)}(s, t)$ in this region is expandable as a sum over partial wave pion nucleon scattering amplitudes. We will take this sum to be saturated by the $P_{\frac{3}{2}, \frac{3}{2}}$ resonance which we take from experiment. From (3.6) this gives that $\alpha^{(+)}(s, t)$ is a first order polynomial in t , the behaviour of which as a function of s is given by the $P_{\frac{3}{2}, \frac{3}{2}}$ partial wave amplitude. As t is not necessarily a physical momentum transfer corresponding to the energy s' in the region of integration of (3.5) an analytic continuation in t of $\text{Im } A(s, t)$ from the physical region of its arguments is implied.

It is clear that the first terms in eq. (3.5a and b), and in the corresponding equations for $B^{(\pm)}$, are identical with the representation used by CHEW, LOW, GOLDBERGER and NAMBU ⁽⁶⁾ since both in their work and in the present one

the integrals are saturated with the (3, 3) resonance. The difference lies in the addition, here, of a strongly t -dependent term representing the contribution of inelastic pion-nucleon scattering.

The weight function $a^{(+)}(t, s, \bar{s})$ is equal to $\text{Im } A^{(+)}(t, s, \bar{s})$ in the region $t > 4\mu^2$ for small value of s and \bar{s} . $t > 4\mu^2$ corresponds to the energy region of pion-pion scattering although for $t < 4M^2$, t is below the threshold for $N\bar{N}$ production. What must be fed in here is the imaginary part of the $\pi + \pi \rightarrow N + \bar{N}$ production amplitude analytically continued to the relevant values of s , \bar{s} and t .

The integral equations for this production amplitude can be derived directly from our representation (3.5) by means of analyticity arguments similar to those of FRAZER and FULCO (7). We shall use the amplitude $f_{\pm}^{(\pm)J}(t)$ as defined in (2.14).

The analytic properties for $A_j^{(\pm)}$ and $B_j^{(\pm)}$ may be deduced from (2.16) and (3.5). For $A_j^{(\pm)}(t)$ for example, one finds a right-hand cut starting at $t = +4\mu^2$ and extending to $t = +\infty$ due to the second term in (3.5) and a left-hand cut from $-\infty$ to 0 arising from the vanishing of the denominators in the first term. The same is true of $B_j^{(\pm)}$ except that the left-hand cut will extend from $-\infty$ to $a = 4\mu^2(1 - (\mu^2/4M^2))$ because of the presence of the pole terms. From eq. (2.15) this leads to the following dispersion relations for f_{\pm}^J , identical with those of FRAZER and FULCO:

$$(3.7) \quad f_{\pm}^J(t) = \frac{1}{\pi} \int_{-\infty}^a \frac{\text{Im } f_{\pm}^J(t') dt'}{t' - t - i\varepsilon} + \frac{1}{\pi} \int_{4\mu^2}^{\infty} \frac{\text{Im } f_{\pm}^J(t') dt'}{t' - t - i\varepsilon},$$

where $\text{Im } f_{\pm}^{(\pm)J}(t)$ on the left hand cut is given in terms of the pion nucleon $P_{\frac{1}{2}, \frac{1}{2}}$ resonance parameters and the single nucleon pole term as given by eq. (5.7) and (5.8) of Ref. (7).

It can be seen from a theorem by FUBINI, NAMBU and WATAGHIN (10) that below the threshold for inelastic processes the phase of the production amplitudes $f_{\pm}^{(\pm)J}$ are equal to the phase shift of the two colliding particles, *i.e.* the π - π scattering phase shift. As there are at present no experimental data on pion-pion scattering we shall make the currently favoured assumption of a resonance in the $J=1$, $T=1$ state.

Returning to eq. (3.5), we can then replace $a^{(\pm)}(t', s, \bar{s})$ by its expansion in terms of $\text{Im } f_{\pm}^{(\pm)J}(t')$ using eq. (2.16). Keeping only the $J=1$, $T=1$ terms in the sums and noting that $A^{(+)}$ and $B^{(+)}$ are unaffected by a $T=1$ pion-pion

(10) S. FUBINI, Y. NAMBU and V. WATAGHIN: *Phys. Rev.*, **111**, 329 (1958).

resonance, we get the following representations for the four invariant amplitudes

$$(3.8) \quad \left\{ \begin{aligned} A^{(+)} &= \frac{1}{\pi} \int_{(m+\mu)^2}^{\infty} \alpha_{\text{el}}^{(+)}(s', t) \left\{ \frac{1}{s' - s} + \frac{1}{s' - \bar{s}} \right\} ds' + C_A^{(+)}, \\ A^{(-)} &= \frac{1}{\pi} \int_{(m+\mu)^2}^{\infty} \alpha_{\text{el}}^{(-)}(s', t) ds' \left\{ \frac{1}{s' - s} - \frac{1}{s' - \bar{s}} \right\} + (s - \bar{s}) \frac{1}{\pi} \int_{4\mu^2}^{\infty} \frac{\varrho(t')}{t' - t} dt', \\ B^{(+)} &= g_r^2 \left(\frac{1}{M^2 - s} - \frac{1}{M^2 - \bar{s}} \right) + \frac{1}{\pi} \int_{(m+\mu)^2}^{\infty} \beta_{\text{el}}^{(+)}(s', t) \left\{ \frac{1}{s' - s} - \frac{1}{s' - \bar{s}} \right\} ds', \\ B^{(-)} &= g_r^2 \left(\frac{1}{M^2 - s} + \frac{1}{M^2 - \bar{s}} \right) + \frac{1}{\pi} \int_{(m+\mu)^2}^{\infty} \beta_{\text{el}}^{(-)}(s', t) \left\{ \frac{1}{s' - s} + \frac{1}{s' - \bar{s}} \right\} ds' + \\ &\quad + \frac{1}{\pi} \int_{4\mu^2}^{\infty} \frac{\sigma(t')}{t' - t} dt' + C_B^{(-)}, \end{aligned} \right.$$

where

$$\begin{aligned} \varrho(t') &= \frac{3\pi}{p'^2} \left(\frac{M}{\sqrt{2}} \operatorname{Im} f_{-}^{(-)1}(t) - \operatorname{Im} f_{+}^{(-)1}(t) \right), \\ \sigma(t') &= \frac{12\pi}{\sqrt{2}} \operatorname{Im} f_{-}^{(-)1}(t'). \end{aligned}$$

In the absence of a solution to the Chew-Mandelstam $\pi\pi$ scattering equations ⁽¹¹⁾ we shall adopt a resonance form that satisfies the requirements of unitarity, correct low energy behaviour and the existence of a cut from $t = 4\mu^2$ to ∞ . Such a form is

$$(3.9) \quad f_{\pi\pi} = \frac{\exp[i\delta_{\pi\pi}] \sin \delta_{\pi\pi}}{q^3} = \frac{\gamma}{t_r - t - i\gamma q^3}, \quad (J = T = 1).$$

If this were a correct solution to the Chew-Mandelstam equations, γ would be a function of t . For $f_{\pi\pi}$ to be a resonance, however, γ would have to be a slowly varying function of t , at least in the resonance region; we shall take it to be a real constant (*).

⁽¹¹⁾ G. F. CHEW and S. MANDELSTAM: UCRL 8728.

(*) Taking γ to be a constant introduces a spurious pole in $f_{\pi\pi}(t)$. However, for a sharp resonance this pole will have a small residue and be distant from the region of interest.

One can now directly write down an expression for $f_{\pm}^{(-1)}(t)$ that satisfies the analyticity requirements of (3.9) and has the desired phase in the region $4\mu^2 < t \leq 16\mu^2$. A solution, equivalent to that of OMNÈS⁽¹²⁾, having all the required properties is

$$(3.10) \quad f_{\pm}^{(-1)}(t) = f_{\pi\pi}(t) \int_{-\infty}^a \frac{\text{Im } f_{\pm}^{(-1)}(t')}{f_{\pi\pi}(t') (t' - t - i\varepsilon)} dt',$$

into which we must now substitute the expressions given by eq. (5.7) and (5.8) of Ref. (7) for $\text{Im } f_{\pm}^{(-1)}(t')$. If we attempt, however, to evaluate these integrals keeping only the contributions from the nucleon pole term and the (3.3) resonance we find that the integrals do not converge, essentially due to the fact that we are using a power series expansion in t' for $\text{Im } f_{\pm}^{(-1)}(t')$ over a region where the expansion no longer converges. FRAZER and FULCO have attempted to estimate the integrals appearing in (3.10) by introducing a cut-off. Our procedure is to replace them by constants representing their value at $t = t_r$, this approximation being based on the assumption that the structure of $f_{\pm}^{(-1)}(t)$ in the region of interest $4\mu^2 < t < \infty$ is dominated by a strongly peaked π - π resonance.

Let us write therefore

$$(3.11) \quad f_{\pm}^{(-1)} = \frac{N_{\pm}}{t_r - t - i\gamma q^3}.$$

In the following section we shall show how one may estimate these constants by comparison with nucleon electromagnetic structure data.

4. - The electromagnetic structure of the nucleon.

It has been pointed out by FRAZER and FULCO^(3,4) that both the magnitude of the isotopic vector part of the anomalous magnetic moment of the nucleon and the radii of the charge and magnetic moment distributions can be adequately explained if the pion-pion interaction is assumed to have a resonance in the $J=1$, $T=1$ state. Earlier attempts by dispersion relation techniques to explain these properties, neglecting the pion-pion interaction, were unable to account for them all simultaneously.

We shall use the notation of FEDERBUSH, GOLDBERGER and TREIMAN⁽¹³⁾. They consider the nucleon current density operator j_{μ} taken between single

⁽¹²⁾ R. OMNÈS: *Nuovo Cimento*, **8**, 316 (1958).

⁽¹³⁾ P. FEDERBUSH, M. L. GOLDBERGER and S. B. TREIMAN: *Phys. Rev.*, **112**, 642 (1958).

nucleon states. From Lorentz and gauge invariance this can be expressed in terms of two scalar functions

$$\langle p' | j_\mu | p \rangle = \left(\frac{M^2}{p_0 p'_0} \right)^{\frac{1}{2}} \bar{u}(p') [F_1(t) i \gamma_\mu - F_2(t) i \sigma_{\mu\nu} p'^\nu - p^\nu] u(p),$$

where $u(p)$ and $u(p')$ are the Dirac spinors for the initial and final nucleons and $t = -(p - p')^2$.

The functions F_1 and F_2 may be subdivided into isotopic scalar and vector parts

$$(4.1) \quad F_1 = F_1^s + \tau_3 F_1^v,$$

$$(4.2) \quad F_2 = F_2^s + \tau_3 F_2^v.$$

We consider here only the isotopic vector parts F_1^v and F_2^v as these are the easiest to handle by dispersion relation techniques. For $t = 0$ they satisfy the relations

$$(4.3) \quad F_1^v(0) = \frac{e}{2},$$

$$(4.4) \quad F_2^v(0) = \frac{\mu_p - \mu_n}{2} = \frac{ge}{2m},$$

μ_n and μ_p are the anomalous magnetic moments of the neutron and proton respectively (experimentally g , the gyromagnetic ratio = 1.83) e is the electron-charge. The functions $F_1^v(t)$ and $F_2^v(t)$ are taken to satisfy the dispersion relations:

$$(4.5) \quad F_1^v(t) = \frac{e}{2} + \frac{t}{\pi} \int_{4\mu^2}^{\infty} \frac{\text{Im } F_1^v(t') dt'}{t'(t' - t)},$$

$$(4.6) \quad F_2^v(t) = \frac{ge}{2m} + \frac{t}{\pi} \int_{4\mu^2}^{\infty} \frac{\text{Im } F_2^v(t') dt'}{t'(t' - t)}.$$

Subtractions have been performed in order to ensure better convergence of the integrals. The reader is referred to the paper by FEDERBUSH, GOLDBERGER and TREIMAN⁽¹³⁾ for a discussion of these equations and for an evaluation of the two pion contribution to $\text{Im } F_1^v(t')$ and $\text{Im } F_2^v(t')$ in terms of the pion electromagnetic form factors and the $\pi + \pi \rightarrow N + \bar{N}$ production amplitudes.

They obtain expressions for this contribution which can be written in terms of the $\pi + \pi \rightarrow N + \bar{N}$ JACOB and WICK ⁽¹⁴⁾ amplitudes as ⁽⁴⁾

$$(4.7) \quad \text{Im } F_i^V(t) = - \frac{e F_{\pi}^*(t) q^3}{2E} \Gamma_i(t),$$

where

$$\begin{aligned} \Gamma_2(t) &= \frac{1}{2\rho^2} \left\{ \frac{M}{\sqrt{2}} f_{-}^{(-)1}(t) - f_{+}^{(-)1}(t) \right\}, \\ \Gamma_1(t) &= \frac{M}{p^2} \left\{ - \frac{E^2}{M\sqrt{2}} f_{-}^{(-)1}(t) + f_{+}^{(-)1}(t) \right\}, \end{aligned}$$

$F_{\pi}(t)$ is the pion electromagnetic form factor. By arguments similar to those used in the derivation of the integral representations for the nucleon electromagnetic form factors it can be shown that $F_{\pi}(t)$ satisfies the integral representation ⁽³⁾

$$(4.8) \quad F_{\pi}(t) = 1 + \frac{t}{\pi} \int_{4\mu^2}^{\infty} \frac{dt' \text{Im } F_{\pi}(t')}{t'(t'-t)}.$$

Also, by the Fubini Nambu, Wataghin theorem ⁽¹⁰⁾ $F_{\pi}(t)$ has the same phase as the $\pi\pi$ scattering amplitude in the $J=1$, $T=1$ state below the inelastic threshold $t=16\mu^2$. The problem of the construction of $F_{\pi}(t)$ is analogous to that of $f_{\pm}^{(-)1}(t)$ except that the former has no left hand cut. A solution arrived at in the same manner, equivalent to the Omnès solution ⁽¹²⁾, is

$$(4.9) \quad F_{\pi}(t) = \frac{t_r + \gamma}{t_r - t - i\gamma q^2}.$$

Using this expression and eq. (4.7) we obtain,

$$(4.10) \quad \text{Im } F_2^V(t) = - \frac{e}{2E} q^3 \frac{t_r + \gamma}{(t_r - t)^2 + \gamma^2 q^6} \frac{1}{2\rho^2} \left(\frac{M}{\sqrt{2}} N_- - N_+ \right),$$

$$(4.11) \quad \text{Im } F_1^V(t) = - \frac{e}{2E} q^3 \frac{t_r + \gamma}{(t_r - t)^2 + \gamma^2 q^6} \frac{M}{p^2} \left(- \frac{E^2}{M\sqrt{2}} N_- + N_+ \right).$$

If we now make the assumption that the resonance is narrow, we can replace

$$\frac{q^3 \gamma}{(t_r - t) + \gamma^2 q^6} \quad \text{by} \quad \pi \delta(t_r - t),$$

⁽¹⁴⁾ M. JACOB and G. C. WICK: *Ann. Phys.*, **7**, 404 (1959).

and obtain by substitution into (4.5) and (4.6)

$$(4.12) \quad F_1^V(t) = \frac{e}{2} \left(1 - \frac{at}{t_r - t} \right),$$

$$(4.13) \quad F_2^V(t) = \frac{ge}{2m} \left(1 - \frac{bt}{t_r - t} \right).$$

The two constants a and b are

$$\begin{aligned} a &= \frac{C_1}{E_r \gamma} \frac{t_r + \gamma}{t_r}, \\ b &= \frac{M}{g} \frac{C_2}{E_r \gamma} \frac{t_r + \gamma}{t_r}, \\ C_2 &= \frac{1}{2p_r^2} \left(\frac{M}{\sqrt{2}} N_- - N_+ \right), \\ C_1 &= \frac{M}{p_r^2} \left(-\frac{E_r^2}{\sqrt{2}M} N_- + N_+ \right), \end{aligned}$$

p_r and E_r are p and E evaluated at $t = t_r$.

The form factors $F_1^V(t)$ and $F_2^V(t)$ have been investigated experimentally by high energy electron scattering from protons and deuterons ⁽¹⁵⁾. It appears from this experimental data that it is consistent to assume that

$$\frac{2}{e} F_1^V(t) = \frac{2m}{ge} F_2^V(t) = \frac{1}{\mu_p} F_2^p(t) = \frac{1}{\mu_n} F_2^N(t) = \frac{1}{e} F_1^p(t), \quad \text{for } 0 > t > -25\mu,^2$$

where $F_2^p(t)$ is the magnetic moment form factor of the proton.

Taking this to be so, the equality of $(2/e)F_1^V(t)$ and $(2m/ge)F_2^V(t)$ gives the relation

$$(4.14) \quad \frac{C_2}{C_1} = \frac{g}{m}.$$

In order to fit the form of $F_2^p(t)$, we note that our form factors (4.12) and (4.13) have the same form as those predicted by the Clementel and Villi model ⁽¹⁶⁾ for the proton charge and magnetic moment distributions. This model is known to give a good fit to the experimental data with values of the

⁽¹⁵⁾ R. HOFSTADTER: High Energy Physics Laboratory, Stanford University, Cal., HEPL 176.

⁽¹⁶⁾ E. CLEMENTEL and C. VILLI: *Nuovo Cimento*, **4**, 1207 (1958).

parameters $a = b = 1.2$ ⁽¹⁷⁾

$$(4.15) \quad t_r = 22.4 \mu^2$$

and

$$(4.16) \quad \frac{C_1}{\Gamma} = -\frac{1.2 E_r}{q_r^2} = -\frac{.286}{\mu^2}, \quad \Gamma = \gamma q_r^3,$$

corresponding to an r.m.s. charge radius of the proton and radius of the proton and neutron magnetic moment distribution of $.8 \cdot 10^{-13}$ cm.

5. - Projection of partial wave amplitudes.

In order to compare the theoretical and experimental phase shifts we need to evaluate expressions for the $f_{l\pm}$ defined in eq. (2.12). This is done by using the relation (2.13) into which we must substitute the expressions for f_1 and f_2 from (2.9) and use the approximate A 's and B 's evaluated in Section 3. In what follows we shall restrict ourselves to the calculation of S , P and D waves only. Applying these operations to a) the pole terms and b) the integrals involving $1/(s' - s)$ and $1/(s' - \bar{s})$ and keeping only the contribution from the (3, 3) state in the absorptive part of f_1 and f_2 , we obtain, in the static limit, expressions identical to those written down by CHEW, GOLDBERGER, LOW and NAMBU ⁽⁶⁾. These are reproduced here.

$$(5.1) \quad f_s = \frac{f_s(T = \frac{1}{2})}{f_s(T = \frac{3}{2})} = -2\lambda^+ + \left(-\frac{2}{-1}\right) \frac{\omega}{M} \lambda^-,$$

where

$$(5.2) \quad \begin{cases} \lambda^+ = \frac{g^2}{2M} - \frac{4M}{3\pi} \int_1^\infty \frac{d\omega'}{q'^2} \left(1 + \frac{2\omega'}{M}\right) \text{Im } f_{33}(\omega'), \\ \lambda^- = \frac{g^2}{2M} - \frac{4M}{3\pi} \int_1^\infty \frac{d\omega'}{q'^2} \text{Im } f_{33}(\omega'), \end{cases}$$

$$(5.3) \quad \begin{cases} f_{11} = -\frac{8}{3} \frac{f^2 q^2}{\omega} + \frac{16}{9} \frac{q^2}{\pi} \int_1^\infty \frac{d\omega'}{q'^2} \frac{\text{Im } f_{33}(\omega')}{\omega' + \omega}, \\ f_{13} = f_{31} = \frac{1}{4} f_{11}, \\ f_{33} = \frac{4}{3} \frac{f^2 q^2}{\omega} + \frac{q^2}{\pi} \int_1^\infty \frac{d\omega'}{q'^2} \text{Im } f_{33} \left(\frac{1}{\omega' - \omega} \right). \end{cases}$$

⁽¹⁷⁾ R. HOFSTADTER, F. BUMILLER and M. R. YEARIAN: *Rev. Mod. Phys.*, **30**, 482 (1958).

With the assumption of a narrow $P_{\frac{3}{2},\frac{3}{2}}$ resonance these expressions become

$$(5.4) \quad \begin{cases} f_{11} = -\frac{8}{3} \frac{f^2 q^2}{\omega} \frac{1}{1 + \omega/\omega_r}, \\ f_{13} \simeq f_{31} \simeq \frac{1}{4} f_{11}, \end{cases}$$

where ω_r is the centre of mass pion energy corresponding to the resonant (3.3) state. For D -waves

$$(5.5) \quad \begin{cases} \delta_{D_{3/2}^{1/2}} = -\lambda_D \left[1 + \frac{112}{9} \left(\frac{\omega}{\omega + \omega_r} \right)^2 \right], \\ \delta_{D_{3/2}^{3/2}} = \lambda_D \left[2 - \frac{28}{9} \left(\frac{\omega}{\omega + \omega_r} \right)^2 \right], \\ \delta_{D_{5/2}^{1/2}} = \lambda_D \left[4 - \frac{32}{9} \left(\frac{\omega}{\omega + \omega_r} \right)^2 \right], \\ \delta_{D_{5/2}^{3/2}} = -\lambda_D \left[8 + \frac{8}{9} \left(\frac{\omega}{\omega + \omega_r} \right)^2 \right], \end{cases}$$

with

$$\lambda_D = \frac{1}{15} \frac{f^2}{M} \frac{q^5}{\omega^2}.$$

We must now evaluate the contribution to f_s of the terms in f_1 and f_2 , representing the effect of the π - π interaction. These terms are given by (2.9), (3.8) and (3.11), and under the assumption of a narrow π - π resonance, are given in the static limit by

$$(5.6) \quad \begin{cases} [f_1^{(\pi\pi)}] = \frac{[f_1^{(\pi\pi)}(T=\frac{1}{2})]}{[f_1^{(\pi\pi)}(T=\frac{3}{2})]} \left(\begin{matrix} 2 \\ -1 \end{matrix} \right) \frac{M}{W} \frac{2}{t_r - t} \left(\frac{3}{2} q^2 \cos \theta C_2 - \frac{3}{2} \omega C_1 \right), \\ [f_2^{(\pi\pi)}] = \left(\begin{matrix} 2 \\ -1 \end{matrix} \right) \frac{M}{W} \frac{-2}{t_r - t} \frac{3}{2} q^2 \left(C_2 + \frac{C_1}{2M} \right). \end{cases}$$

Here the superscript $(\pi\pi)$ denotes the contribution from the terms of (3.13) with denominator $t' - t$. The factor $\left(\begin{smallmatrix} 2 \\ -1 \end{smallmatrix} \right)$ comes from having kept the contribution of the $T=1$ pion-pion scattering state only.

From eq. (2.13),

$$f_s = \frac{1}{2} \int_{-1}^1 (f_1 + f_2 \cos \theta) d \cos \theta,$$

we find that the terms in C_2 do not contribute in the static limit and we get

$$(5.7) \quad [J_s^{(\pi\pi)}] = -\frac{3}{2} \frac{M}{W} \left(-1 \right) \frac{\omega}{t_r} C_1 F_0 \left(\frac{2q^2}{t_r} \right),$$

where

$$F_\alpha \left(\frac{2q^2}{t_r} \right) = \int_{-1}^1 \frac{dc c^\alpha}{1 + (2q^2/t_r)(1-c)}. \quad c = \cos \theta.$$

This result is quite general in the sense that for all higher values of l the terms in C_2 do not contribute in the static limit to the non-spin flip amplitude. Indeed, the non spin flip amplitude for scattering in an l state is

$$(5.8) \quad [(l+1)f_{l+} + lf_{l-}] P_l$$

and one may easily verify, using (2.13), that

$$(5.9) \quad (l+1)f_{l+} + lf_{l-} = \frac{2l+1}{2} \int_1^1 dc (f_1 + f_2 c) P_l,$$

from which the result follows immediately. The spin flip amplitude

$$(5.10) \quad (f_{l-} - f_{l+}) P_l^1 e^{i\varphi}$$

on the other hand, depends, in the static limit, on the linear combination

$$(5.11) \quad C'_2 = C_2 + \frac{C_1}{2M},$$

as can be seen from the relation

$$(5.12) \quad f_{l-} - f_{l+} = \frac{2l+1}{2l(l+1)} \int_{-1}^1 dc (1-c^2) P_l' f_2,$$

and eq. (5.6).

We recall that by the discussion of the preceding section, C_1 and C_2 are related to the vector part of the charge distribution radius and anomalous magnetic moment, respectively. C'_2 corresponds therefore to the total magnetic moment:

$$\mu_{\text{anom}} + \frac{e}{2M}.$$

It is interesting to note that, in so far as the terms depending on the resonance are concerned, the non-spin-flip amplitude is related in the static limit only to the charge distribution radius of the nucleon whereas the spin-flip amplitude is connected only to its total magnetic moment.

Evaluating (2.13) for P and D waves we find that the terms to be added onto the CGLN expressions for f_{P_1} , f_{P_3} , f_{D_3} , f_{D_5} are

$$(5.13) \quad \left\{ \begin{aligned} f_{P_1}^{(\pi\pi\pi)} &= -\frac{3}{2} \frac{M}{W} \begin{pmatrix} 2 \\ -1 \end{pmatrix} \frac{1}{t_r} [\omega C_1 F_1 + q^2 C_2' (F_0 - F_2)], \\ f_{P_3}^{(\pi\pi\pi)} &= -\frac{3}{2} \frac{M}{W} \begin{pmatrix} 2 \\ -1 \end{pmatrix} \frac{1}{t_r} \left[\omega C_1 F_1 - \frac{q^2}{2} C_2' (F_0 - F_2) \right], \\ f_{D_3}^{(\pi\pi\pi)} &= -\frac{3}{4} \frac{M}{W} \begin{pmatrix} 2 \\ -1 \end{pmatrix} \frac{1}{t_r} [\omega C_1 (3F_2 - F_0) + 3q^2 C_2' (F_1 - F_3)], \\ f_{D_5}^{(\pi\pi\pi)} &= -\frac{3}{4} \frac{M}{W} \begin{pmatrix} 2 \\ -1 \end{pmatrix} \frac{1}{t_r} [\omega C_1 (3F_2 - F_0) - 2q^2 C_2' (F_1 - F_3)]. \end{aligned} \right.$$

We must still evaluate the effect on f_s of the extra constants $C_A \dots$ introduced in Section 2 when passing from the Mandelstam representation to the one-dimensional Cini-Fubini form. (The effect on the f_{P_1} amplitude is only a non-static correction and constants have no effect on the other amplitudes.) One easily verifies that these constants simply add to f_s a term of the form

$$(5.14) \quad \alpha + \begin{pmatrix} 2 \\ -1 \end{pmatrix} \beta \omega.$$

This correction is of exactly the same form as the CGLN contribution (5.3),

As for the $P_{\frac{3}{2}, \frac{3}{2}}$ equation, our additional term is small in the region of the resonance itself and hence the resonance solution given in Ref. (4) will be modified simply by the addition of a small real part.

6. - Comparison with experiment and conclusions.

We have postulated a simple possible model for the effect of the pion-pion interaction on the pion-nucleon scattering amplitude. However a direct comparison of the phase-shift predictions of this model with experiment is not very fruitful because of the large uncertainties involved in the phase-shift analysis of the experimental data.

The best established low energy results apart from the existence of the $P_{\frac{3}{2}, \frac{3}{2}}$ resonance are the values of the S -wave scattering lengths. Those quan-

tities, however, are implicitly very dependent on the core contribution to the scattering amplitude, a fact which is reflected in our having taken the high energy contributions to our dispersive integrals as arbitrary constants. These arbitrary constants give contributions to the S -wave scattering amplitude of the same form as the CHEW, GOLDBERGER, LOW and NAMBU terms, namely the expression (5.14). These terms by themselves give an adequate description of the scattering lengths. However, at higher energies the experimental data cannot be adequately explained by the simple dependence given in (5.14). Using our model up to an energy of about $q = 1.5\mu$ enables us to fit all the S -wave data and gives us a value of the « width » Γ of our resonance. Fitting the data with $t_r = 22.4\mu^2$ gives $C_1 \sim -.58$ which corresponds to a value of $\Gamma \sim 2.4\mu^2$; positive, as it must be if our postulate of a resonance is correct. Note that Γ is not the conventional width of the resonance but that with our resonance form (3.11) the energy difference between the points where the resonance reaches half its maximum value is given by $\Gamma/\sqrt{t_r}$.

With this value of t_r and the value of $C_1 = -.58$ the P and D wave threshold behaviour as calculated from (5.13) is shown in the table. If one allows for the uncertainties in F_1^N and F_2^N in the determination of t_r from the isovector parts of the nucleon form factors, then t_r could very well be $15\mu^2$

TABLE I. - Table of threshold values for P and D waves.

Term	π - π contribution		Chew term	Total		Exp.
	$t_r = 22.4$	$t_r = 15$		$t_r = 22.4$	$t_r = 15$	
$f_{P_1}^{1/2}/q^2$.046	.049	-.14	-.094	-.091	-.038 \pm .038
$f_{P_3}^{1/2}/q^2$	-.016	-.013	-.035	-.051	-.048	-.039 \pm .022
$f_{P_1}^{3/2}/q^2$	-.023	-.025	-.035	-.058	-.060	-.044 \pm .005
$f_{P_3}^{3/2}/q^2$.008	.007	.213	.221	.220	.234 \pm .019
$f_{D_3}^{1/2}/q^4$.0013	.0020	-.0019	-.0006	+ .0001	—
$f_{D_3}^{3/2}/q^4$	-.0007	-.0010	.0013	+ .0006	+ .0003	—
$f_{D_3}^{5/2}/q^4$	-.0005	-.0007	.0029	+ .0024	+ .0022	—
$f_{D_3}^{7/2}/q^4$.0003	.0004	-.0065	-.0062	-.0061	—

instead of $22.4\mu^2$. The values of the P and D waves at threshold corresponding to $t_r = 15\mu^2$ are therefore given too. We also give the contribution from the CHEW *et al.* terms as calculated from (5.4) and (5.5) and compare the total with the experimental results (taken from the 1958 Annual International Conference on High Energy Physics at CERN).

While the theoretical numbers quoted in the table are not in exact agreement with the experimental numbers one must remember that the contribution from the π - π interaction may be varied by varying C_1 . The above calculation of C_1 is only reliable as an order of magnitude estimate, since the inclusion of the S wave rescattering corrections in eq. (3.8) could have a significant effect at this energy.

One feature which is not brought out by just inspecting the threshold behaviour of the partial waves is the energy variation of the π - π contribution and of the Chew term. One finds in fact that the energy variation of the π - π contribution is stronger than that of the Chew term and therefore at higher energies the π - π term becomes comparable or larger than the Chew term and determines to a large extent the variation of the phase shifts with energy.

One encouraging feature is the fact that we are able to make the D_{13} phase shift positive at low energies. Also, it is the D_{13} phase shift to which the π - π interaction gives the largest contribution. The C.G.L.N. term alone is negative and so would seem to imply a repulsive interaction for this partial wave whereas experimentally it resonates around 600 MeV.

Of course more extensive calculations must still be done and a direct comparison of theoretical and experimental phase shifts is probably not the best way to put the theory to a severe test. For in analysing an experimental cross-section into partial waves one usually arrives at phase shifts with large uncertainties on them and whose value may depend on the assumed values of other partial waves *e.g.* the D waves. On the other hand, the theory presented here gives simultaneously definite values for S , P and D waves. A better procedure for comparing theory and experiment is therefore to compare directly the differential cross-sections on which the experimental errors are rather small. Such a programme is at present in progress.

In conclusion we would like to remark that it is amusing that one can probably reach an approximation to low energy pion-nucleon scattering identical to the one presented here by considering a model in which both the (3,3) resonance and the π - π , $J=1$, $T=1$ resonance are replaced by isobars having the corresponding masses, spins and isospins. Of course the formulation presented here is much more general since it allows for the insertion of experimental data on π - π scattering in all spin and isospin states when such information becomes available.

* * *

We wish to thank Prof. S. FUBINI for many helpful discussions during the course of this work. We are also indebted to Mr. W. KLEIN for numerical computations.

RIASSUNTO (*)

Dalle proprietà analitiche dell'ampiezza dello scattering pione-nucleone postulate da Mandelstam, deriviamo una relazione fissa di dispersione del trasporto di momento che ha per variabile l'energia, che dovrebbe essere valida a basse energie. Questa formulazione ci permette di valutare l'effetto di una risonanza di scattering di due pioni sullo scattering pione-nucleone. Con una opportuna scelta dei parametri di risonanza pione-pione possiamo approssimare sia gli spostamenti di fase sperimentali pione-nucleone sia i fattori di forma elettromagnetici del nucleone.

(*) *Traduzione a cura della Redazione.*

Calcolo semiempirico dei primi livelli di energia elettronica della molecola HFCO (*).

G. GIACOMETTI, G. RIGATTI e G. SEMERANO

Istituto di Chimica Fisica dell'Università - Padova

(ricevuto il 23 Marzo 1960)

Riassunto. — Vengono calcolati i primi livelli di energia degli elettroni n e π per la molecola HFCO con il metodo LCAO, MO, SCF nella versione semiempirica di Pople-Pariser-Parr. Viene discussa principalmente la frequenza della transizione $n \rightarrow \pi$ prevista dal calcolo, confrontandola con il valore sperimentale recentemente trovato e con quello, già noto da tempo, dell'analogia transizione della formaldeide.

1. - Introduzione.

Si è recentemente intrapreso in questo Istituto lo studio sperimentale dello spettro ultravioletto di molecole simili alla formaldeide e si sono ottenuti i primi risultati per la molecola del fluoruro di formile (¹).

A complemento di queste ricerche ci è parso di un certo interesse iniziare alcune indagini teoriche volte alla elucidazione delle principali caratteristiche elettroniche di questa molecola, con lo scopo di avvalorare le interpretazioni degli spettri ottenuti ed eventualmente contribuire all'assegnazione di bande, alla determinazione delle proprietà di simmetria degli stati elettronici in gioco e così via.

(*) Questa ricerca è stata parzialmente finanziata dall'« Office Chief of Research and Development, U.S. Dept. of Army » tramite il suo Ufficio Europeo, in base al contratto no. DA-91-508-EUC-275.

(¹) A. FOFFANI, I. ZANON, G. GIACOMETTI, U. MAZZUCATO, G. FAVARO e G. SEMERANO: *Nuovo Cimento*, **16**, 861 (1960).

Uno dei metodi più adatti allo studio teorico della struttura elettronica di molecole poliatomiche, specialmente in vista dell'applicazione al calcolo delle transizioni elettroniche, è quello semi empirico proposto nel 1953 da PARISER e PARR ⁽²⁾ per la struttura dei livelli π delle molecole aromatiche e recentemente esteso a composti carbonilici e azotati da ANNO e collaboratori ^(3,4) e da SIDMAN ⁽⁵⁾ tenendo esplicitamente conto, oltre che degli elettroni π , anche degli elettroni non leganti localizzati sugli eteroatomi (elettroni n). Questa estensione è oltremodo importante perchè permette di calcolare le cosiddette transizioni $n-\pi$ che sono responsabili, in generale, degli assorbimenti di questi composti nelle zone più accessibili dello spettro. I risultati ottenuti da ANNO e SADO per la formaldeide ⁽⁶⁾ ci hanno incoraggiato ad intraprendere un calcolo analogo per il fluoruro di formile.

2. - Elementi della teoria.

2'1. *Il calcolo dell'energia.* - Anche se la teoria con tutte le sue modificazioni si trova esposta ormai in numerosi lavori anche italiani ⁽⁷⁾ ci sembra opportuno darne qui le linee essenziali limitandoci alle particolari varianti da noi adottate.

Nell'approssimazione di questo metodo l'hamiltoniano molecolare è espresso nella forma:

$$(1) \quad H = H^0 + \frac{1}{2} \sum_{ij} \frac{e^2}{r_{ij}},$$

in cui e^2/r_{ij} è la repulsione elettrostatica tra le coppie di elettroni che si considerano esplicitamente e H^0 rappresenta il potenziale del campo creato da tutti gli atomi della molecola privati degli elettroni che si considerano esplicitamente. Questo potenziale agisce su ogni elettrone indipendentemente dagli altri e perciò può essere diviso nella somma dei contributi per i singoli elettroni:

$$(2) \quad H^0 = \sum_i H_i^0.$$

⁽²⁾ A. PARISER e R. G. PARR: *Journ. Chem. Phys.*, **11**, 466, 767 (1953).

⁽³⁾ T. ANNO, I. MATUBARA e A. SADO: *Bull. Chem. Soc. Jap.*, **30**, 168 (1957).

⁽⁴⁾ T. ANNO: *Journ. Chem. Phys.*, **29**, 1161 (1958).

⁽⁵⁾ J. W. SIDMAN: *Journ. Chem. Phys.*, **27**, 429 (1957).

⁽⁶⁾ T. ANNO e A. SADO: *Journ. Chem. Phys.*, **26**, 1759 (1957).

⁽⁷⁾ V. ad. es.: M. SIMONETTA: *Struttura delle Molecole*, I Corso Estivo di Chimica; Acc. Naz. dei Lincei (Roma, 1959), pag. 61.

Le autofunzioni monoelettroniche di approssimazione zero vengono prese come combinazioni lineari ortonormalizzate degli orbitali atomici χ_i ,

$$(3) \quad \varphi_i = \sum_j c_{ij} \chi_j.$$

Nel nostro caso gli orbitali χ_i sono di due tipi; quelli di tipo π , che hanno il loro piano nodale coincidente col piano molecolare, e quelli di tipo n , col piano nodale perpendicolare al piano molecolare.

La funzione d'onda di approssimazione zero del sistema elettronico completo, per una determinata configurazione, viene costruita mediante la combinazione lineare antisimmetrizzata dei prodotti delle varie φ_i monoelettroniche:

$$(4) \quad \psi_n = \left(\frac{1}{N!} \right)^{\frac{1}{2}} (-1)^P P \{ \varphi_1(1) \varphi_2(2) \dots \varphi_r(r) \},$$

dove l'indice n sta ad indicare il tipo di configurazione e le varie φ_i differiscono una dall'altra anche solo nella parte di spin. L'energia di ogni singola configurazione è data dall'equazione:

$$(5) \quad E_n = \int \psi_n^* H \psi_n d\tau = H_{nn}.$$

In molti casi, e specialmente per quanto riguarda i più bassi livelli energetici, l'espressione (5) è già una utile approssimazione dell'energia; a volte è però necessario considerare funzioni d'onda ancora migliori delle ψ_n costruendole da combinazioni lineari di queste ultime

$$(6) \quad \Psi_m = \sum_n C_{mn} \psi_n$$

e per le quali i coefficienti C_{mn} e le energie corrispondenti E_m si trovano dalla diagonalizzazione della matrice

$$(7) \quad |H_{nm} - \delta_{nm} E|$$

in cui H_{nm} è un integrale come quello in (5) e δ_{nm} è il simbolo di Kronecker. Quest'ultimo stadio del calcolo si dice mescolamento o interazione delle configurazioni. È in genere troppo laborioso, per sistemi anche non molto complicati, poter includere nel calcolo tutte le configurazioni possibili, anche se l'eventuale simmetria molecolare può permettere di semplificare notevolmente la diagonalizzazione. In generale si fa una opportuna scelta critica delle configurazioni da includere.

2'2. *Il calcolo degli integrali.* — La parte empirica della teoria consiste essenzialmente nel metodo di calcolo degli integrali di tipo (5). Questi ultimi, facendo uso di (4), (3), (2) e (1), vengono ridotti a due tipi fondamentali di integrali su orbitali atomici; gli integrali monoelettronici:

$$(8) \quad H_{ii}^0 = \int \chi_i(1) H_1^0 \chi_i(1) d\tau_1,$$

e quelli bielettronici

$$(9) \quad \chi_i \chi_j / \chi_k \chi_l = \iint \chi_i(1) \chi_j(1) \frac{e^2}{r_{12}} \chi_k(2) \chi_l(2) d\tau_1 d\tau_2.$$

Gli integrali di tipo (8), nel caso $i = j$, vengono approssimati da un'espressione del tipo:

$$(10) \quad H_{ii}^0 = \alpha_i = -I_i - \sum_{j \neq i} [(\chi_i \chi_j / \chi_j \chi_i) + (\chi_j / \chi_i \chi_i)],$$

in cui: I_i è il potenziale di ionizzazione dell'elettrone nell'orbitale χ_i dello stato di valenza dell'atomo; $(\chi_i \chi_j / \chi_j \chi_i)$ sono stati definiti in (9) e $(\chi_j / \chi_i \chi_i)$ sono integrali detti di « penetrazione », che possono essere trascurati, specie nel calcolo delle energie di transizione per le quali si ha una compensazione di errori (4).

Nel caso invece di $i \neq j$ gli integrali H_{ij}^0 si considerano come dei parametri empirici e si trascurano se i due orbitali χ_i e χ_j non si trovano su due atomi formalmente legati.

Questi parametri vengono generalmente indicati con β_{ij} e si può arguire che dipendono essenzialmente dal tipo dei due atomi e dalla loro distanza e non dal resto della molecola.

Gli integrali di respulsione elettronica (9) vengono calcolati in base alle seguenti approssimazioni:

a) Tutti gli integrali di tipo (9) in cui $i \neq j$ oppure $k \neq l$ vengono trascurati. Ciò equivale a trascurare formalmente il cosiddetto « ricoprimento differenziale ». Questa approssimazione fa parte integrante del metodo semi empirico originale e riduce enormemente il numero degli integrali da calcolare limitandoli solamente ai due tipi:

$$(\chi_i \chi_i / \chi_i \chi_i) \quad \text{e} \quad (\chi_i \chi_i / \chi_j \chi_j).$$

Il metodo originale era però limitato ad orbitali di tipo π , mentre noi vogliamo considerare anche gli orbitali di tipo n . È opportuno allora tener conto anche degli integrali di tipo $(\chi_i \chi_j / \chi_i \chi_j)$, limitatamente al caso in cui gli orbitali χ_i e χ_j appartengono allo stesso atomo (sono cioè uno di tipo π e uno di tipo n).

b) Gli integrali monocentrici vengono determinati dall'analisi degli stati di valenza dell'atomo implicato, mediante l'uso di quantità spettroscopiche atomiche, sperimentali.

c) Gli integrali bicentrici ($\chi_i\chi_i/\chi_j\chi_j$) vengono calcolati a distanze grandi, facendo uso delle funzioni atomiche di Slater e si interpolano poi i valori alle distanze molecolari sulla curva che si correla per distanza nulla al valore medio dei due integrali monocentrici. Il metodo è stato descritto abbastanza in dettaglio, per i vari casi di integrali, nei recenti lavori citati (^{3,4}).

2'3. *La scelta delle funzioni molecolari di partenza.* — La scelta delle combinazioni lineari (3) è assolutamente arbitraria nel caso che il calcolo dell'interazione di configurazione venga condotto in maniera completa (tutte le configurazioni incluse). In generale però il numero delle configurazioni è così elevato che rende praticamente impossibile questa completezza. È allora opportuno partire da orbitali molecolari che siano già una soluzione del problema in una approssimazione minore. Si è dimostrato fruttuoso il partire dagli orbitali molecolari che risolvono il problema LCAO, MO di approssimazione zero.

Un metodo ancora migliore è quello di risolvere il problema degli orbitali di campo autoconsistente (orbitali SCF) nel modo con cui viene fatto da Pople (⁸) e cioè con le approssimazioni già contenute nello schema di Pariser e Parr.

Nella applicazione al fluoruro di formile abbiamo impiegato quest'ultimo metodo.

3. -- Applicazione al fluoruro di formile.

La molecola HFCO può essere considerata piana nel suo stato fondamentale, sia attraverso semplici considerazioni teoriche (⁹) sia per evidenze sperimentali di spettroscopia I.R. (¹⁰). I parametri molecolari non sono noti con certezza ma non sono certamente molto lontani da quelli proposti da MORGAN e coll. (¹⁰). I seguenti sono quelli che abbiamo assunto per il calcolo degli integrali elettronici:

$$\text{C—O} = 1.20 \text{ \AA}, \quad \text{C—F} = 1.35 \text{ \AA}, \quad \widehat{\text{FCO}} = 125^\circ.$$

(⁸) J. A. POPL: *Trans. Farad. Soc.*, **49**, 1315 (1953).

(⁹) A. D. WALSH: *Journ. Chem. Soc.*, 2260, 2306 (1953).

(¹⁰) H. W. MORGAN, P. A. STAATS e J. H. GOLDSTEIN: *Journ. Chem. Phys.*, **25**, 337 (1956).

Recenti risultati di spettroscopia a microonde ⁽¹⁾ danno per la distanza C—O un valore alquanto inferiore a quello della formaldeide (che è di 1.22 Å) e molto probabilmente vicino a 1.17 Å. Questa modifica non porta sensibili differenze nel calcolo degli integrali detti ma può essere molto importante per la discussione del parametro β_{CO} .

La molecola appartiene al gruppo di simmetria C_s per cui le funzioni d'onda si possono classificare in due distinte specie di simmetria che vengono indicate con A' e A'' .

Si è tenuto conto esplicitamente di otto elettroni e precisamente: due elettroni n e due elettroni π dell'atomo di fluoro, due elettroni n e un elettrone π dell'atomo di ossigeno e un elettrone π dell'atomo di carbonio. I rispettivi orbitali atomici vengono indicati con n_F , π_F , n_O , π_O , π_C .

I valori di potenziale di ionizzazione negli stati di valenza e degli integrali monocentrici di repulsione elettronica sono stati presi dalla letteratura, tranne gli integrali $(\pi_F n_F / \pi_F n_F)$ e $(\pi_F \pi_F / n_F n_F)$, che sono stati valutati con il metodo riportato in Appendice, e sono riportati in Tabella I.

TABELLA I. — *Potenziali di ionizzazione di stati di valenza ed integrali monocentrici di repulsione elettronica.*

Quantità	Valore (eV)	Fonte	Quantità	Valore (eV)	Fonte
$I\pi_F$	18.06	(1)	$(\pi_O \pi_O / \pi_O \pi_O)$	14.52	(2)
In_F	18.06	(1)	$(\pi_C \pi_C / \pi_C \pi_C)$	11.08	(2)
$I\pi_O$	17.21	(2)	$(\pi_F \pi_F / n_F n_F)$	15.37	(3)
In_O	14.75	(2)	$(\pi_O \pi_O / n_O n_O)$	12.82	(2)
$I\pi_C$	11.54	(2)	$(\pi_C \pi_C / n_C n_C)$	9.84	(2)
$(\pi_F \pi_F / \pi_F \pi_F)$	17.23	(1)	$(\pi_F n_F / \pi_F n_F)$	0.93	(3)
—	—	—	$(\pi_O n_O / \pi_O n_O)$	0.85	(2)

(1) H. A. SKINNER e H. O. PRITCHARD: *Trans. Farad. Soc.*, **49**, 1254 (1953).

(2) T. ANNO, I. MATUBARA e A. SADO: *Bull. Chem. Soc. Jap.*, **30**, 168 (1957).

(3) Vedi Appendice.

Gli integrali bicentrici sugli orbitali atomici sono stati calcolati con le formule di estrapolazione di Pariser e Parr ⁽²⁾ e di Anno e coll. ^(3,4) determinate dai valori alle distanze di 2.79 e 3.80 Å, calcolati mediante l'approssimazione delle sfere uniformemente cariche. Come raggio delle sfere si è preso il valore usato da ANNO ⁽⁴⁾ nella sua seconda approssimazione e precisamente $R = 2.1067/Z$ Å, dove Z è la carica efficace di Slater ($Z_C = 3.25$, $Z_O = 4.55$, $Z_F = 5.20$).

I valori degli integrali per le distanze molecolari scelte sono riportati in Tabella II.

(11) P. FAVERO: comunicazione privata.

TABELLA II. - *Integrali bicentrici di repulsione elettronica.*

Integrale	Valore (eV)	Integrale	Valore (eV)
$\pi_F \pi_F / \pi_O \pi_O$	6.216	$\pi_O \pi_O / n_F n_F$	6.162
$\pi_F \pi_F / \pi_C \pi_C$	8.668	$\pi_C \pi_C / n_O n_O$	8.069
$\pi_F \pi_F / n_O n_O$	6.184	$\pi_C \pi_C / n_F n_F$	8.150
$\pi_O \pi_O / \pi_C \pi_C$	8.703	$n_O n_O / n_F n_F$	6.278

Per applicare il metodo SCF è necessario stabilire *a priori* valori plausibili per le quantità β_{ij} . Ci siamo basati per questa valutazione sul valore di -3.1 eV usato in precedenza per il β_{CO} della formaldeide.

A questo proposito, siccome la nostra impostazione differisce in alcuni particolari da quella di SIDMAN ⁽⁵⁾ e da quella degli autori giapponesi ⁽⁶⁾, abbiamo ricalcolato a scopo di confronto anche i livelli della formaldeide assumendo come distanza C—O per il calcolo degli integrali elettronici il valore di 1.20 \AA , uguale cioè a quello usato per il fluoruro. I risultati, che verranno riportati più oltre, sono essenzialmente in accordo con i calcoli precedenti ed assicurano della bontà del parametro usato.

La scelta dei valori β_{ij} che compaiono nel calcolo è stata quindi fatta in base alla formula di Mulliken ⁽¹²⁾

$$\beta = A \bar{I} S,$$

dove \bar{I} è la media dei potenziali di ionizzazione degli elettroni nei due orbitali interessati ed S l'integrale di sovrapposizione.

Sulla base di -3.1 eV per il β_{CO} della formaldeide risulta un valore di -1.9 eV per β_{CF} . Il β_{CO} va aumentato nel caso del fluoruro di formile data

TABELLA III. - *Orbitali molecolari autoconsistenti π (*) di H_2CO ed $HFCO$.*

$$\begin{aligned} H_2CO: \quad \pi_1 &= 0.530934\pi_C + 0.847416\pi_O \\ \pi_2 &= 0.847416\pi_C - 0.530934\pi_O \end{aligned}$$

$$\begin{aligned} HFCO: \quad \pi_1 &= 0.143872\pi_O + 0.238735\pi_C + 0.960368\pi_F \\ \pi_2 &= 0.833980\pi_O + 0.493165\pi_C - 0.247525\pi_F \\ \pi_3 &= 0.532711\pi_O - 0.836538\pi_C + 0.128160\pi_F \end{aligned}$$

(*) Gli orbitali n , a causa delle approssimazioni usate, non vengono mescolati nel processo di autoconsistenza.

⁽¹²⁾ R. S. MULLIKEN: *Journ. Phys. Chem.*, **56**, 295 (1952).

la suaccennata contrazione del legame. Per una distanza ridotta a 1.17 Å rispetto agli 1.22 Å della formaldeide, l'integrale di sovrapposizione aumenta di circa un fattore 1.13 e pertanto si può assumere $\beta_{CO} = -3.5$ eV.

In Tabella III sono riportati gli orbitali molecolari autoconsistenti ottenuti, per la formaldeide ed il fluoruro di formile rispettivamente.

Il calcolo della interazione configurazionale (I.C.) è stato condotto per tutte le configurazioni della formaldeide derivanti dai tre orbitali considerati (9 configurazioni con $\sum m_s = 0$) mentre per il fluoruro si sono considerate tutte quelle derivanti dai 5 orbitali considerati tranne quelle che si ottengono per eccitazione di più di un elettrone dagli orbitali più bassi, π_3 ed n_F , (in totale 20 configurazioni con $\sum m_s = 0$.)

In Tabella IV sono riportati i valori dei livelli energetici ottenuti sia includendo che trascurando l'interazione configurazionale.

TABELLA IV. - *Livelli elettronici di H₂CO e di HFCO (in eV).*

Configurazione	S. mmetria	Senza I.C.	Con I.C.	Sperim. (*)
H ₂ CO: $n_O^2 \pi_1^2$	1A_1	0	0	—
$n_O^2 \pi_1^2 \pi_2$	3A_2	3.65	3.48	(3.5)
$n_O^2 \pi_1^2 \pi_2$	1A_2	4.13	3.67	4.3
$n_O^2 \pi_1 \pi_2$	3A_1	5.23	5.42	?
$n_O^2 \pi_1 \pi_2$	1A_1	8.55	8.05	(8.0)
HFCO: $n_F^2 n_O^2 \pi_1^2 \pi_2^2$	$^1A'$	0	0	—
$n_F^2 n_O^2 \pi_1^2 \pi_2^2 \pi_3$	$^3A''$	4.23	4.08	—
$n_F^2 n_O^2 \pi_1^2 \pi_2^2 \pi_3$	$^1A''$	4.72	4.27	5.3
$n_F^2 n_O^2 \pi_1^2 \pi_2 \pi_3$	$^3A'$	6.01	6.14	—
$n_F^2 n_O^2 \pi_1^2 \pi_2 \pi_3$	$^1A'$	9.27	—	—
$n_F n_O^2 \pi_1^2 \pi_2^2 \pi_3$	$^3A''$	12.75	12.76	—
$n_F n_O^2 \pi_1^2 \pi_2^2 \pi_3$	$^1A''$	12.87	12.76	—

(*) I valori sperimentali corrispondono ai massimi di assorbimento in solventi inerti (quando esistono).

4. - Discussione.

Lo scopo del nostro calcolo era essenzialmente quello di giustificare lo spostamento verso l'ultravioletto della transizione $^1A' \rightarrow ^1A''$ del fluoruro di formile (cui è stata assegnata la banda con massimo di intensità nell'intorno dei 2200 Å ⁽¹⁾) rispetto alla transizione $^1A_1 \rightarrow ^1A_2$ della formaldeide che, come è ben noto, presenta il suo massimo di intensità nell'intorno dei 2880 Å ⁽¹³⁾.

⁽¹³⁾ A. D. COHEN e C. REID: *Journ. Chem. Phys.*, **24**, 85 (1956).

Lo spostamento previsto dal calcolo è di circa 0.6 eV nel senso desiderato, alquanto inferiore quindi a quello sperimentale che è di 1 eV. Questo risultato è indipendente dall'uso dei valori energetici ottenuti senza la I.C. o di quelli che la comprendono.

Occorre osservare che tale spostamento ipsocromo è praticamente tutto determinato dall'aumentato valore di β , conseguenza della diminuita distanza C—O. Se infatti si eseguono i calcoli con un parametro β uguale a quello usato per la formaldeide (come era stato fatto in una fase preliminare di questo lavoro) la transizione risulta spostata di 0.1 eV solamente. Non vi ha però alcun dubbio che tale variazione del parametro sia pienamente giustificata, oltre che per le evidenze strutturali specifiche più sopra ricordate, anche per il fatto che si riscontra in generale che sostituenti elettronegativi al carbonio del carbonile fanno contrarre la distanza carbonio ossigeno e parallelamente aumentare la costante di forza della vibrazione di allungamento corrispondente ⁽¹⁴⁾. Una soddisfacente spiegazione di questa contrazione non è stata ancora proposta ma noi pensiamo sia principalmente legata all'influenza induttiva trasmessa attraverso i legami σ , influenza che modifica con tutta probabilità anche l'eventuale stato di ibridizzazione *sp* degli orbitali di valenza dell'atomo di ossigeno.

Nel nostro calcolo questa possibilità di ibridizzazione è stata completamente trascurata per non dover introdurre un ulteriore parametro più o meno arbitrario. Il tenerne conto porterebbe delle variazioni nei valori del potenziale di ionizzazione e degli integrali monocentrici dell'ossigeno e potrebbe quindi modificare alquanto i risultati.

Non è escluso che il metodo degli orbitali molecolari autoconsistenti con le approssimazioni semiempiriche di Pariser e Parr possa essere usato con un certo successo per razionalizzare le transizioni $n-\pi$ di tutta la serie dei derivati carbonilici semplici (H_2CO , HFCO , F_2CO , Cl_2CO , CH_3CHO , ecc.). Per ridurre al minimo il numero dei parametri empirici occorrerebbe una verifica della validità dell'uso della formula di Mulliken per la valutazione di β e la determinazione di un criterio sicuro circa lo stato di ibridizzazione degli orbitali dell'ossigeno.

Merita ancora osservare qualche cosa circa l'effetto della interazione delle configurazioni il cui principale risultato è quello di diminuire notevolmente la separazione singoletto-tripletto, che passa da un valore di circa 0.5 ad uno di circa 0.2 eV. I risultati sperimentali non sono tali da permettere un confronto utile ma, data la natura empirica del calcolo e considerato che il parametro fondamentale β è basato su risultati che non tengono conto della I.C., non è escluso che siano più indicativi i risultati del calcolo più semplice.

⁽¹⁴⁾ L. C. KRISHER e E. BRIGHT WILSON jr.: *Journ. Chem. Phys.*, **31**, 882 (1959).

L'abbassamento dello stato 1A_2 rispetto al 3A_2 per la formaldeide, operato dalla interazione delle configurazioni, è stato recentemente calcolato da SENDER e BERTHIER ⁽¹⁵⁾ che hanno usato il metodo SCF non empirico. Le correzioni empiriche di Moffitt e di Hurley ristabiliscono un valore più elevato della separazione singoletto-tripletto ma lasciano ancora molto a desiderare per i valori assoluti delle energie. Il metodo di Pariser e Parr sembra ancora notevolmente superiore a questo riguardo, benchè in casi come il presente, nel quale interessava il confronto tra due composti simili diversamente sostituiti, molti vantaggi vengano perduti dato che le cause delle differenze sono quasi completamente contenute nella differente situazione dello scheletro σ della molecola piuttosto che nel sistema elettronico esplicitamente considerato.

APPENDICE

Il valore teorico dei tre integrali $(\pi_a\pi_a/\pi_a\pi_a)$, $(\pi_a\pi_a/n_an_a)$ e (π_an_a/π_an_a) è dato rispettivamente da ⁽¹⁶⁾:

$$(A.1) \quad \pi_a\pi_a/\pi_a\pi_a = G_a^0 + \frac{4}{25} G_a^2,$$

$$(A.2) \quad \pi_a\pi_a/n_an_a = G_a^0 - \frac{2}{25} G_a^2,$$

$$(A.3) \quad \pi_an_a/\pi_an_a = \frac{3}{25} G_a^2 = \frac{1}{2} \{(\pi_a\pi_a/\pi_a\pi_a) - (\pi_a\pi_a/n_an_a)\},$$

in cui le quantità G_a^i (parametri di Slater Condon) sono definite da:

$$(A.4) \quad G_a^i = e^2 \int_0^\infty \int_0^\infty \frac{r_1^{i-1}}{r_2^{i+1}} R_a^2(r_1) R_a^2(r_2) r_1^2 r_2^2 dr_1 dr_2,$$

dove $R_a(r)$ è la parte radiale (comune) degli orbitali atomici π_a ed n_a .

Questi parametri G_a^i sono generalmente ricavabili da dati spettroscopici relativi all'atomo in questione, ma ciò non è possibile in casi, come quello degli alogeni, di stati monovalenti. In questi casi si può solo sperare di avere un valore empirico per l'integrale (A.1) globalmente.

Se d'altra parte si valutano i G_a^i facendo uso delle funzioni radiali di Slater, essi risultano proporzionali alla carica efficace Z per cui il rapporto, ad esempio, tra gli integrali (A.1) e (A.2) è una quantità ben determinata, indipendente da Z .

⁽¹⁵⁾ M. SENDER e G. BERTHIER: *Journ. Chem. Phys.*, **56**, 946 (1959).

⁽¹⁶⁾ E. U. CONDON e G. H. SHORTLEY: *The Theory of Atomic Spectra* (Camb., 1953).

Si può pensare che le funzioni radiali che darebbero per i G_a^i i valori corretti (cioè quelli determinabili empiricamente dai dati spettrali) siano ancora del tipo di Slater, se pur con un diverso valore della carica efficace. Se questo è il caso, il rapporto tra gli integrali (A.1) e (A.2) è ancora dato dal valore ottenuto con le funzioni di Slater.

Per gli orbitali $2p$, questo rapporto vale 1.121 come si ottiene facilmente eseguendo le integrazioni. La Tabella V mostra per gli elementi del 1° periodo, i valori degli integrali $(\pi_a\pi_a/n_a n_a)$ ottenuti dalla conoscenza di G^2 e quelli calcolati dividendo per 1.121 il valore empirico di $(\pi_a\pi_a/\pi_a\pi_a)$.

TABELLA V (*).

Elemento e stato di valenza	$\pi_a\pi_a/\pi_a\pi_a$ (eV)	$\pi_a\pi_a/n_a n_a$ (eV)		Scarto (%)
		empirico	« teorico »	
Be (sp , V_2)	6.44	(5.96) (**)	5.74	— 4.0
B (sp^2 , V_3)	8.21	(7.20)	7.32	+ 1.6
C (sp^3 , V_4)	11.08	9.84	9.88	+ 0.4
N (s^2p^3 , V_3)	12.95	11.54	11.55	+ 0.1
O (s^2p^4 , V_2)	14.52	12.82	12.95	+ 1.0

(*) I valori della II e III colonna sono ottenuti dai dati riportati da SKINNER e PRITCHARD (loc. cit. in Tabella II).

(**) I valori tra parentesi sono ottenuti mediante estrapolazione.

Come si vede le differenze tra i valori empirici e quelli « teorici » degli integrali $\pi_a\pi_a/n_a n_a$ sono tutte contenute entro il 4% con massimi scarti nei casi in cui il valore empirico è noto con minor precisione. I valori empirici dipendono, d'altra parte, dal metodo usato per fare le medie delle quantità sperimentali usate (vedi SKINNER e PRITCHARD, loc. cit.). In ogni modo si può vedere che differenze anche del 5% su questi integrali non portano a sensibili modificazioni dei risultati finali.

Il valore che si può così calcolare per $\pi_F\pi_F/n_F n_F$ è perciò $17.23/1.121 = 15.37$ eV.

SUMMARY

The low energy levels of the n and π electrons for the HFCO molecule are calculated by the LCAO, MO, SCF method in the semiempirical version given by Pople-Pariser-Parr. The predicted frequency of the $n \rightarrow \pi$ transition is discussed and compared with a recent experimental value and with the value of the analogous formaldehyde transition.

Reazione $^{27}\text{Al} (n, \alpha) ^{24}\text{Na}$ indotta da neutroni di 15,2 MeV.

M. CEVOLANI, S. PETRALIA, B. RIGHINI, U. VALDRÈ e G. VENTURINI

Istituto Nazionale di Fisica Nucleare - Sezione di Bologna

(ricevuto il 4 Aprile 1960)

Riassunto. — Si determina la distribuzione angolare ed energetica delle particelle α risultanti dalla reazione $^{27}\text{Al}(n, \alpha)^{24}\text{Na}$ provocata da neutroni di 15.2 MeV. Le particelle vengono rivelate con emulsioni nucleari Ilford C-2 e K-0. La camera di reazione è stata progettata in modo da ottenere una buona definizione angolare, tra 80° e 160° . La distribuzione angolare risulta notevolmente anisotropa; la distribuzione energetica mostra un gran numero di particelle di bassa energia. Viene calcolata la temperatura del nucleo residuo e si discutono i risultati ottenuti.

1. — Introduzione.

Le ricerche sulle reazioni (n, α) con neutroni veloci sono ancora poco numerose e, se si eccettuano le più recenti di I. KUMABE e coll. ⁽¹⁾, esse si limitano alla misura della sezione d'urto integrale. KUMABE riferisce sui risultati ottenuti nello studio della distribuzione angolare ed energetica delle particelle α emesse da nuclei leggeri e a medio Z , per interazione con neutroni di 14.8 MeV. La distribuzione angolare nel centro di massa appare simmetrica attorno alla direzione di 90° con i neutroni incidenti, ma anisotropa; la distribuzione energetica risulta per qualche nucleo esattamente maxwelliana. Comunque da una supposta distribuzione maxwelliana in un limitato intervallo energetico viene ricavata la temperatura del nucleo residuo.

Le reazioni (n, α) sarebbero le più idonee a verificare le previsioni del modello statistico del nucleo, perchè sembra plausibile l'ipotesi che le particelle α

⁽¹⁾ I. KUMABE, E. TAKEKOSHI, H. OGATA, Y. TSUNEOKA e S. OKIO: *Phys. Rev.*, **106**, 155 (1957); *Journ. Phys. Soc. Jap.*, **13**, 129 (1958); I. KUMABE: *Journ. Phys. Soc. Jap.*, **13**, 325 (1958).

Siano emesse in un processo evaporativo, e non per azione diretta, come sembra oggi più verosimile per la porzione ad energia elevata dello spettro delle reazioni (n, p) .

Qui vogliamo comunicare su alcuni risultati preliminari ottenuti sulla reazione (n, α) nell'alluminio bombardato con neutroni di 15.2 MeV.

2. — Procedimento sperimentale.

I neutroni venivano prodotti per urto di un fascio di deutoni contro una targhetta di tritio assorbito in zirconio. La differenza di potenziale acceleratrice era fornita da una macchina di Cockcroft e Walton ed era regolata a 370 kV; la corrente ionica del fascio era di circa 100 μA . Il flusso di neutroni in tutto l'angolo solido risultò dell'ordine di 10^9 n/s, in base a misure di attività indotta; durante l'irraggiamento della targhetta di alluminio il flusso dei neutroni era controllato da uno scintillatore plastico. L'energia massima dei neutroni era calcolata ⁽²⁾ dal Q della reazione, in corrispondenza alla direzione di emissione e alla energia dei deutoni incidenti.

Per poter avere una definizione abbastanza buona dell'angolo di emissione delle particelle α dalla targhetta di alluminio rispetto alla direzione di incidenza dei neutroni, venne costruita una camera di reazione, nell'interno della quale, su una circonferenza del diametro di 40 cm, trovava posto la targhetta di alluminio, la sorgente di neutroni e la porzione mediana di 8 lastre Ilford C-2 di 100 μm di spessore, scalate angolarmente di 10° , come è indicato in Fig. 1. In tale disposizione tutte le particelle α provenienti da una striscia limitata della targhetta di alluminio e cadenti in una regione media abbastanza ristretta delle emulsioni formano con la direzione di incidenza dei neutroni lo stesso angolo.

Venne usata come targhetta una foglia di alluminio, spessa 2.7 mg/cm², disposta secondo una porzione di superficie cilindrica alta 10 cm e avente lunghezza di 22 cm. La porzione utile della foglia fu però limitata, nel conteggio delle particelle α , a una striscia mediana alta 4 cm e lunga 18 cm. Naturalmente, non potendo limitare le osservazioni ad una striscia infinitamente stretta della targhetta ed a una regione molto limitata delle emulsioni, ed essendo la sorgente dei neutroni alquanto estesa, nasce una indefinizione angolare nelle tracce osservate in ogni emulsione, che per altro risulta abbastanza limitata, anche estendendo l'osservazione a quasi tutta la distesa utile di ogni emulsione — 18 mm \times 30 mm —. Essa è dell'ordine di $\pm 5^\circ$, ad eccezione della emulsione posta a 85° , per la quale l'indefinizione angolare risulta di

⁽²⁾ A. O. HANSON, R. F. TASCHEK e J. H. WILLIAMS: *Rev. Mod. Phys.*, **21**, 635 (1949).

$\pm 10^\circ$. Con una camera di reazione di dimensioni maggiori tali errori verrebbero notevolmente ridotti.

Durante l'irraggiamento del campione di alluminio con i neutroni nella camera di reazione era mantenuta una pressione di $3 \cdot 10^{-2}$ tor.

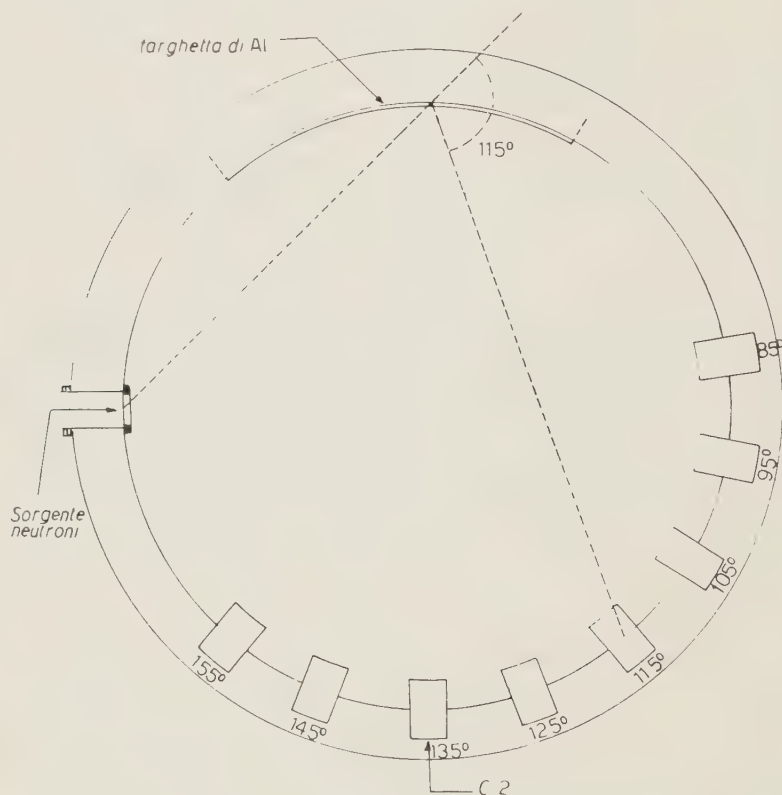


Fig. 1.

Le emulsioni furono trattate col metodo della doppia temperatura, usando sviluppo all'amidolo. Si regolò per tentativi la temperatura e il tempo di permanenza delle emulsioni nello stadio caldo, in modo da avere una buona discriminazione tra protoni e particelle α . Come criterio di discriminazione si prese il numero di grani di argento contenuti in una certa lunghezza R della traccia, a partire dalla fine di questa. Nella Fig. 2 sono riportati alcuni istogrammi che mostrano la frequenza del numero totale dei grani per vari percorsi residui. Tale frequenza è indicata con dischetti neri e con dischetti bianchi, i primi riferentisi a tracce sicuramente dovute a particelle α e i secondi a tracce prodotte da protoni. A partire da un certo valore di R (60 divisioni = $27 \mu\text{m}$) le tracce vengono a distribuirsi in due gruppi distinti di particelle α e di particelle con carica e massa inferiore.

Le curve di Fig. 3 sono state costruite dopo aver riportato nel grafico il numero dei grani in una traccia in funzione della lunghezza della traccia stessa;

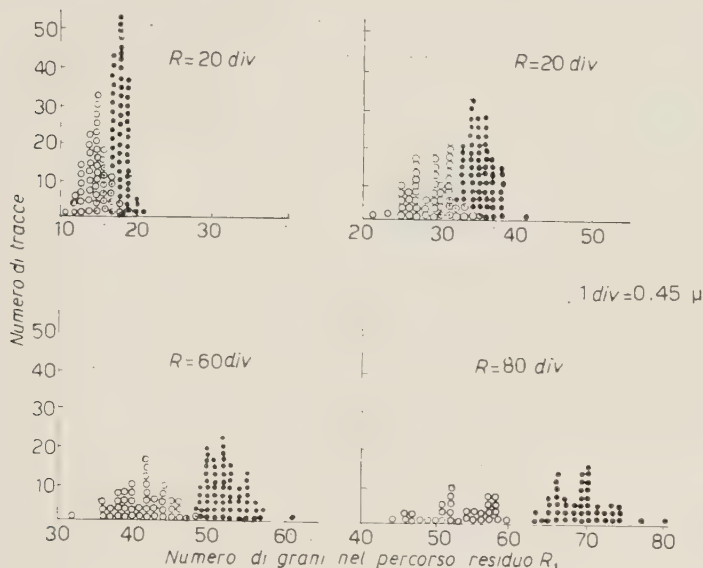


Fig. 2.

esse rappresentano le linee di separazione tra tracce sicuramente dovute a particelle α e tracce dovute a protoni. La regione compresa tra le due curve per percorsi inferiori a $27 \mu\text{m}$ corrisponde ai dischi bianchi centrati di Fig. 2. Pertanto, con i procedimenti di sviluppo delle emulsioni da noi adottati, non è stato possibile distinguere tra le tracce più corte di $27 \mu\text{m}$ e non è stato quindi possibile catalogare particelle α di energie inferiori a 6 MeV.

Più recentemente, venuti in possesso di alcune emulsioni Ilford K-0, siamo riusciti ad avere una discriminazione fino a una energia

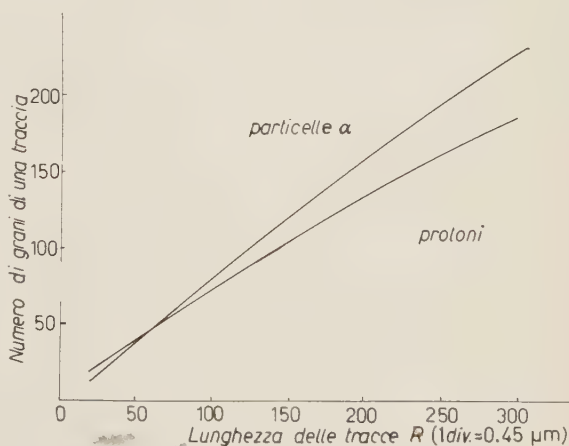


Fig. 3.

delle particelle α di 2 MeV, ed i risultati di un conteggio fatto su una tale emulsione, posta nella camera di reazione in guisa da raccogliere particelle

emesse dall'alluminio sotto un angolo di 85° coi neutroni, sono stati presi in considerazione nella discussione seguente.

Le emulsioni furono osservate da due persone e furono prese come buone le tracce comuni, giudicate dai due osservatori come particelle α in base ai criteri anzidetti. Nei calcoli si tenne conto solo — per quanto riguarda le particelle α elencate nelle C-2 — di quelle ad energia superiore a 7 MeV. Furono poi considerate come tracce corrispondenti a particelle provenienti dalla striscia prescelta della targhetta di alluminio quelle inizianti alla superficie delle emulsioni, aventi inclinazione e direzione di provenienza comprese entro limiti opportuni, variabili a seconda della posizione dell'emulsione.

Per la riduzione della lunghezza delle tracce in energia, si presero in considerazione le tabelle riportate da C. M. G. LATTES, P. H. FOWLER e P. CUER⁽³⁾, sia per le C-2 che per le K-0. Il fattore di contrazione fu determinato da misure meccaniche, fatte su un certo numero di lastre non sviluppate, e da misure fatte con il microscopio sulle lastre sviluppate: il valore medio ottenuto fu

di 2.66. Per le K-0 non si hanno dati sulla relazione percorso-energia; si ritenne perciò, dato che la loro composizione, secondo la Ditta produttrice, non si diversifica molto da quella delle C-2, di poter adottare la stessa relazione valida per quest'ultime.

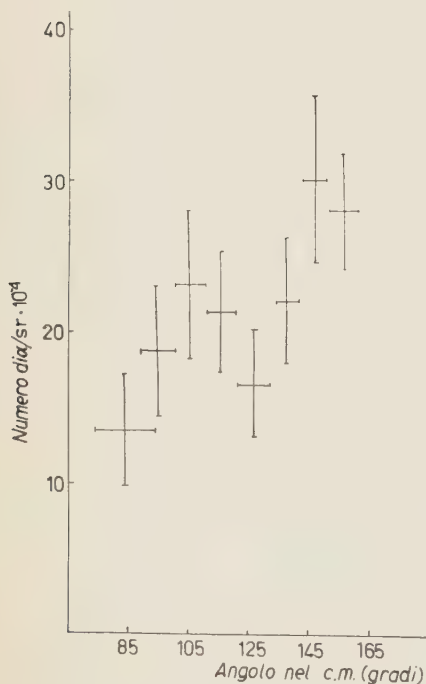


Fig. 4.

3. - Discussione dei risultati.

La distribuzione angolare delle particelle α provenienti dall'alluminio, per tutta la regione energetica ammessa — da 7 a 14 MeV — nel sistema del centro di massa è riportata in Fig. 4. L'errore sul numero delle tracce è l'errore statistico, mentre l'errore sugli angoli risulta dalla somma degli errori determinati dalla estensione della emulsione osservata, dalla estensione della sorgente dei neutroni e dall'altezza della porzione della targhetta di alluminio dalla quale provenivano le tracce.

Dato l'intervallo angolare da noi esplorato, non è possibile rivelare una eventuale asimmetria nella distribuzione delle particelle tra 0° e 180° . Ab-

(³) C. M. G. LATTES, P. H. FOWLER e P. CUER: *Proc. Phys. Soc.*, **59**, 883 (1947).

biamo in corso un esperimento per decidere su tale questione. È evidente invece una notevole anisotropia nella distribuzione, con un massimo secondario attorno a 105° . Tale massimo appare anche nella distribuzione angolare data da KUMABE per l'alluminio.

Nell'ipotesi del nucleo composto la distribuzione angolare delle particelle emesse deve risultare simmetrica e, secondo il linguaggio corrente, isotropa. L. WOLFENSTEIN ⁽⁴⁾ assume come misura del grado di anisotropia il rapporto $\sigma(0^\circ)/\sigma_m$ tra la sezione d'urto a 0° e una sezione d'urto media σ_m , rapporto che con i nostri dati non possiamo valutare. Comunque, nell'ambito del nucleo composto, WOLFENSTEIN, discutendo i vari casi che possono presentarsi per quanto riguarda la densità degli stati del nucleo residuo e i valori del momento angolare massimo, prevede o isotropia o debole anisotropia — al più uguale a 1.3 —. Anche secondo la derivazione di T. ERICSON e V. STRUTINSKI ⁽⁵⁾

l'anisotropia che si può calcolare in base ai nostri risultati è molto inferiore a quella sperimentale. Qui si potrebbe prendere come grado di anisotropia il rapporto tra il numero di particelle emesse attorno a 145° e il numero di particelle emesse attorno a 90° : esso risulta allora di 1.8.

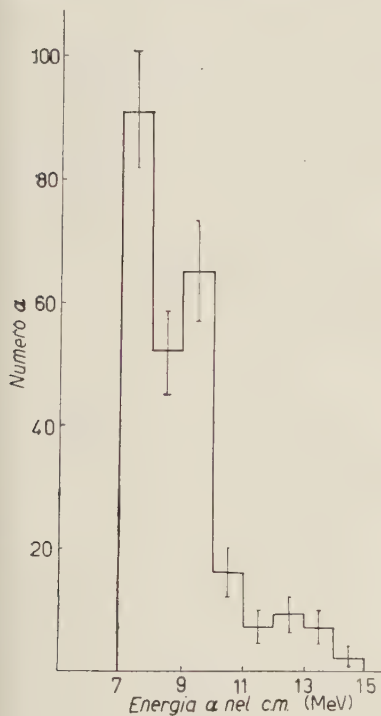


Fig. 5.

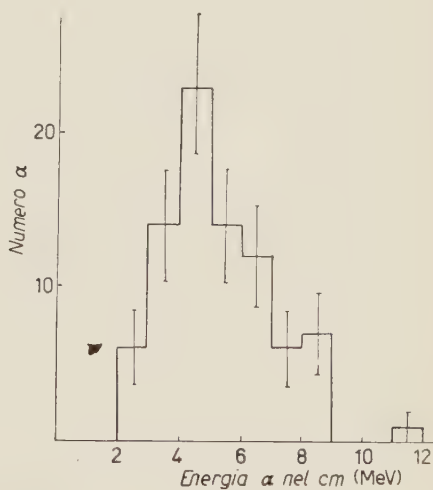


Fig. 6.

La distribuzione energetica delle particelle α nel centro di massa, ottenuta dal conteggio effettuato sulle 8 emulsioni C-2, è mostrata in Fig. 5, mentre nella Fig. 6 c'è l'istogramma relativo alla emulsione K-0, disposta in modo

(4) L. WOLFENSTEIN: *Phys. Rev.*, **82**, 690 (1951).

(5) T. ERICSON e V. STRUTINSKI: *Nucl. Phys.*, **8**, 284 (1958).

da raccogliere le particelle α emesse a 85° con la direzione dei neutroni. In quest'ultima distribuzione, che si estende da 2 MeV a 12 MeV si ha uno spiccato massimo di particelle di energia tra 4 e 5 MeV, che è al disotto della barriera coulombiana. Nella regione di bassa energia il valore di questa è meno definito, date le maggiori perdite subite dalle particelle α nella targhetta di alluminio: in metà spessore le perdite di energia sono di 1.30 MeV per particelle α di 3 MeV e di 0.78 MeV per particelle α di 6 MeV.

Come è noto, lo spettro energetico delle particelle emesse per evaporazione dal nucleo composto è rappresentato dalla equazione ⁽⁶⁾

$$I(E_\alpha) dE_\alpha = \text{cost.}$$

$$\cdot E_\alpha \sigma_c(E_\alpha) W(E_{\alpha m} - E_\alpha) dE_\alpha,$$

E_α essendo l'energia di una particella α , $\sigma_c(E_\alpha)$ la sezione d'urto per la formazione del nucleo composto col processo inverso e $W(E_{\alpha m} - E_\alpha)$ la densità dei livelli del nucleo residuo. Quest'ultima si può esprimere mediante una temperatura nucleare T data da

$$W(E_{\alpha m} - E_\alpha) = \\ = C \exp [-E_\alpha / T(E_{\alpha m})]$$

e quindi

$$\log I/E_\alpha \cdot \sigma_c(E_\alpha) = \mu = \\ = \text{cost} - E_\alpha / T(E_{\alpha m}) .$$



Fig. 7.

I valori di μ , calcolati in base ai risultati ottenuti con la K-0, sono riportati, a meno di un termine additivo, in funzione di E_α in Fig. 7. La curva risultante è composta di due tratti pressochè rettilinei, dalle cui pendenze si ricavano le due temperature di 0.59 MeV e di 1.47 MeV per il nucleo residuo. Probabilmente sulla prima temperatura, corrispondente a particelle α di bassa energia, influisce l'emissione da parte del nucleo composto di coppie di par-

⁽⁶⁾ J. M. BLATT e V. F. WEISSKOPF: *Theoretical Nuclear Physics* (New York, 1952), p. 352.

ticelle — ad esempio, reazioni $(\text{n}, \text{n}\alpha)$ —. L. COLLI e coll. ⁽⁷⁾ ritengono che parte della energia di eccitazione del nucleo si impegni in un processo di eccitazione diverso da quello che determina la evaporazione delle particelle, per cui questa avviene ad una temperatura inferiore.

D'altra parte l'emissione di particelle α di bassa energia potrebbe venire giustificata, secondo K. KIKUCHI ⁽⁸⁾, assumendo un potenziale nucleare diffuso, di tipo esponenziale. Tale potenziale determina un coefficiente di trasmissione superiore a quello calcolabile nel caso di una buca rettangolare, e il rapporto dei due coefficienti, per particelle α di bassa energia nel caso del sodio, può essere superiore a 10.

Nella Fig. 7 sono riportati pure, su scala diversa, i valori di μ calcolati in base ai dati delle emulsioni C-2. La temperatura del nucleo residuo risulta di 1.41 MeV.

KUMABE ottiene un'unica distribuzione maxwelliana considerando le particelle α con energia $E_\alpha \geq 4$ MeV; la temperatura del ^{24}Na è di circa 1.45 MeV.

Concludendo, si è calcolata la temperatura del nucleo residuo ^{24}Na , supponendo che i risultati ottenuti da noi si possano inquadrare nella teoria statistica del nucleo. Non si vede però come in tale teoria possa interpretarsi la notevole anisotropia angolare constatata.

* * *

Gli autori ringraziano il prof. G. PUPPI per l'interesse costante con cui ha seguito questa ricerca e per le numerose discussioni con lui avute.

⁽⁷⁾ L. COLLI, U. FACCHINI, I. IORI, G. MARCAZZAN e A. SONA: *Peaceful Uses of Atomic Energy*, **14**, 147 (Geneva, 1958).

⁽⁸⁾ K. KIKUCHI: *Progr. Theor. Phys.*, **7**, 643 (1957).

SUMMARY (*)

The angular and energetic distribution of α -particles resulting from the $^{27}\text{Al}(\text{n}, \alpha)^{24}\text{Na}$ reaction produced by 15.2 MeV neutrons is determined. The particles are detected with Ilford C-2 and K-0 nuclear emulsions. The reaction chamber was designed so as to obtain a good angular definition, between 80° and 160° . The angular distribution results remarkably anisotropic; the energetic distribution shows a great number of low energy particles. The temperature of the residual nucleus is calculated and the results obtained are discussed.

(*) Editor's Translation.

LETTERE ALLA REDAZIONE

(La responsabilità scientifica degli scritti inseriti in questa rubrica è completamente lasciata dalla Direzione del periodico ai singoli autori).

The Dirac Monopole as a Constituent of Primary Cosmic Radiation.

N. A. PORTER

University College - Dublin

(ricevuto l'8 Febbraio 1960)

In recent years a number of effects have been observed in large extensive air showers which, although well established experimentally, have not been satisfactorily explained. The purpose of this note is to suggest that most of these effects can be understood if it is assumed that a very small fraction, about 10^{-14} , of all primary cosmic ray particles are Dirac monopoles.

a) *Solar time variations.* - Significant variations in solar time have been observed by McCUSKER *et al.* ⁽¹⁻³⁾ in local penetrating showers and dense extensive showers, and by CRANSHAW and GALBRAITH ⁽⁴⁾ in showers containing more than $3 \cdot 10^7$ particles at sea level. The primary energies to which these events correspond are difficult to estimate, but in the latter case are probably of the order 10^{17} eV, with a primary flux of the order $10^{-14}/\text{cm}^2 \text{ s sr}$. The time variations are irregular in character and resemble the small diurnal and semi-

diurnal variations in atmospheric pressure. If the two variations are causally related it would appear necessary to assume that the air shower primaries have very short interaction mean free paths, since the atmospheric variation is negligibly small except at very great altitudes.

b) *Primary spectrum.* - CRANSHAW *et al.* ⁽⁵⁾ and CLARK *et al.* ⁽⁶⁾ have established the number spectrum of extensive air showers at sea level up to shower sizes of about $5 \cdot 10^8$ particles. The energy to which this corresponds is difficult to estimate because of fluctuations in shower development, but is conventionally assumed to be of the order $5 \cdot 10^{18}$ eV. Although the spectrum is becoming steeper there appears to be no cut-off and there are serious difficulties in explaining the acceleration of protons or nuclei in the galaxy to these energies.

c) *Sidereal variations.* - Observations on the largest extensive air showers ^(4,6)

⁽¹⁾ C. B. A. McCUSKER, J. DARDIS and B. G. WILSON: *Proc. Phys. Soc.*, A **68**, 585 (1955).

⁽²⁾ C. B. A. McCUSKER: *Nuovo Cimento*, **11**, 1310 (1955).

⁽³⁾ C. B. A. McCUSKER and B. G. WILSON: *Nuovo Cimento*, **3**, 188 (1956).

⁽⁴⁾ T. E. CRANSHAW and W. GALBRAITH: *Phil. Mag.*, **2**, 804 (1957).

⁽⁵⁾ T. E. CRANSHAW, J. DE BEER, W. GALBRAITH and N. A. PORTER: *Phil. Mag.*, **3**, 377 (1958).

⁽⁶⁾ G. CLARK, J. EARL, W. KRAUSHAAR, J. LINSLEY, B. ROSSI and F. SCHERB: *Nature*, **180**, 353, 406 (1957).

do not show significant sidereal variations, though these would be expected at energies of $\sim 10^{17}$ eV. There is, however, some evidence that showers selected on the basis of special properties, a high local density or the presence of high energy nucleons, do show such variations (¹⁻³).

d) Shower structure. - At all apparent primary energies between 10^{15} and 10^{13} eV showers at sea level have essentially the same structure, contrary to the predictions of cascade theory. There is also some evidence (⁷) that the nucleon component of showers shows a discontinuous change at about 10^{15} eV.

Some of these effects can be explained if it is assumed that the high energy radiation consists of a mixture of electrically charged particles and Dirac monopoles, the protons and light nuclei disappearing at about 10^{16} eV. The magnetic monopole (\cdot) has a pole strength $3.3 \cdot 10^{-9}$ cgsu and will be accelerated linearly in a magnetic field. With an interstellar field of 10^{-6} G it will acquire an energy of 10^{19} eV in a distance of 1 parsec, with ionisation losses (²) in this distance of only $3 \cdot 10^4$ eV. It would be expected, therefore, that if monopoles occur in the primary cosmic radiation they would form the high energy tail of the spectrum. Since they are strongly coupled with magnetic fields, random fields in the galaxy would render them

isotropic and prevent their escape with far greater efficiency than that for electrically charged particles.

Since the monopole fine structure constant, $m^2/\hbar c = 34.2$, compared with 1/137 for electrons, the bremsstrahlung mean free path in air should be of the order 0.01 g/cm² (assuming a mass of the order of the proton) and strongly multiple production of quanta would be expected. Primary monopoles should therefore interact high in the atmosphere, producing showers of energy degraded particles, so that the structure of showers at sea level would not vary strongly with energy.

An upper limit of 10^{-10} monopoles/cm² s at sea level has been set experimentally by MALKUS (¹⁰). This presumably corresponds to a similar flux on the upper atmosphere, since the particles are indestructible except by annihilation. A similar upper limit is set by the strength and constancy of the earth's magnetic field. A flux of 10^{-14} particles/cm² s would, however, be adequate to produce the effects observed in extensive air showers.

The direct detection of monopoles at this intensity presents technical difficulties. An extension of Malkus' experiment with a larger solenoid and longer observation time, could approach this limit.

Indirectly, a measurement of the interaction mean free path of the primaries of the largest extensive air showers, by studying the fluctuations in shower development, seems promising (¹¹).

(⁷) Y. N. VAVILOV, S. I. NIKOLSKII and V. P. SARANTSEV: *Žurn. Ėksp. Teor. Fiz.*, **28**, 505 (1955).

(⁸) P. A. M. DIRAC: *Phys. Rev.*, **74**, 817 (1948).

(⁹) H. J. D. COLE: *Proc. Camb. Phil. Soc.*, **196**, 47 (1951).

(¹⁰) W. V. R. MALKUS: *Phys. Rev.*, **83**, 899 (1951).

(¹¹) A. E. ČUDAKOV and N. M. NESTEROVA: *Suppl. Nuovo Cimento*, **8**, 606 (1958).

Possible Interpretation of an Unusual Hyperon Decay.

C. M. GARELLI, B. QUASSIATI and M. VIGONE

Istituto di Fisica dell'Università - Torino
Istituto Nazionale di Fisica Nucleare - Sezione di Torino

(ricevuto il 1° Aprile 1960)

Studying the interactions of 1.15 BeV/c K^- -mesons in an emulsions stack exposed to the Berkeley Bevatron, an unusual hyperon decay has been observed. The event is reproduced in Fig. 1. A K^- -meson interacts with an emulsion nucleus giving rise to a star with four evaporation tracks, a π^- of 21 MeV kinetic energy that comes to rest in the emulsions producing a σ -star, and a hyperon decaying in flight. The charged decay product is a π^+ of 47 MeV kinetic energy that comes to rest giving a $\pi^+ \rightarrow \mu^+ \rightarrow e^+$ decay.

The kinematics of the decay is in strong disagreement with the normal $\Sigma^+ \rightarrow \pi^+ + n$ decay, because a π^+ of about 120 MeV kinetic energy would be requested.

The event has been experimentally studied in the following way:

A) ionization measurements have been performed in various points of the track, and they are always consistent with the measured range, excluding that the π -meson loosed energy by inelastic scattering;

B) the range of the μ -meson has been measured and it is found to be $600 \pm 10 \mu\text{m}$; this fact rules out the possibility of a decay in flight of a π^- -meson;

C) both ionization-range and ionization-scattering measurements have been performed on the primary track, and the results are consistent with a hyperon mass

The results of all these measurements are collected in Table I and II. We point out that the point of the assumed

TABLE I. - *Primary track.*

$\beta_{\text{emls.}}$	β_{decay}	ΔR	$p\beta$	mass from ionization and scattering measurements
0.33 ± 0.01	0.28 ± 0.01	7.8 mm	$(100 \pm 15) \text{ MeV/c}$	$(1060 \pm 210) \text{ MeV}$



Fig. 1.



TABLE II. - *Secondary track.*

identity	range	kinetic energy	angle with the primary direction
π^+	35 mm	47 MeV	$49^\circ 30' \pm 30'$

decay, carefully observed under high magnification, appears very clean, and that the event is in very lucky geometrical conditions (the dip angle of the hyperon track is $\sim 4^\circ$). Moreover, the ionization is very sensitive to the variation of the β value in the involved velocity region, so that the determination of the β of the hyperon from ionization measurements is very reliable.

We discuss the following interpretations of the event:

1) two body decay of a particle of hyperonic mass.

This particle cannot be a Σ^+ because the $\Sigma^+ \rightarrow \pi^+ + n$ decay, as we already said, is in disagreement with the measured angle of decay and energy of the π^+ -meson. Assuming that we are concerned with an unknown particle whose

strangeness +1 and hypercharge +2. If this is the particle that we observed, a process of production that conserves strangeness, charge and baryonic number is the following:

$$K^- + n + p \rightarrow \pi^- + \Xi^0 + Y^+.$$

This production process is energetically compatible, as one can see from the data of Table III, concerning the parent star.

One serious objection against this interpretation is that, if a hyperon of strangeness +1 and mass of the order of the Λ -mass really exists, there is no reason why this particle should never have been observed in the normal processes of associated production. It would be necessary to assume the existence of some unknown selection rule.

TABLE III. - *Parent star.*

visible prongs	projected angle with the primary direction	dip angle	kinetic energy
Y^+	$+55^\circ$	-4°	65 MeV
π^-	$+11^\circ$	$+45^\circ$	21 MeV
4 evaporation tracks	—	—	120 MeV

decay products are a neutron and a π^+ , we find that the Q value is (36.6 ± 0.5) MeV. This Q value is not in disagreement with the measured mass (1060 ± 210) MeV and is surprisingly equal to that of the Λ^0 hyperon. We suppose that this is a causal fact, because it seems well established that the Λ^0 hyperon does not have a charged counterpart.

In the Gell-Mann scheme place is left for a positively charged hyperon of

2) Interaction of a Σ^\pm -hyperon.

The assumption of the interaction $\Sigma^+ + n \rightarrow \pi^+ + \Lambda^0 + n$ is ruled out by energy conservation, since, within experimental errors, the Σ^+ energy is scarcely sufficient to produce the π^+ and the Λ masses. To explain the production of a π^+ -meson with the observed energy, it would be necessary to assume that both the π^+ -meson and the Λ hyperon

produced do not escape from the nucleus, the meson being absorbed and the Λ hyperon being trapped; that the trapped Λ hyperon decays in the nucleus in $\pi + \pi^0$; that the decay π^0 is also absorbed and that the result of these processes is a π^+ of 47 MeV kinetic energy coming out from the nucleus without any other visible prongs.

The occurrence of a chain of reactions of the type described has to be considered very improbable.

The assumption of an interaction

$$\Sigma^- + p \rightarrow \Lambda^0 + n,$$

followed by a non mesonic decay of the trapped Λ^0 , with emission of a π^+ :

$$\Lambda^0 + p \rightarrow n + n + \pi^+,$$

seems to us very improbable, also owing to the high energy of the π^+ -meson.

3) Radiative decay of a Σ^+ :

$$\Sigma^+ \rightarrow \pi^+ + n + \gamma.$$

In the system where the decaying particle is at rest, for energy and momentum balance, the energy of the γ -ray must range between 65 MeV and 78 MeV, depending from the angle of emission.

This high value of the γ -ray energy excludes a bremsstrahlung process of the π emitted in the decay of the hyperon.

The event can be explained as a direct interaction of the decaying particle with the electromagnetic field.

This type of interaction is analogous to the one that explains the already observed decays: $\Sigma^+ \rightarrow p + \gamma$ ⁽¹⁾, whose occurrence is of about 1%. The event observed by us would be the first example of a decay mode: $\Sigma^+ \rightarrow \pi^+ + n + \gamma$. Of course, further statistics are necessary to give a conclusive interpretation of the event observed. Anyhow we think that the assumption of the radiative decay does not meet with any serious objection.

* * *

Our thanks are due to Prof. FERRETTI, Prof. FRANZINETTI, Prof. FUBINI, Prof. GATTO, Prof. VITALE and Prof. WATAGHIN for very useful discussions.

We are grateful to Prof. LOFGREEN, Prof. SEGRÈ and Prof. GOLDBABER for their help during the exposure.

⁽¹⁾ G. QUARENI, A. QUARENI-VIGNUDELLI, G. D'ASCOLA and S. MORA: *Nuovo Cimento*, **14** 1179 (1959).

Some Aspects of Particle Mixture of Strange Particles (*).

S. OKUBO

*Istituto di Fisica Teorica dell'Università - Napoli**Scuola di Perfezionamento in Fisica Teorica e Nucleare dell'Università - Napoli*

(ricevuto il 5 Aprile 1960)

Purpose of this note is to point out that a certain type of contact interactions (e.g. $\bar{\Lambda}$ -n) can be transformed into new ones corresponding to the direct decay of the particle involved (e.g. $\Lambda \rightarrow p + \pi$) by a simple transformation. Our treatment is essentially the same as had been given by CABIBBO and GATTO and by FEINBERG *et al.* ⁽¹⁾, for the μ -e case.

First consider the Λ -n case. Due to both weak and strong interactions, the virtual transition $\Lambda \leftrightarrow n$ is permissible ⁽²⁾ and as the result, we may have the following effective interaction similar to that of the $\mu \leftrightarrow e$ case ⁽¹⁾.

$$(1) \quad H_1 = f\bar{\Lambda}(a + b\gamma_5)n + f'\bar{\Lambda}(c + d\gamma_5)\gamma \frac{\partial}{\partial x} n + \text{c.c.},$$

where f and f' are of the first order in the weak interaction coupling constant G and, a , b , c , and d are numerical constants. By diagonalizing $H_0 + H_1$, (H_0 being the free Hamiltonian for Λ and n), we have new field operators Λ' and n' ⁽¹⁾:

$$(2) \quad n' = [1 + \alpha\gamma_5]n + [\beta + \delta\gamma_5]\Lambda, \quad \Lambda' = [1 + \alpha'\gamma_5]\Lambda + [\beta' + \delta'\gamma_5]n,$$

where all α , β , δ , α' , β' and δ' are quantities of the order G and the non-diagonal term eq. (1) disappears in terms of new variables. Up to this point, our treatment is not different from that of the μ -e case ⁽¹⁾, and so we don't give the details. However, a new aspect emerges in the present case due to the existence of the strong pion-nucleon (more generally meson-baryons) interaction

$$(3) \quad H_\pi = ig\{\sqrt{2}(\bar{p}\gamma_5 n\pi^+ + \bar{n}\gamma_5 p\pi^-) + (\bar{p}\gamma_5 p - \bar{n}\gamma_5 n)\pi^0\}.$$

(*) The research reported in this document has been sponsored in part by the office Chief of Research and Development, U. S. Department of Army, through its European office under contract no. DA-91-591-EUC-1096.

⁽¹⁾ N. CABIBBO and R. GATTO: *Phys. Rev.*, **116**, 1334 (1959); G. FEINBERG, P. KABIR and S. WEINBERG: *Phys. Rev. Lett.*, **3**, 527 (1959).

⁽²⁾ See e.g. S. OKUBO, R. E. MARSHAK and E. C. G. SUDARSHAN: *Phys. Rev.*, **113**, 944 (1959).

Notice that

$$n \simeq [1 - \alpha\gamma_5]n' - [\beta + \delta\gamma_5]A' + O(G^2).$$

Substitution of this into the right hand side of eq. (3), gives a new additional interaction:

$$(4) \quad H'_\pi = -ig\alpha\{\sqrt{2}(\bar{p}\cdot n')\pi^+ - (\bar{n}'\cdot n')\pi_0\} - \\ -ig\{\sqrt{2}\bar{p}(\delta + \beta\gamma_5)A'\pi^+ - \bar{n}'(\delta + \beta\gamma_5)A'\pi_0\} + \text{c.c.}.$$

Thus, the interaction eq. (1) has been effectively transformed into the new one eq. (4), the second term of which gives rise to the direct decay for $\Lambda \rightarrow p + \pi^-$ and $\Lambda \rightarrow n + \pi^0$. It is interesting to note that it satisfies the $\Delta I = \frac{1}{2}$ rule. Effective interaction eq. (1) has been suggested by some authors⁽³⁾ to be a likely mechanism for Λ -decay in view of this property.

Rigorously speaking, our procedure is not completely self-consistent, since the interaction eq. (4) will give the transition $\Lambda' \leftrightarrow n'$ again. However, this is of higher order in the meson-nucleon coupling constant g . Taking advantage of this fact, we can re-define Λ'' and n'' in terms of Λ' and n' in a similar fashion as before, and so on, successively into the higher order with respect to the coupling constant g . It should be emphasized that the subtraction of the effective interactions like eq. (1) from the given Feynman diagrams is almost analogous to those of self-energy and charge-renormalization terms but the procedure for the former is unfortunately not unambiguous⁽⁴⁾, thus leaving some arbitrariness in the theory⁽⁵⁾.

For the transitions $\Sigma^+ \leftrightarrow p$ and $\Sigma^0 \leftrightarrow n$, we can perform exactly the same procedures as in the $\Lambda \leftrightarrow n$ case, but the corresponding interaction of the type eq. (4) would not in general satisfy the $\Delta I = \frac{1}{2}$ rule. If we neglect the pion interaction but include the electro-magnetic one, then the situation is almost the same as in the μ -e case, and similar to that of the $\mu \rightarrow e + \gamma$ decay⁽¹⁾, as the result $\Sigma^+ \rightarrow p + \gamma$ is forbidden in our approximation, thus explaining the small calculated transition rate⁽⁶⁾ for the process.

Another interesting case is that of the transition $K_2^0 \leftrightarrow \pi_0$ or $K_+ \leftrightarrow \pi_+$. Note that $K_1^0 \leftrightarrow \pi_0$ would be forbidden by the CP-invariance of the theory. Now, we will have an interaction corresponding to eq. (1):

$$(5) \quad H_1 = f(K_2^0 \cdot \pi_0) + f'(\partial_\mu K_2^0 \cdot \partial_\mu \pi_0).$$

Again, by diagonalizing $H_0 + H_1$, we have a new set of field operators:

$$(6) \quad \begin{cases} K_2^{0'} = [1 + \alpha]K_2^0 + \beta\pi_0, \\ \pi_1' = [1 + \alpha']\pi_0 + \beta'K_2^0, \end{cases} \quad \alpha, \beta, \alpha', \beta' \simeq O(G):$$

⁽³⁾ R. F. SAWYER: *Phys. Rev.*, **112**, 2135 (1958); H. OBAYASHI: *Progr. Theor. Phys. Jap.*, **22**, 835 (1959); S. ONEDA, J. C. PATI and B. SAKITA: preprint.

⁽⁴⁾ S. KAMEFUCHI and H. UMEZAWA: *Progr. Theor. Phys. Jap.*, **8**, 579 (1952).

⁽⁵⁾ This is one of the reasons why we discarded the contribution from this type of interaction in our previous work [see ref. (2)].

⁽⁶⁾ R. E. BEHREND: *Phys. Rev.*, **111**, 1691 (1958); P. PRAKASH and A. H. ZIMMERMANN: *Nuovo Cimento*, **11**, 869 (1959).

It is of interest to note that this gives rise to a mass difference between K_1^0 and K_2^0 . If we assume the usual universal Fermi-interaction between $(\Lambda\text{-}p)$ and $(p\text{-}n)$ pairs, then we can estimate the contribution from this specific process mentioned in the above, for the mass-difference. It gives $\Delta m \simeq 10^{-5}$ eV and the resulting characteristic time of order of 10^{-9} s, which is close to that given by OKUN and PONTECORVO ⁽⁷⁾, and not in disagreement with the experimental fact ⁽⁸⁾.

Furthermore, the substitution of eq. (6), into the strong interaction Hamiltonian gives new interactions like $\bar{p}(a+b\gamma_5)pK_2^{0'}$ or $(\bar{p}(a+b\gamma_5)n)K_+$ which is analogous to eq. (4), and might be partly responsible of the $K \rightarrow 3\pi$ decay ⁽⁹⁾ (but not of $K \rightarrow 2\pi$).

Finally, we remark that a similar situation exists even in the region of non-weak interaction. It is the case of the $\Sigma_0 \leftrightarrow \Lambda$ transition made possible by the electromagnetic and strong interactions. Thus it may be necessary to re-define Λ and Σ_0 by a certain linear combination again, though there is ambiguity in this procedure as has been remarked already.

⁽⁷⁾ L. B. OKUN and B. PONTECORVO: *Žurn. Éksp. Teor. Fiz.*, **32**, 1587 (1959).

⁽⁸⁾ E. BOLDT, D. CADMELL and Y. PAL: *Phys. Rev. Lett.*, **1**, 151 (1958).

⁽⁹⁾ If we take account of the pion-pion interaction $\lambda\phi^4$, then we will have a direct decay interaction like $K\cdot\phi^3$ in a similar way.

Poincaré's Epistemological Sum.

G. ROSEN (*)

Institute for Theoretical Physics - Stockholm

(ricevuto il 6 Aprile 1960)

With typical and incisive clarity, Poincaré analysed the epistemological unity of geometry and physics⁽¹⁾. This work preceded general relativity by several years and influenced Einstein's formulation⁽²⁾. Modern physics, hagridden with specialized mathematics, is a collection of beautiful-but-useless and ugly-but-practical theories. Yet the epistemological arguments of Poincaré still remain firm and throw some light on the present situation.

According to Poincaré, the space-time (**) geometry by itself predicates nothing about the behavior of real things. Rather, it is a *union* of the postulated geometry and the totality of non-geometrical laws which is subject to experimental observation. The geometry is defined with or without the help of physical measurements. Then the totality of non-geometrical laws is expressed within the framework of the prescribed geometry. Finally, the *union* of geometrical and non-geometrical postulates, which we shall call *Poincaré's epistemological sum*, is compared with experiment. Essentially a matter of taste, Poincaré asserts that there is no unique way to partition the epistemological sum into a geometrical and a non-geometrical part. A partition of the sum depends on the definition of geometrical and non-geometrical *observables* (modern terminology), and such definitions, in turn, depend on the practicability of experiments. Let us symbolize the epistemological sum by writing:

$$(I) \quad \left\{ \begin{array}{l} \text{a postulated} \\ \text{geometry for} \\ \text{space-time} \end{array} \right\} + \left\{ \begin{array}{l} \text{non-geometrical} \\ \text{laws expressed} \\ \text{within the geometry} \end{array} \right\} = \left\{ \begin{array}{l} \text{an observable} \\ \text{description of the} \\ \text{physical phenomenon} \end{array} \right\}.$$

Relativistic theories provide interesting examples of the epistemological sum. General relativity starts by *defining* the space-time geometry in terms of physical

(*) National Science Foundation Postdoctoral Fellow.

(1) H. POINCARÉ: *Dernières Pensées* (Paris, 1913), p. 35 ff.

(2) A. EINSTEIN: *Ideas and Opinions* (Crown, 1954), p. 232.

(**) POINCARÉ discusses only the geometry of space; the space-time generalization is self-evident, however.

measurements. First Einstein sets up a correspondence between observable events and mathematical points in the space-time continuum. Next, a relation between the practically rigid body and the space-time geometry is postulated: measuring rods and clocks are used to define geometrical intervals of space and time. The theory of general relativity, expressed by a purely geometrical Poincaré sum, stems from these definitions:

$$(2) \quad \left\{ \begin{array}{l} \text{a Ricci-flat} \\ \text{Riemannian geometry,} \\ \text{i.e., } R_{\mu\nu} = 0 \end{array} \right\} + \{0\} = \left\{ \begin{array}{l} \text{an observable} \\ \text{description of} \\ \text{classical gravitation} \end{array} \right\}.$$

Note that a change in the definition of observables would bring about a change in the left side of (2), if the altered theory is to explain the astronomical facts. On the level of macroscopic physics there is no motivation (empirical or aesthetic) for such a change. However, the situation is very different in the microscopic domain. An observable correspondence between physical events and mathematical points in space-time is not precise in the small, according to the quantum theory⁽³⁾. Moreover, measuring rods are operationally useless and small clocks obey quantum limitations. For these reasons the definitions which underlie general relativity are not particularly appropriate in the microscopic domain. It follows that general relativity may not be the most desirable epistemological sum for sub-atomic (classical) gravitation. An alternative description of gravitation, based on the definition of genuine microscopic observables, is awaited with great interest.

As an example of the flexibility of a Poincaré sum, we mention the laws which govern classical gravitation and electromagnetic radiation. The relativistic theory of gravitation and electromagnetic radiation, in the form originally proposed by Einstein, is represented by:

$$(3) \quad \left\{ \begin{array}{l} \text{a Riemannian geometry with} \\ R_{\mu\nu} = 2F_{\mu\sigma}F^{\nu\sigma} - \frac{1}{2}g_{\mu\nu}(F_{\rho\sigma}F^{\rho\sigma}) \end{array} \right\} + \left\{ \begin{array}{l} \text{a source-free electro-} \\ \text{magnetic field, i.e.,} \\ F_{\mu\nu;\sigma} + F_{\nu\sigma;\mu} + F_{\sigma\mu;\nu} = 0; \\ F^{\mu\nu}{}_{;\nu} = 0 \end{array} \right\} =$$

$$= \left\{ \begin{array}{l} \text{an observable} \\ \text{description of classical} \\ \text{gravitation and electro-} \\ \text{magnetic radiation} \end{array} \right\}.$$

Here the space-time geometry (to be measured with rods and clocks) and the electromagnetic field (to be measured with test charges) enter as fundamental observables.

RAINICH⁽⁴⁾ and more recently MISNER⁽⁵⁾ have repartitioned the Poincaré sum (3) in order to obtain a purely geometrical form of the theory. The result, so-called

⁽³⁾ E. P. WIGNER: *Rev. Mod. Phys.*, **29**, 255 (1957).

⁽⁴⁾ G. Y. RAINICH: *Trans. Am. Math. Soc.*, **27**, 106 (1925).

⁽⁵⁾ C. W. MISNER and J. A. WHEELER: *Ann. Phys.*, **2**, 525 (1957).

« Rainich geometry », is represented by:

$$(4) \quad \left\{ \begin{array}{l} \text{a Rainich Riemannian geometry,} \\ \text{i.e., } R = 0, R_{00} > 0, \\ R_{\mu\sigma} R_{\nu}{}^{\sigma} - \frac{1}{4} g_{\mu\nu} (R_{\rho\sigma} R^{\rho\sigma}) = 0, \\ \oint [\sqrt{-g} \varepsilon_{\mu\nu\rho\lambda} R^{\mu}{}_{\sigma} R^{\nu\sigma;\rho} dx^{\lambda} / (R_{\rho\sigma} R^{\rho\sigma})] = 0 \end{array} \right\} + \{0\} = \left\{ \begin{array}{l} \text{an observable description} \\ \text{of classical gravitation} \\ \text{and electromagnetic radiation} \end{array} \right\}.$$

Although the theories described by (3) and (4) are formally equivalent, an important change in the definition of observables accompanies the passage from (3) to (4). The space-time geometry and the electromagnetic field appear as fundamental observables in (3), whereas the electromagnetic field (to be computed from the metric) does not appear as a fundamental observable in (4). Again we see that a change in the definition of observables accompanies a change in the Poincaré sum.

Strikingly dissimilar Poincaré sums are associated with the more useful theories of modern physics. Before field quantization these theories take the form:

$$(5) \quad \left\{ \begin{array}{l} \text{a Minkowski-flat} \\ \text{Riemannian geometry,} \\ \text{i.e., } R_{\mu\nu\rho\sigma} = 0 \end{array} \right\} + \left\{ \begin{array}{l} \text{a linear or} \\ \text{quasi-linear} \\ \text{classical field} \\ \text{theory} \end{array} \right\} = \left\{ \begin{array}{l} \text{an observable} \\ \text{description of} \\ \text{the physical} \\ \text{phenomenon} \end{array} \right\}.$$

Maxwell's theory of electromagnetism, Dirac's theory of the electron, and Yukawa's theory of the meson all serve to exemplify (5). In theories of this type the geometry is supposed defined *à la Einstein*, a point-event correspondence with geometrical intervals of space and time measured with rods and clocks. However, we have already noted that Einstein's definitions are impracticable in the small. Hence, when theories like (5) apply to the microscopic domain, the geometry is really defined to be Minkowski-flat *without evoking experimental measurements*, and such a definition must stand or fall on its practical merits. Since quantum electrodynamics is a very successful theory, and since the customary Poincaré sum for quantum electrodynamics is of the type (5), virtually all theories for the microscopic domain have taken the Minkowski-flat definition as a starting point. Clearly this is not the only way to proceed, for with a new interpretation of observables it is possible to repartition Poincaré sums like (5).

We illustrate the last remark with a simple example. Choosing coordinates for the Minkowski-flat geometry such that the metric tensor is given by

$$(6) \quad \bar{g}_{\mu\nu} = \text{diag} \left[-1, 1, 1, 1 \right],$$

let us consider the Poincaré sum (5) for a scalar wave theory:

$$(7) \quad \left\{ \begin{array}{l} \text{a Minkowski-flat} \\ \text{Riemannian geometry} \\ \text{with } g_{\mu\nu} = \bar{g}_{\mu\nu} \end{array} \right\} + \left\{ \begin{array}{l} \text{the equation} \\ \bar{g}^{\mu\nu} \varphi_{,\mu\nu} = 0 \end{array} \right\} = \left\{ \begin{array}{l} \text{a scalar} \\ \text{wave theory} \end{array} \right\}.$$

Here the scalar function φ is an observable, measured experimentally and expressed in terms of the Minkowski-flat coordinates prescribed by (6). With an appropriate geometrical interpretation of the observable φ , it is possible to repartition the Poincaré sum (7) in order to obtain a purely geometrical form of the theory:

$$(8) \quad \left\{ \begin{array}{l} \text{a Riemannian geometry with} \\ R_{\mu\nu\rho\sigma} = \frac{1}{2}(g_{\mu\sigma}R_{\nu\rho} + g_{\nu\rho}R_{\mu\sigma} - g_{\mu\rho}R_{\nu\sigma} - g_{\nu\sigma}R_{\mu\rho}) \end{array} \right\} + \{0\} = \left\{ \begin{array}{l} \text{a scalar} \\ \text{wave theory} \end{array} \right\}.$$

To prove the formal equivalence of (7) and (8), let us consider the relation

$$(9) \quad R_{\mu\nu\rho\sigma} = \frac{1}{2}(g_{\mu\sigma}R_{\nu\rho} + g_{\nu\rho}R_{\mu\sigma} - g_{\mu\rho}R_{\nu\sigma} - g_{\nu\sigma}R_{\mu\rho}).$$

By contracting μ and σ in this expression, we find that

$$(10) \quad R = 0.$$

Hence (9) implies the weaker condition

$$(11) \quad R_{\mu\nu\rho\sigma} + \frac{1}{2}(g_{\mu\rho}R_{\nu\sigma} + g_{\nu\sigma}R_{\mu\rho} - g_{\mu\sigma}R_{\nu\rho} - g_{\nu\rho}R_{\mu\sigma}) + \frac{1}{6}(g_{\mu\sigma}g_{\nu\rho} - g_{\mu\rho}g_{\nu\sigma})R = 0,$$

an equation which merely states that the Riemannian geometry is *conformally flat* ⁽⁶⁾. Thus, the metric tensor of the geometry takes the form

$$(12) \quad g_{\mu\nu} = (\varphi - \varphi_0)^2 \bar{g}_{\mu\nu},$$

where $\bar{g}_{\mu\nu}$ is the metric tensor of a flat space, and where the scalar function φ (at this point an arbitrary function) is greater than φ_0 , a constant which remains at our disposal. Choosing coordinates such that

$$(13) \quad \bar{g}_{\mu\nu} = \text{diag} \left[-1, 1, 1, 1 \right],$$

it follows from (12) that

$$(14) \quad R = 6(\varphi - \varphi_0)^{-3} \bar{g}^{\mu\nu} \varphi_{,\mu\nu},$$

and in view of (10) we have

$$(15) \quad \bar{g}^{\mu\nu} \varphi_{,\mu\nu} = 0.$$

Therefore the relation (9) describes a conformally flat Riemannian geometry with

$$(16) \quad \varphi \equiv \varphi_0 + (-\det g_{\mu\nu})^{\frac{1}{4}},$$

satisfying the scalar wave eq. (15) if the coordinates are prescribed by (13).

(*) L. P. EISENHART: *Riemannian Geometry* (Princeton, 1949), p. 91.

Measured experimentally, the observable φ is obtained in terms of coordinates prescribed by (13). Thus, nothing prevents us from interpreting φ in accordance with eq. (16). That is, let us interpret $(\varphi - \varphi_0)^4$ as the four-volume density of a Riemannian geometry characterized by (9). In so doing, we relax the definitions for geometrical measurements proposed by Einstein, definitions which are impracticable in the microscopic domain. The purely geometrical Poincaré sum (8) is thereby established.

It may be possible to work out a similar repartition of the Poincaré sum for quantum electrodynamics. The motivation for this is not just aesthetic, because attempts to generalize the customary Poincaré sum have produced theories which are not as useful as quantum electrodynamics.

CP Invariance and Non-Linear Pion Interactions.

V. GUPTA and S. N. BISWAS

Tata Institute of Fundamental Research - Bombay

(ricevuto il 19 Aprile 1960)

FEINBERG ⁽¹⁾, SOLOVIEV ⁽²⁾ and GUPTA ⁽³⁾ have recently shown that the requirement of invariance under CP and charge symmetry results in a parity conserving pion-nucleon interaction, the neutral pion and charged pion interactions being treated separately. The above result is true for any fermion isotopic spin doublet; consequently for simplicity we will speak of the nucleon doublet only.

The above authors only considered interactions linear in the pion field. The aim of this note is to investigate whether non-linear (in the pion field) interactions also turn out to be parity conserving or not under the two above mentioned requirements.

We follow the notation of FEINBERG ⁽¹⁾. We treat the n-n, p-p and the n-p interactions separately. The general n-n and p-p parity violating the non-linear interaction Lagrangian (with scalar and pseudoscalar couplings only) is

$$(1) \quad L_0 = \sum_{r=0}^{\lambda} \{ \bar{\psi}_1 (g_r + i g'_r \gamma_5) \psi_1 + \bar{\psi}_2 (f_r + i f'_r \gamma_5) \psi_2 \} \varphi_0^{m-2r} (\varphi \varphi^*)^r.$$

L_0 involves the pion field « m » times, ψ_1 and ψ_2 refer to the neutron and proton fields respectively. The coupling constants g_r , f_r etc. are real numbers because of the hermiticity of L_0 . The π^0 , π^+ and π^- fields are denoted by φ_0 , φ and φ^* respectively and $\lambda = m/2$ or $(m-1)/2$ according as « m » is even or odd. The requirement of CP invariance ⁽¹⁾ on L_0 gives

$$(2) \quad \begin{cases} g_r = \eta_0^{m-2r} g_r, & g'_r = -\eta_0^{m-2r} g'_r; \\ f_r = \eta_0^{m-2r} f_r, & f'_r = -\eta_0^{m-2r} f'_r; \end{cases}$$

where $\eta_0 = \pm 1$ is the real phase factor which arises from φ_0 , i.e. $CP \varphi_0(x) (CP)^{-1} = \eta_0 \varphi_0(-x)$. If « m » is even, clearly $f'_r = g'_r = 0$, and if « m » is odd then for $\eta_0 = +1$,

⁽¹⁾ G. FEINBERG: *Phys. Rev.*, **108**, 878 (1957).

⁽²⁾ V. G. SOLOVIEV: *Nuclear Physics*, **6**, 618 (1958).

⁽³⁾ S. N. GUPTA: *Can. Journ. Phys.*, **35**, 1309 (1957).

$f'_r = g'_r = 0$, and for $\eta_0 = -1$; $f_r = g_r = 0$. Thus, L_0 , as in the linear case, becomes parity conserving. The requirement of charge symmetry, (cfr. (5)), in this case, serves to relate the coupling constants.

The general n-p interaction with « m » pion fields can be written as

$$(3) \quad L_1 = \sum_{r=0}^{\lambda} \{ \bar{\psi}_1 t (G_r + i G'_r \gamma_5) \psi_2 \varphi_0^{m-(2r+1)} (\varphi \varphi^*)^r \varphi^* + \text{h.c.} \}.$$

The G_r and G'_r are complex and are essentially the coupling constants. The upper limit « λ » in the « r » summation is $(m-1)/2$ for odd « m », while $\lambda = (m-2)/2$ for even « m ». The requirement of CP invariance on L , leads to the relations

$$(4) \quad G_r = G_r^* \eta_0^{m-(2r+1)} \eta, \quad G'_r = -G_r'^* \eta_0^{m-(2r+1)} \eta;$$

where η is the complex phase factor from the charged pion field (i.e. $CP \varphi(x) (CP)^{-1} = \eta \varphi^*(-x)$). Applying charge symmetry ⁽¹⁾

$$(5) \quad \psi_1 \rightarrow \psi_2, \quad \psi_2 \rightarrow \psi_1, \quad \varphi \rightarrow \varphi^*,$$

we obtain $G_r = G_r^*$ and $G'_r = G_r'^*$. Thus G_r and G'_r are real and it follows from (4) that η is real and equal to ± 1 . We, then, have two cases:

(i) « m » even. If $\eta_0 = +1$ then $\eta = +1$ gives $G'_r = 0$, while $\eta = -1$ gives $G_r = 0$. $\eta_0 = -1$, $\eta = +1$ or -1 gives G_r or G'_r , respectively, equal to zero.

(ii) « m » odd. In this case $m - (2r+1)$ is even, so that $\eta_0^{m-(2r+1)} = 1$ for both $\eta_0 = \pm 1$. Again, for $\eta = +1$, $G'_r = 0$, while for $\eta = -1$, $G_r = 0$.

Hence, the non-linear n-p interaction becomes parity conserving under the requirements of CP invariance and charge symmetry.

Thus, the hypothesis, that CP invariance and charge symmetry should lead to a parity conserving interaction, permits both linear and non-linear pion interactions with fermion isotopic doublets.

On the Connection between Scattering and Photoproduction of Pions at High Energies.

C. PELLEGRINI

Laboratori Nazionali di Frascati del C.N.R.N. - Frascati, Roma

L. TAU

*Istituto di Fisica dell'Università - Roma
Istituto Nazionale di Fisica Nucleare - Sezione di Roma*

(ricevuto il 26 Aprile 1960)

It is known that between the elements of the S matrix for scattering and photoproduction of pions on nucleons

$$(1) \quad \begin{cases} \pi + N \rightarrow N + \pi, \\ \gamma + N \rightarrow N + \pi, \end{cases}$$

a relation exists which follows from the unitarity and time reversal invariance of S ⁽¹⁾. One can indeed show that, if the amplitudes of (1) with well defined total angular momentum J , isotopic spin T and parity P are written as $\langle \pi | S | \pi \rangle = A \exp [2i\alpha]$, $\langle \pi | S | \gamma \rangle = C \exp [i\gamma]$, with A , α , C , γ real numbers, then — at energies which do not allow two or more pions in the final states — one obtains $A=1$, and also

$$(2) \quad \cos 2(\alpha - \gamma) = -1.$$

Recently the measurements of cross sections for reactions (1) have been extended to energies where two pion processes contribute appreciably, and we wish to present in this note a formula of the same type as (2), which takes these processes into approximate account ⁽²⁾.

⁽¹⁾ K. M. WATSON: *Phys. Rev.*, **95**, 228 (1954); see also M. GELL-MANN and K. M. WATSON: *Ann. Rev. Nucl. Sci.*, **4**, 219 (1954).

⁽²⁾ An analysis of the same type as the one given here has been made by R. H. CAPPS: *Phys. Rev. Lett.*, **2**, 475 (1959). Due to his exact treatment, Capps deduces only an inequality for the phase differences.

Let us introduce elements

$$\langle 2\pi, \lambda | S | \pi \rangle = B_\lambda \exp [i\beta_\lambda] \quad \text{and} \quad \langle 2\pi, \lambda | S | \gamma \rangle = D_\lambda \exp [i\delta_\lambda],$$

which are responsible for two pion reactions. The index λ which figures here explicitly serves to indicate all the quantum numbers which, together with JTP , are necessary to specify the state of a two-pion, one-nucleon system. Invariance of S for time reversal means that S is symmetrical, $\langle b | S | a \rangle = \langle a | S | b \rangle$, and the unitarity condition $SS^+ = 1$ is now written

$$(3) \quad 0 = \langle \pi | SS^+ | \gamma \rangle = \sum_n \langle \pi | S | n \rangle \langle n | S^+ | \gamma \rangle = \\ = \langle \pi | S | \pi \rangle \langle \pi | S^+ | \gamma \rangle + \langle \pi | S | \gamma \rangle + \sum_\lambda \langle \pi | S | 2\pi, \lambda \rangle \langle 2\pi, \lambda | S^+ | \gamma \rangle.$$

We have of course made $\langle \gamma | S | \gamma \rangle = 1$. We have also restricted ourselves to an energy region in which final states with three or more pions can be neglected. In this region S and P waves only should be adequate in describing two pion processes.

In order to proceed further and be able to connect (3) with the cross sections, we now assume the isobaric model⁽³⁾. This describes the two pion processes as reactions which — due to the strong resonant interaction in the $P \frac{3}{2} \frac{3}{2}$ state of the pion nucleon system — proceed essentially through an intermediate state in which an excited nucleon N^* with spin $\frac{3}{2}$, isotopic spin $\frac{3}{2}$, parity $+$ and sharp mass is present. Thus we write

$$(4) \quad \begin{cases} \pi + N \rightarrow \pi + N^* \rightarrow \pi + \pi + N, \\ \gamma + N \rightarrow \pi + N^* \rightarrow \pi + \pi + N. \end{cases}$$

Experimental evidence supports this model⁽⁴⁾.

Reactions (4) proceed then, in this approximation, as though they were two body processes, and the sum over λ in (3) reduces now to only one term. This allows us to write

$$A C \exp [i(2\alpha - \gamma)] + C \exp [i\gamma] = -BD \exp [i(\beta - \delta)].$$

Finally, squaring this equation, and using the other condition, $\langle \pi | SS^+ | \pi \rangle = 1$, which furnishes $A^2 + B^2 = 1$, we obtain the result

$$(5) \quad \cos 2(\alpha - \gamma) = \frac{1}{\sqrt{1 - B^2}} \left[\frac{1}{2} B^2 \left(1 + \frac{D^2}{C^2} \right) - 1 \right].$$

Let us indicate now by X^2 any one of the squared matrix elements B^2 , C^2 , D^2 . The connection with the corresponding partial cross section of the same JTP is then

⁽³⁾ S. J. LINDENBAUM and R. M. STERNHEIMER: *Phys. Rev.*, **109**, 1723 (1958).

⁽⁴⁾ V. ALLES-BORELLI, S. BERGIA, E. PEREZ-FERREIRA and P. WALOSCHEK: *Nuovo Cimento*, **14**, 211 (1959).

given by the well known formula

$$\sigma = \frac{\pi \lambda^2 (2J + 1)}{2n} X^2.$$

Here λ is the wave length of the incident particle, and n is 1 if this particle is a pion, 2 if it is a photon.

Unfortunately, the experimental results for reactions (4) are too scanty to allow a numerical evaluation of (5). There is one point to be noted, however, and this is that the existence of only S and P waves in (4), together with the isobar hypothesis, prevents the $J = \frac{1}{2}$, $P = -1$ state from going into a two pion channel. This follows from the usual rules for the addition of angular momenta, and makes relation (2) still valid at the energies here considered for the S wave of reactions (1).

A question could be raised, which concerns the inadequacy of the isobar model, due to the coexistent pion-pion interaction. Actually, experimental evidence seems to indicate that this interaction becomes important only at energies where three pion processes should also be important, that is at energies where the present analysis becomes inadequate anyway.

* * *

In conclusion, we should like to thank Prof. G. STOPPINI for posing the problem and for his encouragement, and Prof. M. CINI for a clarification regarding the pion-pion interaction.

LIBRI RICEVUTI E RECENSIONI

J. S. R. CHISHOLM and A. H. DE BORDE - *An Introduction to Statistical Mechanics*. Pergamon Press, 1958, pp. 160.

È difficile giudicare fino a che punto risulti utile moltiplicare il numero dei libri su un dato argomento. Tale osservazione è particolarmente valida qualora si tratti di una materia che presenti notevoli difficoltà concettuali, come è il caso della meccanica statistica; tanto più che su questo argomento esistono già parecchi ottimi trattati. Mi sembra quindi che un nuovo testo di meccanica statistica sia giustificato solo se l'impostazione è completamente nuova o se i concetti fondamentali vengono posti in più chiara luce o ancora se si tratta di un testo di aggiornamento. Nessuna di queste condizioni è soddisfatta dal libro di CHISHOLM e DE BORDE, il quale riflette piuttosto lo sforzo compiuto da due valorosi insegnanti per dare un'impronta personale al corso da loro svolto.

Il giudizio tuttavia non vuole essere

negativo: la materia è chiaramente impostata con l'intento di darle uno sviluppo armoniosamente logico (si noti che il libro è dedicato a studenti « undergraduate » del corso di laurea in matematica e fisica e non a futuri ricercatori); il punto di vista classico e quantistico sono portati avanti in modo parallelo, con un metodo semplificato alla Darwin-Fowler; alle questioni di principio sono alternate applicazioni di carattere vario, ad esempio i calori specifici di H_2 , D_2 e HD , gli equilibri isotopici, la teoria di Debye, il concetto di fonone, ecc.

L'impostazione di alcuni concetti può essere criticabile: per esempio l'introduzione dell'insieme gran canonico (§ 15) può apparire correlata, al lettore non provvisto, ai principi della meccanica quantistica. Si può anche dissentire sulla denominazione di « gas reale » data a un gas composto di molecole bi- o poliatomiche non interagenti tra di loro e quindi obbediente all'equazione dei gas perfetti.

G. BOATO

PROPRIETÀ LETTERARIA RISERVATA

Direttore responsabile: G. POLVANI

Tipografia Compositori - Bologna

Questo fascicolo è stato licenziato dai torchi il 28-VI-1960